An investigation into the effect of oxLDL and cyclic nucleotides on platelet cytoskeletal function

Yusra Ahmed

PhD Medical Sciences

The University of Hull and The University of York

Hull York Medical School

September 2020

Abstract

Atherosclerosis is a major underlying cause in cardiovascular disease and a significant health concern in developed countries. Part of the mechanism by which platelets are linked to this process is via their activation by oxidised Low-Density Lipoproteins (oxLDL), which drives both atherogenesis and thrombosis. However, the mechanism by which oxLDL drives platelet activation and thrombosis is unclear.

The combinations of matrix protein within the vascular wall and within the thrombus, especially if oxLDL is present can affect the size and strength of the thrombus formed. We have previously shown that platelets bind effectively to fibrinogen, but that this can be reversed by prostacyclin (PGI$_2$). We now demonstrate that the combination of fibrinogen and oxLDL as a matrix protein induced a significant increase in platelet adhesion and spreading in a dose-dependent manner. Furthermore, we identified that oxLDL partially blocked the reversal of spread platelets by PGI$_2$, as the surface area of the platelet was unaffected in contrast to those platelets spread only on fibrinogen. This suggested that oxLDL modulated the reversal of platelet spreading by PGI$_2$. However, oxLDL mediated inhibition of surface area reduction by PGI$_2$ was independent of the secondary mediators ADP and TxA$_2$.

To understand how oxLDL might cause this change in PGI$_2$ mediated reversal of platelet function, we first identified the cAMP production in spread cells. This indicated that cAMP production was inhibited by oxLDL but was still significantly higher than control spread platelets. This indicated that the reversal of stress fibres could be induced by limited increases in cAMP whilst higher increases then affected lamellipodia and reduced overall platelet surface

area. These two pieces of data suggested that the RhoGTPases, Rac and RhoA might be differentially controlled within spread platelets. This was confirmed as platelets spread on oxLDL and fibrinogen in the presence of PGI_2 showed elevated levels of Rac activity, whilst RhoA activity was significantly inhibited. Furthermore, we found that pMLC was elevated in platelets spread on fibrinogen, fibrinogen and nLDL as well as oxLDL, in line with stress fibre formation and increase in Rho activity in the absence of PGI_2.

To understand the effect of this reversal of stress fibres on thrombus formation, we post perfused cAMP elevating agents over platelet aggregates preformed on fibrinogen +/- oxLDL or nLDL. Our data suggest that at high shear PGI_2 or the AC (adenylyl cyclase) activator, forskolin cannot induce reversal of stress fibres, whilst the phosphodiesterase 3 inhibitor, milrinone can. In contrast at low shear, PGI_2 and forskolin can induce a complete reversal of stress fibres. This data indicates that shear stress can alter PGI_2 effects on spread platelets, potentially due to changes in PDE3 activity, and therefore can help to provide a prothrombotic environment.

In summary, our data shows that oxLDL and fibrinogen play an important role in promoting a prothrombotic and proinflammatory phenotype, contributing to atherogenicity and atherothrombosis. Investigating the contribution of oxLDL and fibrinogen and their involvement in atherothrombosis, in the context of these results will provide novel insights and identify new pathways of immunothrombosis.

Publications

- Atkinson L, Yusuf M., Aburima A, **Ahmed Y**, Thomas S, Naseem K & Calaminus S., 2017. Reversal of stress fibre formation by Nitric Oxide mediated RhoA inhibition leads to reduction in the height of preformed thrombi. *Scientific Reports. 3032. 21167-6.*

- Kinnon, M; **Ahmed Yusra (coauthor)**, Atkinson, L; McClew, B; Price, T; Calaminus, S; Stasiuk, G, 2019. Development of a fluorescent probe for understanding the role of zinc in platelets. Manuscript submitted to *Chemistry-A European Journal*. (Manuscript submitted).

- **Ahmed Yusra**, Atkinson L., Naseem, K., Calaminus S., 2020. Oxidized low-density lipoprotein modulates the activity of RhoGTPases altering the reversal of platelet activation to PGI$_2$. *Manuscript in preparation to Journal of Thrombosis and Haemostasis. (*Manuscript in preparation).

Oral presentations

- Ahmed Yusra, Atkinson L., Naseem, K., Calaminus S, 2018. Oxidized low-density lipoprotein modulates the activity of RhoGTPases altering the reversal of platelet activation to PGI$_2$. *North of England Cell Biology.*

Poster presentation

- Ahmed Yusra, Atkinson L., Naseem, K., Calaminus S., 2019. Oxidized low-density lipoprotein modulates the activity of RhoGTPases altering the reversal of platelet activation to PGI$_2$. *Postgraduate Research Conference. Hull York Medical School. UK.*

- Ahmed Yusra, Atkinson L., Naseem, K., Calaminus S, 2018. Oxidized low-density lipoprotein modulates the activity of RhoGTPases altering the reversal of platelet activation to PGI$_2$.. *European Platelet Network Meeting. Belgium*.

- Ahmed Yusra, Kinnon, M; Atkinson, L; McClew, B; Price, T; Calaminus, S; Stasiuk, G., 2017. Development of a fluorescent probe for understanding the role of zinc in platelets. *UK Platelet meeting. University of Manchester. UK.*

Contents

List of Figures

List of Tables

Abbreviations

ApoB	Apolipoprotein B
ApoB-100	Apolipoprotein B - 100
α2β1	Integrin alpha 2 beta 1
αIIbβ3	Integrin alpha IIb beta 3
5-HT 5	5-hydroxytryptamine (serotonin)
AC	Adenylyl cyclase
ACD	Acid citrate dextrose
ADP	Adenosine 5'-diphosphate
AKAP	A-kinase anchoring protein
ANOVA	Analysis of variance
APS	Ammonium persulfate
Arp2/3	Actin-related protein 2/3
ATP	Adenosine triphosphate
ATPase	Adenosine 5'-triphospatase
BSA	Bovine Serum Albumin
Ca2+	Calcium
cAMP	Cyclic adenosine 3',5'-monophosphate

CD36	Cluster of differentiation 36
Cdc42	Cell division control protein 42
cGMP	Cyclic guanosine 3',5'-monophosphate
COX	Cyclooxygenase
COX-1	Cyclooxygenase 1
COX-2	Cyclooxygenase 2
CRIB	Cdc42/Rac1 Binding Domain
c-Src	Cellular sarcoma
C-terminal	Carboxyl terminal
CVD	Cardiovascular Diseases
CXCR4	Chemokine receptor type 4
DAG	Diacylglycerol
dH2O	distilled water
DiOC6	3,3'-Dihexyloxacarbocyanine iodine
DNA	Deoxyribonucleic acid
DTS	Dense tubular system
ECM	Extracellular matrix
EDTA	Ethylenediaminetetraacetic acid
EGTA	Ethyleneglycoltetraacetic acid

eNOS	Endothelial nitric oxide synthase
ER	Endoplasmic reticulum
F-actin	Filamentous actin
FAK	Focal adhesion kinase
FcR γ-chain	Fc receptor gamma chain
FITC	Fluorescein isothiocyanate
FSK (Fsk)	Forskolin
G-actin	Globular actin
GAF	(cGMP) binding domain on PDE2 and PDE5
GAP	GTPase activating protein
GAPDH	Glyceraldehyde 3-phosphate dehydrogenase
GDI	Guanine-nucleotide dissociation inhibitor
GDP	Guanosine diphosphate
GEF	Guanine-nucleotide exchange factor
GP	Glycoprotein
GPCR	G-Protein coupled receptor
GPIb-V-IX	Glycoprotein Ib-V-IX receptor complex
GPIIb/IIIa	Glycoprotein IIb/IIIa
GPO	Gly-Pro-Hyp

GPVI	Glycoprotein VI
GTP	Guanosine 5'-triphosphate
HDL	High-density Lipoprotein
HEPES	4-(2-Hydroxyethyl)-1-piperazineethanesulfonic acid
IDL	Intermediate-density Lipoprotein
IL-6	Interleukin 6
iNOS	Inducible nitric oxide synthase
IP3	Inositol 1, 4,5-triphosphate
ITAM	Immuno-receptor Tyrosine-based activation motif
ITIM	Immunoreceptor tyrosine-based inhibitory motif
kDa	Kilo Dalton
LAT	Linker for activation of T cells
LCAT	Lethicin Cholesterol Acyl Transferase
Lp(a)	Lipoprotein (a)
LPL	Lipoprotein Lipase
MAPK	Mitogen activated protein kinase
Mg2+	Magnesium
MLC	Myosin light chain
MLCK	Myosin Light Chain Kinase

MLCP   Myosin Light Chain Phosphatase

MMPs   Matrix metalloproteinases

mRNA   Messenger ribonucleic acid

nLDL   native low-density lipoprotein

NO   Nitric oxide

NOS   Nitric oxide synthase

NPFs   Nucleation promoting factors

N- terminal   Amino terminal

OCS   Open canalicular system

oxLDL   oxidized low-density lipoprotein

P2Y1   Purigenic class of G-protein-coupled receptor 1

P2Y12   Purigenic class of G-protein-coupled receptor 12

PAGE   Polyacrylamide gel electrophoresis

PAR   Protease activated receptor

PAR1   Protease-activated receptor-1

PAR4   Protease-activated receptor-4

PBS   Phosphate Buffer Saline

PC   Phosphatidylcholine

PDE   Phosphodiesterase

PF4   Platelet factor 4

PGE1   Prostaglandin E1

PGE2   Prostaglandin E2

PGF2   Prostaglandin E2

PGG2   Prostaglandin G2

PGH2 2   Prostaglandin H

PGI_2 Prostacyclin

PI3K   Phosphatidylinositol 3-kinase

PIP2   Phosphatidylinositol 4, 5-bisphosphate

PIP3   Phosphoinositol Tri (3) Phosphate

PKA   Protein kinase A

PKC   Protein kinase C

PKG   Protein Kinase G

PLA2   Phospholipase A2

PLCγ   Phospholipase Cγ

PLC2   Phospholipase Cγ2

PLCβ   Phospholipase C beta

PLCγ2   Phospholipase C gamma 2

PPACK	Phenylalanyl-Prolyl-Arginyl Chloromethyl KetonePhosphatidylserine
PS	
Rac1	Ras-related C3 botulinum toxin substrate 1
RhoA	Ras homologous A
RhoGEF	Rho guanine nucleotide exchange factor
Rif	Rho in filopodia
ROCK	Rho kinase
ROS	Reactive Oxygen Species
SCCS	Surface connected open canalicular system
SD	Standard Deviation
SDS	Sodium dodecyl sulphate
SFK	Src family kinase
sGC	Soluble guanylyl cyclase
SH2	Src homology 2
SH3 domain	Src homology 3 domain
SLP-76	Src homology 2 domain-containing leukocyte protein of 76 kDa
SMCs	Smooth muscle cells
SNARE	Soluble N-ethylmaleimide-sensitive fusion protein
Syk	Spleen tyrosine kinase

TAE	Tris-Acetate-EDTA
TBS-T	Tris buffered saline with Tween 20
TEMED	N,N,N',N'-tetramethylethylenediamine
TPO	Thrombopoietin
Tris	Trishydroxyaminomethane
TXA2	Thromboxane A2
VASP	Vasodilator Simulated Protein
VCA	Verprolin, Cofilin, Acidic domain
VCAM-1	Vascular Cell Adhesion Molecule 1
VLDL	Very Low-density Lipoprotein
vWF	von Willebrand factor
WAS	Wiskott-Aldrich Syndrome
WASp	Wiskott-Aldrich Syndrome protein
WAVE	WASp-family verprolin-homologous protein
WHO	World Health Organization

Acknowledgement

First, I would like to thank God Almighty for giving me the strength and good health to embark on this challenging journey.

Heartfelt thanks to my supervisor, Dr Simon Calaminus, for his invaluable guidance, patience and understanding throughout the course of my PhD research. I could not have asked for a more considerate and supportive supervisor. I would like to extend my gratitude to the University of Hull for funding my PhD.

My appreciation extends to Dr Hassan, Dr Aden and Dr Arabeyyat for being great colleagues, friends, role models and mentors. Your encouragements have been especially valuable.

I would like to thank my laboratory colleagues as well as our blood donors. This work would not have been possible without their help. Special thanks to Dr Atkinson, Dr Berger, Matt, Adam and Paulo for the advice and support.

I would like to give special thanks to Jawad for being an older brother and a great friend. Thank you for all the stories, life lessons and support during the challenging times. Thank you Anisha for being like a sister to me. Thank you for all the spontaneous adventures and laughter. I thank God for finding a great friend like you.

This PhD would not have been possible without my family and friends. Further thanks go to my siblings Yasmin, Sara, Samia and Hassan for being understanding and giving me the strength throughout this journey.

I am indebted to my Mama and Baba, who have made an untold number of sacrifices for me and always believed in my dreams. Thank you for the continuous support and prayers. I love you both Mama and Baba.

As for my fiancé Fatih, I find it difficult to express my appreciation because it is so boundless. I am grateful for your love and support throughout this entire journey. Thank you for all those nights you stayed up, giving me endless support and encouragement while I pushed through lab work. Seni çok seviyorum aşkım.

Author's declaration

'I confirm that this work is original and that if any passage(s) or diagram(s) have been copied from academic papers, books, the internet or any other sources these are clearly identified by the use of quotation marks and the reference(s) is fully cited. I certify that, other than where indicated, this is my own work and does not breach the regulations of HYMS, the University of Hull or the University of York regarding plagiarism or academic conduct in examinations. I have read the HYMS Code of Practice on Academic Misconduct, and state that this piece of work is my own and does not contain any unacknowledged work from any other sources'.

Chapter 1: General Introduction

Cardiovascular disease is increasing in epidemic proportions in the developing world and is considered as the leading cause of death globally (Guilbert, 2003). Clinicians and researchers rely heavily on mortality data from both developing and developed countries to draw conclusions in order to establish therapeutic interventions and policies. It can be argued that the prevalence of cardiovascular disease in developing countries is not very accurate, as mortality data collected from developing countries are subject to limitations i.e., patients that die without health records or death certificates (Pagidipati and Gaziano, 2013). However, it is evident that cardiovascular disease is a common social, economic and health burden in these nations.

Ischemic heart disease, stroke and congestive heart failure account for 80% of CVD morbidity and mortality. Ischemic heart disease is the leading cause of death in developed regions and a major disease burden in developing nations. Although epidemiological transition and significant decline in CVD mortality is a public health success story, the emergence of racial, gender and geographic disparities in CVD mortality need to be thoroughly tackled.

There are well-established racial and social disparities in cardiovascular health outcomes between minority and non-minority group across globe (Graham, 2015). Generally, ethnic minorities have not benefitted from the epidemiological shift and decline in CVD related deaths (Mensah et al., 2017). Risk assessment is a public health challenge in specific populations and therefore, preventative strategies focusing on lifestyle interventions should be emphasised. Thus, it is important for physicians and clinicians to understand the nuances in CVD presentation, risk factors as well as therapeutic strategies in different population groups as "better understanding and awareness of the disparities of CVD risk factors by race and ethnicity

may help clinicians and public health professionals develop culturally sensitive interventions, prevention programs, and services specifically targeted toward risk burdens in each of these populations" (Kurian and Cardarelli, 2007).

Although contemporary preventative measures focus on risk factors, public health professionals should therefore consider social, economic, and political structures that impede preventative efforts in order to prevent CVD mortality.

1.1 Atherosclerosis

Atherosclerosis is a major element in cardiovascular disease and a major health concern in developed countries. In a Horus study, atherosclerosis was discovered in pre-modern human beings from four preindustrial populations with significant differences in lifestyle and diet, suggesting that the disease is an inherent aspect of ageing in humans and not necessarily characterized by a specific lifestyle or diet (Thompson et al., 2013).

Atherosclerosis is linked to the mis-regulation of lipids within the blood. This pathological condition causes thickening of the intimal layers of the arteries, causing a loss in elasticity. This mis regulation not only causes the build-up of fatty plaques within the vasculature, but also causes the blood cell platelet to become more reactive, and therefore provides a prothrombotic environment. An important risk factor for the onset of atherosclerotic lesion and ischemic heart disease is increased levels of LDL in the plasma which is one example of hyperlipidaemia. Furthermore, hyperlipidaemia is an important risk factor in increased platelet reactivity. Increased platelet reactivity has been described in elevated levels of LDL, inducing a prethrombotic risk and the opposite effect was reported in low levels of LDL (Carvalho, Colman and Lees, 1974; Stuart, Gerrard and White, 1980; Davi et al., 1992). For instance,

Lacoste et al., 1995 have illustrated the involvement of excessive blood lipids in promoting the formation of a platelet thrombus in coronary artery disease patients, enhancing the propensity for acute thrombosis. Consequently, the rationale behind preventing thrombosis as a therapeutic approach for preventing unstable coronary syndromes is compelling.

1.1.1 Pathogenesis of atherosclerosis

The earliest hallmark of atherosclerosis is the fatty streak caused by the accumulation of lipids in the vascular bed (figure 1.1). The build-up of lipid causes foam cell formation in the tunica intima (Libby et al., 2019). Following the death of these foam cells, soft lipids are formed causing the formation of an atheromatous plaque. As the plaque continues to develop, vascular smooth muscle cells, endothelial cells and macrophages undergo cell death by apoptosis and necrosis. The cell death of each of these types of cell, affects the plaques in different manners. Endothelial cell death and dysfunction can induce plaque erosion, which underpins the pro-inflammatory and pro-thrombotic phenotypes associated with atherosclerotic plaques whilst smooth muscle cell death can initiate the destabilisation of the rupture- prone fibrous cap. Interestingly, although the most abundant of the apoptotic cells found in atherosclerotic lesions are macrophages, the role of apoptotic macrophages in these lesions remains to be elucidated.
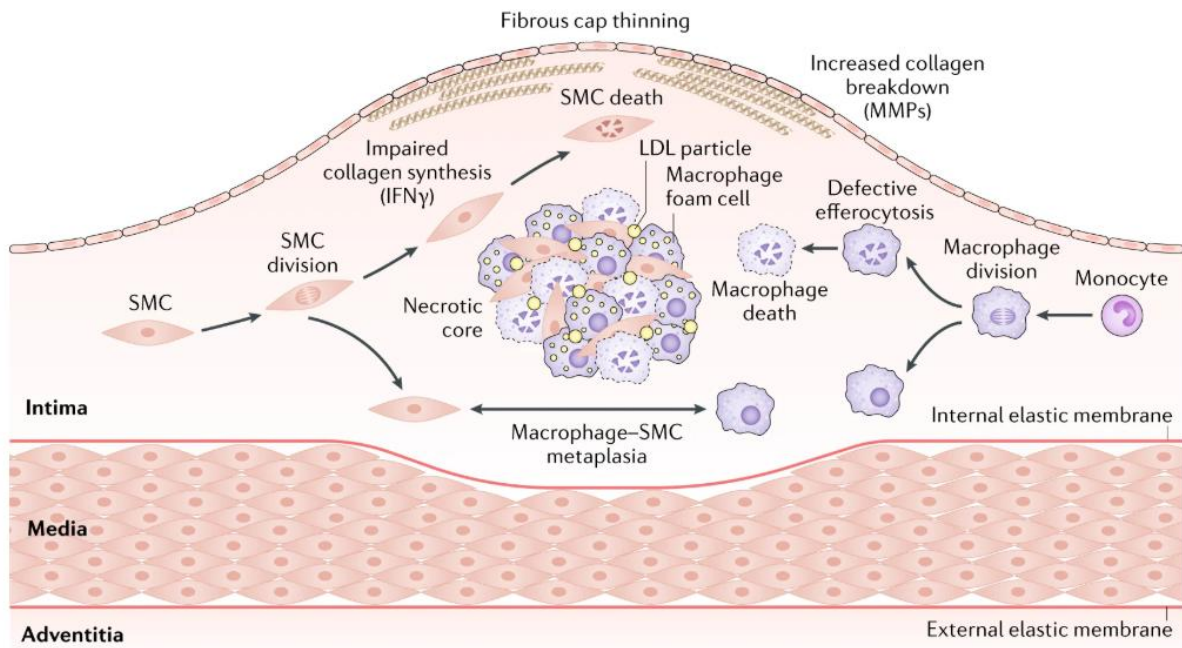
Figure 1.1 The evolution of the atherosclerotic plaque.

The recruitment of smooth muscle cells includes the production of extracellular matrix proteins such as collagen, proteoglycans and elastin causing the thickening of the tunica intima. Activated macrophages generate MMPs, degrading extracellular matrix components which in turn weakens the fibrous cap and increases plaque rupture risk. As the atherosclerotic lesion progresses, smooth muscle cells and macrophages undergo apoptosis and clearance of these dead cells results in the formation of foam cells. Image adapted from Libby et al., 2019.

1.1.2 Calcification

Calcification is a marker of coronary plaque deposition and an active process that recapitulates biological processes in bone formation and is regulated by an array of cellular pathways, resulting in the calcification of connective tissues and lipids as well as arterial stiffness (Ruiz, Hutcheson and Aikawa, 2015). This process is correlated with the instability of plaques, inducing plaque rupture and thrombus formation (Ruiz, Weinbaum, Aikawa and Hutcheson, 2016). The amount and level of calcification provides insight into the total coronary plaque burden and rapid calcium progression is associated with poor cardiovascular prognosis (Alexopoulos and Raggi, 2009).

1.1.3 Inflammation and chronic endothelial injury

Endothelial injury occurs during the early stages of atherosclerosis. The inflammatory cascade regulates this process. Endothelial injury results in the phenomenon of neovascularization which stimulates the expression of adhesion molecules such as (vascular cell adhesion molecule 1) VCAM-1, encouraging the recruitment of erythrocytes, inflammatory cells and cytokines as well as plasma proteins. Accumulation of leukocytes to the endothelium leads to the recruitment and subsequent proliferation of smooth muscle cells. As a result, adhesion of monocytes to the endothelium is observed, orchestrating the progression of atherosclerosis through the release of cytokines as well as lipid accumulation. Differentiation of monocytes into macrophages drives the atherosclerotic development due to the production of matrix metalloproteases (MMPs), causing the vascular wall to weaken as a result of extracellular matrix degradation (Galis, Sukhova, Lark and Libby, 1994). An increase in expression and activity of MMPs has been described in atherosclerotic lesions (Galis, Sukhova, Lark and Libby, 1994).

1.1.4 Plaque rupture

Plaque rupture is "an area of fibrous cap disruption whereby the overlying thrombus is in continuity with the lipid core" (Virmani et al., 2000). Vulnerable plaques are characterised by an increase in inflammatory cells, MMP expression, lipid content and a reduction in the number of vascular smooth muscle cells and collagen. Vascular smooth muscle cells are thought to play a role in promoting plaque instability as there are more apoptotic vascular smooth muscle cells unstable in contrast to stable plaques (Bauriedel, Hutter and Welsch, 1999). Infiltration of macrophages leads to a reduction in the tensile strength of the fibrous cap, promoting plaque rupture. The accumulation of lipid by macrophages also encourages the formation of foam cells, expanding the lipid core, degrading the tissues found in the intima which is thought to cause the dysfunction of the tunica media (Shah et al., 1995).

1.1.5 Does cell death play a role in thrombosis?

Apoptosis also plays a key function in the thrombogenicity of atherosclerotic lesions. Apoptotic cells in the intima are a major source of tissue factor, activating the coagulation cascade (Mallat & Tedgui, 2001). Apoptotic cells also increase tissue factor activity and are thought to colocalise with tissue factor (Kockx & Herman, 2000). An increase in procoagulant activity is also observed in apoptotic bodies in atherosclerotic plaques, inducing local and systemic thrombosis (Mallat et al., 1999).

1.2 Theories of Atherosclerosis

Following the early studies investigating the pathogenesis of atherosclerosis, three principal theories dominated the discussion concerning atherogenesis: the incrustation hypothesis developed by Karl Rokitansky, Virchow's inflammatory theory and finally the response to injury theory that was proposed by Ross that eventually led to the unification of the concepts.

1.2.1 The Incrustation or *"Thrombogenic"* Theory

Elucidated by Karl Freiherr von Rokitansky in 1852, the incrustation theory of atherosclerosis asserts that the thickening of the inner lining of the arteries is due to the conversion of fibrinogen to fibrin on the luminal surface of arteries inducing the formation of a thrombus. More recently, the role of platelets in atherogenesis has been heavily investigated (Wu, Atkinson and Lindner, 2017). It is believed that inflammation during the initial stages of atherosclerosis stimulates endothelial cells, inducing activation of platelets (Massberg et al., 2002). Reactive oxygen species generated from atherosclerotic risk factors are also though to initiate and exacerbate platelet activation further. Indeed, the activation of the endothelium enhances P-selectin mediated platelet rolling and results in platelet-endothelium adhesion (Bröijersén et al., 1998).

1.2.2 Insudation Theory

Virchow however challenged Rokitansky's thrombogenic theory in 1856 by proposing the *"endarteritis deformans"* which essentially described the different stages of atherosclerosis. In

his theory, he described atherosclerosis as a process that is initiated by intimal inflammation and is subsequently followed by thickening of the fibrous cap. This theory was later developed by Anitschkow who proposed the basis of the lipid theory, suggesting a correlation between elevated cholesterol to lipid accumulation. The deposition of lipids in the vessel wall plays a critical role in atherosclerosis. Although studies are yet to elucidate how the lipids accumulate in the vessels, to date, this concept is widely accepted. There is strong evidence to suggest that the lipid found in atherosclerotic lesions is from the blood and a positive correlation between elevated cholesterol levels and atherosclerotic plaques (Steinberg, 2002; Gardener et al., 2009). Anitschkow's hypothesis was used as the key basis for developing Ross' *"reaction to injury"* hypothesis.

1.2.3 The "Response to Injury" Theory

The response to injury hypothesis was initially proposed by Ross and Glomset in 1973. They proposed that the initiation and development of atherosclerotic plaques was driven by cells at the site of the lesions. It was believed that the injury to the endothelium modified their functional roles as barriers. The damage of the endothelial barrier resulted in platelet adhesion to the subendothelium matrix. Once platelets adhere, increased levels of growth factors such as platelet derived growth factor (PDGF) (20-fold) are released from α granules which stimulate the migration of smooth muscle cells from the tunica media to the tunica intima, inducing proliferation and subsequent release of collagen thus, causing the hardening of the atherosclerotic plaque (Jawien et al., 1992).

1.3 Plasma lipoproteins

Cholesterol and triglycerides are relatively insoluble in water and thus these lipids must be transported in association with lipoproteins *in vivo*. Plasma lipoproteins are divided into seven functionally distinct groups: Chylomicrons, chylomicron remnants, very low-density lipoprotein (VLDL), intermediate density lipoprotein (IDL), low-density lipoprotein (LDL), high-density lipoprotein (HDL) and lipoprotein (a) (Lp(a)) (Table 1.1). The classes are traditionally separated by fractionating the lipoproteins by ultracentrifugation and the particles are distinguished by their flotation density.

Plasma lipoproteins have an imperative role in carrying out the absorption and transport of dietary lipids by the small intestine, transporting triglycerides from the liver to peripheral tissues and transport of cholesterol from the peripheral tissues to the liver and intestine. Lipoproteins have a central hydrophobic core consisting of cholesterol esters and triglycerides and are surrounded by hydrophilic groups of phospholipids, free cholesterol, and apolipoproteins. Hydrophobic portions of phospholipid acyl chains interact with apolipoproteins. There are different apoproteins on different lipoproteins. Apolipoprotein sequences can fold into amphipathic α-helices that contain a nonpolar face that associates with the fatty acid chains of phospholipids and nonpolar lipids (Segrest et al., 1974).

Several principal functions have been established for apolipoproteins. Firstly, they are involved in the delivery of lipids to a variety of different tissues. This involves lipoprotein receptors on the cell surface to recognize specific apolipoproteins. Secondly, apolipoproteins have an important role as cofactors for enzymes of lipid metabolism and thirdly, they maintain the lipoprotein structure, providing stability.

Table 1.1 Classes of lipoproteins.

Lipoprotein	Density (g/ml)	Size (nm)	Major Lipids	Major Apoproteins
Chylomicrons	<0.930	75-1200	Triglycerides	Apo B-48, Apo C, Apo E, Apo A-I, A-II, A-IV
Chylomicron Remnants	0.930- 1.006	30-80	Triglycerides Cholesterol	Apo B-48, Apo E
VLDL	0.930- 1.006	30-80	Triglycerides	Apo B-100, Apo E, Apo C
IDL	1.006- 1.019	25-35	Triglycerides Cholesterol	Apo B-100, Apo E, Apo C
LDL	1.019- 1.063	18- 25	Cholesterol	Apo B-100
HDL	1.063- 1.210	5- 12	Cholesterol Phospholipids	Apo A-I, Apo A-II, Apo C, Apo E
Lp (a)	1.055- 1.085	~30	Cholesterol	Apo B-100, Apo (a)

Plasma lipoproteins are divided into seven functionally distinct groups: Chylomicrons, chylomicron remnants, VLDL, IDL, LDL, HDL and Lp(a). lipoproteins are classified according to size, lipid composition, and apolipoproteins. Adapted from (Feingold and Grunfeld, 2000).

1.3.1 Structure of Low-density lipoproteins

Human LDL particles are major carriers of cholesterol in the systemic circulation and their role in cholesterol transfer and metabolism is well established. LDL particles are approximately 22 nm in diameter and have a mass of three million daltons. They lie within the density limits of 1.019-1.063 g/ml (Glomset et al., 1973). LDL particles consist of about 170 triglycerides and 1600 cholesterol esters forming the highly hydrophobic core, surrounded by an outer monolayer of 700 phospholipid molecules and one copy of Apo B-100. Furthermore, 600 molecules of unesterified cholesterol are found in LDL particles of which the majority are found on the surface monolayer (Miller and Shyy, 2017). Phosphatidylcholine and sphingomyelin are the two major components of the phospholipids. However, lysophosphatidylethanolamine, diacylglycerol, ceramide and phosphatidylinositol are also other components of the phospholipid (figure 1.2).

LDL particles also contain lipophilic antioxidants such as, α-tocopherol (6 molecules per LDL particle/1.03μg/ml of LDL), a smaller proportion of γ-tocopherol, carotenoids, oxycarotenoids and ubiquinol-10 (Esterbauer et al., 1992). There is a variation in LDL size and composition because of variable fatty acid molecules which can be visualised as light and heavy subfractions using ultracentrifugation techniques.

A single copy of Apo B-100 containing 4563 amino acids is associated with every LDL particle (Feingold and Grunfeld, 2000). Apo B-100 has a distinct role in preserving structural stability as well as the regulation of LDL particle interaction. It is synthesized in the liver and as a result of metabolic processes is produced from modified VLDL. Thus, ApoB-100 is a molecule with the ability to undergo changes due to structural changes in the carrier particles (Feingold and

Grunfeld, 2000). In addition, ApoB-100 serves as ligand for lipoprotein receptors, induces lipoprotein formation and regulates enzymes important for lipoprotein metabolism.
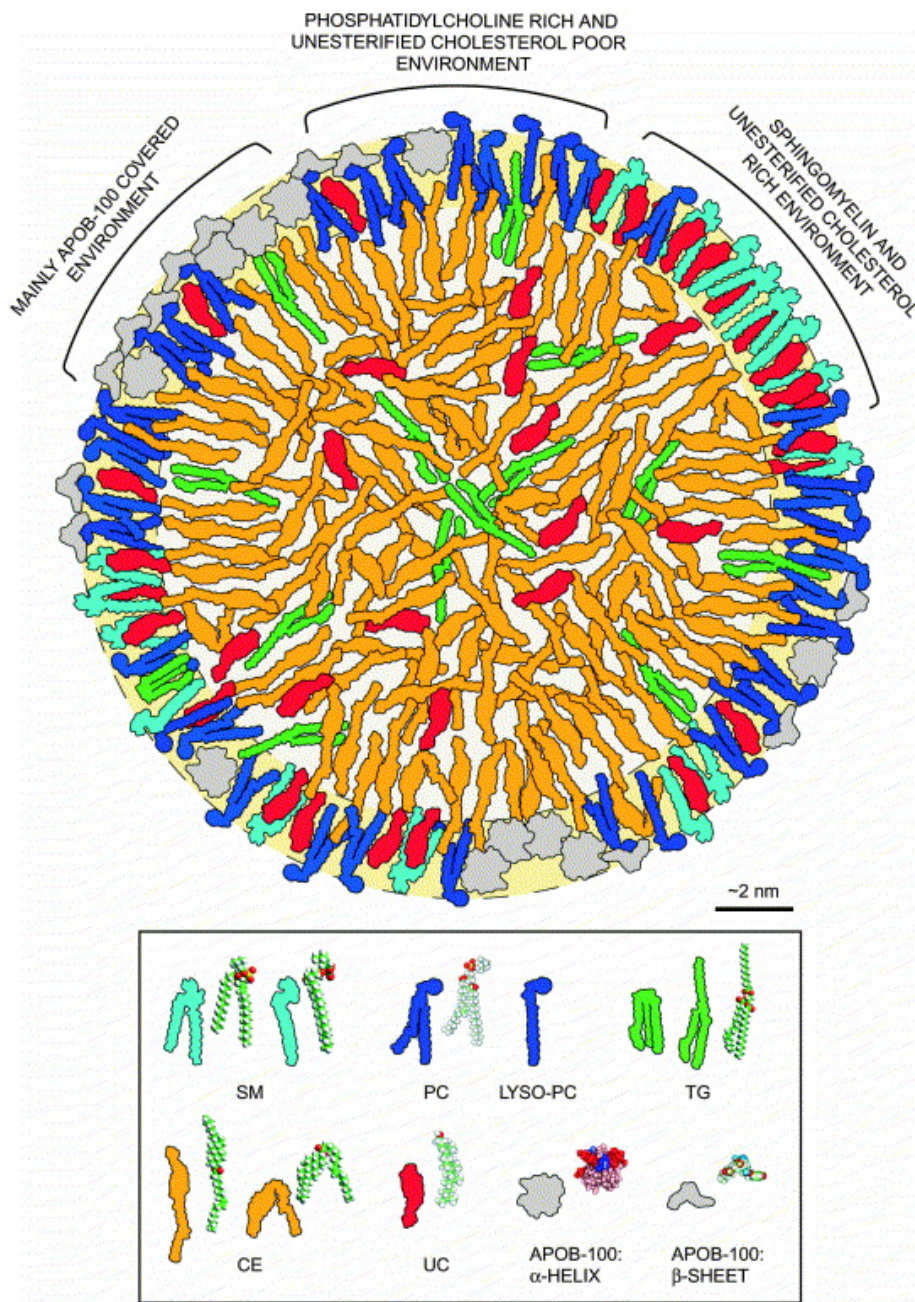
Figure 1.2. Schematic representation of an LDL.

The depicted particle has a surface monolayer of 2 nm (pale yellow background), and an average composition of 20% protein, 20% phospholipids, 40% CEs, 10% UC, and 5% TGs. Note the different domains illustrated at the particle surface and the interpenetration of core and surface lipids. Adapted from (Hevonoja et al., 2000).

1.3.2 Lipoprotein metabolism

The concentration of cholesterol in the circulation is regulated by the endogenous and exogenous pathways of lipoprotein metabolism. The exogenous pathway begins with the absorption of dietary lipids into Apo B-48 coated chylomicron particles rich in triglycerides located in the intestine (Shepherd, 2001) (figure 1.3). The thoracic duct drains the chylomicrons in the lymph into the systemic circulation via the left subclavian vein, delivering nutrients to muscle and adipose tissue (Feingold and Grunfeld, 2000. Lipoprotein lipase (LPL) anchored to the surface of the capillary endothelium by electrostatic interactions with glycosaminoglycans is expressed in high concentrations in these tissues. LPL is activated by ApoC-II (alongside Apo A-V) on the chylomicrons, facilitating the hydrolysis of the triglycerides in the chylomicron core and thus resulting in the production of free fatty acids which are absorbed by muscle and adipose tissues (Wang et al., 2015). Once the majority of the triglycerides from parent chylomicrons are metabolised, they become chylomicron remnants rich in cholesterol esters. Chylomicron remnants acquire Apo E on their surface and are cleared from the circulation via specific hepatic receptors on the liver (Feingold and Grunfeld, 2000).

On the contrary, the endogenous pathway begins with synthesis of triglyceride rich VLDL from the liver (figure 1.4). VLDL is hydrolysed by LPL and the depletion of triglycerides from VLDL results in VLDL remnants known as IDL. IDL particles can be depleted from the circulation by the liver through the binding of Apo E to LDL receptors (Olivecrona, 2016). Additionally, IDL can be converted to LDL as a result of hydrolysing the triglycerides in IDL by hepatic lipase, reducing the concentration of triglycerides and leading to the subsequent loss of Apo E. The principal apolipoprotein for these LDL particles is Apo B-100. The majority of the LDL in the circulation is cleared by a specific high affinity hepatocyte LDL receptor.

Furthermore, excess cellular cholesterol undergoes reverse cholesterol transport whereby HDL particles deliver the cholesterol from cells to the liver for excretion by the bile duct or to be recycled (Oram, 1990). The reverse cholesterol transport pathway is mediated by the ATP-binding cassette A-1 transporter (ABCA1), facilitating the efflux of cholesterol to Apo A-I, the main structural protein for HDL. Apo A-I activates a HDL associated enzyme termed lecithin cholesterol acyl transferase (LCAT). The activation of this enzyme induces the esterification process whereby free cholesterols on the surface of the HDL particle move to the hydrophobic core, producing mature large HDL particles.
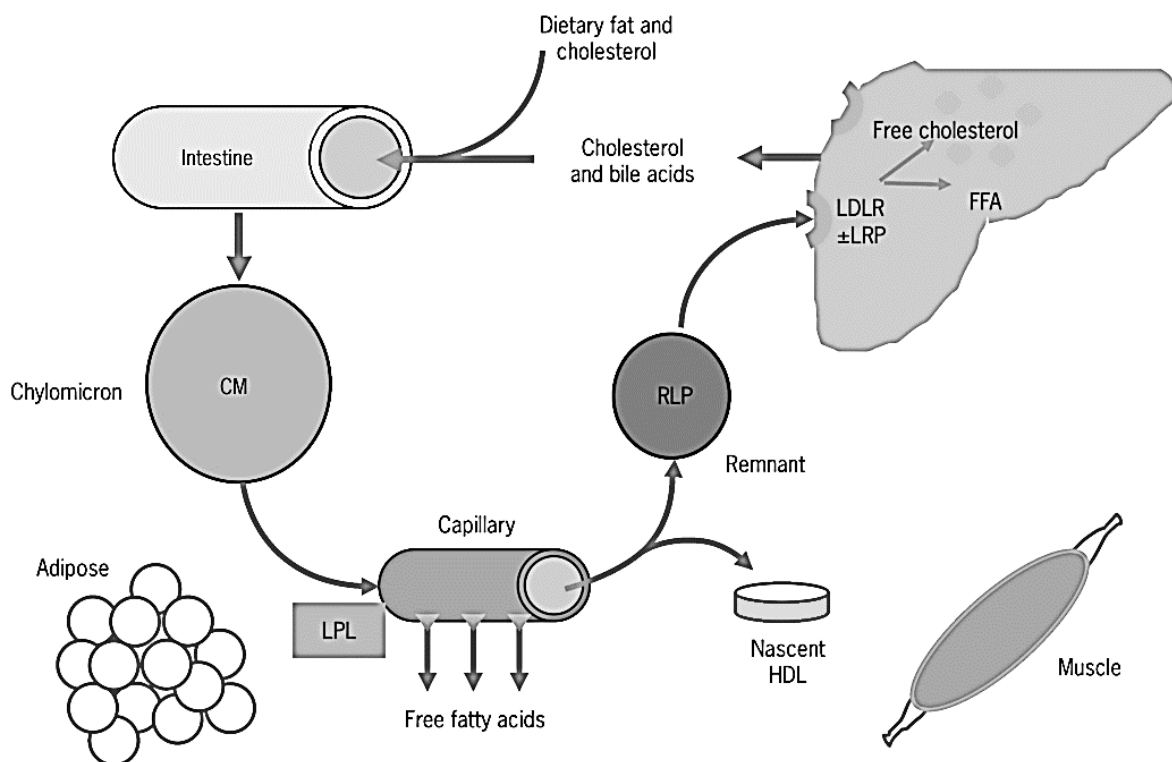
Figure 1.3 Exogenous pathway. Absorption of cholesterol and triglycerides derived from dietary lipids in the gut and incorporated into chylomicrons. Triglyceride-rich lipoproteins are made by the liver and are involved in the transport of dietary triglycerides and cholesterol to the peripheral tissues and liver. The chylomicron remnants are removed from plasma via ApoE by specific LDL receptors of the liver. Image adapted from (The British Journal of Cardiology, 2019).

Key: CM = chylomicron; FFA = free fatty acids; HDL= high density lipoprotein; LDR = low density lipoprotein receptor; LPL = Lipoprotein lipase; LRP = LDL receptor-relate protein; RLP = remnant lipoprotein.
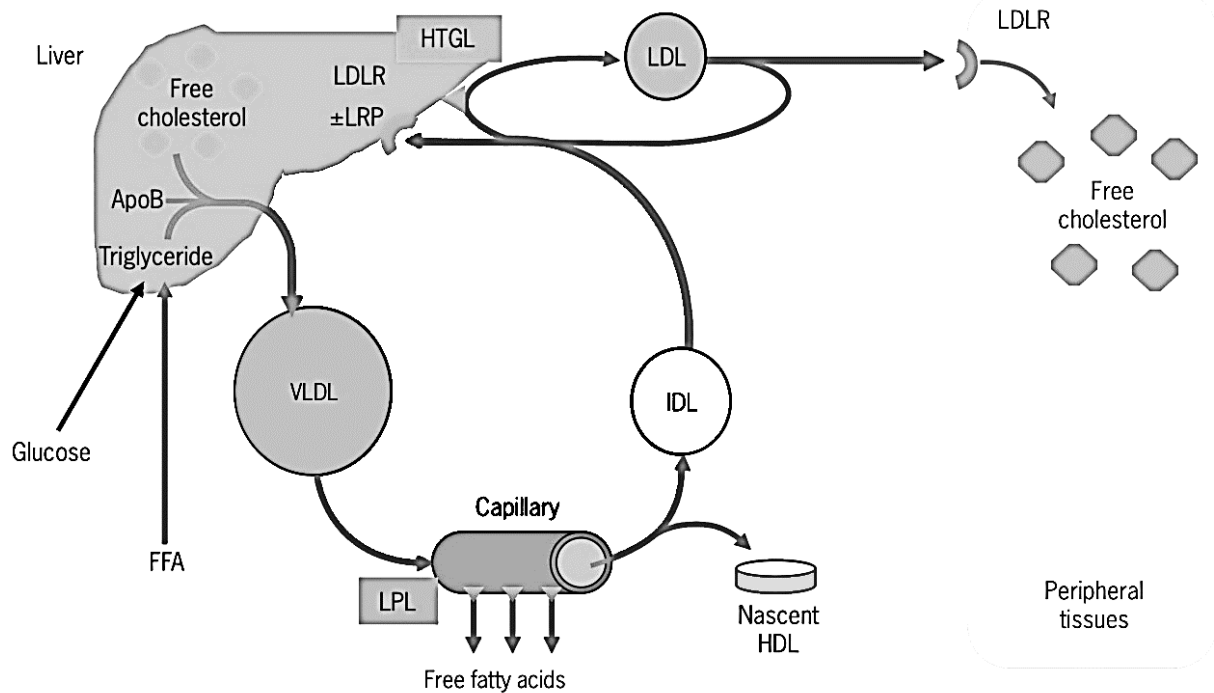
Figure 1.4 Endogenous pathway.

Triglyceride rich VLDL is synthesised by the liver. VLDL is hydrolysed by LPL and the depletion of triglycerides from VLDL results in VLDL remnants known as IDL. IDL particles can be depleted from the circulation by the liver through the binding of Apo E to LDL receptors. IDL can be converted to LDL as a result of hydrolysing the triglycerides in IDL by hepatic lipase. Apo B-100 is the major apolipoprotein for these LDL particles. LDL in the circulation is cleared by hepatocyte LDL receptor. Image adapted from (The British Journal of Cardiology, 2019).

Key: ApoB = apolipoprotein B; FFA = free fatty acids; HDL = high density lipoprotein cholesterol; HTGL= hepatic triglyceride lipase; IDL= intermediate- density lipoprotein cholesterol; LDR = low density lipoprotein receptor; LPL= lipoprotein lipase; LRP= LDL receptor related protein; VLDL = very low- density lipoprotein.

1.4 Oxidised low-density lipoproteins

In 1979, Goldstein & Brown observed that in patients with familial hypercholesterolaemia including those with a non-functional LDL receptor, foam cells were deposited in the arterial walls similar to patients that have functional LDL receptors. Indeed, this paradox was resolved when they observed that the acetylation of LDL facilitated high affinity binding of LDL to macrophages 20 times greater than nLDL, enabling internalisation and increased concentration of intracellular cholesterol. It was therefore postulated that chemically modified (acetylated) LDL binds specifically to (acetylated LDL) receptors on scavenger cells later characterised as scavenger receptor A (SRA) by Kodama and colleagues in 1988. However, this raised the question: *Is LDL acetylated in vivo?*

1.4.1 Acetylation of LDL

There was no evidence suggesting the possibility of LDL acetylation occurring in vivo. Nevertheless, in 1981, Henrisken and colleagues discovered that the overnight incubation of native LDL (nLDL) with cultured endothelial cells in the presence of transition metal ions, produced a modified version of LDL that is taken up by peritoneal macrophages with a high affinity. Shortly after, it was proposed that LDL is subject to oxidative changes during incubation with endothelial cells and umbilical veins, establishing the oxidative modification theory of atherosclerosis. LDL oxidation is believed to occur in the tunica intima and is considered a key event of atherogenesis (Steinbrecher et al., 1984).

1.4.3 Oxidative modification of LDL

Daniel Steinberg and his colleagues proposed the oxidative modification hypothesis in 1989. The hypothesis predicts that the oxidation of LDL (oxLDL) is an early event in the atherosclerotic process-giving rise to foam cells. Following the hypothesis proposed by Steinberg, a plethora of studies have demonstrated a role for oxLDL in foam cell formation through scavenger receptor pathways (Rahaman et al., 2006). As a result, scavenger receptor A (SRA) was the first to be characterised by Kodama et al in 1988. As well as SRA, oxLDL encounter various other scavenger receptors such as CD36, CD68, LOX-1 and SR-PSOX (Riazy et al., 2011).

Oxidative modification of LDLs is induced by cultured cells such as endothelial cells (Steinbrecher et al 1984), macrophages (Cathcart et al, 1985, Leake and Rankin 1990) as well as smooth muscle cells (Morel et al 1984, Heinecke 1986). Lipid peroxidation is mediated by free radicals leading to the subsequent structural changes and involves three important steps: initiation, propagation and termination. The peroxidation of polyunsaturated fatty acids (PUFA) is considered as the initiating event whereby a H· is abstracted from the double bond in PUFA. This results in the formation of the carbon radical (-C·H-). Molecular rearrangement of this carbonyl radical occurs, inducing stabilisation of this radical thus, forming a conjugated diene.

Molecular oxygen reacts with the conjugated dienes to form the lipid peroxyl radical

$$\textbf{-C·H- + O}_2 \rightarrow \textbf{-HCOO·-}$$
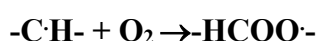
The production of lipid peroxyl radicals undergo propagation, resulting in the abstraction of hydrogen from another PUFA and formation of organic hydroperoxide such as lipid hydroperoxide and carbonyl radical.

$$\text{-CH- + -HCOO}^{\cdot} \to \text{-C}^{\cdot}\text{H- + -COOH-}$$
$$\text{-HCOO}^{\cdot}\text{- + -HCOO}^{\cdot}\text{- } \to \text{-CHOOH- + O}_2$$
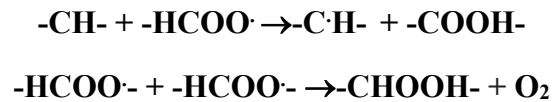
In the termination step, a hydrogen atom is donated by antioxidants to the lipid peroxyl radicals which induces the generation of nonradical products.

$$\text{-H}_2\text{COO}^{\cdot} + \alpha\text{-tocopherol} \to \text{-H}_2\text{COOH+ } \alpha\text{-tocopherol}^{\cdot}$$
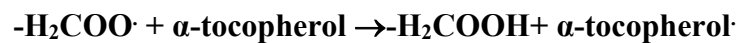
As mentioned above, the main products of lipid peroxidation are the lipid hydroperoxides (figure 1.5). However, a plethora of aldehydes are produced during this complex process such as malondialdehyde (MDA), propanal, hexanal as well as 4-hydroxynonenal (4-HNE). Of these aldehydes, MDA is deemed to be the most mutagenic while on the other hand, 4-HNE is considered to be extremely toxic. The aldehydes generated form Schiff bases with lysines of Apo B-100, cause an increase in net negative charge and (relative electrophoretic mobility) REM status (Morel, DiCorleto & Chisolm, 1984). The formation of adducts between aldehydes and Apo B-100 causes modification of the domain normally recognised by the classic LDL receptor, consequently enabling recognition by scavenger receptors and increasing LDL uptake and encouraging the development of foam cells (Esterbauer et al., 1990).

As noted previously, one of the major antioxidants found in the LDL particle, α-tocopherol inhibits oxidation by scavenging the lipid peroxyl radicals (Esterbauer et al., 1987).

In earlier studies, the addition of α-tocopherol to plasma before the isolation of LDL increased the level of α-tocopherol and a delay in the propagation step of lipid peroxidation was observed (Jessup et al., 1990, Esterbauer et al., 1991). However, large quantities of α-tocopherol and oxidised lipids are found in the atherosclerotic plaque and protection against oxidation is only evident at concentrations above the physiological levels, suggesting that α-tocopherol is not acting as an antioxidant physiologically (Suarna et al., 1995; Priemé et al., 1997). Nevertheless, superoxide radicals and nitric oxide exhibit antioxidant properties by reacting with lipid peroxyl radicals (Rubbo et al., 2000; Kowald, Lehrach & Klipp, 2006). The role of the redox-active transition metals, copper, and iron as key players in LDL oxidation in atherosclerosis is strongly emphasized in the literature. Transition metals have been observed in atherosclerotic plaques previously (Lamb et al., 1995, Stadler et al.,2008). Furthermore, copper appears in the blood in the form of ceruloplasmin while the physiological forms of iron are termed haemin and ferritin. Although copper has the competency to oxidise LDL in vitro, only trace amounts are found in the circulation as ceruloplasmin (Ehrenwald, Chisolm and Fox, 1994). Notably, ceruloplasmin has both prooxidant and antioxidant properties (Patel et al., 2002). On the other hand, iron is carried in circulation as haemoglobin in high millimolar concentrations in the form of haem, myoglobin, several enzymes as well as the glycoprotein, transferrin. Iron that is not in this form is stored as ferritin and haemosiderin.

Although access to redox-active transition metals is meticulously controlled, it is important to note that when Fenton reactions are catalysed by transition metal ions at trace levels, OH· radicals are produced.

$$M^{(n)} + + O_2^- \rightarrow M^{(n-1)+} + O_2$$

$$M^{(n-1)} + + H_2O_2 \rightarrow M^{(n)+} + HO^{\cdot} + HO-$$
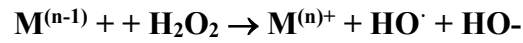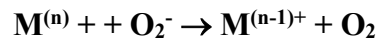
Thus, negligible amounts of intracellular and circulating transition metal ions to catalyse the Fenton reaction in vivo (Repetto et al., 2010). Likewise, copper also has oxidative properties with respect to the Fenton reaction.

$$-H2COOH + Cu^{2+} \rightarrow -H_2COO* + Cu^+ + H^+$$

$$H2COOH + Cu^+ \rightarrow -H_2CO* + Cu^{2+} + OH^-$$
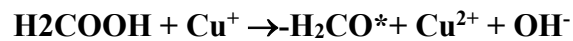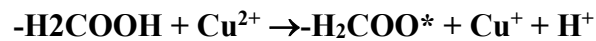
Once lipid hydroperoxides are formed, they can readily react with Cu^{2+}, breaking down the O-O bond of the organic peroxide and generating alkoxyl radicals and therefore inducing the propagation of the chain reaction.
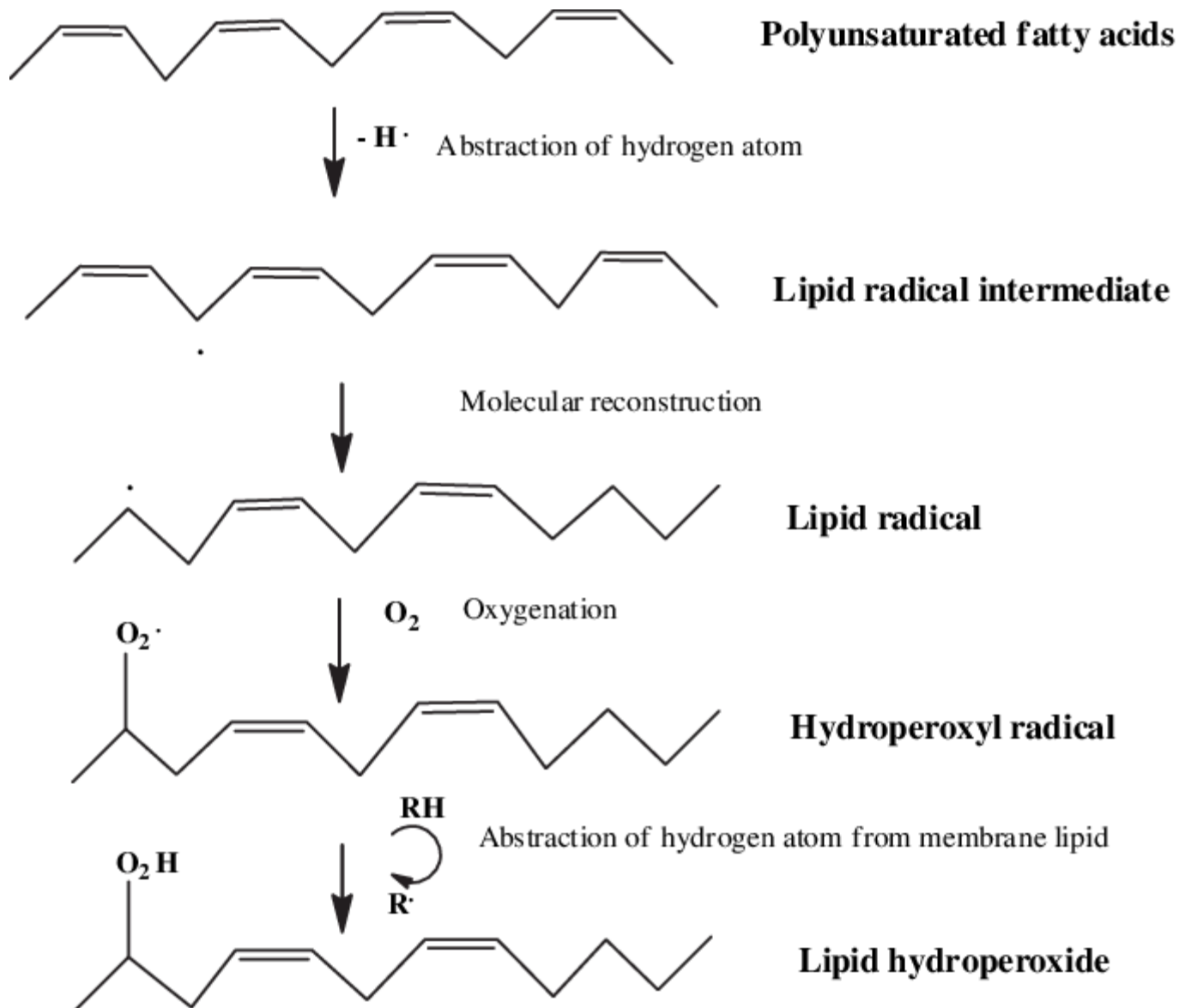
Figure 1.5. Lipid peroxidation. Lipid peroxidation involves three important steps: initiation, propagation and termination. Image Adapted from (Jairam, Uchida and Narayanaswami, 2019).

1.5 Formation of Platelets

Within the bone marrow, the haematopoietic stem cells (HSCs) will undergo differentiation to produce the megakaryocyte-erythroid progenitors, which in the presence of thrombopoietin, will terminally differentiate and mature into megakaryocytes (Liu et al., 2011). Megakaryocyte maturation is a very complex process involving, proliferation and polyploidisation. Mature megakaryocytes are polyploid cells that no longer have the capacity to develop or proliferate but are distinctly capable of shedding cytoplasmic fragments, generating 2000-3000 platelets from a 32N megakaryocyte (Winkelmann, Pfitzer and Schneider, 1987; Italiano et al., 1999).

1.5.1 Platelet shedding

During the maturation process the megakaryocyte is thought to migrate from the osteoblastic niche to the vascular niche (Yin and Linheng, 2006). Within the vascular niche the megakaryocyte will encounter matrix proteins such as fibrinogen, which will initiate platelet biogenesis (Patel, Hartwig and Italiano, Jr, 2005). Platelet biogenesis was first identified in 1906 by Wright but more recently has been shown *in vitro* and *in vivo* to involve the generation of multiple cytoplasmic extensions known as proplatelets, which stem from the plasma membrane of the megakaryocyte (Italiano, Stewart and Roberts, 1999; Junt et al., 2007). Initially thick, these cytoplasmic extensions become elongated, thin and form a beaded appearance, leading to the development of intricate branching structures (Italiano, Stewart and Roberts, 1999). These proplatelet extensions protrude through the vascular endothelium and into the sinusoid lumen where they are liberated into the bloodstream as nascent platelets (Avecilla et al., 2004; Junt et al., 2007; Balduini et al., 2012). The distribution of organelles

and platelet-specific granules into the nascent platelets is a crucial part in the process of platelet release from proplatelets tips (Richardson et al., 2005).

The release of platelets from megakaryocytes was believed to be a bone marrow event. However, megakaryocytes have been identified within the lungs (Aschoff, 1893 , Howell and Donahue, 1937) and recently it has been shown that lung megakaryocytes produce up to 50% of the platelets within mice, potentially producing platelets which have a more immune function than those produced within the bone marrow (Lefrançais et al., 2017). Thus, there is controversy surrounding where platelet release occurs *in vivo*.

1.5.2 Platelet Structure

Platelets are small anucleate cells with an average diameter of 2-3 µm. Healthy individuals have a platelet count of 150 to 450 x 10^3 per microlitre of blood. Platelets circulate in a discoid shape in their inactive state. The structure of the platelet can be divided into the peripheral, sol-gel and organelle zones as well as the membrane systems (figure 1.6).

1.5.3 Peripheral zone

The glycocalyx is the dynamic structure that covers the exterior of the platelet. It consists of glycoproteins such as GPIb-IX-V and $\alpha_{IIb}\beta_3$ responsible for targeting adhesive receptors for platelet activation. Beneath the glycocalyx is an incompressible lipid bilayer that is not able to stretch. The open canalicular system (OCS) is connected to the glycocalyx and is responsible for the exchange of molecules in the extracellular environment and serves as conduits for granule release during platelet secretion (Flaumenhaft, 2003; van Nispen tot Pannerden et al., 2010). The OCS also provides an additional membrane required for spreading. The lipid bilayer acts as a surface for coagulation factors Va, VIIa, and Xa.

1.5.5 Sol-gel zone

The matrix of the cytoplasm known as the sol-gel zone consists of several fibre systems that differ in polymerisation states (Heijnen and Korporaal, 2017). The most prominent of the systems are the tightly circumferential coiled microtubules which maintain the platelet resting shape and thus, supports the contractility of the cytoskeleton membrane. Actin microfilaments are also another fibre system found in the sol-gel zone (Heijnen and Korporaal, 2017). This zone is essential for providing contractility in platelets and anchors the plasma membrane glycoproteins and proteoglycans. Although a plethora of constituents are found in the zone, the microfilaments are the major structural components involved in pseudopod formation and shape change. Upon platelet activation, the cytoplasmic actin microfilament cytoskeleton constricts the microtubules, enabling the movement of α-granules and dense bodies to the centre of the platelet and therefore resulting in granule secretion via the OCS (Krumwiede and White, 2007).

1.5.6 Organelle zone

The organelle zone is not a distinct zone but rather a storage zone for granules such as the α granules and dense granules, dense bodies, peroxisomes, lysosomes, glycosomes and mitochondria. (Behnke, 1967). In comparison to the dense granules, the α granules are the most abundant in platelets. There are 50-80 α granules per platelet that measure 200-500 nm in diameter. Platelet α granules also contain a plethora of mediators that play a role in haemostasis, inflammation, wound repair as well as angiogenesis. They contain haemostatic factors such as vWF, fibronectin, vitronectin, thrombospondin, fibrinogen and factor V. Platelet factor 4 (PF4), CXCL7 and IL-8 are the most abundant chemokines present in α

granules and have a key function in inflammatory processes (Yadav and Storrie, 2016). In addition, growth factors such as platelet-derived growth factor (PDGF), transforming growth factor β (TGF-β) alongside angiogenic factors like vascular endothelial growth factor (VEGF) and membrane- associated receptors such as $\alpha_{IIb}\beta_3$ and P-selectin are also present in the α granules. On the other hand, dense granules are less abundant with 3 to 8 granules per platelet and have fewer molecules at high millimolar concentrations such as serotonin, ADP, ATP, Ca^{2+}, pyrophosphate and polyphosphates including Mg^{2+} and K^{+}(Heijnen and Korporaal, 2017). Contents of the dense granules play a role in primary haemostasis by being involved in the positive feedback mechanism, activating the P2Y12 receptor via ADP release and thus causing the amplification of platelet activation.
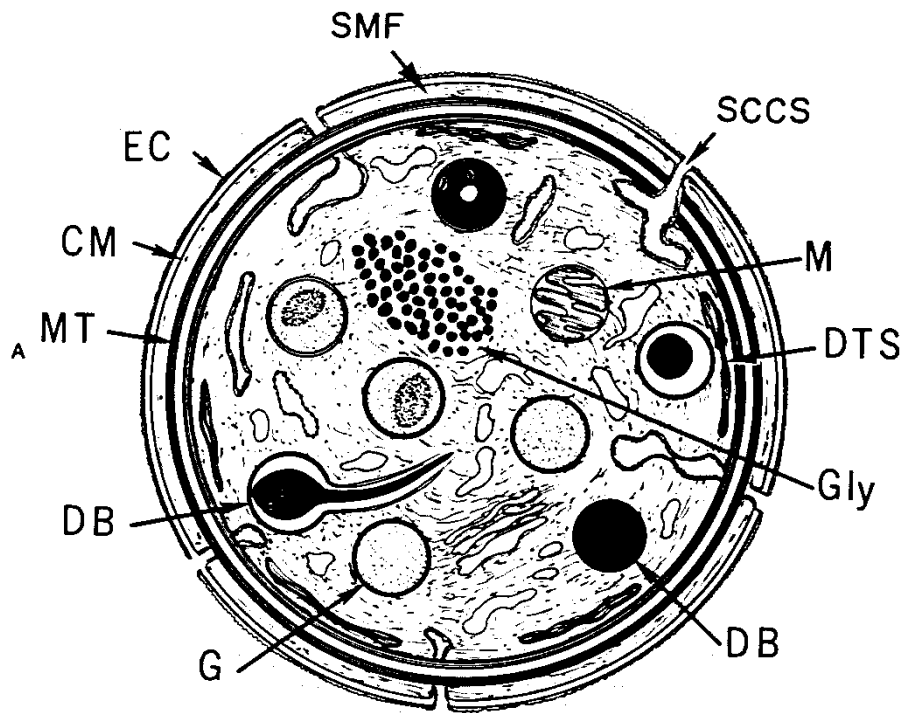
Figure 1.6. A schematic representation of the ultrastructure of blood platelets as shown via electron microscopy. The peripheral zone consists of the exterior coat (EC), trilaminar unit membrane (CM), the submembrane area (SMF) and open canalicular system (SCCS) (White and Gerrard, 1976). The sol-gel zone is composed of submembrane filaments (SMF), microfilaments, circumferential band of microtubules (MT) as well as glycogen (Gly), mitochondria (M), alpha granules (G), dense granules (DB) and the dense tubular system (DTS) (White and Gerrard, 1976). Image adapted from White and Gerrard, 1976.

1.6 Platelet adhesion and activation

Platelet adhesion does not occur in normal conditions where the vasculature is intact as a result of a repertoire of substances such as prostacyclin (PGI_2) and nitric oxide (NO) released by the endothelium that inhibit platelet activation (Nagy and Smolenski, 2018). However, upon endothelial injury, circulating platelets are exposed to pro-thrombogenic components of the extracellular membrane (ECM) such as collagen, vWF and other ECM proteins. Under high shear, collagen and vWF activate platelets leading to shape change and granule secretion, amplifying the platelet activation process (Ruggeri and Mendolicchio, 2007). The platelet activation signalling events converge at the common pathway whereby integrin adhesion receptors are upregulated thus activating $\alpha_{IIb}\beta_3$, promoting the formation of platelet aggregates and subsequently generating a thrombus. This process is meticulously regulated and is comprised of a series of distinct steps such as, tethering, rolling, integrin activation, secretion, aggregation and clot retraction (figure 1.7).

1.6.1 Platelet aggregation

Following vascular injury, thrombogenic proteins of the ECM such as collagen and vWF become exposed which leads to the formation of a thrombus. It is believed that there are two independent pathways to platelet activation: one pathway is the principal concept whereby exposure of the subendothelial collagen propagates the activation of platelets whereas the other pathway suggests that thrombin produced by tissue factor (present in the vessel wall and in circulation) initiates platelet activation (Yun et al., 2016). Both pathways are crucial for platelet activation and thrombus formation however, the dominating pathway is dependent on the injury. As mentioned previously, the binding of collagen to platelet GPVI and GPIb-V-IX with

collagen bound vWF leads to platelet adhesion. The shear rate at the vessel wall is a major determinant for the initial tethering of platelets (Savage, Saldívar and Ruggeri, 1996).

At high shear rates 1000-10000 s^{-1} i.e. arterial blood flow, reversible aggregation is mediated by vWF which binds to immobilized collage via GPIb-IX-V. This results in the formation of thin membrane protrusions referred to as tethers. The formation of platelet tethers is independent of soluble agonists such as ADP, serotonin, TXA_2 and thrombin. Additionally, tethers are formed by the binding of vWF to its receptor GPIbα at the A1 region before firm irreversible platelet adhesion and stable aggregation via $α_{IIb}β_3$ (Savage, Saldívar and Ruggeri, 1996; Parise, 1999; Kasirer-Friede et al., 2004). vWF-GPα is essential for the formation of tethers as inhibiting the A1 domain of vWF results in reduced tether formation (Dopheide, Maxwell and Jackson, 2002). The formation of tethers is essential for causing the platelets in circulation to slow down for sustained interactions to occur between platelets, enabling firm and stable platelet aggregation.

Under low shear rates (<1000 s^{-1}) in large veins and venules, GPVI binds to collagen and thus activates $α_{IIb}β_3$ integrin mediated platelet activation. It is thought that $α_{IIb}β_3$ is more predominant in mediating platelet aggregation at low shear rates as inhibition of vWF does not inhibit platelet aggregation, suggesting that platelet aggregation at low shear rates is independent of vWF-GPIbα (Savage, Almus-Jacobs and Ruggeri, 1998). Nevertheless, other *in vivo* studies have shown that vWF also plays a role in platelet aggregation under these conditions (Brill et al., 2011).

1.6.2 Platelet secretion

Cytoskeletal reorganization results in the secretion of platelet granules. In the resting platelet the granules are distributed in a random manner however, once activated, the α-granules come together to the centre of the platelet where fusion with the OCS takes place (Stenberg et al., 1984). Due to increase in intracellular calcium and PKC activation, fusion between the granules and the plasma membrane occurs, releasing the granule contents into the OCS which subsequently results in their release into the extracellular environment by exocytosis (Escolar and White, 1991). The fusion between the granules and plasma membrane is regulated by vesicle-soluble N-ethylmaleimide–sensitive fusion protein attachment receptor (v-SNARE) proteins. It is believed that v-SNAREs associate with target membranes known as t-SNAREs (Sutton et al., 1998).

As aforementioned, there are three different types of granules found in platelets: α-granules, dense granules and lysosomes. A plethora of adhesion proteins such as fibrinogen, vWF, vitronectin, thrombospondin, cytokines including coagulation, fibrinolytic and growth factors are found in the α-granules. Additionally, dense granules contain nucleotides such as ADP, ATP, GTP, serotonin, pyrophosphates and divalent cations whereby lysosomes contain an array of proteolytic enzymes (Ren, Ye and Whiteheart, 2008). ADP is bound to two GPCRs, $P2Y_1$ and $P2Y_{12}$. The $P2Y_1$ receptor is coupled Gq and the $P2Y_{12}$ receptor is coupled to Gi. Gq signalling is involved in GPCR mediated granule secretion in platelets and it also plays an important role in ADP mediated platelet shape change because of activating PLCβ thus, increasing intracellular calcium. $P2Y_{12}$ coupled Gi signalling amplifies platelet activation while inhibiting adenylyl cyclase activity and cAMP synthesis. A defect in $P2Y_{12}$ results in impaired platelet aggregation but a normal shape change is observed (Foster et al., 2001; André et al.,

2002). On the other hand, platelet aggregation is markedly reduced, and shape change is not observed in mice lacking the $P2Y_1$ receptor (Léon et al., 1999).

TXA_2 is also an important secondary agonist that plays a role in amplifying platelet activity. Increase levels of intracellular calcium induces the activation of phospholipase A_2 (PLA_2), releasing arachidonic acid which is consequently converted into prostaglandin cyclic endoperoxides PGG2 and PGH2 by cyclo-oxygenase-1 (COX-1) and thromboxane synthase to produce TXA_2. TXA_2 binds to its TP receptor in an autocrine and paracrine fashion. The TP receptor is coupled to Gq and G12/13 thus, aiding in platelet shape change, platelet aggregation and amplification of platelet activation. Mice lacking TP display prolonged bleeding times and a defect in platelet aggregation (Thomas et al., 1998).
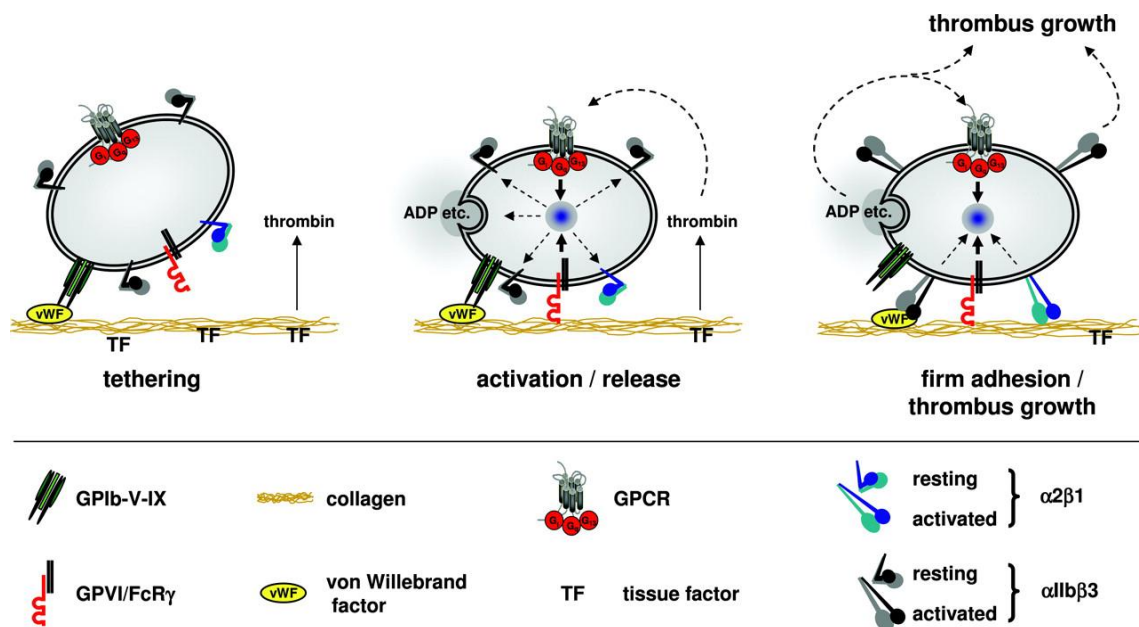
Figure 1.7. Platelet adhesion to subendothelial matrix at the sites of vascular injury.

Platelet tethering to the ECM is initiated primarily by the interaction of by GPIb –vWF. This is then followed by the interaction of GPVI–collagen interactions which as a result, switches $\alpha_2\beta_1$ and $\alpha_{IIb}\beta_3$ to a high affinity state, releasing ADP, ATP and TXA_2 to amplify platelet activation. Tissue factor (TF) induces thrombin formation, activating platelets. Image adapted from (Sachs & Nieswandt, 2007).

1.6.3 Thrombus formation

The stable adhesion and aggregation mediated by $\alpha_{IIb}\beta_3$ results in the initiation of the haemostatic plug. Upon endothelial injury, phosphatidylserine is produced, leading to calcium-mediated binding between factor Xa to the platelet surface with factor Va and resulting in the formation of prothrombinase complex. The conversion of prothrombin to thrombin takes place in this complex which promotes the coagulation cascade by cleaving soluble fibrinogen to fibrin. Recent studies give further insight into the architecture of the platelet-rich thrombi. Studies *in vivo* show that platelet activation does not occur in an even fashion throughout the haemostatic plug but rather display a defined structure and very distinct architecture. Early observations in vivo show that the distribution of activated platelets varies in the platelet rich thrombi. It is believed that platelet rich thrombi are composed of two zones: the growing thrombi also known as the core which consists of tightly packed activated platelets and a high concentration of thrombin (Stalker et al., 2013). The second zone has an outer shell of less active platelets that are arranged in a loose manner and is predominantly mediated by ADP. Inhibition of the $P2Y_{12}$ blocks the formation of the outer shell. It was reported that transport of soluble agonists such as thrombin was slower in the core than the outer shell of the growing thrombus (Welsh et al., 2014). These observations identify that platelet activation and granule release occurs in the core of the thrombi and not at the outer shell which highlights that platelets in the thrombi release their contents into the core of the growing thrombus and not into the circulation (Stalker et al., 2013).

There is now a strong emphasis in the field in understanding the architecture of the thrombus as targeting the specific pathways that mediate thrombus shell formation without affecting haemostasis in general are crucial (figure 1.8). Exploring the architecture of clots can also give

insight into the different regions of the thrombus and may play a role in potential therapeutic

strategies in terms of which areas of the thrombus to target.
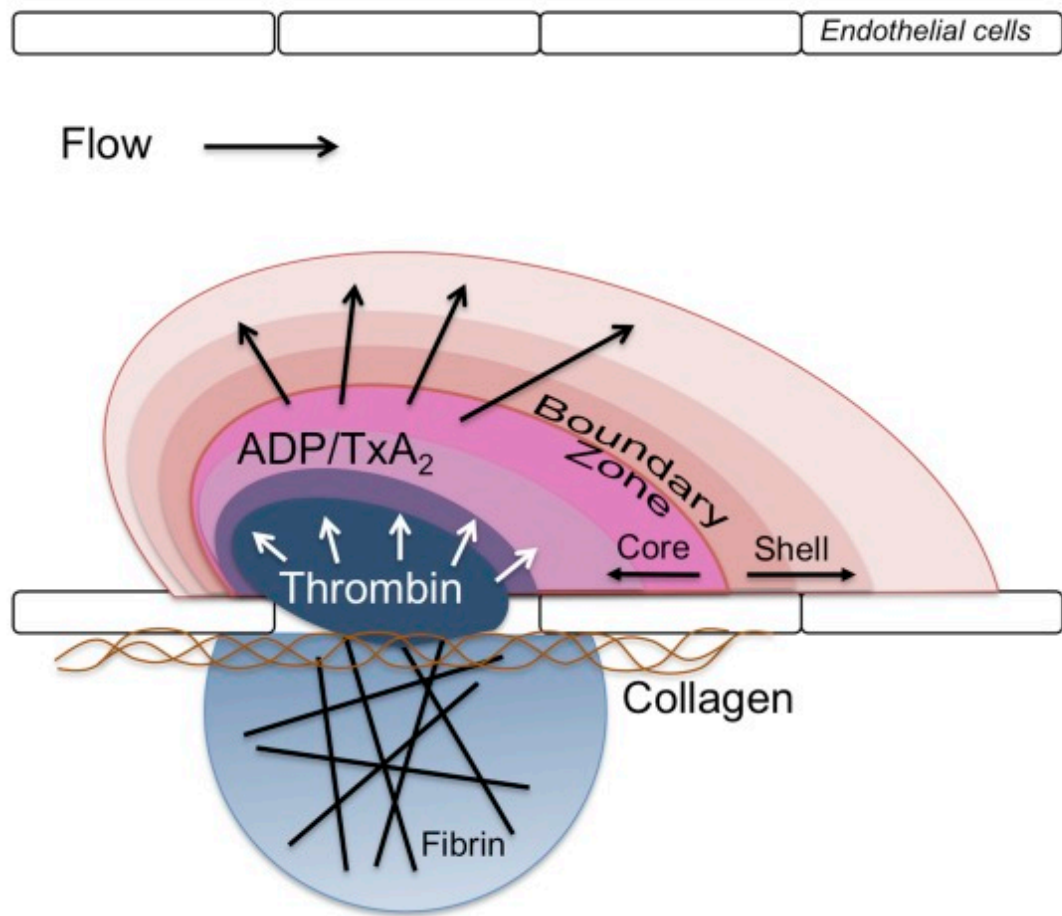
Figure 1.8. The architecture of a thrombus.

The thrombus consists of a fibrin mesh, an inner core and an outer shell. The fibrin mesh is in proximity with the endothelium and penetrates the extravascular space. The inner core is composed of activated tightly packed platelets whereas the outer shell is formed of loosely packed platelets recruited by soluble agonists such as ADP and TXA_2. Image adapted from (Stalker et al., 2013).

1.7 Platelet receptors and activation

1.7.1 Interaction of von Willebrand factor with platelet

Under high shear rate flow (>1000 s^{-1}), initial platelet adhesion occurs when interaction between circulating vWF and collagen. Interaction with vWF occurs via its A1 and A3 domain upon vessel injury (Lankhof et al., 1996; Hoylaerts et al., 1997). Subsequently, immobilised VWF binds to the GPIbα platelet specific glycoprotein GPIb-V-IX via interaction with its A1 domain, allowing platelets to respond to the components of the extracellular matrix such as collagen.

The high affinity interaction is induced as a result of high shear stress of blood flow on immobilised (but not soluble) vWF in the subendothelial matrix or stimulated platelets. vWF and GPIb-IX play a crucial role in haemostasis as mice lacking vWF and GPIb-IX have severe bleeding whilst patients lacking these receptors suffer from the bleeding disorders von Willebrand disease and Bernard-Soulier syndrome respectively. (Denis et al., 1998; Ware, Russell & Ruggeri, 2000). GPIb-IX-vWF interactions induce the rolling process of the platelet and thus, platelet activation which eventually results in the conformational transition of $\alpha_2\beta_1$, enabling adhesion to collagen and therefore causing platelet interaction with the low affinity GPVI receptor at low shear rates (<1000 s^{-1}).

1.7.2 Interaction of collagen with platelets

Collagen is the most abundant protein in the body and is comprised of more than 28 different subtypes. It is thought that collagen I (70-75%), III (20-25%) and V (1-2%) are the major subtypes of collagen found in the arterial wall (Barnes, Knight and Farndale, 1999). Collagen

is one of the first subendothelial matrix components that are exposed during vessel injury. Out of the four abundant forms of collagen, type I and type III are the most thrombogenic found in the subendothelial layers. Collagen induced platelet activation is triggered by the constitutively active receptor, GPVI and is only exposed in the state of an injury. GPVI is a 62kDa type I transmembrane receptor and is considered to be the most potent platelet signalling receptor (Clemetson et al., 1999). Synthetic ligands such as CRP, which is GPVI specific and the snake venom, convulxin that binds to GPVI as well as GPIb-IX have been described in the literature (Andrews et al., 2001). GPVI binds to GPO (Gly-Pro-Hyp) repeat regions of collagen. GPVI is an example of a tyrosine kinase linked receptor.

The importance of GPVI signalling is emphasized in in vitro studies to help explore downstream signalling pathways that are $\alpha_2\beta_1$ independent. GPVI is structurally composed of two immunoglobulin-like extracellular domains (D1 & D2) associated to the transmembrane region and cytoplasmic tail and are held by a mucin-like stalk rich in O-glycosylation sites. GPVI exists as a monomer in resting platelets and is associated with the Fc Receptor-γ chain (FcRγ) chain via the transmembrane domain (Nieswandt & Watson, 2003). The clustering that forms as a result of collagen binding to GPVI results in the tyrosine phosphorylation of ITAM thus, recruiting small family kinases Lyn and Fyn which are attached to the cytoplasmic domain of GPVI by the Src homology 3 domain (SH3) (Ezumi et al., 1998; Schmaier et al., 2009). Phosphorylation enables the ITAM motif to recognize the Src homology 2 domain of Syk. Once Syk associates with FcRγ, Syk becomes activated and phosphorylates downstream targets such as transmembrane adapter linker for activated T cells (LAT) and the Src homology 2 domain-containing leukocyte phosphoprotein of 76 kDa (SLP-76). This generates a signalosome complex containing LAT, SLP-76, Btk/Tec family, Gads, the Vav family of guanine nucleotide exchange factors (GEF) and phospholipase C γ2 (PLCγ2) (Nieswandt &

Watson, 2003). PLCγ2 also interacts with phospho inositide 3-kinase (PI3K), activating PLCγ2 and subsequently hydrolysing phosphatidylinositol (3,4)-bisphosphate (PIP2) (Pasquet et al., 1999).

Activation of PLCγ2 also generates inositol (1,4,5)-trisphosphate (IP3). IP3 releases calcium from intracellular stores and consequently promotes the release of extracellular calcium that is crucial for platelet activation. Diacylglycerol (DAG) is also another critical messenger released and it plays an important role in activating Protein Kinase C (PKC). Although the roles of the distinct isoforms remain to be elucidated, PKC is thought to have a role in platelet secretion and activation.

In addition, to GPVI, platelets have an additional collagen receptor, the integrin $\alpha_2\beta_1$. The role of both receptors in platelet function is controversial however, it is generally believed that GPVI is essential for inducing activation and aggregation of platelets while $\alpha_2\beta_1$ promotes stable adhesion of platelets (Varga-Szabo et al., 2008).

Finally, the activation of $\alpha_{IIb}\beta_3$ triggers inside out signalling enabling stable platelet adhesion to the ECM by binding fibrinogen or vWF and inducing platelet aggregation. Although GPVI cannot propagate adhesion independently, it has been reported that platelets from GPVI-knockout mice fail to show stable adhesion, highlighting the significance of this receptor (Nieswandt et al., 2001).

1.7.3 Platelet activation via fibrinogen

Fibrinogen binding to the platelet integrin $\alpha_{IIb}\beta_3$ activates platelet spreading on fibrinogen coated surfaces. Clinical studies have consistently shown elevated levels of fibrinogen in patients with cardiovascular disease and thrombosis (Wilhelmsen et al., 1984). Studies have also shown that platelet spreading is increased at lower concentrations of fibrinogen compared to higher fibrinogen concentrations (Jiroušková, Jaiswal and Coller, 2007; Qiu et al., 2014).

In addition, the platelet integrin $\alpha_{IIb}\beta_3$ is kept in an inactive, low affinity conformation state in resting platelets. Once activated, the integrin undergoes a conformational change and results in high affinity ligand binding to fibrinogen and vWF. The conformational change in the extracellular domains of integrins from a low-high affinity are mediated by the binding of talin and kindlins to the cytoplasmic domain of β_3, triggering inside-out signalling (Tadokoro et al., 2003). It is believed that the active conformation of $\alpha_{IIb}\beta_3$ is established when talin binds to β_3 (Calderwood et al., 1999). Thus, the membrane-proximal regions of both α_{IIb} and β_3 are disrupted which enables the conformation of $\alpha_{IIb}\beta_3$ from its low affinity bent state to its high affinity extended form, propagating extracellular ligand binding and initiating platelet adhesion, aggregation and thrombus formation (Vinogradova et al., 2002; Li et al., 2003). It is important to note that kindlins also play a role in integrin activation. Notably, mice deficient in kindlin-3 fail to activate the integrin even though talin expression is unaffected suggesting that kindlin-3 plays a pivotal role in inducing a conformational change in $\alpha_{IIb}\beta_3$ (Moser et al., 2008).

Furthermore, the increase in intracellular calcium observed following platelet activation results in the activation of guanine nucleotide exchange factor I (CalDAG-GEF1) and its downstream target Rap1 (Crittenden et al., 2004). CalDAG-GEF1 activates Rap1 a member of the Ras

family of small GTPases and converts Rap1 from its inactive GDP form to its active GTP state. This consequently leads to the interaction with the Rap1 GTP interaction adaptor molecule (RIAM), stimulating talin interaction and $\alpha_{IIb}\beta_3$ activation (Lafuente et al., 2004). The role of Rap1b and CalDAGGEF1 in integrin activation remain to be elucidated as platelets deficient in both proteins do not completely inhibit $\alpha_{IIb}\beta_3$ (Lafuente et al., 2004). Moreover, a deficient or non-functional $\alpha_{IIb}\beta_3$ due to mutations of the (integrin subunit alpha 2b) ITGA2B or (integrin alpha IIb/beta3) ITGB3 genes coding for α_{IIb} β_3 respectively results in a bleeding disorder known as Glanzmann thrombasthenia, highlighting the importance of a functional integrin for platelet activation (Nurden et al., 2011).

An array of intracellular signalling events known as outside-in signalling occur once the integrin $\alpha_{IIb}\beta_3$ is activated which leads to stable adhesion, platelet spreading, secretion and clot retraction (Bernardi et al., 2006). Interaction between $G\alpha 13$ and β_3 takes place after integrin binding, activating SFKs and thus the GPVI and ITAM signalling pathway (Gong et al., 2010; Aslan and McCarty, 2013).

1.7.4 Platelet activation mediated by soluble agonists

A variety of soluble platelet agonists such as ADP, thrombin and TXA$_2$ play an important role in platelet activation and thrombus formation. These platelet agonists cause activation of platelets via G-protein coupled receptors (GPCRs). GPCRs are expressed on platelets and induce signals via heterotrimeric G proteins. Heterotrimeric G-proteins are formed of α, β and a γ subunits. Once receptors are bound to their ligands, the α subunit bound to GDP converts to its active form, GTP alongside the dissociation of both the β and γ subunits. Heterotrimeric G proteins expressed on platelets consist of: Gq, G12/13, Gi/Gz and Gs which are crucial for

GPCR activity as they are coupled to specific receptors and agonists required for platelet regulation. Gq is coupled to thrombin receptors PAR1 and PAR4, TXA_2 receptor (TP), ADP receptor ($P2Y_1$) as well as the serotonin receptor (5HT2A). Signalling through this receptor activates $PLC\beta2$ via the ITAM pathway, hydrolysing PIP2 and generating IP3 and DAG. This causes an efflux calcium as a result, increasing intracellular calcium levels.

G12/13 proteins are coupled to PAR1 and PAR4 including (thromboxane receptor) TP and are responsible for activating the Rho/Rho kinase pathway, inhibiting MLC phosphatase and inducing the phosphorylation of MLC. p115 RhoGEF, a subgroup of Rho-specific guanine nucleotide exchange factors become activated following the activation of $G\alpha13$ (Hart et al., 1998; Fukuhara, Chikumi and Gutkind, 2001). This triggers a shape change in platelets and release of granules. $G\alpha13$ is thought to play an important role in integrin outside-in signalling. In addition, Gi is coupled to $P2Y_{12}$ and activates platelets via TXA_2. It has a primary role in activating PI3K, stimulating downstream effectors such as Rap1b which subsequently causes the activation of the integrin.

1.8 Platelet actin cytoskeleton

Upon exposure to biochemical or physiological stimuli, platelets undergo remarkable changes which orchestrate the reorganisation of the platelet cytoskeleton. Following platelet activation, platelets undergo a dramatic shape change, which is regulated by the actin cytoskeleton (Fox, 2001). If the platelet is in suspension it changes from a discoid shape to spherical form (figure 1.9). Alternatively, if the platelet is adhered to a surface it will initially produce finger like projections termed filopodia, followed by lamellipodia filling the gaps and spaces between the adjacent filopodia, and actin nodules, an actin-rich structure implicated in successful platelet adhesion under high shear (Calaminus et al., 2008). Finally, the actin cytoskeleton will rearrange into stress fibres, which help to resist shear force. Each of these actin structures has been shown to play a crucial role in thrombus formation or stability (Calaminus et al, 2008).

Actin is the most abundant protein present in platelets, constituting of approximately 15-20% of the total protein. It exists in either the monomeric, globular form (G-actin) or the polymeric, filamentous form (F-actin). In platelets, G-actin and F-actin are both in a dynamic equilibrium with each other. In the resting platelets, 40-50% of the total actin is present as filaments which increases to approximately 70% upon stimulation with thrombin. In each platelet there is an average of 2000 filaments with a filament length of 1.1µm (Hartwig, 1992).
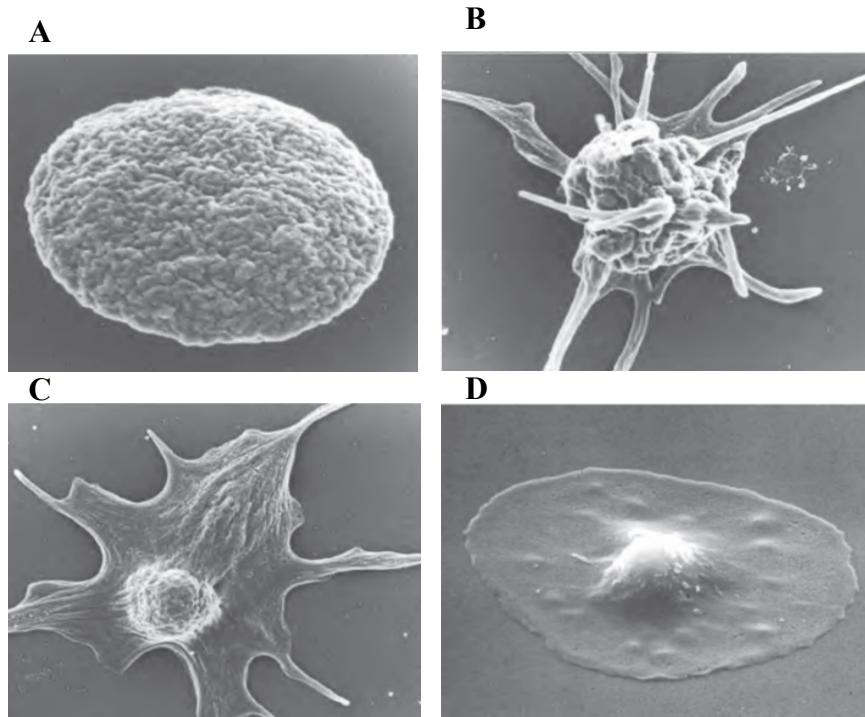
Figure 1.9. Scanning electron microscopic images showing platelet shape change.

Discoid platelet in its resting state imaged in low-voltage, high resolution scanning electron microscope (LVHR-SEM). B) Early stage of dendritic platelet displaying smooth pseudopods (filopodia formation) that protrude from the platelet. C) Early platelet spreading and lamellipodia formation. As the cytoplasm extends and fills the gaps between pseudopods, the central body begins to disappear. D) Fully spread platelet (White, 2007).

Actin polymerisation underpins the formation of every actin structure formed (figure 1.10). Actin polymerisation proceeds in a sequential manner that is initiated by a lag period that is characterised by actin nucleation followed by the polymerisation phase (elongation phase) whereby the short actin filaments rapidly elongate as a result of actin monomers joining both ends (Bearer, 1993). Eventually, a steady state is established as the rate of addition and loss of actin is in equilibrium. Actin filaments have a fast-growing 'barbed' end and a slow growing 'pointed' end and are thus polarised inherently. The polymerisation of actin filaments is dependent on the addition of ATP or ADP bound actin monomers. Attachment of ATP to G-actin monomer increases the actin polymerisation rate whereas the binding of ADP reduces this. Actin monomer addition is observed at the barbed end in the presence of ATP while on the other hand, the depolymerization of the filament occurs at the pointed end (Bearer, 1993). Critical concentration of actin polymerization is determined by the composition of ions of the solution. Divalent cations like Mg^{2+} and Ca^{2+} regulate the polymerisation of actin as well as ATP hydrolysis (Martonosii, Molino and Gergely, 1964).

De novo nucleation is facilitated via the Arp2/3 complex which consists of seven subunits. The Arp2/3 complex is a nucleation factor. Nucleation promoting factor (NPFs) are proteins that activate this complex (i.e. Wiskott Aldrich (WASp) family proteins, SCARE/WAVE family). WASp family proteins are well characterised NPFs that bind to the Arp2/3 complex. The NPF bound to the actin monomer binds to Arp2/3, inducing the polymerisation of new daughter actin filaments from the edge of existing mother filaments in a Y-branch orientation that has a distinctive 70° angle (Mullins, Heuser and Pollard, 1998).

In addition, formin proteins induce the assembly of actin filaments. The formin homology 2 (FH2) domain causes actin nucleation and the formin homology 1 (FH1) domain is responsible for the delivery of profilin–actin complexes to the filament's barbed end (Ireton, 2013).
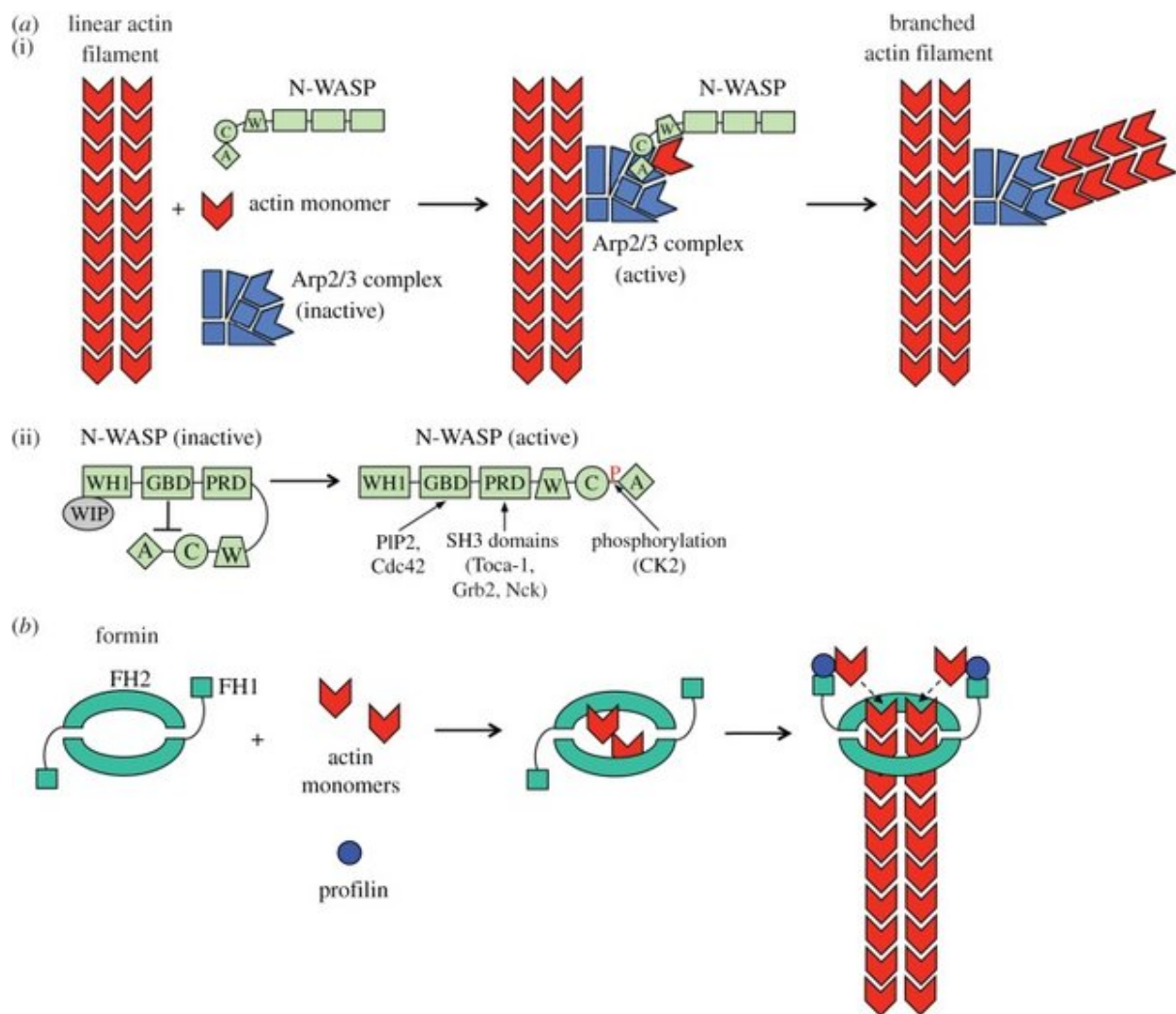
Figure 1.10. Actin polymerisation.

(a) Actin polymerization mediated by Arp2/3. (i) Actin filament assembly by Arp2/3 and N-WASP. N-WASP uses its WCA domain to activate Arp2/3 dependent actin polymerization. (ii) phosphorylation of a serine residue in WCA domain induces N-WASP activation. (b) Formin proteins acts as dimers and activate the assembly of linear actin filaments. The formin homology 2 (FH2) domain is responsible for actin nucleation and the formin homology 1 (FH1) domain delivers profilin–actin complexes to the filament's barbed end. Image adapted from (Ireton, 2013).

1.8.1 Regulation of actin assembly

An array of actin binding proteins that promote or inhibit actin assembly of the filaments play a role in the regulation of cellular mechanisms (figure 1.11). Profilin binds to actin monomers as well as to the barbed end of the actin filament. It also has a higher affinity for ADP-actin filament barbed ends and binds weakly to ATP-actin (Courtemanche and Pollard, 2013). Thus, dissociation of profilin occurs following the attachment of profilin-actin complex to the actin filament, releasing the end of the filament for elongation. Upon platelet activation, profilin competes with thymosin- β4 for actin monomers binding to filaments. This promotes the exchange of ADP-actin monomers with ATP to initiate elongation (Pantaloni and Carlier, 1993). Actin-monomer binding proteins such as thymosin- β4 and DNase I sequester G-actin and result in depolymerisation.

Actin severing and actin capping proteins play a crucial role in the regulation of actin assembly. Severing proteins shorten the length of the actin filament whereas capping proteins inhibit elongation. The two major families of actin filament severing proteins are cofilin and the gelsolin family. Cofilin inhibits ADP-actin monomer exchange as it has a high affinity for ADP-actin monomers. Although cofilin inhibits the nucleotide exchange, profilin on the other hand promotes the exchange of ADP-actin to ATP-actin. Likewise, CapZ induces the depolymerisation of actin filaments converting F-actin to G-actin. Furthermore, gelsolin binds to the barbed end or pointed the actin filament causing the severing of the filament. In addition, tropomodulin caps the end of the actin filament inhibiting nucleotide exchange at the pointed end.

A key family of proteins that play fundamental roles within the actin cytoskeleton are the Rho family of small guanine nucleotide binding proteins (Aslan and McCarty, 2013). They are a member of the Ras superfamily and RhoA, Rac1 and Cdc42 are some of the best characterised Rho GTPases in mammals (Nobes and Hall, 1995). The Rho GTPases act as molecular switches, shifting from an inactive to active state by exchanging GDP for GTP. This cycle is regulated by GEFs which are responsible for switching on signalling as a result of catalysing the exchange of GDP to GTP and GAPs which terminate signalling by inducing the hydrolysis of GTP (Aslan and McCarty, 2013).
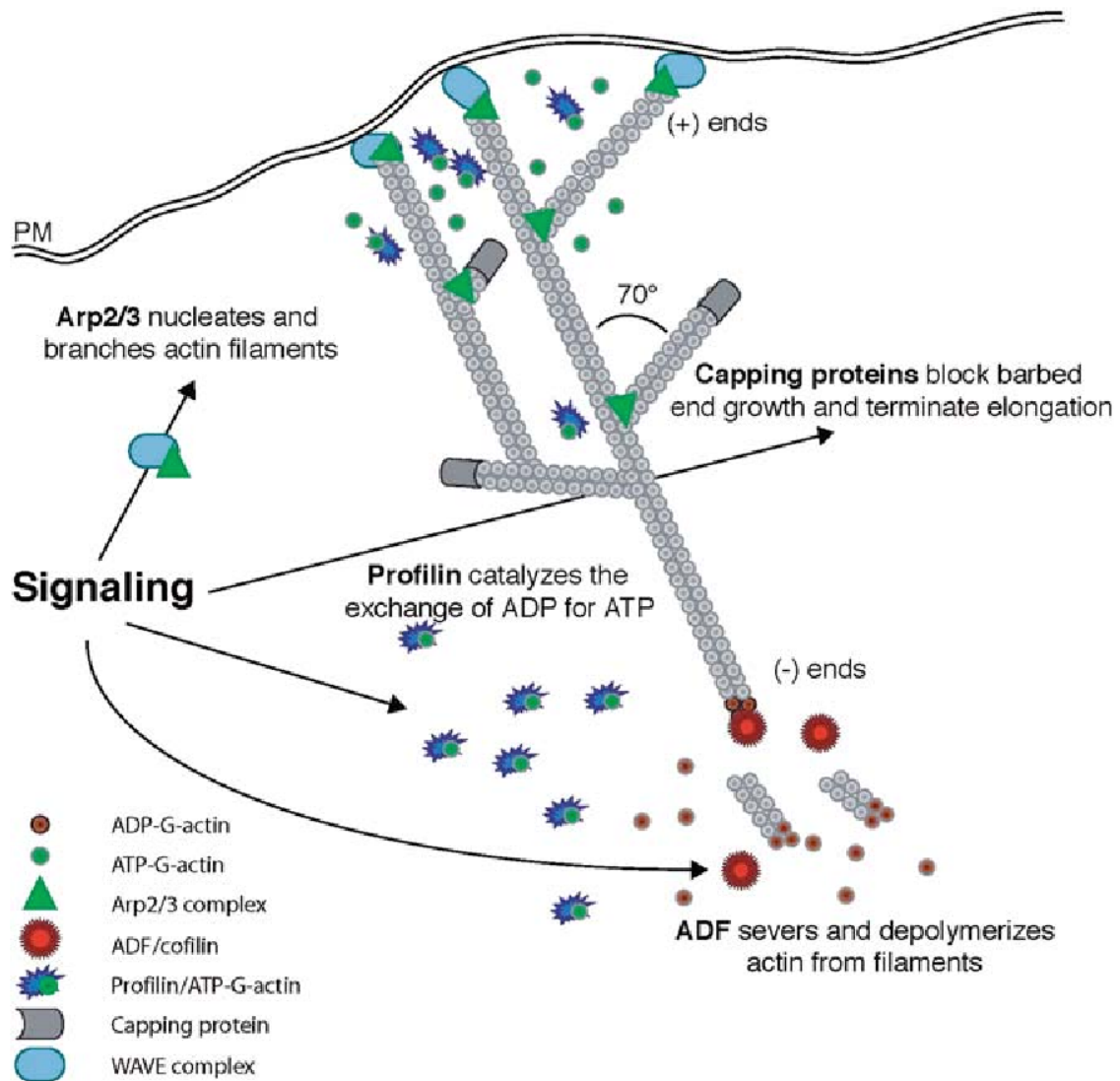
Figure 1.11. Actin polymerisation.

Arp2/3 activation causes nucleation and induces branched actin filaments at the leading edge. Capping proteins regulate the half-life of filaments by inhibiting elongation of filaments. ADF/cofilin triggers the dissociation of ADP-actin from filament pointed ends and causes the severing of existing filaments, inducing new barbed ends. Profilin triggers the exchange of ADP for ATP- actin. Image adapted from Disanza et al., 2005.

1.8.2 Cdc42 and Rif in filopodia formation

Upon platelet activation, GTP bound Cdc42 binds to the CRIB/GBD motif domain of WASP. Autoinhibition of WASP is caused by the binding of the CRIB domain to the VCA domain thus, the C and A domains are unable to activate Arp2/3 complex. However, the competitive binding of PIP2, Cdc42 and other ligands allow interaction with the Arp2/3 complex by exposing the VCA domain and promoting actin recruitment. Cdc42 binds to regulatory proteins like formins (mDia2 and mDia3) responsible for actin nucleation. These multidomain proteins interact with an array of cytoskeletal proteins, associating with the rapidly growing barbed end and inhibiting capping proteins. Nonetheless, the roles of Cdc42 in platelet function are not well established. Translocation of Cdc42 to the platelet cytoskeleton occurs in an integrin-mediated fashion (Dash, Aepfelbacher & Siess, 1995). However, the mechanisms of filopodia formation is unclear and remains controversial. While on one hand, Cdc42 is thought to have an important role in filopodia formation as platelets treated with the GTPase inhibitor Secramine A inhibited collagen induced adhesion and aggregation, results from different Cdc42 knockout strategies were contradictory (Chang et al., 2005; Pula & Poole, 2008; Pleines et al., 2010; Akbar et al., 2011). Akbar et al., 2011 have described reduced platelet function such as, filopodia formation, spreading, secretion as well as low platelet counts in Cdc42 knock-out models, indicating that Cdc42 might be involved in megakaryocytic platelet production as well. However, Pleines and co-workers have shown that Cdc42 has a role in forming filopodia downstream of GPIb but not GPVI and $\alpha_{IIb}\beta_3$ as Cdc42 deletion reduced the ability for platelets to form filopodia on vWF but not on fibrinogen and collagen. In addition, they found that Cdc42 knock out platelets increase granule secretion and produced larger aggregates and increased the size of the thrombus.

Furthermore, it has been reported that filopodia formation and actin dynamics are independent of WASP, suggesting that platelet spreading may be driven by a Rac-WAVE-Arp2/3 dependent pathway (Yarar et al., 1999; Kahiwagi et al., 2005). Other RhoGTPases like Rif are also thought to be involved in the formation of filopodia independent of Cdc42. Studies have shown that Rif directly activates mDIA1 and mDIA2 and induces longer and more flexible filopodia compared to Cdc42 in other cell types (Aspenstrom, Franson & Saras, 2004; Passey, Pellegrin & Mellor, 2004; Pellegrin & Mellor, 2005; Lammers et al., 2005). However, in platelets Rif knockout mice display no phenotype in their platelets and megakaryocytes (Goggs et al., 2013). Likewise, mDIA1 deficiency showed no phenotypic alterations in clot retraction, P-selectin expression or spreading (Thomas et al., 2011). Therefore, the data from both mDIA1 and Rif knockout studies are consistent, highlighting that pathways independent of Rif and mDIA1 mediate filopodia formation.

1.8.3 Rac and lamellipodia

Rac 1 and Rac 2 have been reported to be expressed in platelets. Nevertheless, Rac1 has been shown to be the most principal isoform in platelets as shown in the murine platelets from Rac1$^{-/-}$Rac2$^{-/-}$ mice (McCarty et al., 2005). Rac regulates the formation of lamellipodia by activating the Arp2/3 complex, which is responsible for nucleation and hence, the formation of branched networks. Rac1 and Arp2/3 are linked by the SCAR/WAVE family. Upon platelet stimulation, the WAVE complex is activated by Rac. However, WAVE proteins do not interact with Rac GTPases directly like in the case seen with WASP with Cdc42. Components of the wave regulatory complex (WRC) for instance, Sra-1 and Nap1 expose the VCA (verprolin domain (WASP homology 2), cofilin homology domain and acidic region (activates Arp2/3) region of WAVE, promoting Rac-dependent lamellipodia formation (Steffen et al., 2004). Sra is bound

to the V and C domains of the WAVE protein, blocking WAVE activation. Mutations of Sra1 exposes the V region and promotes the activation of Arp2/3 and therefore increase the affinity between Rac and WRC. Likewise, deletion of the VCA region removes Sra1, inducing actin branching (Chen et al., 2010). Rac GTPases, PIP3 and kinases indirectly activate SCAR/WAVE, initiating actin polymerisation. Deletion of WAVE1 reduced lamellipodia formation on laminin and CRP and not on collagen or fibrinogen suggesting a major role for Scar/WAVE1 downstream of GPVI (Calaminus et al.,2007). Arp2/3 deficiency results in a defect in lamellipodia formation including marked microthrombocytopenia in mice, as a result of premature platelet release and reduced platelet survival in circulation (Paul et al., 2017).

Due to this critical role for Rac1 in lamellipodia formation, McCarty et al have shown that Rac 1 is important for stabilising the thrombus under shear flow on collagen. Interestingly though it has also been reported that Rac has non-cytoskeletal roles in platelet function. McCarty et al implicated Rac in GPVI signalling as Rac deletion inhibited aggregation in response to CRP, suggesting the importance of Rac-mediated platelet activation (McCarty et al., 2005). Furthermore, it has been reported that Rac1 drives PKC activity and PLCγ_2 activity as well as IP$_3$ subsequently, increasing intracellular calcium levels (Piechulek et al., 2005; Pleines et al.,2005; Guidetti et al.,2009). Deletion of Rac1 is also thought to inhibit downstream effects of ITAM signalling that activate PLCγ_2, regulate the early signalling events of integrin outside in signalling (Hall, 2005), mediate GPIb signalling upstream of PI3K/Akt pathway (Lyn dependent) (Delaney et al., 2012) and it is also established that integrin mediated MAPK and MLC activation is Rac1 dependent (Flevaris et al., 2008).

1.8.4 RhoA

RhoA is activated downstream of various heterotrimeric G protein coupled receptor pathways to regulate platelet shape change response (figure 1.11). It is well established that G-proteins of the G_{12} and G_{13} family couple to GPCRs to the activation of RhoA. RhoGEF proteins such as P115RhoGEF interact with $G\alpha_{12}$ and $G\alpha_{13}$, inducing RhoA activity by converting RhoA into the active GTP form. Once active, RhoA-GTP binds to and activates the Rho kinase ROCK, remodelling the actin cytoskeleton. This subsequently leads to the phosphorylation and inhibition of myosin light chain phosphatase, stimulating the phosphorylation of myosin light chain (MLC) and MLC- dependent contraction. Indeed, $G\alpha_{13}$ binds to the cytosolic domain of integrin β_3 inducing $G\alpha_{13}$-GPCR-integrin cross talk. Following this the Src family kinase become activated which mediates the activation of p190RhoGAP and as a result, hydrolyse RhoA-GTP to its GDP form, inhibiting platelet contractility and enable spreading. Calcium-dependent calpain proteases cleave integrin β_3 inhibiting c-Src activity and therefore inducing platelet contraction and clot retraction. Activation of RhoA results in the formation of contractile actomyosin bundles, which is important for platelet adhesion and contraction. RhoA activation regulates stress fibre assembly as a result of inactivating actin polymerisation factors like cofilins and causing platelet contractility via the phosphorylation of MLC.

1.8.5 Cross talk between Rac and RhoA

The ability of RhoA to induce shape change is dependent on the G12/G13 signalling pathway although Rac1 is mediated by Gq, illustrating that Rho and Rac are differentially regulated (Gratacap et al., 2001). Although Rac activation is Gq mediated, it is also thought that Rac releases mediators which can therefore activate Gi-coupled receptors.

During the early stages of outside-in signalling, Rac1 drives actin polymerisation as well as lamellipodia formation while RhoA is inhibited to allow spreading, highlighting their antagonistic relationship (Flevaris et al., 2007). Ultimately, calcium-dependent proteases like calpain promote platelet contraction and clot retraction, facilitating the interaction between RhoA and Rac to phosphorylate MLC. While Rho and Rac are both involved in the first pMLC peak activated by the inside-out signalling during clot retraction, Rac1 is also involved in the second pMLC peak that is mediated by actin polymerisation and Rac1 activation (Egot et al., 2013). Furthermore, a role for Rac1 in inducing MLC phosphorylation and regulating Rac1-MAPK dependent integrin outside-in signalling has been established (Flevaris et al., 2008).

1.9 Inhibitory regulation of platelets

The structure and function of the endothelium is essential for maintaining the vascular wall and systemic circulation however, it is not inert but rather metabolically active and involved in the regulation of body homeostasis. The endothelium plays an important role in providing vascular tone and mediating thrombosis. It functions as a partially permeable membrane, regulating the exchange of macromolecules between the vascular lumen and smooth muscle cells.

Under normal physiological conditions, the endothelium is intact and spontaneous activation of platelets is prevented to avoid thrombosis. Intracellular signalling that promote platelet activation are controlled meticulously by mechanisms that negatively regulate platelet activation. Negative regulators of platelet activation such as NO and PGI_2 are platelet antagonists that inhibit adhesion, activation and aggregation. However, their concentration decreases following vascular injury and platelets are activated by the components of the ECM and soluble agonists via ITAM signalling pathways and GPCRs respectively. Immunoreceptor Tyrosine-based Inhibition Motif (ITIM)-coupled receptors are antagonists for ITAM-coupled receptors and inhibit the activating kinases as well as some of the key players of the ITAM signalling pathway. Platelet endothelial cell adhesion molecule-1 (PECAM-1/CD31) a member of the ITIM family inhibits collagen induced platelet aggregation and secretion (Patil, Newman and Newman, 2001). Under physiological in vitro conditions, PECAM-1 deficient mice produce larger thrombi, suggesting its major role in inhibiting thrombus formation (Jones et al., 2001).

Potent platelet antagonists like NO and PGI$_2$ are both from the endothelium and are essential in regulating platelet function, leading to an increase in intracellular cyclic nucleotides cGMP and cAMP respectively.

1.9.1 Nitric oxide

NO is a free radical gas released from the endothelium, functioning as a negative regulator of platelet activity. NO is synthesized by an enzyme called nitric oxide synthase (NOS). There are three isoforms of NOS: neuronal NOS (nNOS), inducible NOS (iNOS) and endothelial NOS (eNOS) (Naseem, 2005; Forstermann and Sessa, 2011). NO is synthesized by NOS from the amino acid L-arginine and molecular oxygen, producing L-citrulline and water as by-products of this enzymatic reaction (Forstermann and Sessa, 2011). NO released from vascular smooth muscle cells stimulates vasodilation and prevents the remodelling of vascular cells and smooth muscle proliferation. Once released from the endothelium, NO markedly inhibits secondary aggregation and thrombus formation (Freedman et al., 1997). In NOSIII knock-out mice, a defect in the ability to inhibit platelet activation and reduced bleeding times have been observed (Freedman et al., 1999).

When NO diffuses across the plasma membrane of the platelet and into the cytoplasm, it activates soluble guanylyl cyclase (sGC) causing an increase in cyclic guanosine 3', 5'monophosphate (cGMP). This results in the activation of cGMP-dependent protein kinase (PKG), inhibiting several pathways responsible for platelet activation. PKG decreases intracellular levels of Ca^{2+} by activating the sarcoplasmic reticulum ATPase (SERCA) which inhibits the influx of Ca^{2+} (Trepakova, Cohen and Bolotina, 1999). IP3 mediated Ca^{2+}release

is also inhibited, leading to further decrease in Ca^{2+} in the cytosol (Schlossmann et al., 2000). sGC and cGMP both play important inhibitory roles in platelet regulation. However, a stimulatory role of sGC in platelets have been described in sCG knock-out mice by Zhang et al., 2010. On the contrary, it has been argued by Gambaryan, Friebe and Walter, 2012 that sGC has a strict inhibitory role in platelets as they have not found a stimulatory effect in platelets in sGC deficient mice.

1.9.2 Prostacyclin

Prostacyclin is a member of the prostanoid family that was discovered by John Vane and co-workers in 1976 as a potent vasodilator and cAMP-dependent platelet inhibitor (Moncada et al., 1976). It is a 20-carbon unsaturated carboxylic acid with a cyclopentane ring that is produced in the smooth muscle cells as well as the vascular endothelial cells. PGI_2 is the main product of arachidonic acid metabolism and has a half-life of about three minutes in the blood. PGI_2 metabolism is initiated when the phospholipid membrane releases arachidonic acid by phospholipase A_2 which is induced by high levels of intracellular Ca^{2+} which occurs in the first few minutes of cellular activation (Lückhoff et al., 1988). Subsequently, oxidation of arachidonic acid by cyclooxygenase enzymes results in the production of hydroperoxyl endoperoxide (PGG_2) and this is further reduced by COX to hydroxy endoperoxide (PGH_2). The enzyme prostacyclin synthase converts this unstable PGH_2 into PGI_2 in endothelial cells which is consequently released from the vascular endothelium. This is because COX-1 and PGI_2 synthase are abundantly found in the endothelial cells. In contrast, PGI_2 synthase is not the main enzyme expressed in platelets instead, thromboxane synthase is predominantly expressed and thus, PGH_2 is converted to the principal product, thromboxane (TXA_2) (a vasoconstrictor) (Needleman et al., 1976). Notably, the released PGI_2 is converted and spontaneously broken down non-enzymatically to 6-keto prostaglandin F1a (PGF1α) (Epstein

et al., 1990). The endothelial cells producing PGI_2 are sandwiched by neighbouring platelets on the luminal side and vascular smooth muscle cells on the basal side of the endothelium.

1.9.2.1 IP receptor

The prostacyclin receptor, IP is a member of the prostanoid receptor superfamily coupled to the Gαs protein and is enriched in platelets as well as vascular smooth muscle cells. The extracellular domain consists of a small N-terminal domain and three extracellular loops. Ligands bind to the seven membrane-spanning alpha-helices in the transmembrane domain. (Stitham et al., 2003). Additionally, the intracellular domain is comprised of three loops, a putative eighth helix and a C-terminal tail (Narumiya, Sugimoto and Ushikubi, 1999; Reid et al., 2010). For normal function of IP receptors, a variety of post-translational modifications occur such as N-linked glycosylation, palmitoylation, disulphide bond formation and isoprenylation. Upon binding on the IP receptor, PGI_2 releases Gαs from the catalytic subunit of AC, elevating cAMP levels.

The human IP receptor consists of two N-glycosylation sites: N7 which is in the extracellular loop and N78 which is in the first extracellular loop (Smyth and FitzGerald, 2002). A greater degree of glycosylation has been described in HEK and COS-7 cells at the N78 residue compared to N7, suggesting a function on signal transduction, membrane localisation and ligand binding of the IP receptor (Zhang, Austin and Smyth, 2001). The C-terminal domain of the IP receptor alongside a few sites in the intracellular loops are targets for phosphorylation by protein kinase A (PKA) and protein kinase C (PKC). Ser328 is the principal phosphorylation site of PKC on human IP receptor. Phosphorylation of Ser328 by PKC is essential for desensitisation for cAMP and the inositol pathway signalling (Smyth, Li and

FitzGerald, 1998). Activation of IP receptors triggers $G\alpha_s$ mediated activation of adenyl cyclase dependent cAMP synthesis, activating PKA which in turn inhibits platelets.

An increased tendency to thrombosis has been observed in IP receptor knockout mice (Murata et al., 1997). TXA_2 production was increased and an obstruction of the carotid artery has been observed in mice lacking the IP receptor (Cheng, Austin and Rocca, 2002). It is thought that the lack of IP receptor may play a role in atherogenesis. Furthermore, another study showed that the lack of IP receptor resulted in the loss of protective effect seen in cardiomyocytes (Xiao et al., 2001).

1.9.3 Adenylyl cyclase and cAMP synthesis

Elevation of cAMP is dependent on the activation of adenyl cyclase (AC) and degradation by phosphodiesterases. The transmembrane enzyme AC is responsible for converting ATP into the cAMP nucleotide. Thus far, out of the 9 isoforms of AC, AC3, AC6 and AC7 have been identified in platelets (Rowley et al., 2011). However, AC6 has been established definitively (Burkhart et al., 2012). The AC enzyme is made up of transmembrane domain 1 (TMD1) that is connected with a loop to transmembrane domain 2 (TMD2) (figure 1.12). The TMDS have six transmembrane spanning α helices each. The loop between TMD1 and TMD2 is known as the C1 domain, the portion after TMD2 is known as C2. Both C1 and C2 domains are broken into subdomains whereby C1 is divided into C1a and C1b and the C2 domain into C2a and C2b. Once the C1a domain dimerises with C2a, it induces the active adenylyl cyclase. This active AC catalyses the cyclic reaction the conversion of ATP to cAMP and pyrophosphate (PPi).

Calcium calmodulin complexes regulate AC3 (AC3 is part of group 1 of ACs). AC7 are regulated by G$\beta\gamma$ subunits (group 2) and AC6 is inhibited by Gαi/calcium (group 3). All plasma membrane adenylyl cyclase enzymes are inhibited by calcium if the calcium concentrations are higher than physiological concentrations. Nonetheless, it is only the A5 and A6 isoforms that are inhibited by calcium at physiological concentrations as they have a higher affinity for binding calcium. All AC enzymes have a divalent cation (Mg^{2+}) at their catalytic site which is essential for the catalysis and conversion of ATP into cAMP + PPi. Indeed, it is involved in coordinating the ATP and bringing it into the catalytic subunit of ACs. Hence, at high concentrations of Ca^{2+}, the calcium displaces the magnesium from the catalytic site. However, calcium has a bigger valency than magnesium so the PPi generated from the conversion of ATP to cAMP is not released and so blocks the catalytic subunit, inhibiting the AC enzyme. Calcium concentrations in the cytoplasm can be increased by the extracellular fluid or through the endoplasmic reticulum. Voltage gated calcium channels open in response to depolarisation of the electrical potential difference of the membrane, driving calcium back into the cell. Alternatively, calcium can be released by the ER via G-protein coupled receptors. Activation of Gαq activates PLC$\gamma\beta$, degrading the PIP2 and generating IP3 and DAG (remain attached in the phospholipid bilayer meanwhile the IP3 is translocated into the cytoplasm). IP3 then acts on IP3 receptors on the endoplasmic reticulum membrane (major calcium store), causing the release of calcium from the endoplasmic reticulum.

Another way calcium activates AC1,3 and AC7 while inhibiting AC5 and AC6 is through store operated calcium entry (SOCE). When calcium levels in the ER go down, stromal interaction molecule 1 (STIM1) aggregate in the ER membrane, activating the calcium channels (calcium release activated calcium (CRAC)) on the plasma membrane and allowing the SERCA pump to drive calcium back into the ER.

It is important to note, all ACs are only affected by calcium from the CRAC and voltage gated calcium channels. It is believed that this is due to calcium signalling being localised to microdomains.
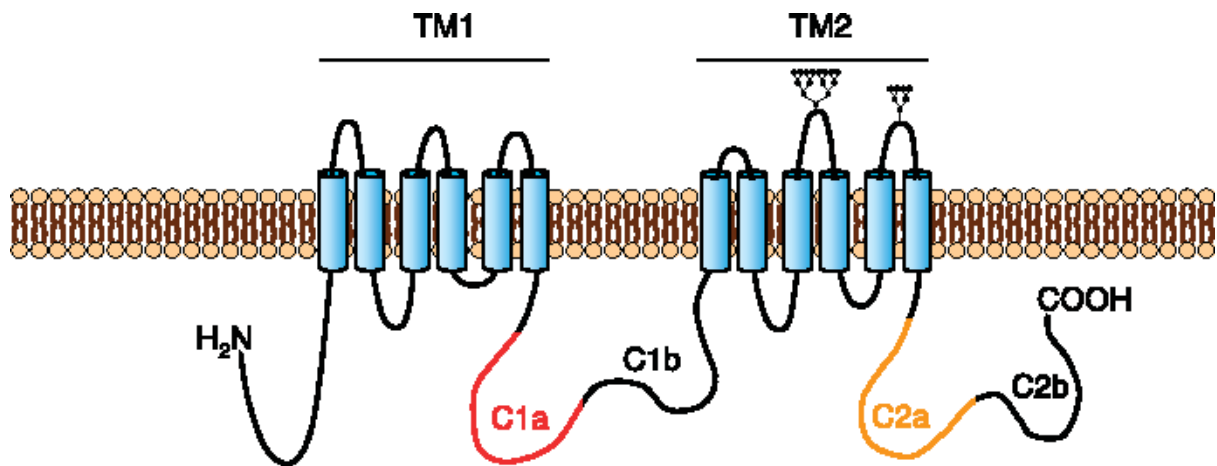
Figure 1.12. Structure of adenylyl cyclase.

The structure of ACs are divided into the NH2 terminus, the first transmembrane domain (TMD1, blue cylinders) containing six transmembrane spanning α helices, the first cytoplasmic loop consisting of C1a (red) and C1b (black). This loop is connected to the second transmembrane domain (TMD2, blue cylinders) with extracellular N-glycosylation sites with the carboxylic tail consisting of the C2a (orange) and C2b(black) domain. The dimerisation of the C1a and C2a domains forms the catalytic core with ATP binding sites (Willoughby and Cooper, 2007).

1.9.4 Protein kinase A

PKA consists of two regulatory subunits which dimerise and are attached to two catalytic subunits, forming the inactive PKA (figure 1.13). Increases in cAMP concentration cause the PKA catalytic core to activate. It is thought that both regulatory subunits bind to cAMP molecules which induces a conformational change in the dimer, causing the catalytic subunits to disassociate from the regulatory subunits, exposing the active sites and activating the catalytic core (Sjoberg, Kornev and Taylor, 2010). Thus, the catalytic subunit phosphorylates substrate proteins at serine and threonine residues that contain the sequence :(Arg-Arg-X-Ser/Thr, Arg-Lys-X-Ser/Thr, Lys-Arg-X-Ser/Thr) (Taylor et al., 2008). However, some catalytic subunits do not completely disassociate as they are thought to undergo substrate phosphorylation (Smith et al., 2013). Although some hallmarks of cytoskeletal reorganisation need the activation of PKA others are inhibited as a result of it. A-kinase anchoring proteins (AKAPs) drive PKA to some of the components of the actin cytoskeleton, enhancing cAMP and PKA signalling. PKA(I) and PKA(II) are the two main isoforms of PKA. They are classified due to their differences in regulatory subunits RI and RII which interact with the catalytic domain (Taylor, Buechler and Yonemoto, 1990). Four distinctive regulatory subunit genes have been established: Riα, Riβ, RIIα and RIIβ (Lee et al., 1983; Scott et al., 1987; Clegg, Cadd and McKnight, 1988). In addition, three catalytic subunit genes: Cα, Cβ, and Cγ, have been identified in the literature.
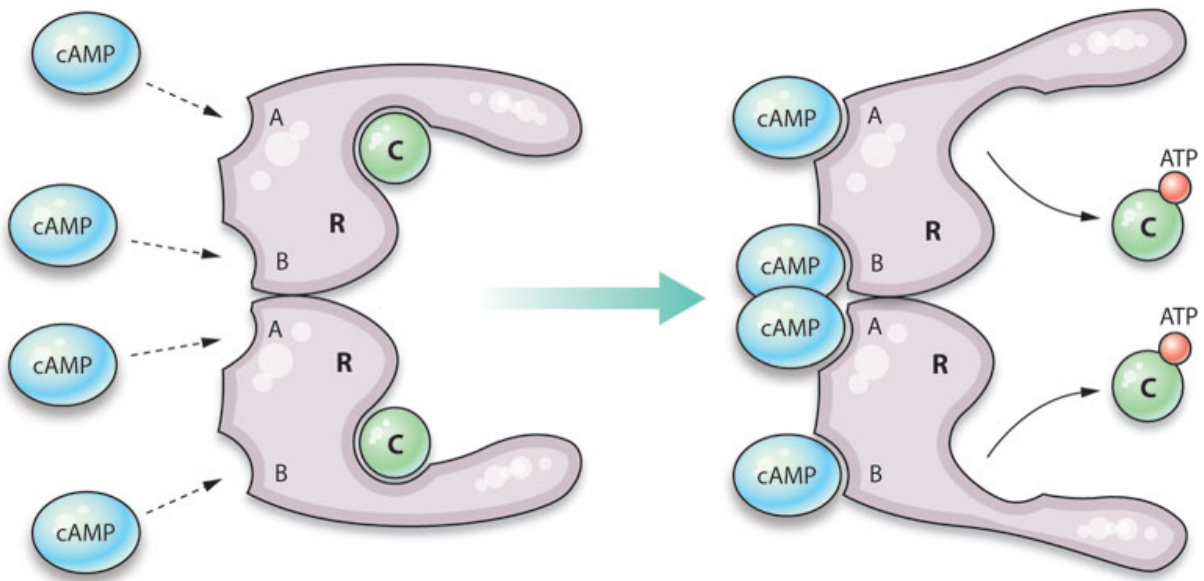
Figure 1.13. The activation of cAMP-dependent protein kinase.

Once cAMP binds to the regulatory subunits conformational change is induced which causes the disassociation of subunits from the complex, activating the catalytic core. Two cAMP molecules bind to each regulatory subunit which reduces their affinity for the catalytic subunits. This greatly sharpens the response of the kinase to changes in cAMP concentration. Image adapted from (Murray, 2008).

1.9.5 cAMP degradation by phosphodiesterases

Following the discovery of cAMP, cyclic nucleotide phosphodiesterases (PDEs) were identified. Immediately after the discovery of cGMP it became evident that both cAMP and cGMP are hydrolysed by cyclic nucleotide PDE activity (Butcher and Sutherland, 1962). PDEs regulate the degradation of cAMP and cGMP by selectively hydrolysing the 3' cyclic phosphate bond into inactive 5' cAMP/cGMP.

It is believed that there are 60 isoforms of PDEs and eleven different families (PDEs-1-11) comprising 21 different genes. The different families of PDEs are grouped according to amino acid sequences, characteristics of catalytic activity and their regulatory properties. PDEs are regulated by several protein interactions, binding of Ca^{2+}/calmodulin as well as binding to cAMP or cGMP allosterically. The roles of the different isoforms of PDEs in platelet function remain to be elucidated. Furthermore, the function of PDEs in a specific cell type vary across different species thus making it difficult to comprehend their functions. (Rybalkin et al., 1997; Dlaboga, Hajjhussein and O'Donnell, 2006; Abi-Gerges et al., 2009). It is believed that PDEs 4,7 and 8 are cAMP specific, PDEs 5,6 and 9 are cGMP specific and PDEs 1,2,3,10 and 11 are specific to both cAMP and cGMP (Bender and Beavo, 2006). PDE3 and PDE4 have a high affinity for cAMP in most cells. PDEs 2,3 and 5 are expressed in platelets (Hidaka and Asano, 1976). PDE3 can hydrolyse cGMP and cAMP however it is inhibited by cGMP and is commonly referred to as "the cGMP-inhibited cAMP PDE" as competitive inhibition of AMP hydrolysis occurs (Grant and Colman, 1984). The PDE2 enzyme consists of two GAF domains: GAF-A and GAF-B. It catalyses both cAMP and cGMP which bind GAF-B causing a conformational change and thus increases enzyme activity. PDE2 is stimulated by high concentrations of cGMP. Additionally, PDE5 is known as the cGMP specific/cGMP binding PDE. PDE5 specifically catalyses cGMP. While cGMP binding in PDE2 occurs in GFA-B,

cGMP has a high affinity binding to PDE5 occurs in the GAF-A domain. Biochemical studies have also reported the phosphorylation dependent activation of PDE5 by PKA and PKG that may possibly provide negative feedback on cGMP levels (Corbin et al., 2000).

1.9.6 The role of *"scavenger receptors'* in atherosclerosis

Brown and Goldstein discovered scavenger receptors (SR) in macrophages in the 1970s. They identified that modified oxLDL but not nLDL undergoes internalisation and degradation. There are different recognition patterns of the major receptors for oxLDL to the various forms of oxLDL. SRs are recognized by their biochemical ability to bind to various modified forms of LDL, such as oxLDL, inducing the differentiation of macrophages into foam cells and stimulating the formation of atherosclerotic lesions.

1.9.7.1 Class A scavenger receptors: Scavenger receptor A (SRA)

SR-A was the first scavenger receptor to be characterized and can preferentially bind acetylated, modified or oxidized LDL. This receptor is a type II trimeric transmembrane glycoproteins of 400-500 residues consisting of an N-terminal cytoplasmic transmembrane domain and a collagenous extracellular domain which facilitates ligand recognition and has collagen binding activity, allowing macrophage adhesion to collagens (Gowen et al., 2001). There are two different isoforms of SR-A (SR-AI and SR-AII) produced from the splicing of a single gene product. The only difference between these two receptors are in the cysteine-rich C-terminus whereby the 110-amino acids in SR-AI is replaced by a 6-amino acid sequence in SR-AII (Kodama et al., 1988; Rohrer et al., 1990; Gowen et al., 2001). SR-A are expressed in various cells such as, macrophages (predominantly expressed in macrophage derived foam

cells in atherosclerotic plaques), smooth muscle cells as well as sinusoidal endothelial cells in the liver (Takahashi et al., 1992; Dejager, Mietus-Synder and Pitas, 1993; Li, Freeman and Libby, 1995; Gough et al., 1999). Although SR-AI and SR-AII both bind to a variety of ligands, different binding affinities for acetylated and oxidized LDL have been described in the literature. oxLDL has a lower affinity for binding compared to acetylated LDL (Freeman et al., 1991). Furthermore, it is widely accepted that SR-A are more specific for extensively oxidised LDL.

1.9.7.2 Class B scavenger receptors: CD36

CD36 was the first-class B scavenger receptor to be identified as a receptor for oxLDL. CD36 is an 88kDa glycoprotein. It consists of two short intracellular domains, two transmembrane domains as well as a glycosylated extracellular domain consisting of three disulphide bridges crucial for ligand binding. It is believed that the hydrophobic sequence is involved in lipid ligand binding. The C-terminus is activated in signal transduction via interaction with Src tyrosine kinases, propagating CD36 mediated signalling. In contrast to SR-A, CD36 can bind to moderately oxidised LDL (Endemann et al., 1993). Additionally, unlike SR-A, oxLDL binding to CD36 is not inhibited by acetylated oxLDL (Endemann et al., 1993).

CD36 is an important player in an array of pathophysiological processes, from metabolism, angiogenesis and apoptosis to immunity, sensing of lipids and atherogenesis (Febbraio, Hajjar and Silverstein, 2001; Bodart et al., 2002; Hoebe et al., 2005; Philips, Rubin and Perrimon, 2005). To gain an insight into the role of oxLDL in platelet activation, various receptors and signalling pathways are being studied in detail. The glycoprotein CD36 (GP IV) is expressed

abundantly in platelets and acts as a receptor to its proposed ligands: thrombospondin-1 and oxLDL. However, the function of CD36 in vivo and how these agents induce the activation of platelets remain unclear. As well as being expressed on platelets, CD36 is found on a variety of cell types including monocytes, macrophages and endothelial cells. Macrophage CD36 is involved in the formation of the atherosclerotic lesion. The scavenger receptor mediates the uptake of oxLDL, forming foam cells. The interaction between oxLDL and macrophage CD36 causes the inhibition of macrophage migration contributing to the trapping of macrophages in the atherosclerotic lesions.

Platelet CD36 induces the inflammation in the plaque and is actively involved in the formation of the thrombus following the rupture. The way in which oxLDL and CD36 stimulate the activation of platelets remains unclear and understanding it may lead to the discovery of new therapeutic strategies. The interaction between platelet CD36 with oxLDL has been reported to activate platelets, as supported by the induction of P-selectin expression as well as the activation of integrin $\alpha_{IIb}\beta_3$ (Podrez et al., 2007). oxLDL binding to CD36 activates platelets via Src kinases as well as the activation of protein kinase-dependent pathways (Chen et al., 2008). Moreover, another study also showed that CD36-oxLDL ligation causes activation of Src kinases alongside Syk, which causes tyrosine phosphorylation and subsequent PLCγ2 activation resulting in platelet shape change, spreading and MLC phosphorylation (Wraith et al., 2013). Thus, this suggests that the subsequent downstream signalling events can involve Ca^{2+} mobilisation in a CD36-dependent manner. Indeed, it has already been identified that immobilised oxLDL can induce CD36-dependent Ca^{2+} mobilisation (Nergiz-Unal et al., 2011).

1.9.8 Role of oxLDL in inflammation

There is increasing evidence for the role of oxLDL in the pathogenesis of atherosclerosis and cardiovascular disease (Kiyan et al., 2014). Following the build-up of oxLDL in the vascular wall, macrophages play a pivotal role in taking up oxLDL, inducing the macrophage differentiation to lipid-laden foam cells and thus, initiating the first hallmark of the formation of atherosclerotic lesions (Quinn et al., 1987; Korporaal et al., 2007; van Tits et al., 2011; Kiyan et al., 2014). oxLDLs do not only induce transformation into foam cells but are central players in endothelial dysfunction, promoting vascular endothelium injury and the subsequent pathogenic process of atherogenesis (Watt et al., 2016). In addition, the interaction that occurs between platelets and oxLDL induces the activation of platelets, resulting in the release of inflammatory modulators such as chemokines and cytokines that contribute to atherosclerosis (Badrnya et al., 2014). Autoantibodies that react with oxidation specific epitopes of oxLDL are found in the blood of atherosclerotic patients, suggesting that oxLDL should also be present in the blood circulation (Korporaal et al., 2007). Therefore, platelets in the circulation become activated once they associate with oxLDL, promoting the thrombus formation after the rupture of the atherosclerotic plaque.

1.9.9 The role of oxLDL in platelets and megakaryocytes

Interestingly, studies have shown an increase in P-selectin expression in the atherosclerotic plaque endothelium, indicating that platelet adhesion is essential in early atherogenesis (Johnson-Tidey et al., 1994; Vora et al., 1997). The endothelium and platelets both express P-selectin which plays an important role in mediating the platelet-endothelium interactions, enabling the platelets and neutrophils to roll and adhere to the activated endothelium (Frenette

et al., 1995). oxLDL have been reported to upregulate the expression of P-selectin by the endothelium (Gebuhrer et al., 1995; Vora et al., 1997). The exposure of oxLDL to platelets via scavenger receptors such as CD36 results in the release of pro-atherogenic chemokines from platelets. This causes the chemokines to attract more monocytes and thus, exacerbating the atherosclerotic process by inducing monocyte to macrophage conversion and subsequent foam cell formation (Curtiss et al., 1987; Siegel-Axel et al., 2008; Daub et al., 2010). Theoretically speaking, since platelets are derived from the megakaryocyte and megakaryocytes are found near the endothelium where oxLDL are present, there is a possibility that they may come into contact with oxLDL during proplatelet formation (proplatelet cytoplasmic extensions protrude through the vascular endothelium), therefore, producing platelets that are pre-activated by oxLDL and consequently, contributing to the promotion of the atherosclerosis process and thrombus formation. Thus, it can be postulated that oxLDL may play a pivotal role in atherosclerotic behaviour of megakaryocytes.

As previously discussed, Aschoff, 1893 observed intravascular megakaryocytes in human lungs. Circulating oxLDL is an important atherogenic factor that could be found in pulmonary arteries and atherosclerosis in these arteries is accelerated in patients with atherosclerosis of the systemic arteries (Moore, Smith and Hutchins, 1982). Therefore, it can be hypothesised that intravascular megakaryocytes found in the lungs of these patients may encounter circulating oxLDL, encouraging the production of pre-activated platelets involved in the development of the atherosclerotic process. The internalisation of oxLDL also results in the inhibition of endothelium regeneration. Furthermore, the lysophosphatidylcholine component of oxLDL have also been described to directly interfere with atherogenesis by inhibiting prostacyclin, causing monocytes to adhere to the endothelial wall (Thorin et al., 1994; Mahfouz and Kummerow, 2001). As discussed in the first section of this review, PGI_2 is the most potent

inhibitor of platelet aggregation. Its receptor PGI2-R mediates its action. The receptors expressed on the platelets must have originated from the megakaryocytes as platelets only have very few remnant RNA transcribed from the megakaryocyte nucleus. It has been observed that PGI_2 receptor is expressed in megakaryocytes and cytokines upregulate this receptor and its upregulation can also direct the development of megakaryocyte maturation (Sasaki et al., 1997). We know that megakaryocytes are found next to the endothelium where oxLDL is also present. Hypothetically speaking, in the presence of oxLDL, PGI_2 may be attenuated, which may lead to a reduced maturation event in megakaryocytes as well as the production of platelet aggregates, following the proplatelet formation event and therefore, amplifying the atherosclerotic process. This would pose *clinical* significance as a defect in megakaryocyte maturation could result in thrombocytopenia.

In addition, oxLDL has also been reported to decrease the PGI_2 to thromboxane ratio, inducing platelet aggregation and adhesion (Mahfouz and Kummerow, 1998; Mahfouz and Kummerow, 2001). Upon activation, platelets attach to blood leukocytes as well as monocytes. Platelet-monocytes aggregates are currently believed to be an early predictor for cardiovascular disease. oxLDL inhibit NO production from the endothelial cells and this is believed to be one of the most crucial characteristics of endothelial dysfunction and hence, a key event in the atherosclerotic process (Blair et al., 1999). Lox-1 is involved in the endothelial dysfunction caused by oxLDL and is associated with the ability of oxLDL to inhibit NO production. Upregulation of Lox-1 expression has been reported in early stages of atherogenesis, suggesting that Lox-1 may have some significance in initiating atherosclerosis (Chen et al., 2000).

1.10 Aims of the study

Atherosclerosis is a major element in cardiovascular disease and a significant health concern in developed countries. Furthermore, modified LDL triggers the pathogenesis of atherosclerosis by altering the functions of cells. oxLDL adheres to endothelial cells and triggers their activation, leading to adhesion and rolling of leukocytes and thus, promoting an inflammatory response. It is well established that a variety of cells play a role in the atherosclerotic process such as monocytes, macrophages, endothelial cells, smooth muscle cells as well as platelets.

In the blood of atherosclerotic patients, autoantibodies that react with oxidation specific epitopes of oxLDL are present, suggesting the presence of oxLDL in the circulation (Korporaal et al., 2007). Furthermore, elevated fibrinogen levels are related to the formation of plaques in atherosclerosis as well as inducing a prothrombotic or hypercoagulable state (Levenson et al., 1995; Zhang et al., 2014). Therefore, we investigated whether a hypercoagulable state was induced upon the interaction between circulating oxLDL and fibrinogen.   The main aims of this thesis were:

1. To determine the effect on actin cytoskeleton caused by spreading platelets on fibrinogen and oxLDL

2. To identify how PGI_2 affected platelets spread on oxLDL and fibrinogen

3. To identify the role of AC and PDEs in oxLDL modulation of fibrinogen spreading

4. To determine the effect of oxLDL and fibrinogen in thrombus formation in high and low shear stress in vitro.

Chapter 2: Materials and Methods

2.1 Materials

PGI_2 (Cayman Chemical, Michigan, USA), Forskolin (Sigma-Aldrich, UK), Fibrinogen (Enzyme Research, Swansea, UK), ProLong Diamond Antifade Mountant (GE healthcare, Little Chalfont, Buckinghamshire, UK)). Multichannel biochips (Cellix, Dublin Ireland). Ultracentrifuge tubes & 70ti rotor (Beckman Coulter, USA), Beckman Coulter counter (Beckman Coulter, USA), Aggregometer (Chrono-Log, USA), Micro magnetic stir bars (Chrono-Log, USA). All other reagents stated below are from Sigma Ltd (Poole, UK) unless otherwise stated. PBS, Paraformaldehyde, $CuSO_4$, Glucose, Tris-Na Citrate, NaCl, Citric acid, EGTA EDTA, KCl, HEPES, NaH_2PO_4, Na_2HPO_4 $NaHCO_3$, $MgCl_2$, Triton X-100, KH_2PO_4, Acrylamide 30%, methanol, PVDF, BSA, ethanol, milk powder, TEMED, APS, Tris base, SDS, Glycine, Glycerol, Bromophenol blue, Dithiothreitol, Tween-20, 24-well plate, 6-well plate, 10 cm dish, 21-gauge butterfly needle, coverslips, glass slides, plate reader, licor_Odyssey, phosphatase and protease inhibitors.

2.1.1 Primary antibodies

Table 2. 1.1. List of primary antibodies.

No	Antibody	Host	Dilution		2% Blocking	Source
			WB	IF		
1	pVASP^{Ser157}	Rabbit monoclonal	1:1000	-	BSA	Cell Signalling
2	pMLC^{Ser19}	Rabbit polyclonal	1:1000	-	BSA	Cell Signalling
3	pPKA Substrate	Rabbit monoclonal	1:1000	-	BSA	Cell Signalling
4	GAPDH	Mouse monoclonal	1:6000	-	Milk	Millipore
5	EO6	Mouse monoclonal	-	1:400	BSA	Avanti Polar Lipids inc

2.1.2 Secondary antibodies

Table 2.1.2 List of secondary antibodies.

No	Antibody	Host	Dilution		Source
			WB	IF	
1	IR Dye 680RD anti-rabbit	Goat	1:20000	-	LI-COR Biotechnology, Cambridge, UK
2	IR Dye 800CW anti-mouse	Goat	1:2000	-	LI-COR Biotechnology, Cambridge, UK
3	Alexa 594 anti-mouse	Goat	-	1:1000	Thermo Fisher

2.1.3 Fluorescent dyes

Table 2.1.3. List of fluorescent dyes.

No	DYE	Source
1	FITC-Phalloidin 2mM	Sigma
2	Rhodamine B 2mg/ml	Sigma
3	Alexa 488 Anti-Fibrinogen 1:200	Abcam, Cambridge
4	$DIOC_6$ 10 µM	Enzo

2.1.4 Inhibitors

Table 2.1.4. List of inhibitors.

No	Inhibitor	Source
1	Apyrase 2U/ml	Sigma
2	Indomethacin 10 µM	Sigma
3	Y27632 10 µM	Abcam, Cambridge
4	NSC23766 50 µM	Enzo Scientific
5	Milrinone 10 µM	Enzo

2.1.5 Protein ladder

Table 2.1.5. Protein ladder.

No	Name	kDa	Source
1	Precision Plus Protein Standards (Kaleidoscope standards)	15, 20, 50, 100-250	Bio-rad

2.1.6 List of kits

Table 2.1.6. List of kits.

No	Kits	Source
1	RhoA Pull-down Activation Assay Biochem Kit	Cytoskeleton
2	Rac1 Pull-down Activation Assay Biochem Kit	Cytoskeleton
3	cAMP Biotrak Enzymeimmunoassay System	GE Healthcare Life Sciences
4	Precision Red advanced protein assay	Cytoskeleton

2.2. Low density lipoprotein preparation

2.2.1. Isolation of low-density lipoproteins

LDL (1.019-1.063 g/mL) was isolated from human plasma by density gradient ultracentrifugation as described by (Chung, Wilkinson, Geer and Segrest, 1980; Naseem, Goodall and Bruckdorfer, 1997). Whole blood from healthy volunteers was collected in 0.15M EDTA (pH 7.4). Blood was centrifuged at 1500g for 30 mins at 4ºC. Plasma yield was adjusted to 1.019 g/mL by the addition of high-density solution (HDS) (2.97 M KBr, 2.62 M NaCl, 297 µM EDTA). KBr was slowly dissolved into the plasma and gently stirred. The plasma was subsequently dialysed against a 2 litre 1.019 g/mL KBr solution and transferred into ultracentrifuge tubes and centrifuged at 33400 rpm for 18 hours at 4ºC on a fixed angle rotor (70Ti) in a Beckman XL70 centrifuge. LDL was isolated by removing chylomicrons and VLDL using a 19-gauge needle and the density of the plasma was adjusted to 1.063 g/mL by adding HDS with gentle stirring and plasma was dialysed against 1.063 g/mL density solution (68mM NaBr, 0.3mM EDTA and 5mM NaOH). The plasma was subject to a second centrifugation for 18 hours at 4ºC and the upper golden layer was removed, dialysed against a 1.063 g/mL solution. The plasma was then centrifuged a final time at 33400 rpm for 18 hours at 4ºC to achieve concentrated LDL.

LDL was dialysed against a dialysis buffer (140 mM NaCl, 8.1 mM Na_2HPO_4, 1.9 mM NaH_2PO_4, 100 µM EDTA) for 8 hours at 4ºC with several changes and gentle stirring to remove the KBr. EDTA solution was added into the dialysis buffer to remove transition metal ions. Dialysis was carried out in the dark and air-tight conditions to prevent oxygenation. The LDL was filtered using a 0.22 µm pore size filter and stored at 4 ºC in the dark.

A

| 1 | 2 | 3 | 4 |

1.019 g/ml

Adjusted plasma

Chylomicrons, VLDL

LDL

HDL & Albumin

LDL

1.063 g/ml solution impurities

LDL

Corresponding images

B

Golden layer: LDL
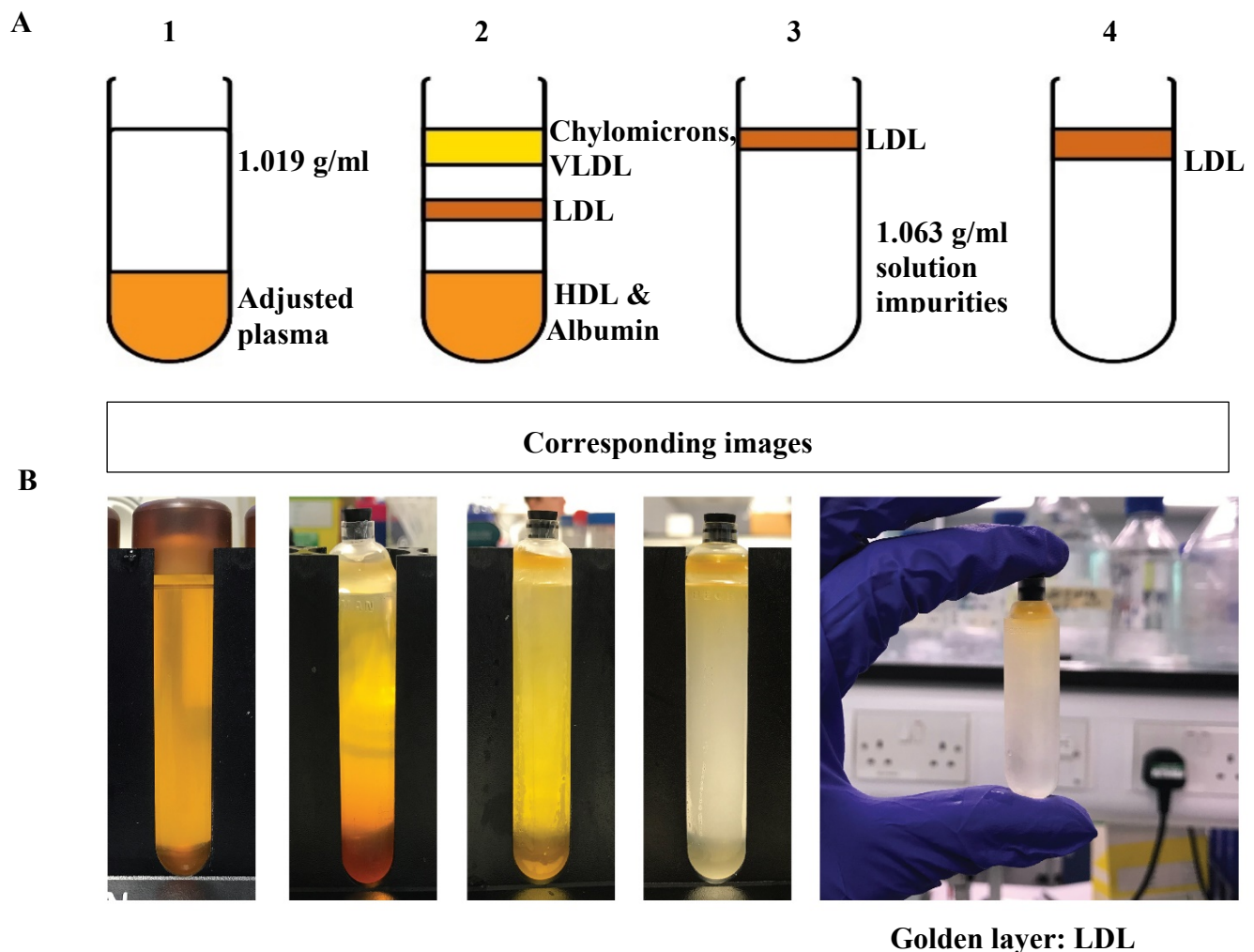
Figure 2.1. Isolation of LDL from density gradient ultracentrifugation.

LDL (1.019-1.063 g/mL) was isolated from human plasma by density gradient ultracentrifugation as described by (Chung, Wilkinson, Geer and Segrest, 1980; Naseem, Goodall and Bruckdorfer, 1997). **A)** Schematic representation of LDL isolation. **1)** Plasma yield was adjusted to 1.019 g/mL by the addition of 1.316 g/mL solution and dialysed. **2)** After ultracentrifugation, the chylomicrons were removed and the remainder of the plasma was adjusted to 1.063 g/mL, dialysed and centrifuged again. **3)** The golden layer at the top is the LDL. **4)** To increase the concentration of LDL, the density of plasma was checked and adjusted to 1.063 g/mL and centrifuged a final time. **B)** Images (taken by me) representing the isolation steps of LDL by density ultracentrifugation.

2.3. Oxidation of low-density lipoproteins

2.3.1. Preparation of extensively oxidised low-density lipoproteins

LDL (2 mg/ml) was oxidised by the addition of 10 µmol/L $CuSO_4$ for 24 hours at 37 °C. Further oxidation was stopped by dialysing LDL in dialysis buffer (140 mM NaCl, 8.1 mM Na_2HPO_4, 1.9 mM NaH_2PO_4) and 100 µM EDTA to chelate Cu^{2+} ions for 24 hours (Gerry, Satchell and Leake, 2008).

2.3.2. Identification of oxidised low-density lipoproteins: Determining the REM of LDL

Upon oxidation of LDL, the $ApoB_{100}$ protein undergoes modification, increasing its net negative charge as well as reducing its affinity to LDL receptor (Brown and Goldstein, 1986). This is measured on agarose gel electrophoresis by the increased anodic electrophoretic mobility of LDL as described by Morel et al., 1984. 1% agarose gel was prepared and 20 µg of oxLDL and nLDL (control) were loaded into separate wells in the electrophoresis cassette, the tank was filled with TAE buffer and subsequently ran for 30 min at 100V. The gel was stained with0.1% Coomassie- Brilliant-Blue R-250 and imaged using LiCor Odyssey imaging system to visualise ApoB of LDLs.

TAE buffer (pH 8.3)	Coomassie blue stain	De-staining solution
40 mM Tris base	0.1% Coomassie- Brilliant- Blue R-250	10% Ethanol
20 mM Acetic acid	50% Methanol	7% Acetic acid
2 mM EDTA	10% Acetic Acid	

2.4. Platelet preparation

2.4.2. Preparation of washed human platelets

Platelets were isolated from whole blood taken from healthy volunteers that were not on any medication for 14 days. Blood was taken via a 21-gauge butterfly needle and directly into a sterile plastic syringe that contained an anticoagulant, acid-citrate-dextrose (ACD, ratio 1:5 – 29.9 mM Tri-sodium citrate, 2.9 mM citric acid, 72.6 mM NaCl and 113.8 mM D-glucose (pH 6.5)). To avoid early platelet activation as a result of traces of thrombin or tissue factor contamination, the first 5 ml of blood was discarded. The blood was then transferred into a 50 ml conical tube and gently inverted. After collecting blood, the blood samples were centrifuged at 200g for 15 min at 21ºC and platelet-rich plasma (PRP) was isolated, and 0.3 M citric acid was added to prevent platelet activation. PRP was then centrifuged at 800g for 12 mins at 21ºC and the platelet-poor plasma (PPP) was discarded. The platelet pellet was carefully resuspended with 5 ml wash buffer (0.036 mM citric acid, 0.01 mM EDTA, 0.005 mM D-glucose, 0.005 mM KCl, 0.09 mM NaCl (pH 6.5)), centrifuged at 800g for 12 min at 21ºC, and the supernatant discarded. The platelet pellet was gently resuspended in modified Tyrode's buffer (150 mM NaCl, 5 mM HEPES, 0.55 mM NaH_2PO_4, 7 mM $NaHCO_3$, 2.7 mM KCL, 0.5 mM $MgCl_2$, 5.6 mM D-glucose (pH 7.4)). After isolation, washed platelets were counted using a Beckman Coulter Z1 Counter. 5 µl of platelet suspension was added to 10 ml of isotonic buffer in a cuvette (Beckman Coulter Accuvette) and platelet numbers were recorded three times using the counter before an average was taken. Platelets were rested for 30 min at 37 ºC before conducting experiments.

2.4.3. Preparation of washed platelets (spread) for SDS-PAGE

For SDS-PAGE experiments, 10 cm dishes were coated with the desired matrix (fibrinogen at 100 µg/ml or fibrinogen +/- oxLDL at 50 µg/ml or nLDL (50 µg/ml)) and blocked with fatty acid free BSA (5 mg/ml). To denature the proteins, BSA was boiled for 10 mins and cooled down at room temperature and subsequently filtered. Plates were blocked with BSA for 1 hour. Platelets ($2x10^8$/ml) were isolated as per washed human platelets protocol (2.4.2) and spread. Plates were washed with PBS twice. After spreading platelets, 50 µl of lysis buffer was added and spread platelets were collecting by scraping the cells using a cell scraper. Protein concentration was estimated using Precision Red Advanced Protein Assay (Cytoskeleton). 3 µl of platelet sample was incubated into a total volume of 300 µl in a 96 well plate for 1 min. Samples were prepared in triplicates and read in a platelet reader at 600 nm.

Table 2.4.4. SDS- PAGE gel electrophoresis.

Lysis buffer	X4 Laemmli Buffer (pH 6.8)
10 mM Tris base	4.0g SDS
150 mM NaCl	0.1g bromophenol blue
1 mM EDTA	20 ml glycerol
1 mM EGTA	10 ml Tris 1.0 M (pH 6.8)
2% Triton-100	10 ml β-Mercaptoethanol
Protease inhibitor cocktail (1:1000)	50 ml dH$_2$0
Phosphatase inhibitor (1:1000)	

Samples were run on SDS-PAGE in a discontinuous buffer system described by (Laemmli, 1970). Protein was separated by a 1.5 mm thick polyacrylamide gels in 10%, 14% resolving gels and 4% stacking gel (depending on experiment). The gels were placed in an electrophoresis tank with running buffer and samples were run at 70 volts for 30 min and the remainder of the run was at 120 volts for 1 hour (time varied according to protein of interest).

After the run was complete, the protein was transferred onto a PVDF membrane in order of cassette electrode, filter paper, PVDF membrane, gel, filter paper and another electrode cassette using a Bio-Rad Trans-Blot Turbo at 2.5 V, 1.3A for 10 min. The PVDF membrane was subsequently blocked with 5% milk or 10% BSA for 1 hour to avoid non-specific binding. Thus, membranes were incubated with a primary antibody (1:1000) in TBS-T supplemented with 2% milk or 2% BSA overnight, with gentle shaking at 4ºC. Membranes were washed with 0.1% TBS-Tween twice for 10 min with gentle shaking 5 times and incubated with a fluorescent secondary antibody (1:20000) 1 hour at room temperature under dark conditions to avoid bleaching of fluorescent dyes. Blots were then imaged using an Odyssey CLx imaging system (Li-Cor, Nebraska, USA) and analysed using Image Studio Lite (Li-Cor, Nebraska, USA).

Table 2.4.5. Recipe for resolving gels (two resolving gels).

Resolving Gel	10%	14%
30% Acrylamide (ml)	5	7
10% SDS (µl)	150	150
1.5 M Tris HCl (pH 8.8) (mL)	3.75	3.75
dH$_2$O (ml)	6.03	4.03
10% ammonium persulfate (APS) (µl)	75	75
TEMED (µl)	7.5	7.5

Table 2.4.6. Recipe for stacking gels (two stacking gels).

Stacking Gel	4%
30% Acrylamide (ml)	1.98
10% SDS (µl)	150
0.5 M Tris HCl (pH 8.8) (mL)	3.78
dH$_2$O (ml)	9.0
10% ammonium persulfate (APS) (µl)	75
TEMED (µl)	15

Table 2.4.7. Recipe for TBS and TBS-T.

TBS	TBS-T
19. 97 mM Tris Base	19. 97 mM Tris Base
141.78 mM NaCl	141.78 mM NaCl
1L dH$_2$O	1L dH$_2$O
	1 ml Tween 20

Running buffer

0.1% SDS

192 mM Glycine

25 mM Tris base

2.4.5. Measurement of platelet aggregation in vitro: Light transmission aggregometry

Platelet aggregation was tested using light transmission aggregometry as described by Born, 1962. In an unstimulated platelet suspension, increased scattering of light occurs through the suspension (figure 2.2). Upon adding platelet agonists, platelet aggregates are formed and the amount of light that scatters decreases, whilst the amount of light transmitted through the suspension increases and is detected by the photocell. Therefore, light transmission is directly proportional to platelet aggregation measured in the light transmission aggregometry. The aggregation of washed human platelets was measured using a Chrono-log dual-channel light aggregometer (Chronolog, USA). 250 µl washed platelets ($2x10^8$ /ml) were incubated at 37 ºC in aggregation tubes under stirring conditions (1000 rpm). After incubations, suspended platelets were stimulated with agonists (thrombin at 0.1U/ml or oxLDL at 10, 30 or 50 µg/ml) and the traces were recorded. The aggregometer was calibrated against tyrodes buffer before each experiment.
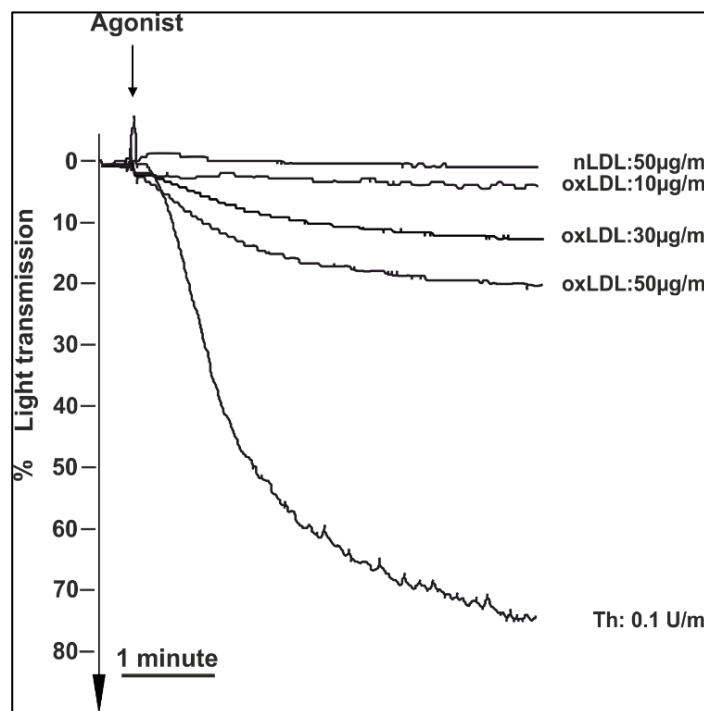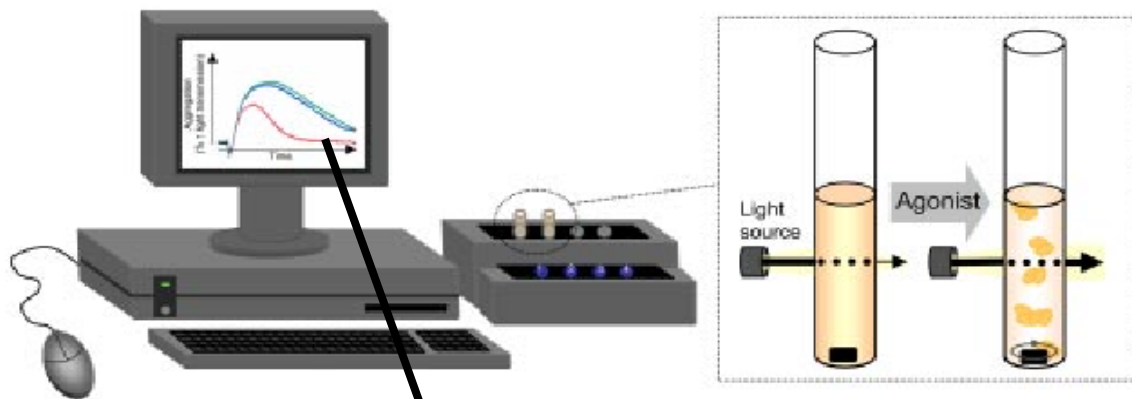
Figure 2.2. Light transmission aggregometry

Schematic representation of a platelet aggregation experimental set up adapted from Jackson (2007) (TOP). Representative aggregation trace showing platelets stimulated with thrombin (0.1 U/ml), oxLDL (10 μg/ml, 30 μg/ml, 50 μg/ml) and nLDL (50 μg/ml) (BOTTOM).

2.4.6. Platelet spreading assays

Glass coverslips were coated with 3, 30 and 100 µg/ml fibrinogen overnight at 4°C or with 10, 30 and 50 µg/ml oxLDL or nLDL for 1 hour at room temperature. In combination experiments, glass coverslips were coated with 3, 30 and 100 µg/ml fibrinogen overnight at 4°C, washed twice with PBS and then coated with 10, 30 and 50 µg/ml oxLDL or nLDL for 1 hour at room temperature. Fatty acid free BSA (5 mg/ml) was boiled for 10 minutes, prior to filtering, and was then used to block the coverslips for 1 hour at room temperature. After washing coverslips twice with PBS, washed human platelets ($2x10^7$/ml) were then spread on coverslips at room temperature to stay consistent throughout the experiment and avoid premature activation. Platelets were spread at multiple different times as explained in sections below.

2.4.7.1. Apyrase and indomethacin inhibitors

Human platelets ($2x10^7$/ml) were then pre-treated 2 U/ml apyrase, 10 µM indomethacin or the combination of both inhibitors for 10 minutes. Platelets were spread for 20 minutes and subsequently treated with the inhibitors again alongside 10 nM PGI_2 for 10 minutes.

2.4.7.2. Y27632 and NSC23766 inhibitors

Human platelets $2x10^7$/ml were pre-treated with either 10 µM Y27632 or 50 µM NSC23766 for 30 minutes prior to spreading for 30 minutes.

2.4.8. Post incubation of platelets with inhibitors

Human platelets (2×10^7/ml) were incubated on coverslips for 20 minutes at room temperature. Platelets were then washed twice with PBS before addition of either Tyrodes (control), 10 nM PGI_2, 10 nM PGI_2 and 1 µM forskolin, 1 µM forskolin, 10 µM milrinone, 10 µM Y27632 or 50 µM NSC23766 for 10-30 minutes.

For all spreading experiment, at the relevant timepoint, adhered platelets were subsequently fixed using 4% formaldehyde for 10 minutes, permeabilised using Triton X-100 (0.1%) for 5 minutes and stained using FITC phalloidin for 1 hour in the dark. The coverslips were then mounted on glass slides using Diamond anti fade mounting medium.

2.4.7. Microscopy and image analysis

A fluorescence microscope (Zeiss Axio Observer -Zeiss, Cambridge, UK) was used to visualise platelets and obtain images. Three randomised images of each condition were taken, and acquired images were deconvolved in Zen Pro software (Carl Zeiss, Cambridge, UK) and then processed in CorelDraw X7 (Corel). All the images were analysed for platelet adhesion, platelet surface area, and the number of platelets with actin nodules and stress fibres. Image analysis was performed using Image J software (NIH, Bethesda, USA).

2.5. cAMP assay

2.5.1. Identifying cAMP levels in platelets

The cAMP assay facilitates the extraction of cAMP from the platelet. Isolated washed plates were prepared using the technique described in section 2.4.3. cAMP kit (GE Healthcare Life Sciences- Amersham cAMP Biotrak EIA system- RPN 225) was used to measure the cAMP levels within the platelet lysates as per the manufacturer's instructions. Briefly 100 µl of sample and 100 µl of standards were transferred to the wells of 96-well plate. The samples were labelled in duplicated and 100 µl of antiserum was added into each well and the samples were gently mixed and incubated at 4ºC for 2 hours with gentle shaking. 50 µl of cAMP-peroxidase conjugate was added into the samples post incubation, gently mixed and incubated for 1 hour at 4ºC. After incubation, the volume of each well was aspirated and washed four times with wash buffer provided in the commercial kit. 150 µl of an enzyme substrate was added to the wells for 1 hour at room temperature with gentle shaking. To stop the reaction, 100 µl of 1.0 M H_2SO_4 was added to each well and the samples were immediately read using a Tecan plate reader at 450 nm. A standard curve was acquired from the experiment which enabled the identification of the cAMP levels of each sample.

2.6. RhoA pull down assay

Washed human platelet lysates were prepared and protein concentration was estimated using the technique described in section 2.4.3. RhoA activity of samples were determined using a RhoA pulldown kit (Cytoskeleton Inc) as per the manufacturer's instructions. Briefly 250 µg of lysate were incubated with 50 µg of Rhotekin-RBD-beads for 1 hour at 4ºC with gentle shaking. Rhotekin-RBD beads were pelleted by centrifuging at 5000 g at 4ºC for 1 min. 90% of supernatant was carefully removed, not disturbing the pellet. The beads were subsequently washed with 500 µl wash buffer (provided in the commercial kit). Rhotekin-RBD beads were pelleted once again by centrifuging at 5000g at 4ºC for 3 min. The supernatant was gently removed without disturbing the pellet and Laemmli buffer was added to each sample and samples were ready to be analysed by SDS-PAGE. As the protein of interest was small, the samples were run on 14% resolving gel using the western blot techniques described in section 2.4.4.

2.7. Rac pull down assay

Washed human platelets were isolated and prepared as described in section 2.4.3. Rac activity of samples were determined using a Rac pulldown kit (Cytoskeleton Inc) as per the manufacturer's instructions. Briefly 250 µg of lysate were incubated with 50 µg of PAK-PBD-beads for 1 hour at 4ºC with gentle shaking. It was previously established the 50 µg beads show optimal results (Verma and Ihler, 2002; Yusuf et al, 2017). PAK-RBD beads were pelleted by centrifuging at 5000g at 4ºC for 1 minute. 90% of supernatant was carefully removed, not disturbing the pellet. The beads were subsequently washed with 500 µl wash buffer (provided in the commercial kit). PAK-PBD beads were pelleted once again by centrifuging at 5000g at 4ºC for 3 minutes. The supernatant was gently removed without disturbing the pellet and Laemmli buffer was added to each sample and samples were ready to be analysed by SDS-PAGE. As the protein of interest was small, the samples were run on 14% resolving gel using the western blot techniques described in section 2.4.4.

2.8. Flow

Biochips were coated with the desired matrix protein (fibrinogen at 100 µg/ml, 300 µg/ml or 1000 µg/ml) and/or oxLDL/nLDL at 50 µg/ml) and blocked for 1 hour with denatured and filtered fatty acid free BSA (5 mg/ml). Whole blood was collected into an anticoagulant, 100 µM PPACK (Phenylalanyl-Prolyl-Arginyl Chloromethyl Ketone) to inhibit thrombin irreversibly. The whole blood was stained with 10 µM $DIOC_6$ 20 min before flowing into the multichannel biochips at a low sheer rate of 200 s^{-1} or high shear rate of 1000 s^{-1} (depending on the experiment) at 37 ºC. The thrombi were fixed with 4% formaldehyde for 15 minutes and stained with 10 µM $DIOC_6$ and/or 2 mg/ml Rhodamine B for 1 hour. Images were obtained using an Apotome 2.0 on Zeiss Axio Observer (Carl Zeizz, Cambridge, UK) at 63X magnification with oil and deconvolved on Zen Pro Softwares (Carl Zeiss, Cambridge, UK). Images were analysed on Image J and processed on CorelDraw X7 (Adobe).

2.9. Statistical analysis

Data was expressed as mean ± standard deviation (SD) and were analysed using T-Test or one-way analysis of variance (ANOVA) with P value 0.05 which was followed by a post hoc Tukey HSD (Honestly Significant Difference) to compare the means of the one-way ANOVA between the groups. The data was analysed using Microsoft Excel 2017 and Graphpad (Prism 7).

CHAPTER 3: Platelets spread on oxLDL and Fibrinogen display a prothrombotic phenotype

3.1. Introduction

Dyslipidaemia is a major risk factor in atherosclerosis and results in increased platelet reactivity inducing a prothrombotic risk. Increased platelet reactivity has been described in elevated levels of LDL whilst the opposite effect was reported in low levels of LDL (Carvalho, Colman and Lees, 1974; Stuart, Gerrard and White, 1980; David et al., 1992). Hyperlipidemia induces the formation of a platelet thrombus and increases the development of coronary thrombosis at the site of the thrombus formation in the plaque rupture (Lacoste et al., 1995). Part of the mechanism is due to the modification of LDL which promotes the pathogenesis of atherosclerotic lesions.

The most common method of LDL oxidation in vitro thus far is oxidation by copper. It is believed that the oxidation products formed from LDL oxidised this way are physiologically similar to the oxidation products found in cells. Oxidation of LDL by copper leads to peroxidation of PUFA, decomposition of lipid hydroperoxides to aldehyde products as well as the formation of oxysterol-rich LDL (Gerry, Satchell and Leake, 2008). It has previously been established that the extent of LDL oxidation is crucial in determining the degree of platelet activation (Naseem, Goodall and Bruckdorfer, 1997). In vitro studies show that modified lipoproteins directly affect platelet activation and aggregation and cause the potentiation of platelet activation stimulated by several agonists such as thrombin, collagen, ADP as well as epinephrine (Ardlie, Selley and Simons, 1989; van Willigen, Gorter and Akkerman, 1994).

Fibrinogen also plays a key role in arterial thrombosis as a result of promoting the crosslinking of platelets during thrombus growth. The conformational change in the platelet integrin receptor $\alpha_{IIb}\beta_3$ triggers inside-out signalling, changing the integrin from a low affinity to a high affinity state. Fibrinogen binding results in the elevation of intracellular calcium levels and induces MLC phosphorylation and thus, the formation of stress fibres. As well as having a crucial role in platelet activation and aggregation, fibrinogen also plays an important role in atherogenesis. Increasing evidence from studies have reported that elevated fibrinogen levels are related to the formation of plaques in atherosclerosis as well as inducing prothrombotic or hypercoagulable state (Levenson et al., 1995; Zhang et al., 2014). It was previously established that the combination of oxLDL and collagen enhances the formation of a thrombus at high shear rates in vitro (Nergiz-Unal et al., 2011). Thus, it can be hypothesised that the combination of oxLDL and fibrinogen may lead to a prothrombotic phenotype.

The aims of this chapter are to:

- Identify the role of oxLDL and nLDL in platelet aggregation
- Identify the effect on actin cytoskeleton caused by spreading platelets on different concentrations of fibrinogen, and combinations of fibrinogen and nLDL/oxLDL
- Assess the effect that addition of oxLDL has on PGI_2 mediated rearrangement of the actin cytoskeleton in platelets.

3.2. oxLDL, but not nLDL induces platelet aggregation in a dose-dependent manner

A plethora of studies have shown that oxLDL can cause platelet activation and potentiation by platelet agonists (Wraith et al, 2013). However, the mechanisms by which platelet activation and thrombosis occurs remain to be elucidated as oxLDL are a group of heterogenous modified particles. oxLDL in circulation induce platelet hyperactivity and subsequent thrombosis while nLDL does not cause platelet aggregation (Wraith et al., 2013; Berger et al., 2018). Before exploring the effects of oxLDL and nLDL in the actin cytoskeleton of the platelet, it was necessary to determine the oxidative level of LDL. Thus, after oxidation of LDL in MOPS containing 10 µM of $CuSO_4$ across a 24-hour period, the relative electrophoretic mobility of LDL was determined by loading 20 µg of LDL protein into a 0.5% agarose gel. Figure 3.1 demonstrates that the REM of oxLDL was almost 3-fold (2.86±0.27) the control.

Furthermore, to ensure that the oxLDL produced induced the expected aggregation response, washed human platelets were isolated and their activity was studied with thrombin (0.1 U/ml), as a positive control, alongside oxLDL (10, 30 and 50 µg/ml) and nLDL (50 µg/ml) using light transmission aggregometry.

Consistent with previous findings the positive control, thrombin, induced strong aggregation at 2 minutes (figure 3.2). Importantly oxLDL induced a dose-dependent increase in platelet aggregation with the maximum aggregation response and shape change at 50 µg/ml, whereas no aggregation response was observed for nLDL (figure 3.2).

OxLDL can induce platelet activation and aggregation, but we also wanted to understand how it can affect platelet spreading. Before we could identify this, it was necessary to ensure that oxLDL would effectively bind to glass coverslips, and also effectively bind to additional matrix proteins such as fibrinogen. Therefore, glass coverslips were blocked with BSA (5 mg/ml) and coated with fibrinogen Alexa-488, oxLDL (50 μg/ml) as well as the combination of both fibrinogen Alexa-488 and oxLDL (50 μg/ml). The oxLDL was then incubated with E06 (binds to phosphocoline headgroup of oxidised phospholipids present in oxLDL but absent in nLDL) (1.5 mg/ml) for 1 hour at room temperature, before addition of a secondary antibody for 30 minutes at room temperature. Figure 3.3 showed colocalization between the Alexa-488 labelled fibrinogen and E06 stain.

0.5% Agarose gel

A

CuSO$_4$ 10μM   -   +

B
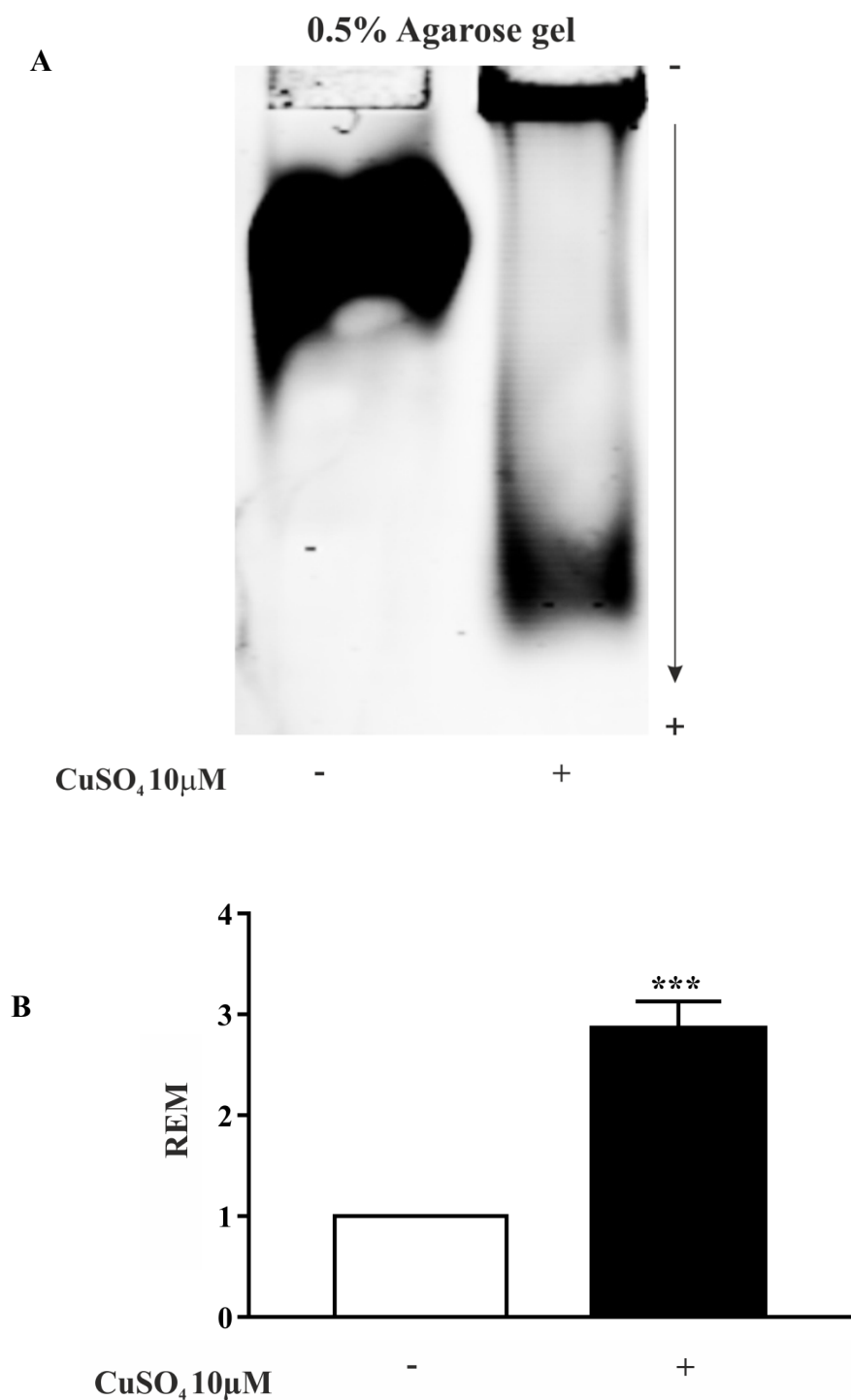
Figure 3.1. Increased relative electrophoretic mobility in oxLDL compared to nLDL.

Isolated LDL was treated with the presence of 10 μM CuSO$_4$ at 37°C (OS-rich) to induce complete oxidation. A) Representative image of 0.5% agarose gel containing 20 μg samples of LDL across 24 hours. Electrophoresis was performed at 100 V for 1 hour in TAE buffer. REM was calculated as the distance travelled from origin. Data shown as mean ± SD (n=4). ***$p<0.001$ relative to control.
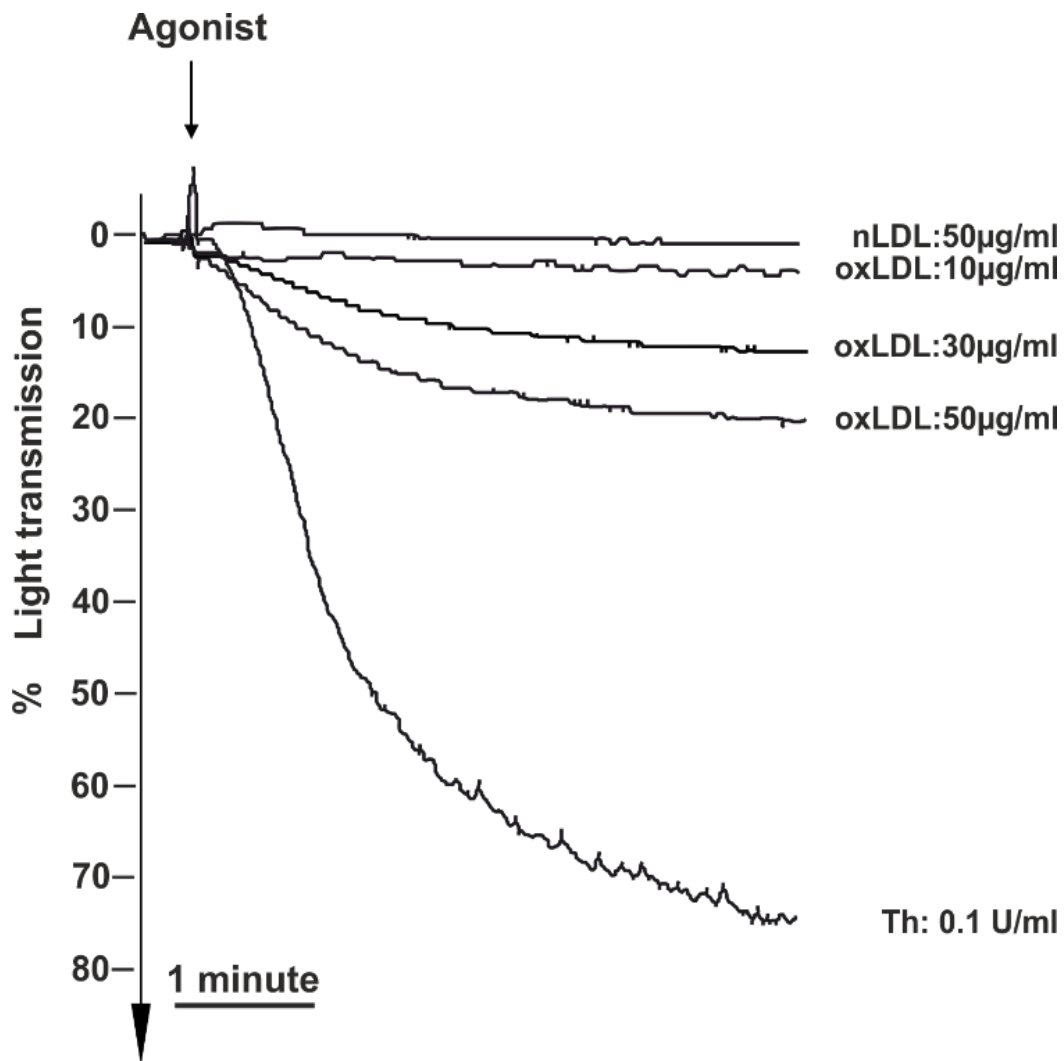
Figure 3.2 oxLDL, but not nLDL induces platelet aggregation in a dose-dependent manner.

Human platelets 3×10^8/ml were treated with thrombin (0.1 U/ml), oxLDL (10 µg/ml, 30 µg/ml, 50 µg/ml) and nLDL (50 µg/ml) for 4 minutes. Aggregation was recorded using a Chrono-Log aggregometer. Traces shown are representative of n=3.
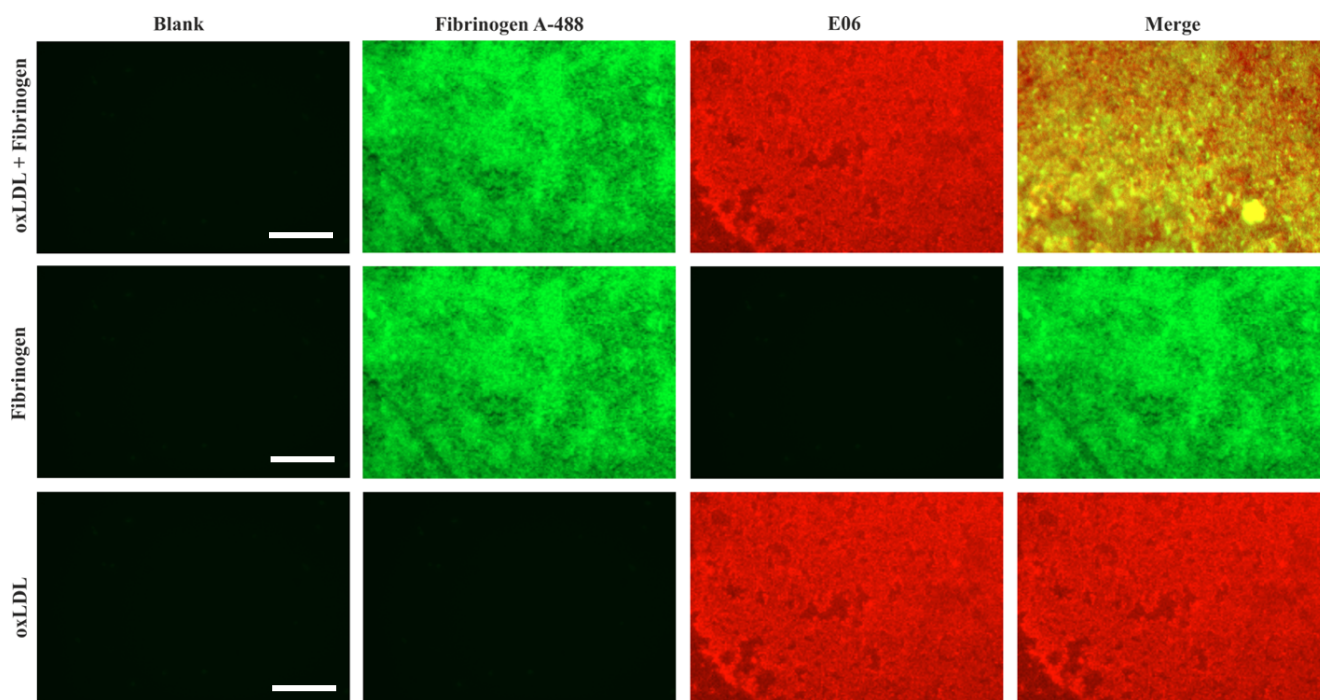
Figure 3.3. Immunofluorescence binding of fibrinogen and oxLDL on coverslips.

Glass coverslips were blocked with BSA (5 mg/ml) and coated with fibrinogen Alexa-488 (green stain), oxLDL (50 µg/ml) as well as the combination of both fibrinogen Alexa-488 and oxLDL (50 µg/ml). oxLDL was incubated with E06 (red stain) (1.5 mg/ml) for 1 hour at room temperature, before addition of a Alexa-594 for 30 minutes at room temperature. Images were taken using an immunofluorescence microscope and images shown are representative of n=3. Scale bar= 20µm.

3.3. Platelet spreading on fibrinogen varies with concentration.

The regulation of platelet activation involves the rapid reorganisation of the actin cytoskeleton. Platelet activation induces the shape change of platelets from biconcave discs to spread cells and is critical for haemostasis and the formation of the haemostatic plug. Having established that fibrinogen and oxLDL effectively bind to glass coverslip, it was then sought to understand how platelets spread on each of these surfaces. Therefore, initially platelets were spread on different concentrations of fibrinogen to determine how the concentration of matrix protein affected platelet spreading. Human platelets ($2x10^7$/ml) were spread on fibrinogen (3-100 µg/ml) coated coverslips for 45 minutes at room temperature. Adhered platelets were subsequently fixed, permeabilised and stained using FITC phalloidin and visualised under a fluorescence microscope. Platelet spreading was measured and analysed using the ImageJ software and the number of platelets was counted to determine platelet adhesion.

As previously published, the concentration of fibrinogen altered platelet spreading (Jiroušková, Jaiswal and Coller, 2007; Qiu et al., 2014). As the concentration of fibrinogen increased, there was a significant reduction in platelet surface area reducing from 37.25±5.74 µm^2 at 3 µg/ml to 23.47±3.66 µm^2 at 30 µg/ml and 20.79±2.98 µm^2 at 100 µg/ml (figure 3.4 A,B). However, there was no significant change in platelet adhesion for all concentrations of fibrinogen (figure 3.4C).

A

3μg/ml Fibrinogen   30μg/ml Fibrinogen   100μg/ml Fibrinogen

B

C
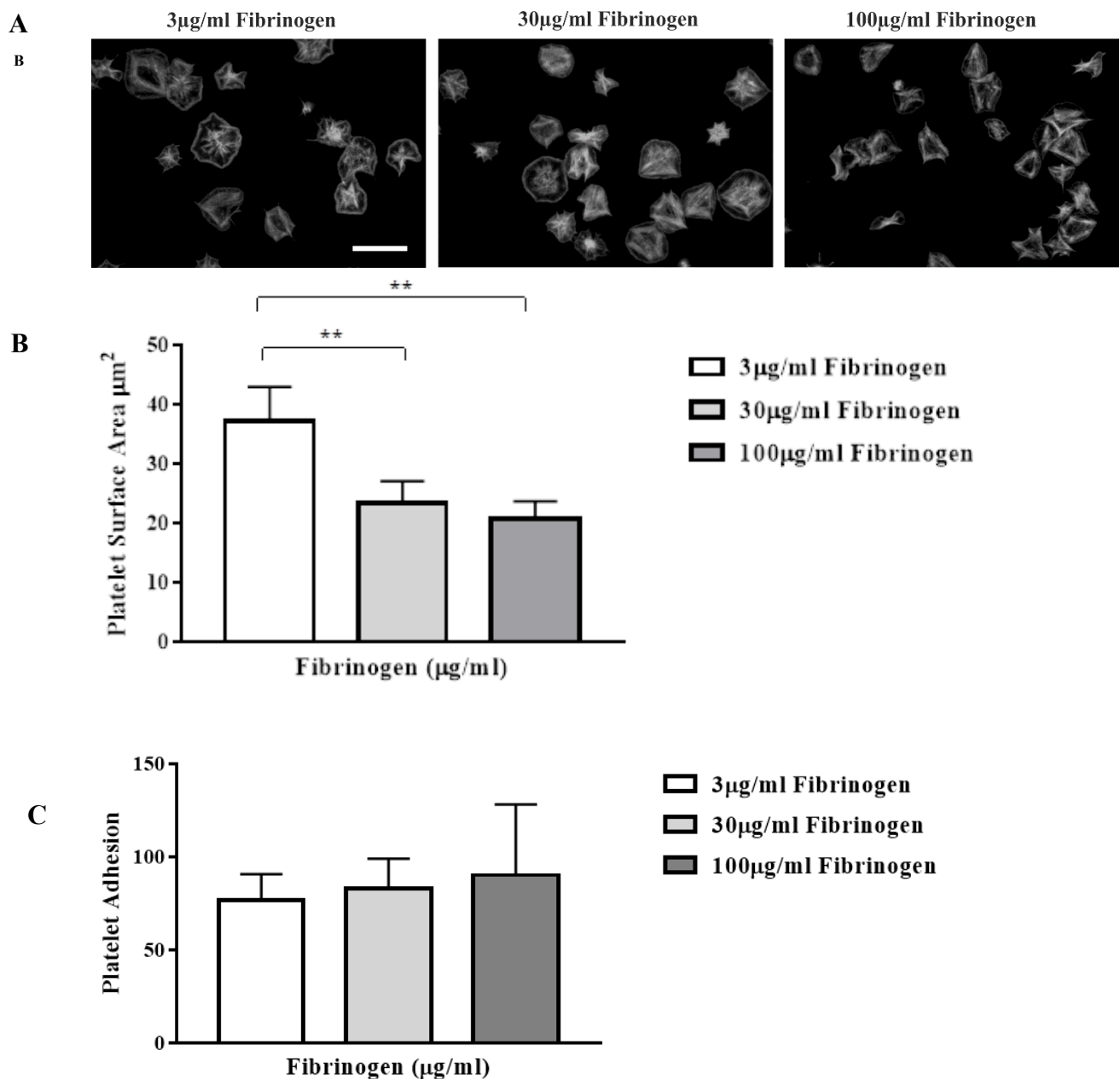
Figure 3.4. Fibrinogen reduces the surface area of platelets in a dose-dependent manner.

Coverslips were coated with 3-100 μg/ml fibrinogen overnight at 4°C before coating with BSA (5 mg/ml) for 1 hour at room temperature. Human platelets (2×10^7/ml) were then incubated on coverslips for 45 minutes at room temperature. Adhered platelets were fixed using formaldehyde, permeabilised using Triton X-100 (0.1%) and stained using FITC phalloidin. **A)** Images are representative of each condition. **B)** Fibrinogen reduces the surface area of platelets in a dose-dependent manner. **C)** Platelet adhesion is not affected by fibrinogen concentration. Data shown as mean ± SD (n=3). ** $p<0.01$ relative to control. Scale bar= 20μm.

3.4. oxLDL but not nLDL induces an increase in platelet spreading in a dose-dependent manner

To determine the platelet actin cytoskeletal rearrangements induced in response to oxLDL and nLDL, human washed platelets ($2x10^7$/ml) were spread on oxLDL or nLDL coated coverslips (10 µg/ml, 30 µg/ml, 50 µg/ml) for 45 minutes. Adhered platelets were subsequently fixed using formaldehyde, permeabilised, stained using FITC phalloidin and visualised under a fluorescence microscope. Platelet spreading was measured and analysed using the ImageJ software and the number of platelets was counted to determine platelet adhesion.

As expected, there was little platelet adhesion to nLDL, even with increasing concentrations. Furthermore, those platelets that did adhere did not spread, even at 50 µg/ml nLDL (figure 3.5A). However, in contrast, oxLDL induced a dose-dependent increase in both platelet adhesion and platelet surface area. oxLDL induced an increase in platelet adhesion from (38.89±37.73) at 10 µg/ml to (109.22±29.73) at 50 µg/ml (figure 3.5 B and C). Furthermore, the surface area of the platelets spread on oxLDL at 10 µg/ml was 22.70±3.74 μm^2 which increased to 31.45±1.48 μm^2 at 30 µg/ml and 40.88±4.18 μm^2 at 50 µg/ml. Importantly, there was also a significant increase in platelet adhesion and platelet surface area between oxLDL and nLDL for all concentrations.
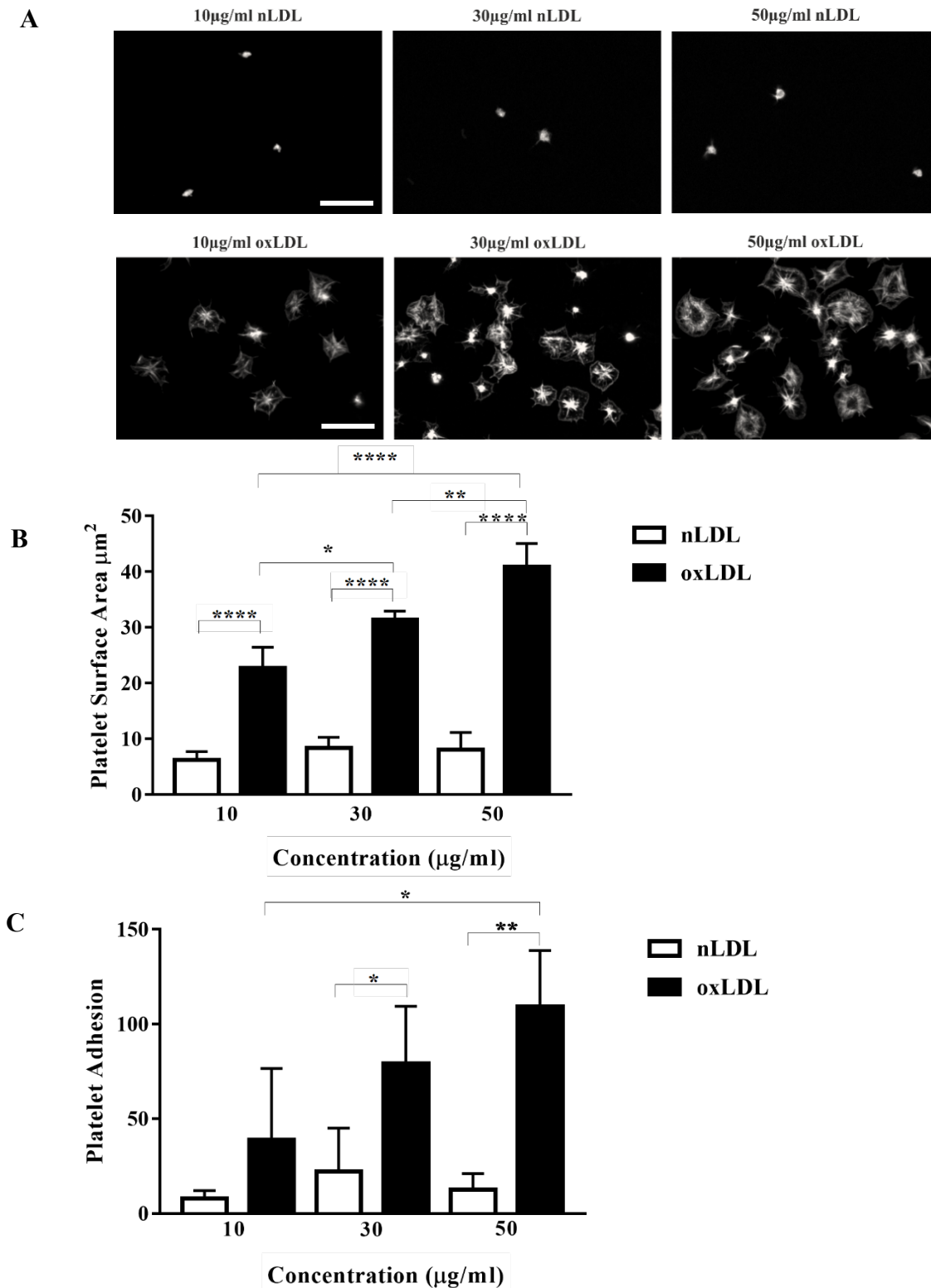
Figure 3.5. OxLDL but not nLDL induces an increase in platelet adhesion and spreading in a dose-dependent manner.

Human platelets (2×10^7/ml) were incubated on oxLDL or nLDL treated coverslips (10 µg/ml, 30 µg/ml, 50 µg/ml) for 45 minutes at room temperature. Adhered platelets were subsequently fixed using formaldehyde, permeabilised using Triton X-100 (0.1%) and stained using FITC phalloidin. **A)** Representative images for each condition. **B)** OxLDL induces an increase in platelet surface area in a dose-dependent manner. **C)** oxLDL induces an increase in platelet adhesion in a dose-dependent manner. Data shown as mean ± SD (n=3). * $p<0.05$. ****$p<0.0001$. ** $p<0.01$ relative to control. Scale bar= 20µm.

3.3.1. Combination of fibrinogen with oxLDL induces a change in platelet spreading

Upon determining the individual effects of fibrinogen, nLDL and oxLDL on platelet spreading, the effect of combining nLDL or oxLDL with fibrinogen was studied. As a result, coverslips were coated with 3-100 μg/ml fibrinogen overnight at 4°C before coating with nLDL or oxLDL (10 μg/ml, 30 μg/ml and 50 μg/ml) for 1 hour at room temperature. Human platelets $(2x10^7/ml)$ were then incubated on the coverslips for 45 minutes at room temperature before fixation, permeabilization, stained using FITC phalloidin and imaged under a fluorescence microscope. Platelet spreading was measured and analysed using the ImageJ software and the number of platelets was counted to determine platelet adhesion.

Analysis of the fibrinogen in combination with nLDL demonstrates that nLDL induces an inhibitory effect on low dose fibrinogen (3 μg/ml). In combination with 10 μg/ml nLDL the platelet surface area reduced to 18.59 ± 5.55 μm^2 whilst at 30 μg/ml and 50 μg/ml the surface area of the platelets was reduced to 20.75 ± 7.24 μm^2 and 23.60 ± 6.13 μm^2 respectively in comparison to the control (37.26 ± 5.74 μm^2) (figure 3.6B). However, combination with nLDL had no effect on platelet adhesion (Figure 3.6C).

In contrast, at higher concentrations of fibrinogen there was no effect of addition of nLDL on platelet spreading or platelet adhesion. (figure 3.7 &3.8)

A

3μg/ml Fibrinogen

10μg/ml oxLDL   30μg/ml oxLDL   50μg/ml oxLDL

B

Platelet Surface Area μm²

□ Control
▨ 10μg/ml nLDL
▨ 30μg/ml nLDL
■ 50μg/ml nLDL

3μg/ml Fibrinogen

C

Platelet Adhesion

□ Control
▨ 10ug/ml nLDL
▨ 30ug/ml nLDL
■ 50ug/ml nLDL
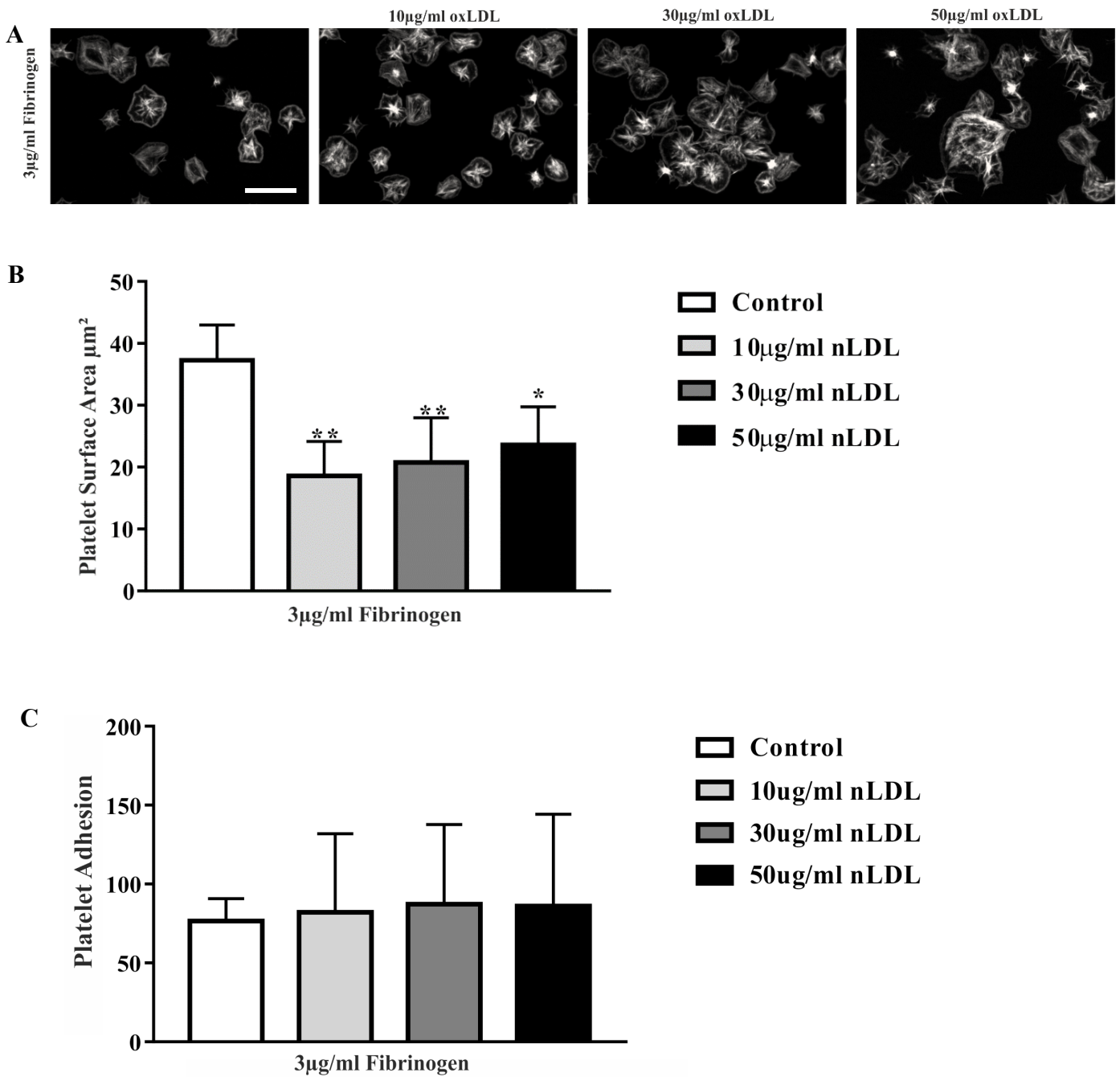
3μg/ml Fibrinogen

Figure 3.6. **nLDL induces a reduction in platelet spreading in low dose fibrinogen**

Coverslips were coated with 3 μg/ml fibrinogen overnight at 4°C and nLDL (10 μg/ml, 30 μg/ml and 50 μg/ml) for 1 hour at room temperature. Human platelets ($2x10^7$/ml) were incubated for 45 minutes at room temperature. Adhered platelets were subsequently fixed using formaldehyde, permeabilised using Triton X-100 (0.1%) and stained using FITC phalloidin. **A)** immunofluorescence was detected by FITC labelled phalloidin. **B)** nLDL induces reduced surface area of platelets. **C)** No effect observed in platelet adhesion. Data shown as mean ± SD (n=3). ** $p<0.01$ * $p<0.05$ relative to control. Scale bar= 20μm.

A

10μg/ml nLDL   30μg/ml nLDL   50μg/ml nLDL

30μg/ml Fibrinogen

B

Platelet Surface Area μm²

30μg/ml Fibrinogen

Control
10μg/ml nLDL
30μg/ml nLDL
50μg/ml nLDL

C

Platelet Adhesion

30μg/ml Fibrinogen

Control
10μg/ml nLDL
30μg/ml nLDL
50μg/ml nLDL
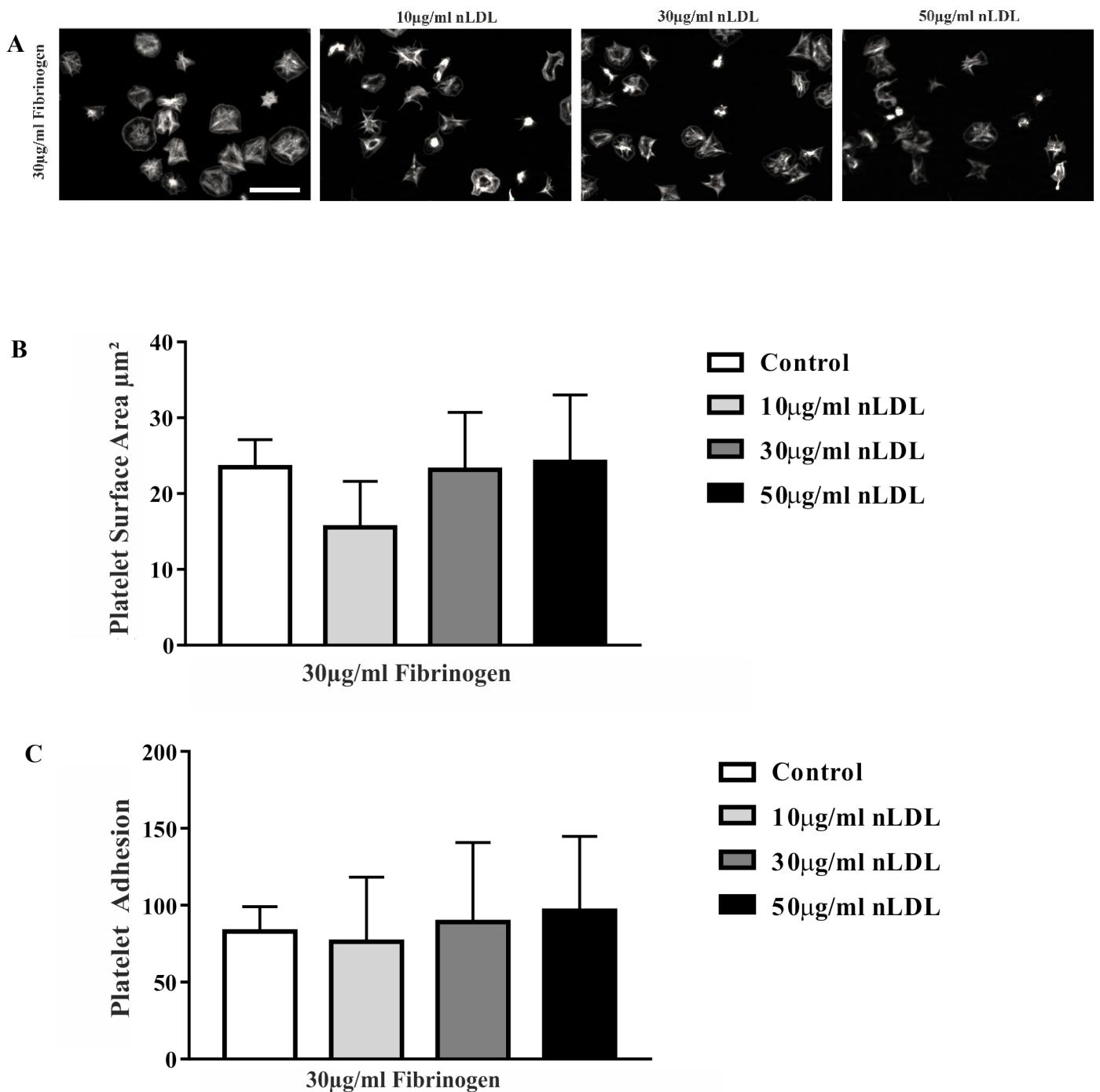
Figure 3.7. nLDL does not induce platelet spreading or adhesion.

Coverslips were coated with 30 μg/ml fibrinogen overnight at 4°C and nLDL (10 μg/ml, 30 μg/ml and 50 μg/ml) for 1 hour at room temperature. Human platelets (2×10^7/ml) were incubated for 45 minutes at room temperature. Adhered platelets were subsequently fixed using formaldehyde, permeabilised using Triton X-100 (0.1%) and stained using FITC phalloidin. **A)** immunofluorescence was detected by FITC labelled phalloidin. **B)** nLDL does not affect the surface area of platelets in a dose-dependent manner. **C)** No affect observed in platelet adhesion. Data shown as mean ± SD (n=3). ** $p < 0.01$ * $p < 0.05$ relative to control. Scale bar= 20μm.
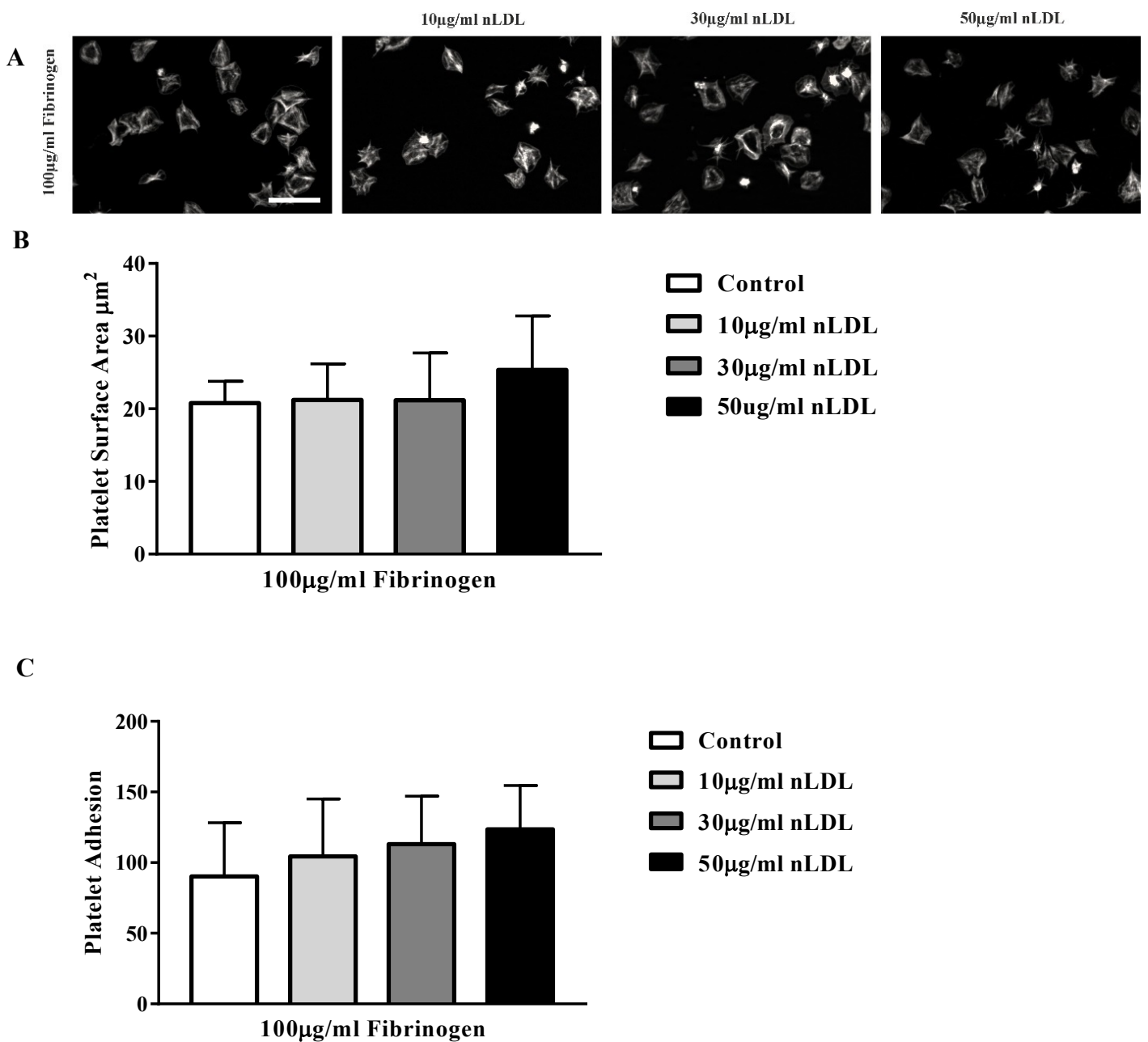
Figure 3.8. nLDL does not induce platelet spreading or adhesion on high dose fibrinogen.

Coverslips were coated with 100 µg/ml fibrinogen overnight at 4°C and nLDL (10 µg/ml, 30 µg/ml and 50 µg/ml) for 1 hour at room temperature. Human platelets ($2x10^7$/ml) were incubated for 45 minutes at room temperature. Adhered platelets were subsequently fixed using formaldehyde, permeabilised using Triton X-100 (0.1%) and stained using FITC phalloidin. **A)** Images are representative of each condition. **B)** nLDL does not affect the surface area of platelets in a dose-dependent manner. **C)** No affect observed in platelet adhesion. Data shown as mean ± SD (n=3). ** $p<0.01$ * $p<0.05$ relative to control. Scale bar= 20µm.

3.4.1. Increase in platelet surface area in high dose oxLDL combination

Analysis of the fibrinogen and oxLDL combinations identified that platelets spread on 3 µg/ml fibrinogen with oxLDL showed a reduction of the surface area from 21.53 ± 9.40 µm^2 in comparison to 37.26 ± 5.74 µm^2 for the control (figure 3.9 B). However, with 30 µg/ml and 50 µg/ml oxLDL the surface area increased back to the level of the control (figure 3.9 B). Interestingly there was no change in platelets adhesion in the presence of oxLDL for all concentrations (figure 3.9 C).

Analysis of spread platelets on 30 µg/ml fibrinogen with or without oxLDL identified that there was a significant increase in platelet surface area between the lowest dose of oxLDL,10 µg/ml oxLDL (18.74 ± 1.83 µm^2) and highest dose, 50 µg/ml oxLDL (34.29 ± 6.71 µm^2) (figure 3.10 B). Although an increasing trend in platelet adhesion was observed with increasing concentrations of oxLDL, there was no significant increase in number of platelets adhered across all concentrations (3.10 C).

Analysis of spread platelets on 100 µg/ml fibrinogen in combination with varying concentrations of oxLDL identified that there was a significant increase in platelet surface area between fibrinogen & 10 µg/ml oxLDL ($20.54+7.09$ µm^2) and fibrinogen & 50 µg/ml oxLDL (33.43 ± 6.61 µm^2) (figure 3.11 B). Although an increasing trend in platelet adhesion was observed with increasing concentrations of oxLDL, there was no significant increase in number of platelets adhered across all concentrations (3.11 C).

A

3µg/ml Fibrinogen | 10µg/ml oxLDL | 30µg/ml oxLDL | 50µg/ml oxLDL

B

Platelet Surface Area µm²

Control
10µg/ml oxLDL
30µg/ml oxLDL
50µg/ml oxLDL

3µg/ml Fibrinogen

C

Platelet Adhesion

Control
10µg/ml oxLDL
30µg/ml oxLDL
50µg/ml oxLDL
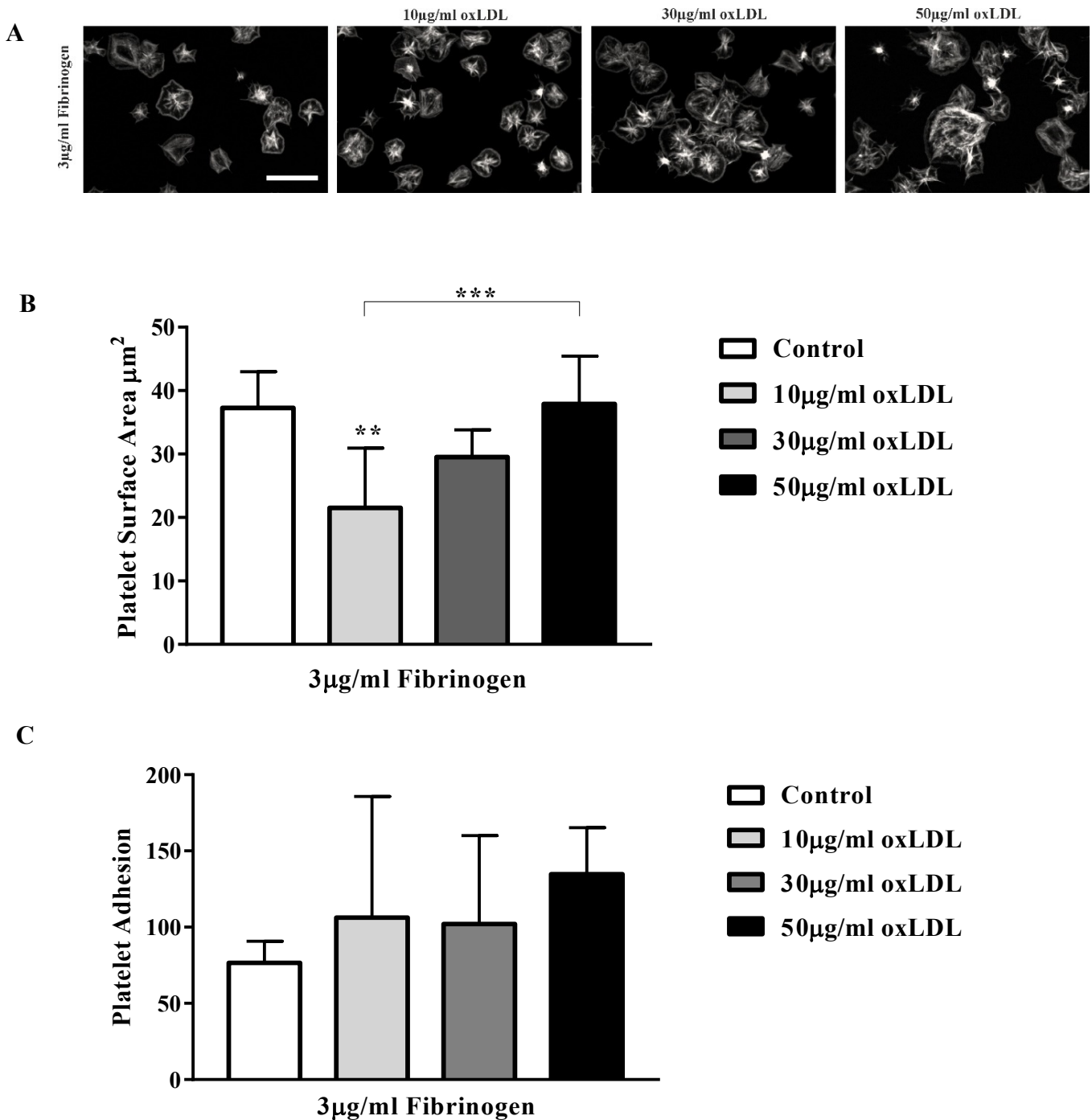
3µg/ml Fibrinogen

Figure 3.9. Increase in platelet surface area observed in high dose oxLDL combination.

Coverslips were coated with 3 µg/ml fibrinogen overnight at 4°C before coating with oxLDL (10 µg/ml, 30 µg/ml and 50 µg/ml) for 1 hour at room temperature. Human platelets ($2x10^7$/ml) were then incubated on the coverslips for 45 minutes at room temperature before fixation, permeabilization, stained and imaging. **A)** Images are representative of each condition. **B)** The combination of oxLDL and fibrinogen induces platelet spreading. **C)** oxLDL does not induce a change in platelet adhesion. Data shown as mean ± SD (n=3 for control and n=5 for combinations). *** $p<0.001$ relative to control. Scale bar= 20µm.

135

A 30µg/ml Fibrinogen | 10µg/ml oxLDL | 30µg/ml oxLDL | 50µg/ml oxLDL

B

C

Figure 3.10. The combination of oxLDL and fibrinogen enhances platelet surface area.

Coverslips were coated with 30 µg/ml fibrinogen overnight at 4°C before coating with oxLDL (10 µg/ml, 30 µg/ml and 50 µg/ml) for 1 hour at room temperature. Human platelets (2×10^7/ml) were then incubated on the coverslips for 45 minutes at room temperature before fixation, permeabilization, staining and imaging. **A)** Images are representative of each condition **B)** The combination of oxLDL and fibrinogen induces platelet spreading. **C)** oxLDL does not induce a change in platelet adhesion. Data shown as mean ± SD (n=3 for control and n=5 for combinations). *** $p<0.001$ relative to control. Scale bar= 20µm.

A

B

C
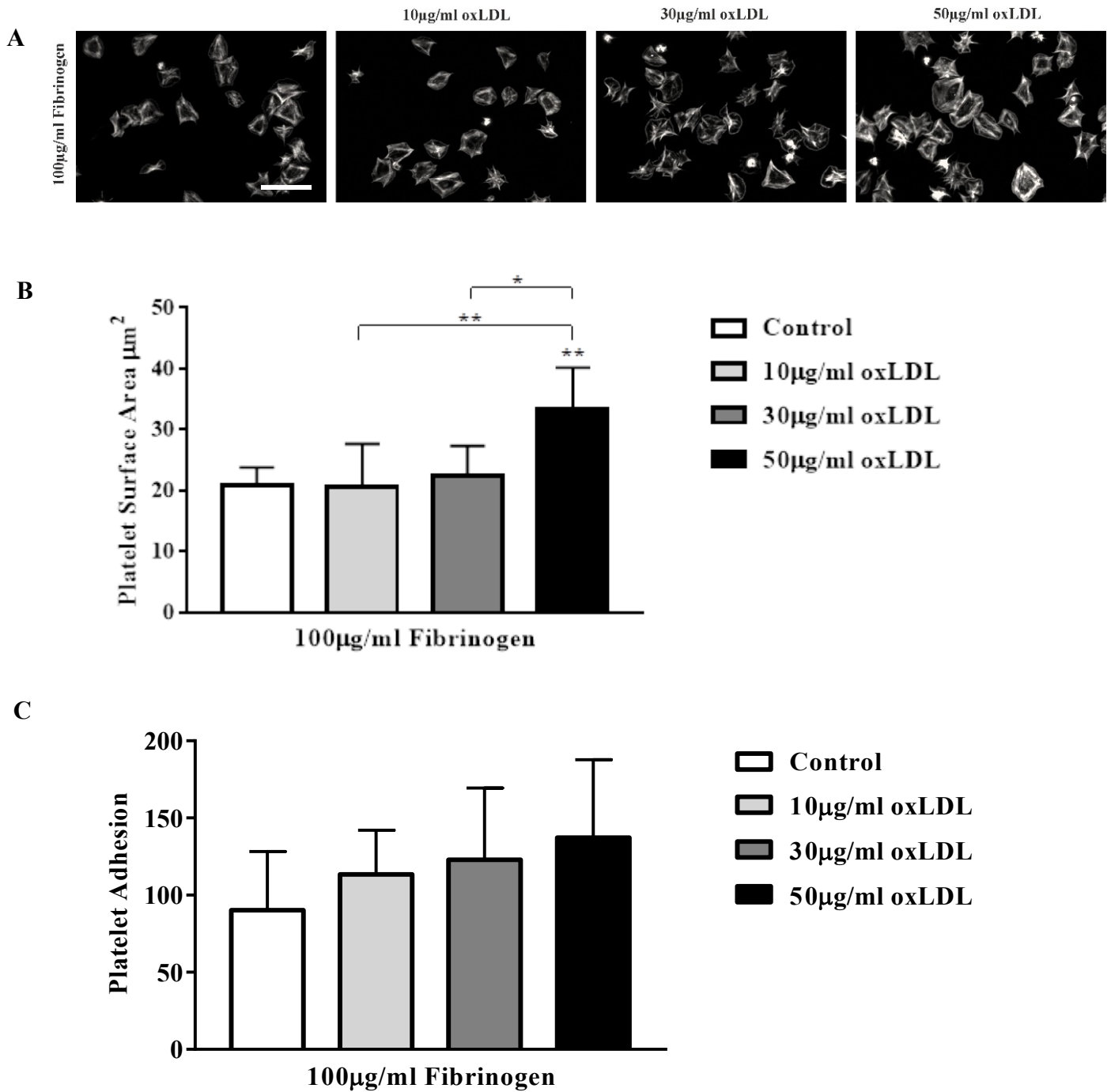
Figure 3.11. The combination of high dose oxLDL and fibrinogen increases platelet surface area.

Coverslips were coated with 100 µg/ml fibrinogen overnight at 4°C before coating with oxLDL (10 µg/ml, 30 µg/ml and 50 µg/ml) for 1 hour at room temperature. Human platelets (2×10^7/ml) were then incubated on the coverslips for 45 minutes at room temperature before fixation, permeabilization, stained and imaging. **A)** Images are representative of each condition **B)** The combination of oxLDL and fibrinogen induces platelet spreading**. C)** oxLDL does not induce platelet adhesion. Data shown as mean ± SD (n=3 for control and n=5 for combinations). * $p<0.05$ ** $p<0.01$ relative to control. Scale bar= 20µm.

3.5. PGI$_2$ causes reversal of platelet spreading on fibrinogen spread platelets

Under normal physiological conditions, the endothelium is intact and spontaneous activation of platelets is prevented to avoid thrombosis. Intracellular signalling pathways that promote platelet activation are controlled meticulously by mechanisms that negatively regulate platelet activation. Negative regulators of platelet activation such as NO and PGI$_2$ are platelet antagonists that inhibit adhesion and activation of platelets (Mitchell et al., 2007). It has been described that PGI$_2$ is involved in continuously inhibiting platelets before activation and is present in the circulation at 10 pM which is the threshold concentration necessary in the body (FitzGerald et al., 1981).Therefore, as PGI$_2$ is crucial in the regulation of a thrombus and plays a pivotal role in inhibiting platelets in the vasculature, understanding how other signalling pathways can modulate its function in spread platelets would help identify how platelets activate thrombus formation.

To identify if PGI$_2$ induces cytoskeletal rearrangements in platelets already spread on Fibrinogen and oxLDL combinations, washed human platelets ($2x10^7$/ml) were incubated on coverslips coated with 100 μg/ml fibrinogen, 50 μg/ml nLDL, or 50 μg/ml oxLDL for 20 minutes at room temperature and treated with 10 nM PGI$_2$ for 10 minutes. Adhered platelets were subsequently fixed using formaldehyde, permeabilised, stained using FITC phalloidin and imaged under a fluorescence microscope.

Analysis of the spread platelets on fibrinogen alone identified that incubation with 10 nM PGI$_2$ for 10 minutes resulted in a significant decrease in platelet surface area 17.72 ± 1.50 μm^2 in comparison to the control 26.55 ± 2.03 μm^2 (figure 3.12 B). However, there was no effect observed on platelet adhesion in the presence of 10 nM PGI$_2$ in comparison to the control

138

(figure 3.12 C). In alignment with this, figure 3.12 D showed that 10 nM PGI_2 stimulation induced an increase in actin nodule formation from 23.41±4.21% in the control platelets, to 78.45±3.28% in the platelets stimulated with 10 nM PGI_2. Additionally, as expected, stress fibre reversal in the presence of 10 nM PGI_2 was observed from 69.50±5.75% in the control to 18.81±3.80% upon treatment with 10 nM PGI_2 (figure 3.12 E).

Analysis of the spread platelets indicated that the surface area of platelets spread on 100 µg/ml fibrinogen and 50 µg/ml nLDL showed no difference to those spread on fibrinogen alone, in terms of platelet adhesion, surface area, actin nodule number, or stress fibre containing platelets (figure 3.13). As expected, figure 3.13 B demonstrated that treatment with PGI_2 significantly reduced the surface area from 20.68± 2.03 μm^2 to 17.72±1.50 μm^2 whilst the percentage of platelets with actin nodules significantly increased from 20.49±3.36% in the control sample to 80.11±5.65% (figure 3.13 D). Further, figure 3.13 E showed a significant reduction in percentage of platelets with stress fibres was evident with 10.48±2.67% of the platelets spread on 100 µg/ml fibrinogen in combination with 50 µg/ml nLDL having stress fibres after stimulation with 10 nM PGI_2 in comparison to 71.23±4.49% in the control. The number of platelets adhered was not affected in any condition.
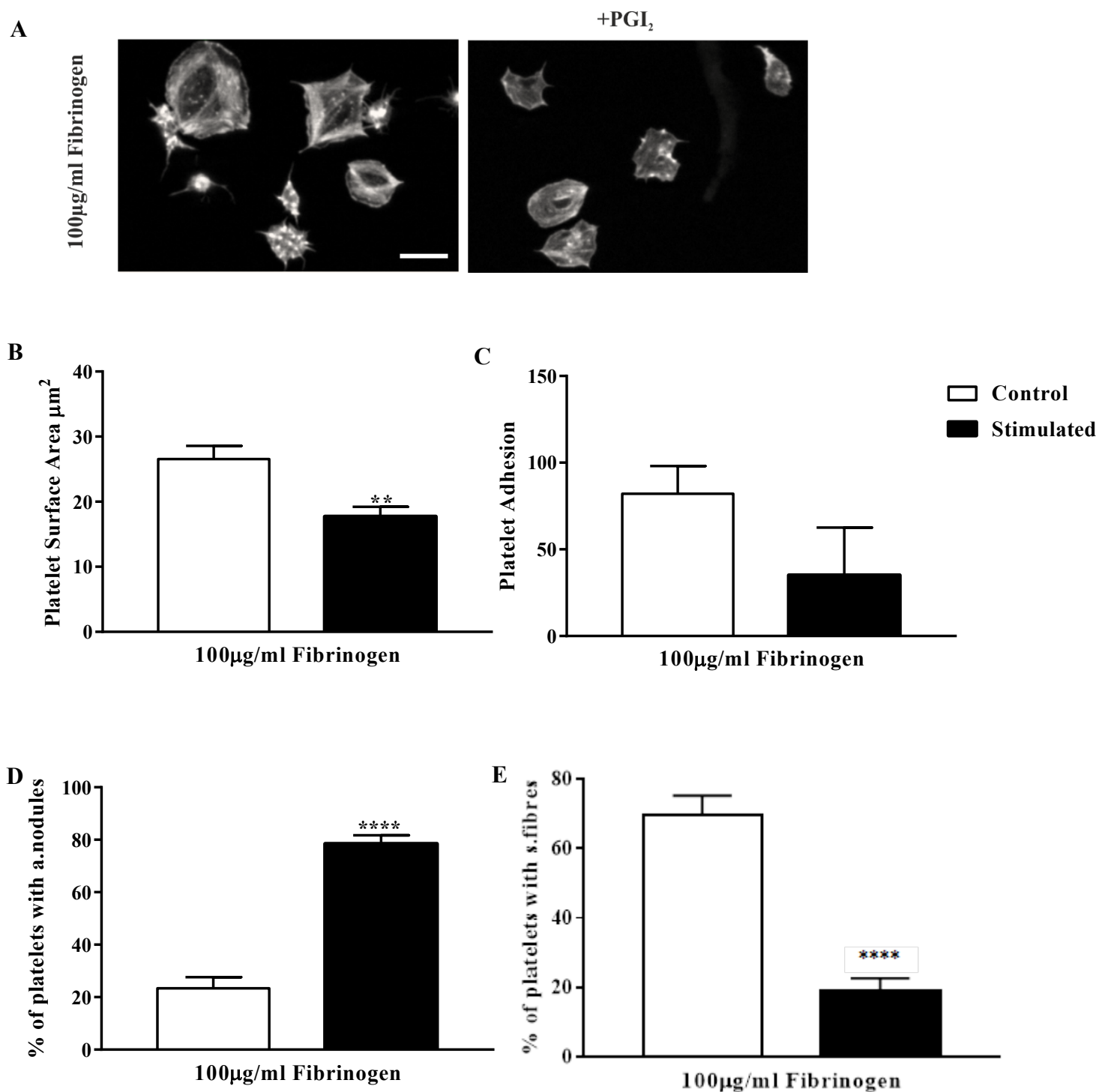
Figure 3.12. PGI$_2$ has an inhibitory effect on fibrinogen spread platelets.

Coverslips were coated with 100 µg/ml fibrinogen overnight at 4°C. Human platelets ($2x10^7$/ml) were incubated on coverslips for 20 minutes at room temperature. Platelets were treated with 10 nM PGI$_2$ for 10 minutes. Adhered platelets were subsequently fixed using formaldehyde, permeabilised using Triton X-100 (0.1%) and stained using FITC phalloidin. **A)** Images are representative of each condition. **B)** PGI$_2$ reduces the surface area of fibrinogen spread platelets. **D)** PGI$_2$ induces actin nodule formation. **E)** PGI$_2$ induces stress fibre reversal ** $p<0.01$ *** $p<0.001$ relative to control. Scale bar= 20µm.
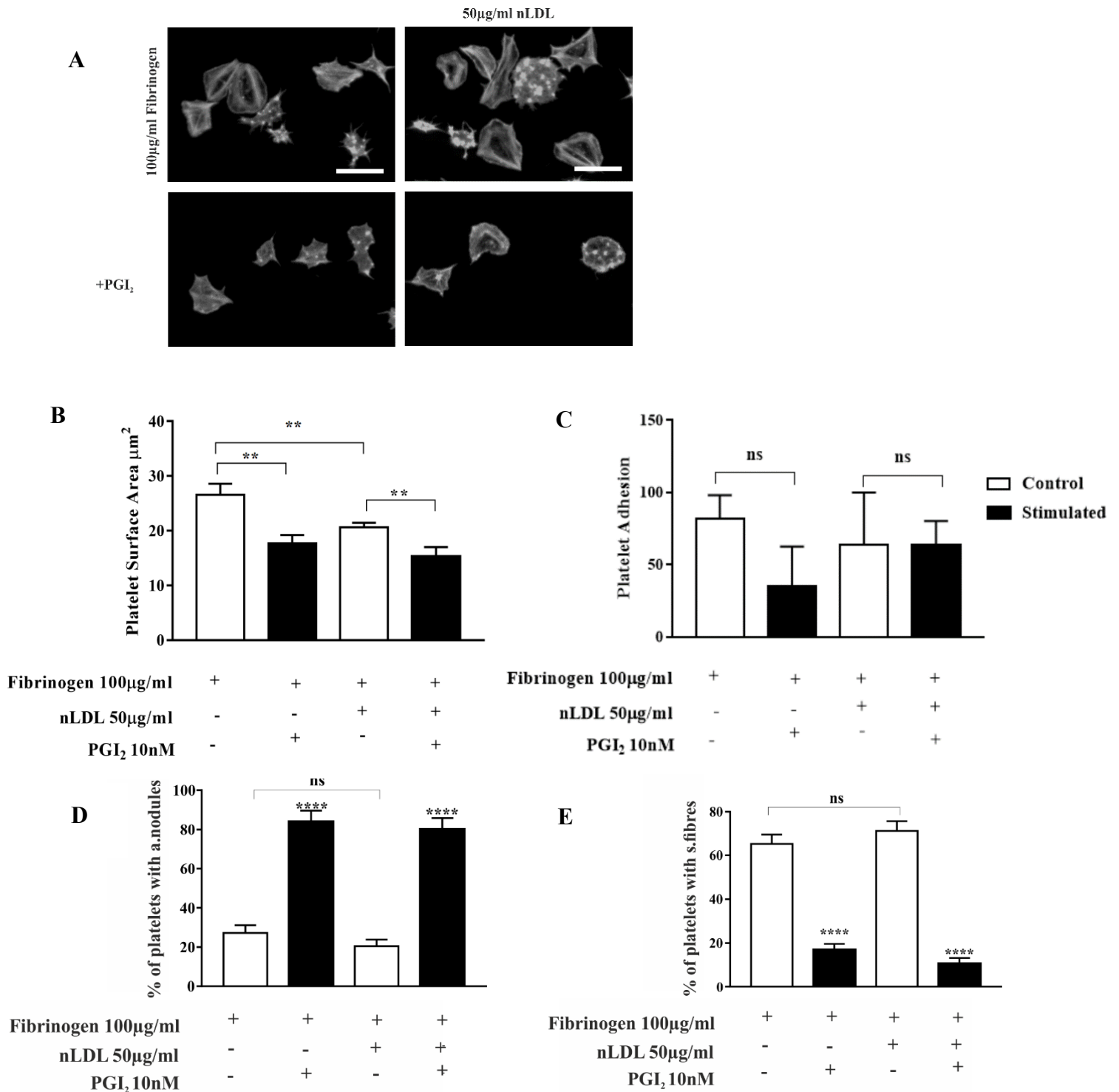
Figure 3.13. PGI$_2$ has an inhibitory effect on nLDL and fibrinogen spread platelets.

Coverslips were coated with 100 µg/ml fibrinogen overnight at 4°C and 50 µg/ml nLDL for 1 hour at room temperature. Human platelets (2x10^7/ml) were incubated on coverslips for 20 minutes at room temperature. Platelets were treated with 10 nM PGI$_2$ for 10 minutes. Adhered platelets were subsequently fixed using formaldehyde, permeabilised using Triton X-100 (0.1%) and stained using FITC phalloidin. **A)** Images are representative of each condition **B)** PGI$_2$ reduces he surface area of nLDL and fibrinogen spread platelets. **D+E)** PGI$_2$ induces actin nodule formation and stress fibre reversal. ** $p<0.01$ *** $p<0.001$ relative to control. Scale bar = 20 µm.

141

3.6. oxLDL but not nLDL attenuates the effect of PGI$_2$ in platelets

Having identified that platelet spreading on fibrinogen induced stress fibre reversal in the presence of PGI$_2$, we then investigated the effect of combining oxLDL and fibrinogen. Therefore, washed human platelets (2×10^7/ml) were incubated on coverslips coated with 100 µg/ml fibrinogen, 100 µg/ml fibrinogen & 50 µg/ml nLDL, or 100 µg/ml fibrinogen & 50 µg/ml oxLDL for 20 minutes at room temperature and treated with 10 nM PGI$_2$ for 10 minutes. Adhered platelets were subsequently fixed using formaldehyde, permeabilised, stained using FITC phalloidin and imaged under a fluorescence microscope.

nLDL induced little platelet adhesion and supported no platelet spreading (figure 3.14). Therefore, PGI$_2$ had little effect on platelet adhesion, or surface area. Stress fibre and actin nodule formation was not possible to analyse due the lack of platelet spreading. However, oxLDL attenuated the effect of post treatment of 10 nM PGI$_2$ in spread platelets as there was no significant change in platelet surface area from oxLDL control sample (44.53 ± 2.78 µm^2) to 43.97 ± 5.01 µm^2 in the presence of 10 nM PGI$_2$. There was also no change in platelet stress fibre formation nor in platelet adhesion (figure 3.14C).

Importantly there was a significant increase in surface area of spread platelets spread on oxLDL+ fibrinogen (36.43 ± 7.98 µm^2) in comparison to fibrinogen alone ($26.55 + 17.71$ µm^2) (Figure 3.15 B). Analysis of platelets spread on fibrinogen and oxLDL indicated that there was no significant difference in the number of platelets adhered in the presence of both 100 µg/ml fibrinogen and 50 µg/ml oxLDL after stimulation with 10 nM PGI$_2$ (figure 3.15 C). However, treatment with PGI$_2$ induced a significant reduction in surface area in control conditions but caused no change in surface area in platelets in the presence of oxLDL and fibrinogen.

Although there was no change in platelet surface area, interestingly there was a difference in the actin structures. Analysis of stress fibres and actin nodules indicated that addition of PGI_2 still induced stress fibre reversal and actin nodule formation, with 86.91±6.43% of platelets spread on 100 µg/ml fibrinogen and 50 µg/ml oxLDL combination had actin nodules after treatment with 10 nM PGI_2 in comparison to the control (8.05±2.52%) figure 3.15 D. This was mirrored by a significant reduction in platelets containing stress fibres, from 95.59±5.96% in the control to 5.93±2.98% in 10 nM PGI_2 stimulated platelets (figure 3.15 E).

This demonstrates that although oxLDL prevented the reduction in platelet surface area induced by PGI_2, it did not prevent the collapse of stress fibres and the formation of actin nodules in the presence of fibrinogen.

A

50μg/ml nLDL   50μg/ml oxLDL

+PGI$_2$

B

nLDL 50μg/ml	-	-	+	+
oxLDL 50μg/ml	+	+	-	-
PGI$_2$ 10nM	-	+	-	+

C

nLDL 50μg/ml	-	-	+	+
oxLDL 50μg/ml	+	+	-	-
PGI$_2$ 10nM	-	+	-	+
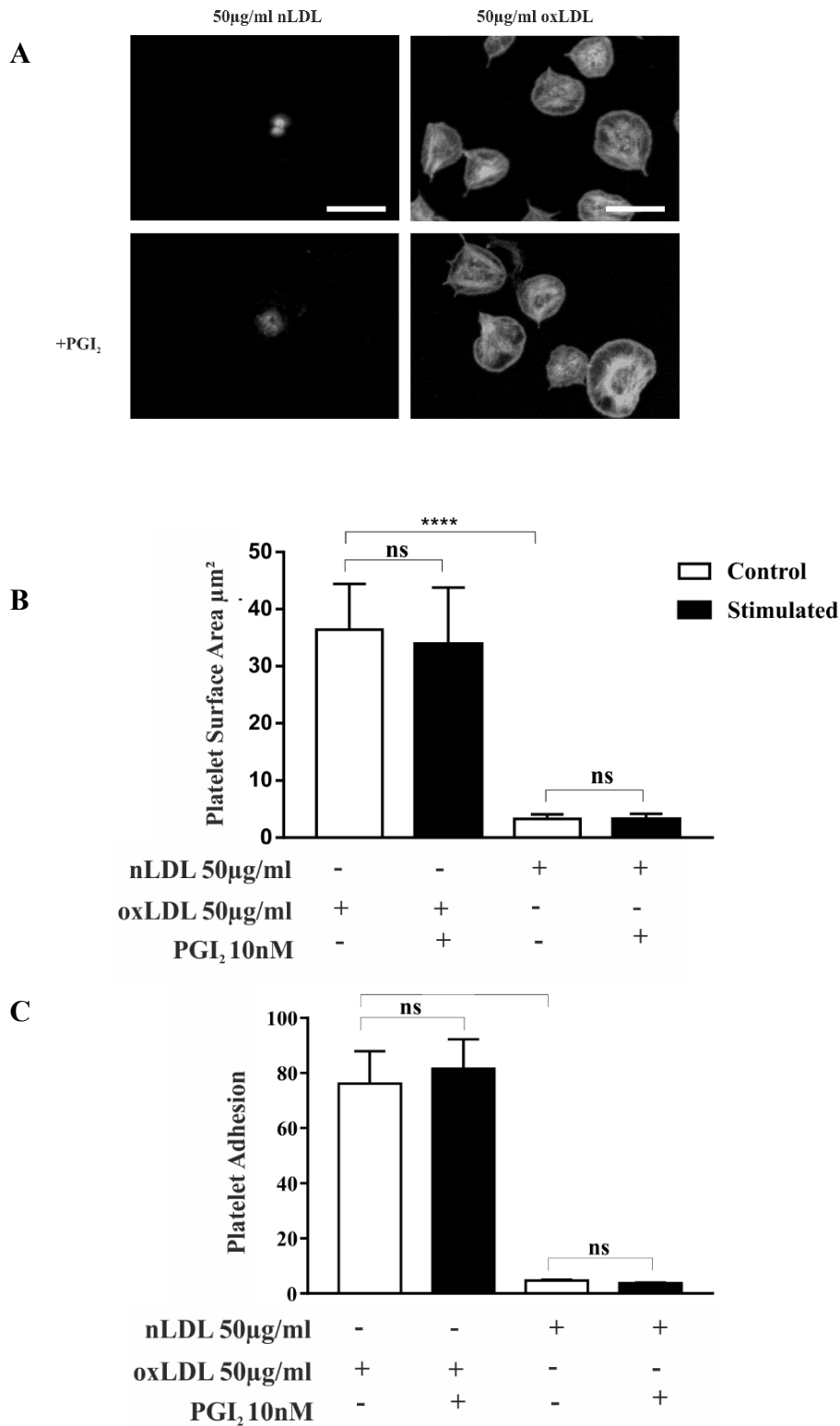
Figure 3.14. oxLDL attenuates the effect of PGI$_2$ in platelets.

Coverslips were coated with 50 μg/ml oxLDL or nLDL for 1 hour at room temperature. Human platelets ($2x10^7$/ml) were incubated on coverslips for 20 minutes at room temperature. Platelets were treated with 10 nM PGI$_2$ for 10 minutes. Adhered platelets were subsequently fixed using formaldehyde, permeabilised using Triton X-100 (0.1%) and stained using FITC phalloidin. **A)** Images are representative of each condition. **B)** Average Surface Area **C)** Platelet adhesion. n=3 * P>0.05 relative to control. Scale bar= 20μm.
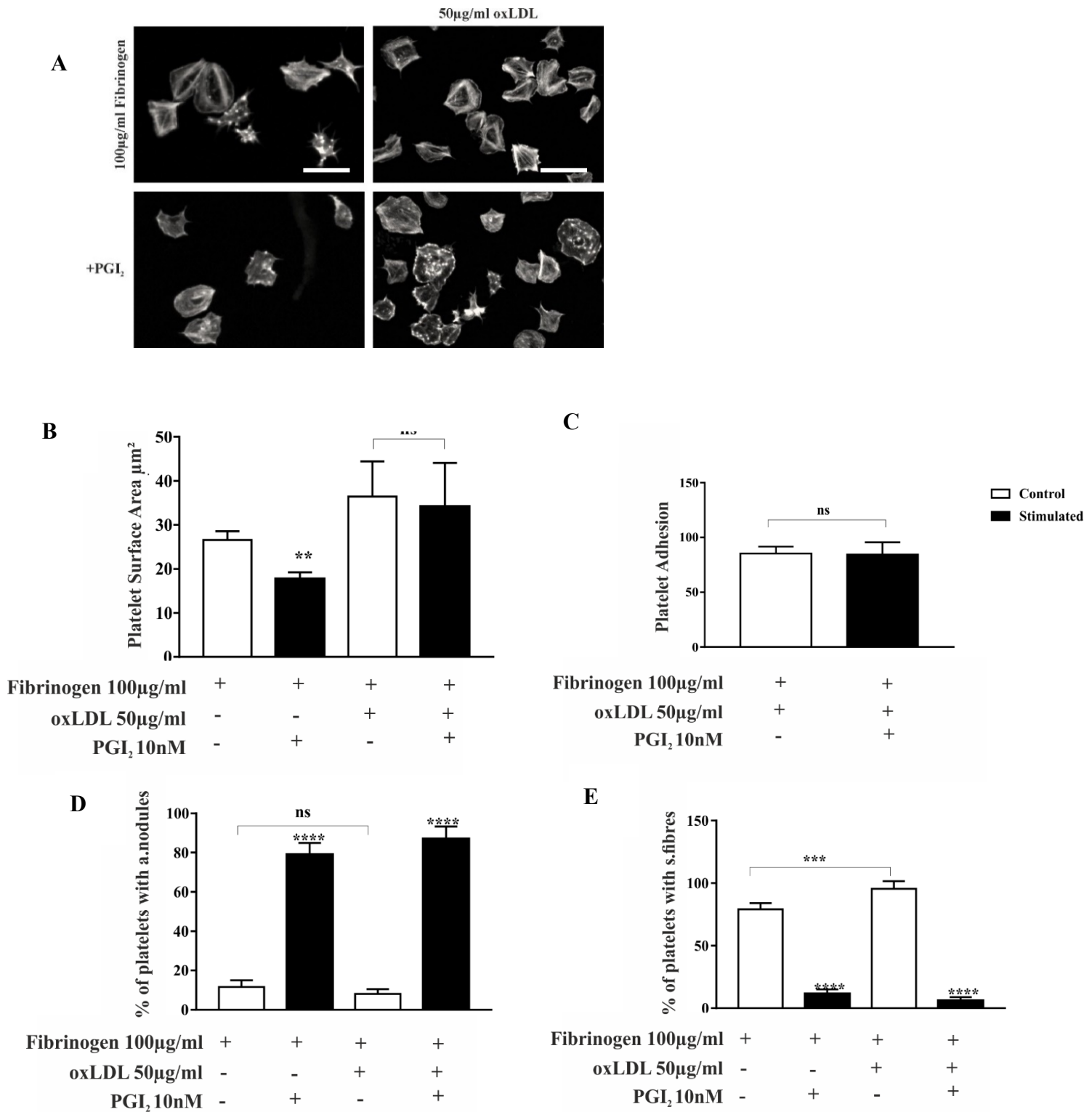
Figure 3.15. The effect of PGI$_2$ is attenuated in the presence of oxLDL.

Coverslips were coated with 100 µg/ml fibrinogen overnight at 4°C and 50 µg/ml oxLDL for 1 hour at room temperature. Human platelets (2×10^7/ml) were incubated on coverslips for 20 minutes at room temperature. Platelets were treated with 10 nM PGI$_2$ for 10 minutes. Adhered platelets were subsequently fixed using formaldehyde, permeabilised using Triton X-100 (0.1%) and stained using FITC phalloidin. **A)** Images are representative of each condition. B) Average surface area **C)** Platelet adhesion. **D)** % of platelets with actin nodules **E)** %of platelets with stress fibres. n=3. * $p<0.05$ ** $p<0.01$ *** $p<0.001$ **** $p<0.0001$ relative to control. Scale bar= 20µm.

145

3.7. Platelet surface area is significantly reduced in the presence of apyrase and indomethacin

To understand if the actin cytoskeletal changes induced by PGI_2 were dependent on ADP and TXA_2, washed human platelets ($2x10^7$/ml) were pre-treated with 2 U/ml apyrase and 10 μM indomethacin or the combination of both inhibitors. Platelets were then incubated on the coverslips coated with 100 μg/ml fibrinogen, 50 μg/ml nLDL and 100 μg/ml fibrinogen, or 50 μg/ml oxLDL and 100 μg/ml fibrinogen for 20 minutes and treated with 10 nM PGI_2 for 10 minutes. Control samples for each condition without 10 nM PGI_2 used for comparison. Adhered platelets were fixed using formaldehyde, permeabilised, stained using FITC phalloidin and visualised using an immunofluorescence microscope.

In the presence of apyrase and indomethacin there was a significant reduction in surface area of platelets in all conditions in comparison to the control. However, there were additional significant reductions in surface area in the presence of 10 nM PGI_2 and 10 μM indomethacin (12.63 ± 0.42 μm^2) and the combination of 2 U/ml apyrase and 10 μM indomethacin (13.63 ± 0.59 μm^2) in comparison to the control treated with 10 nM PGI_2 alone (17.45 ± 0.48 μm^2). This aligned with a reduction in stress fibre formation with just $1.39\pm0.57\%$ of platelets in the presence of apyrase containing stress fibres, $1.35\pm0.39\%$ in the presence of indomethacin and $0.98\pm0.14\%$ in the combination of both. There was also a reduction in adhesion upon treatment with apyrase 32.28 ± 0.69 and with apyrase and indomethacin (32.00 ± 4.67) as well as in all the respective conditions with 10 nM PGI_2 when compared to the control (figure 3.16 C). In agreement actin nodules increased for all samples in comparison to the control condition (figure 3.16 D). Analysis for percentage of platelets with stress fibres showed a reduction from the control platelets at $88.78\pm1.47\%$ to $12.61\pm1.24\%$ in the presence of 10 nM PGI_2 (figure 3.16 E). In addition to the cytoskeletal effects there was a reduction in number of platelets

adhered between the control condition 48.22±3.20 to 37.00±3.61 in the presence of 10 nM PGI$_2$.

Analysis of platelets spread on nLDL and fibrinogen showed a very similar effect to that seen on fibrinogen alone in regards platelet adhesion, platelet surface area, and analysis of actin nodules and stress fibres (figure 3.17)

Analysis of platelets spread on oxLDL and fibrinogen identified that the effect of 10 nM PGI$_2$ was attenuated in the presence of oxLDL as platelets spread on 50 µg/ml oxLDL and 100 µg/ml fibrinogen showed no significant change in surface area of platelets (figure 3.18 B). However, interestingly, platelet surface area reduced from 18.87±0.95 µm^2 in platelets treated with 2 U/ml apyrase and 10 µM indomethacin combined to 15.72±0.62 µm^2 in the respective condition containing 10 nM PGI$_2$ (Figure 3.18B). Figure 3.18C shows that the number of adhered platelets reduced from the control platelets spread on 50 µg/ml oxLDL and 100 µg/ml fibrinogen (75.89±2.83 µm^2) to 61.22±3.56µm^2 upon treatment with 10 nM PGI$_2$. Platelet adhesion was significantly reduced in all the other platelet samples when compared to the control (figure 3.18 C). Furthermore, figure 3.18 D shows an increase in the percentage of platelets with actin nodule formation was seen from the control sample 51.62±0.81% to 96.90±.1.28% under 10 nM PGI$_2$ stimulation. The formation of actin nodules increased in conditions treated with apyrase, and indomethacin irrespective of 10 nM PGI$_2$ stimulation. (figure 3.19 D). In agreement, figure 3.18 E shows that stress fibre reduced from 92.21±1.86% in the control to 5.42±0.86% once treated with 10nM PGI$_2$. Furthermore, a reduction in percentage of platelets with stress fibres was observed in all conditions treated with apyrase, and indomethacin irrespective of post-treatment with 10nM PGI$_2$ in contrast to the control.
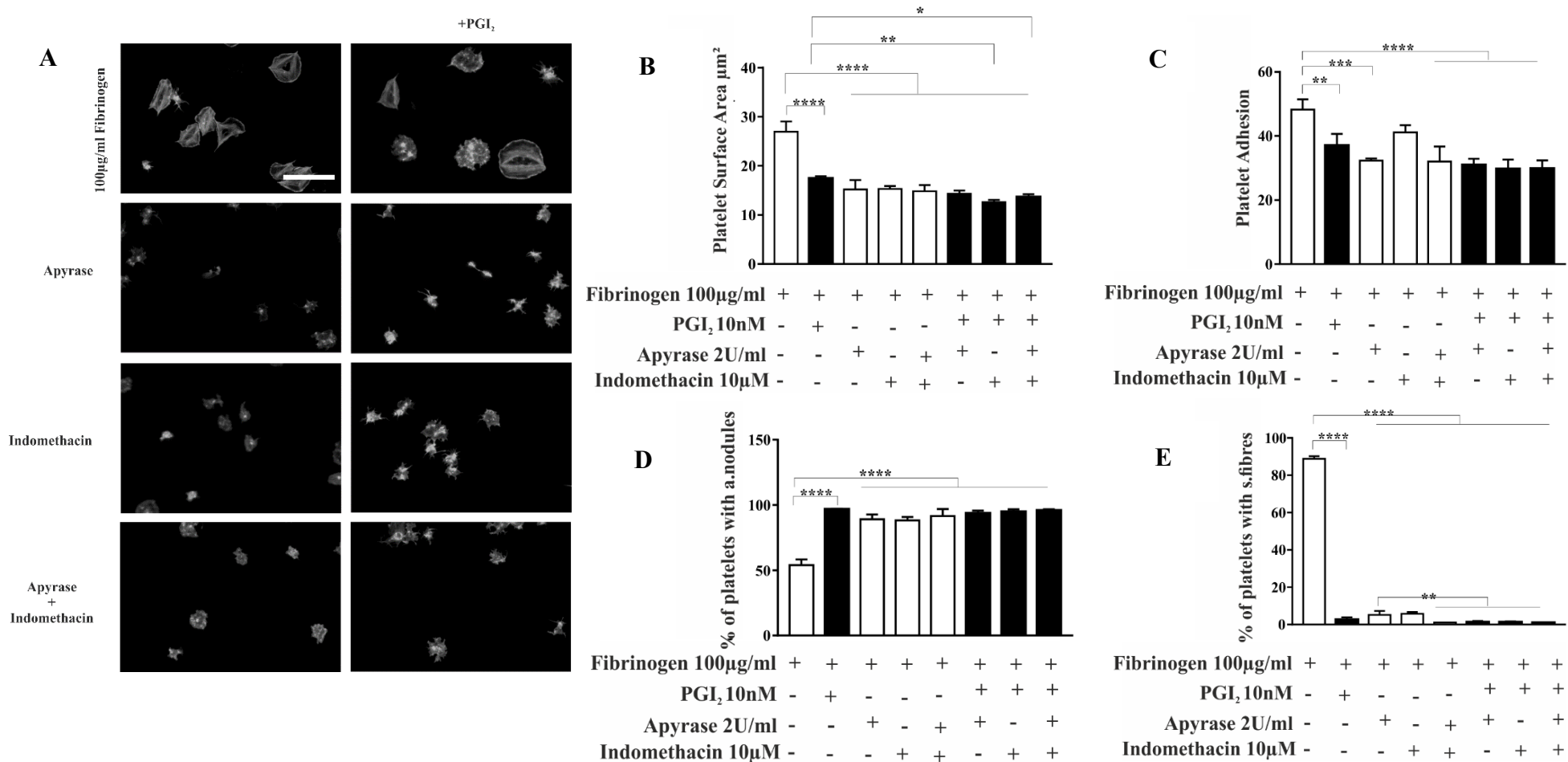
Figure 3.16. Platelet surface area is significantly reduced in the presence of apyrase and indomethacin.

Coverslips were coated with 100 μg/ml fibrinogen overnight at 4°C. Human platelets (2×10^7/ml) were then pre-treated 2 U/ml apyrase, 10 μM indomethacin or the combination of both inhibitors for 10 mins. Platelets were spread for 20 mins and subsequently treated with the inhibitors and PGI$_2$ for 10 mins. Adhered platelets were fixed using formaldehyde, permeabilised using Triton X-100 (0.1%) and stained using FITC phalloidin. **A)** Images are representative of each condition **B+C)** Platelet surface area and adhesion are reduced in the presence of Apyrase and Indomethacin. **D+E)** Apyrase and indomethacin induce stress fibre reversal and actin nodule formation in platelets. n=3 * $p<0.05$ ** $p<0.01$ *** $p<0.001$ **** $p<0.0001$ relative to control. Scale bar= 20μm.

Figure 3.17. Platelet surface area is significantly reduced in the presence of apyrase and indomethacin.

Coverslips were coated with 100 μg/ml fibrinogen or 50 μg/ml nLDL for 1 hour at room temperature. Human platelets 2×10^7/ml were pre-treated with apyrase, indomethacin or the combination of both inhibitors for 10 mins. Platelets were spread for 20 mins and subsequently treated with the inhibitors and PGI$_2$ for 10 mins. Adhered platelets were fixed using formaldehyde, permeabilised using Triton X-100 (0.1%) and stained using FITC phalloidin. **A)** Images are representative of each condition **B+C)** Platelet surface area and adhesion are reduced in the presence of Apyrase and Indomethacin. **D+E)** Apyrase and indomethacin induce stress fibre reversal and actin nodule formation in platelets. n=3. * $p<0.05$ *** $p<0.001$ **** $p<0.0001$ relative to control. Scale bar= 20μm.

A

50µg/ml oxLDL   +PGI₂

100µg/ml Fibrinogen

Apyrase

Indomethacin

Apyrase + Indomethacin

B

Platelet Surface Area µm²

oxLDL 50µg/ml	+	+	+	+	+	+	+	+
Fibrinogen 100µg/ml	+	+	+	+	+	+	+	+
PGI₂ 10nM	-	+	-	-	-	+	+	+
Apyrase 2U/ml	-	-	+	-	+	+	-	+
Indomethacin 10µM	-	-	-	+	+	-	+	+

ns **** ***

C

Platelet Adhesion

oxLDL 50µg/ml	+	+	+	+	+	+	+	+
Fibrinogen 100µg/ml	+	+	+	+	+	+	+	+
PGI₂ 10nM	-	+	-	-	-	+	+	+
Apyrase 2U/ml	-	-	+	-	+	+	-	+
Indomethacin 10µM	-	-	-	+	+	-	+	+

* **** ***

D

% of platelets with a.nodules

oxLDL 50µg/ml	+	+	+	+	+	+	+	+
Fibrinogen 100µg/ml	+	+	+	+	+	+	+	+
PGI₂ 10nM	-	+	-	-	-	+	+	+
Apyrase 2U/ml	-	-	+	-	+	+	-	+
Indomethacin 10µM	-	-	-	+	+	-	+	+

**** *** **** ****

E

% of platelets with s.fibres

oxLDL 50µg/ml	+	+	+	+	+	+	+	+
Fibrinogen 100µg/ml	+	+	+	+	+	+	+	+
PGI₂ 10nM	-	+	-	-	-	+	+	+
Apyrase 2U/ml	-	-	+	-	+	+	-	+
Indomethacin 10µM	-	-	-	+	+	-	+	+

**** **** * **

Figure 3.18. Presence of apyrase and indomethacin induces actin nodule formation and stress fibre reversal.

Coverslips were coated with 100 µg/ml fibrinogen overnight at 4°C or 50 µg/ml oxLDL for 1 hour at room temperature. Human platelets 2×10^7/ml were pre-treated with apyrase, indomethacin or the combination of both inhibitors for 10 mins. Platelets were spread for 20 mins and subsequently treated with the inhibitors and PGI₂ for 10 mins. Adhered platelets were fixed using formaldehyde, permeabilised using Triton X-100 (0.1%) and stained using FITC phalloidin. **A)** Images are representative of each condition. **B+C)** Platelet surface area and adhesion are reduced in the presence of Apyrase and Indomethacin. **D+E)** Apyrase and indomethacin induce stress fibre reversal and actin nodule formation in platelets. n=3**.** * $p<0.05$ ** $p<0.01$ *** $p<0.001$ **** $p<0.0001$ relative to control. Scale bar= 20µm.

3.8. Discussion

Previous studies have found that oxLDL but not nLDL induces platelet aggregation, adhesion and shape change (Wraith et al.,2013). However, the role of oxLDL in combination with fibrinogen in inducing prothrombotic phenotype remains to be elucidated. It is believed that hyperlipidaemia triggers the formation of a platelet thrombus and increases the development of thrombosis at the site of the thrombus formation in the atherosclerotic lesions (Eitzman et al., 2000). The oxidation of LDL is an early marker, indicating the progression and development of the atherosclerotic process-giving rise to foam cell formation as initially described by Steinberg, 1997. Modified LDL drives the pathogenesis of atherosclerosis by altering the functions of cells. Various cells play a role in the atherosclerotic process such as monocytes, macrophages, endothelial cells, smooth muscle cells as well as platelets. In the blood of atherosclerotic patients, autoantibodies that react with oxidation specific epitopes of oxLDL are present, highlighting the presence of oxLDL in the circulation (Korporaal et al., 2007). It is thought that once the atherosclerotic plaque rupture, platelets in the circulation associate with oxLDL, initiating the formation of a thrombus.

It was therefore important to indicate whether LDL was oxidatively modified by measuring the extent of protein modification that occurs as a result of the reaction between amino acid residues such as lysine and arginine on apoB and lipid derived oxidation products. Thus, a REM assay was performed whereby the REM of nLDL was regarded as 1. The REM of oxLDL was almost 3-fold, suggesting that protein modification is due to lipid oxidation products which is consistent with previous findings (Brown, Dean and Davies, 2005).

After extensive oxidation of LDL, the ability of oxLDL to cause platelet aggregation was tested. Platelets were therefore stimulated with thrombin (0.1 U/ml) and increasing concentrations of oxLDL (10, 30 and at 50 μg/ml) and nLDL (50 μg/ml). It was identified that oxLDL but not nLDL induced platelet aggregation in a dose dependent manner and maximum aggregation was observed at 50 μg/ml oxLDL, consistent with findings reported by Wraith et al.,2013; Magwenzi et al., 2015 and Berger et al., 2019. Although oxLDL can cause platelet aggregation, the combination with fibrinogen in reorganising the actin cytoskeleton of spread platelets and inducing a prothrombotic phenotype remains to be elucidated. Thus, to ensure fibrinogen and oxLDL bind together on glass coverslips, coverslips were coated with BSA (5 mg/ml) control, fibrinogen Alexa-488, E06 (1.5 μg/ml) as well as the combination of both fibrinogen Alexa-488 and E06. Figure 3.3 showed colocalization between the Alexa-488 labelled fibrinogen and E06 stain, suggesting that oxLDL and fibrinogen can bind to coverslips. It is believed that exposure of platelet receptors and coagulation factors in the microenvironment of atherosclerotic lesions leads to platelet activation, aggregation and thrombus formation. Fibrinogen is the major constituent of the atherosclerotic microenvironment and studies have now demonstrated a plethora of mechanisms highlighting the key function of fibrinogen in accelerating plaque vulnerability due to its high affinity to bind hydrophobic and atheromatous negatively charged lipid surfaces thus, increasing thrombogenicity ((Zwaal, Comfurius and Bevers, 1998; Wang et al., 2019). The oxidised phospholipids such as oxysterols generated during the preparation of oxLDL resemble the domains of phosphatidylserine membranes in terms of polarity and charge. Together, this indicates that the presence of the oxidised products in the LDL may predispose to thrombotic events due to their inherent ability to bind fibrinogen.

Subsequently, it was postulated that platelets spread on oxLDL would also induce platelet activation in a dose dependent manner under static conditions. Thus, platelets were spread on increasing doses of oxLDL and it was determined that the ability for oxLDL to propagate platelet spreading and adhesion was indeed dose dependent. Following this, it was further conceptualised that the combination of immobilised fibrinogen and oxLDL would enhance platelet activation. Although previous research showed that the combination of oxLDL and collagen enhanced thrombus formation, major platelet ligands such as fibrinogen were not studied (Nergiz-Unal et al., 2011). As a result, platelets were initially spread on immobilised fibrinogen at increasing doses and it was established that increasing concentrations of fibrinogen reduce the surface area of platelets, as described previously (Qiu et al., 2014; Safiullin et al., 2015). Further, the effect of spreading oxLDL on immobilised fibrinogen under a static system was consequently studied. Here, platelets were spread for 45 minutes on increasing concentrations of fibrinogen and oxLDL and a prothrombotic phenotype was observed in platelets spread on 50 μg/ml oxLDL and 100 μg/ml fibrinogen likely as a result of sensitising platelets for activation. The interaction of platelets with oxLDL is a key feature in atherothrombosis which inevitably leads to platelet hyperreactivity. Although the mechanism by which this happens is poorly understood, studies have suggested this phenotype is due to an increase in Ca^{2+} levels and increased secretion of P-selectin in a CD36 dependent manner (Chen, Febbraio and Silverstein, 2007).

Another reason for the prothrombotic activity we observed can be due to changes in the platelet lipidome as a result of lipid uptake via CXCL12/CXCR4-7 axis through oxidation and peroxidation processes regulated by mitochondrion-dependent ROS generation (Chatterjee et al., 2015). As a result, it is evident that platelets can store large amounts of oxLDL to atherosclerotic lesions which further signifies the role of platelets on atherothrombosis.

Having identified that platelets are potentiated on a combination of fibrinogen and oxLDL, we then investigated how the effect of PGI_2 on spread platelets was to be modulated. Here as expected platelets spread on fibrinogen readily reversed their stress fibres, formed actin nodules and reduced their surface area in the presence of PGI_2. In contrast those spread on oxLDL alone no longer responded to PGI_2 treatment in agreement with Berger et al 2019. However, those spread on oxLDL and fibrinogen, surprisingly partially reversed. This was identified as although the surface area of the platelet was maintained, the platelet stress fibres were readily reversed, and actin nodules formed. This clearly identified that the presence of oxLDL was preventing some of the actions of PGI_2 but could not prevent them all. This therefore identified that differing levels of cAMP within the platelet might induce differing responses, which could then impact on platelet function.

Importantly, we then asked the question if platelets spreading in the presence and absence of PGI_2 was dependent on ADP and TxA_2. Therefore, a series of spreading experiments were carried out in the presence of apyrase and indomethacin separately and in combination. On fibrinogen adhesion and platelet surface area was dependent on ADP and TxA_2. This is in agreement with (Borgognone et al., 2014) paper, who showed that early timepoints showed a marked inhibition, but by 45 minutes this inhibition was gone. Importantly this inhibition was still present on fibrinogen and oxLDL. However interestingly actin nodule formation was independent of ADP and TxA_2.

Conclusion

Together, the data in this chapter provides insight into the role of oxLDL and fibrinogen on platelet spreading. This chapter identifies that combinations of oxLDL and fibrinogen

potentiate platelet adhesion and spreading. Furthermore, this combination partially blunts the

effect of PGI$_2$, preventing a reduction in platelet surface area, and only allowing the reversal

of platelet stress fibres. These two effects most likely help to induce a prothrombotic

phenotype.

CHAPTER 4: cAMP causes the differential regulation RhoGTPases in oxLDL and fibrinogen spread platelets

4.1. Introduction

PGI$_2$ is a potent inhibitor of platelet function. It induces cAMP signalling, causing PKA activation leading to inhibition of Ca^{2+} mobilisation, granule secretion, integrin activation, the reorganisation of the cytoskeletal proteins and platelet aggregation. Control of cAMP signalling is mediated via changes in the activity of AC, the enzyme that drives cAMP production, and PDEs, which metabolise cAMP, particularly the PDE2 and PDE3 subtypes (Sun et al., 2007). Therefore, changes in the concentration of cAMP caused by changes in activity of either AC or PDEs may cause the formation of a prothrombotic or a bleeding phenotype.

Critical to understanding how cAMP is linked to aberrant platelet function is how it helps to modulate the actin cytoskeleton. The actin cytoskeleton has been heavily linked to effective production of stable thrombi (Auger and Watson, 2008). PKA can target multiple important proteins within the cytoskeleton, such as the Rho family proteins, Rac and RhoA (Yusuf et al, 2017).

RhoA activation is implicated in stress fibre formation and the activation of RhoA results in the formation of contractile actin myosin bundles which is important for platelet adhesion and contraction (Klages et al., 1999). Rac has a specific role in platelet lamellipodia formation, spreading and reorganising the cytoskeleton (McCarty et al., 2005). The ability of RhoA to induce shape change is dependent on the G12/G13 signalling pathway although Rac1 is mediated by Gq, suggesting that Rho and Rac are differentially regulated (Gratacap et al., 2001). While Rac activation is Gq mediated, it also thought that Rac releases mediators which

can therefore activate Gi-coupled receptors. Rac1 drives actin polymerisation as well as lamellipodia formation while RhoA is inhibited to allow spreading highlighting their antagonistic relationship during outside-in signalling. Platelet contraction and clot retraction is thought to be mediated by calcium-dependent proteases like calpain, facilitating the interaction between RhoA and Rac to trigger MLC phosphorylation. Although Rho and Rac are both involved in the first pMLC peak activated by the inside-out signalling during clot retraction, Rac1 is also involved in the second pMLC peak that is mediated by actin polymerisation and Rac1 activation (Egot et al., 2013). Furthermore, in platelets it has been shown that PDE activity can be activated by oxLDL, therefore preventing the inhibitory action of PGI_2 on platelet function (Berger et al, 2019).

In chapter 3, we identified that platelets spread on oxLDL and fibrinogen were only partially inhibited by PGI_2. Stress fibre formation was fully reversed, but lamellipodia was maintained (using platelet surface as a proxy for lamellipodia formation). As a result, it was postulated that under these conditions, the level of cyclic nucleotide cAMP can inhibit RhoA activity whilst having no effect on Rac activity. Therefore, this Chapter aims to:

- To identify the level of cAMP produced in oxLDL and fibrinogen spread platelets

- To identify the role of AC and PDEs in oxLDL modulation of fibrinogen spreading

- To determine the role of PGI_2 in regulating RhoA and Rac activity in oxLDL and fibrinogen spread platelets

- To identify if PGI_2 signalling induces the phosphorylation of VASP and downregulates the phosphorylation of MLC.

4.2. cAMP levels are modulated in the presence of oxLDL in spread platelets

To further understand the spreading phenotype identified in chapter 3 (figure 3.15) we sought to identify if this was due to changes in cAMP level induced by PGI_2 within the platelet. Therefore, initially we confirmed that the cAMP assay was working well. Platelets were stimulated for 1 minute with different concentrations of PGI_2 (0.3, 10, 100 nM) before undergoing lysis with Triton X-100 (0.1%) and analysis using a cAMP kit.

Figure 4.1 shows that cAMP levels were significantly elevated in a dose responsive manner after stimulation with 0.3 nM (908.11±160.24 fmol/µg/ml), 10 nM (2175.03±841.09 fmol/µg/ml) and 100 nM (2306.51±1555.39 fmol/µg/ml) PGI_2 compared to the basal control (268.58±198.26 fmol/µg/ml). In addition, a marked increase in cAMP levels was seen in platelets treated with 10 nM PGI_2 than 0.3 nM PGI_2 (figure 4.1).

To establish the role of PGI_2 in regulating cAMP levels in spread platelets, washed human platelets ($2x10^8$/ml) were spread on 100 µg/ml fibrinogen, 100 µg/ml fibrinogen & 50 µg/ml nLDL or 100 µg/ml fibrinogen & 50 µg/ml oxLDL for 20 mins and subsequently treated with tyrodes as a control or 10 nM PGI_2 for 2mins. Adhered platelets were lysed using Triton X-100 (0.1%) and analysed using a cAMP kit and subsequently measured for fluorescence on a spectrophotometer.

Importantly, figure 4.2 shows that PGI_2 significantly increased cAMP in platelets spread on fibrinogen (937.53±616.43 fmol/µg/ml) and 100 µg/ml fibrinogen & 50 µg/ml nLDL to (1272.87±646.41 fmol/µg/ml) in comparison with the 100 µg/ml fibrinogen control (134.53±123.39 fmol/µg/ml). Interestingly cAMP levels in platelets spread on 50 µg/ml

oxLDL and 100 µg/ml fibrinogen were elevated but to a markedly lower level (346±196.01 fmol/µg/ml) upon 10 nM PGI$_2$ treatment in comparison to the control platelets (152.09±123.39 fmol/µg/ml) (figure 4.2). This demonstrates that cAMP concentration was compromised by the presence of oxLDL.

After confirming that PGI$_2$ stimulation induced different cAMP levels dependent on the matrix protein on which the platelets were spread, the effect on PKA signalling downstream of cAMP was therefore explored. Washed human platelets (2x10^8/ml) either in suspension or spread on 100 µg/ml fibrinogen, 100 µg/ml fibrinogen & 50 µg/ml nLDL or 100µg/ml fibrinogen & 50 µg/ml oxLDL were stimulated with 10 nM PGI$_2$ for 1 minute. before lysis, and western blotting for downstream markers of PKA activation (pVASP^{Ser157} and pPKA substrate).

Stimulation of spread platelets on 100 µg/ml fibrinogen, 100 µg/ml fibrinogen & 50 µg/ml nLDL by 10 nM PGI$_2$ induced elevation of pPKA substrate phosphorylation and the level of pVASP^{Ser157} to 15.60±10.94 and 15.69±10.84 respectively (figure 4.3 A and B respectively). However, the addition of 10 nM PGI$_2$ did not increase pVASP^{Ser157} induce pPKA substrate phosphorylation in the presence of 50 µg/ml oxLDL (figure 4.3 A). Densitometry analysis in figure 4.3 C showed that pVASP^{Ser157} levels were 0.714±0.31 in suspended basal conditions which increased to 11.20±9.07 in suspended platelets stimulated with 10 nM PGI$_2$. Platelets treated with 0.1 U/ml thrombin had a similar pPKA profile to platelets spread on 100 µg/ml fibrinogen.
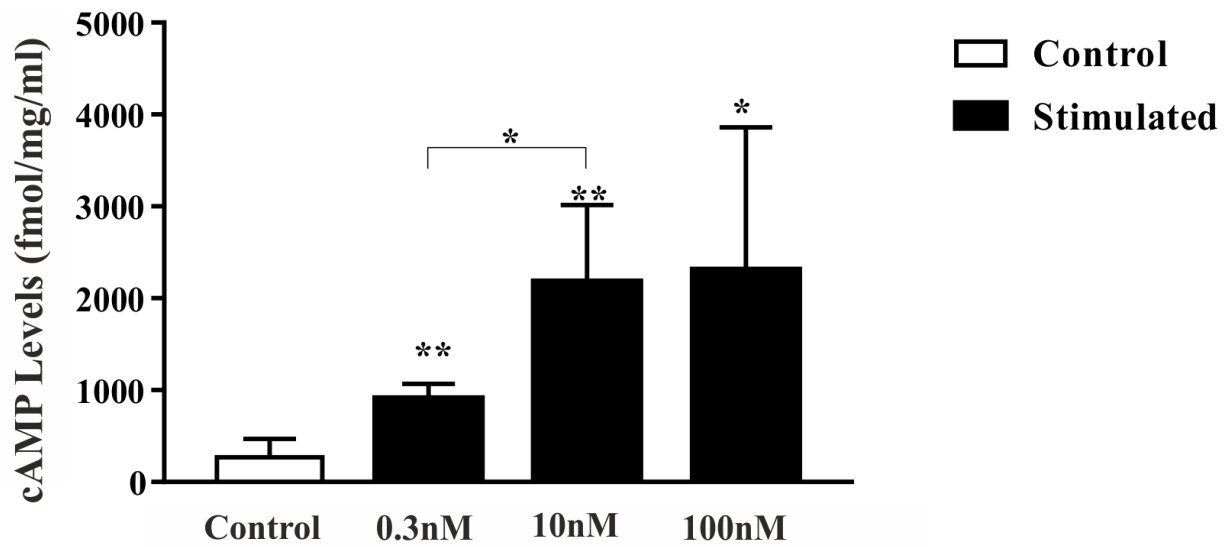
Figure 4.1. cAMP levels are elevated in suspended platelets treated with increasing concentrations of PGI$_2$.

Human platelets 2×10^8/ml in suspension were treated with 0.3,10 and 100 nM PGI$_2$ for 1 minute. Platelets were lysed using Triton X-100 (0.1%) and analysed using a cAMP kit. Absorbance was measured on a spectrophotometer. Data shown as mean ± SD (n=5) * $p<0.05$. ** $p<0.01$ relative to control.
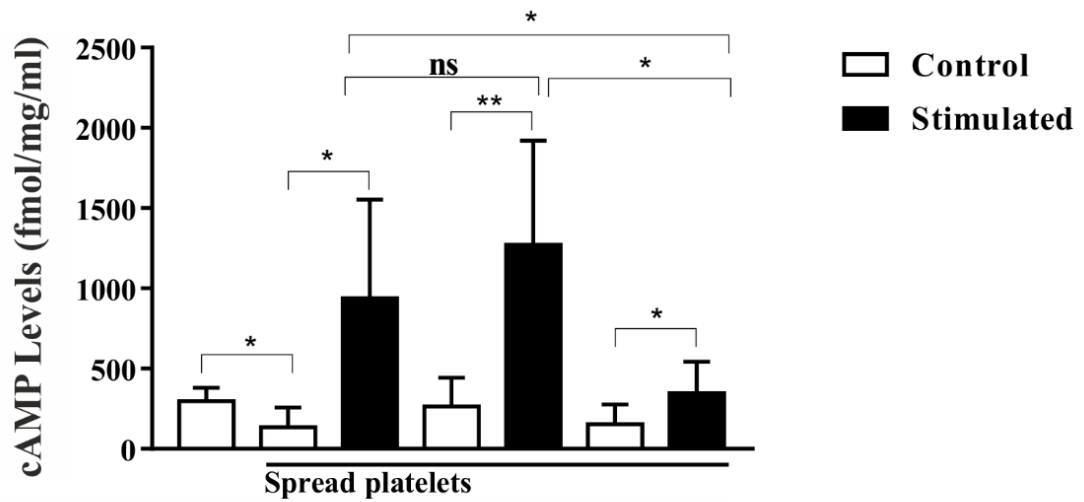
Figure 4.2. cAMP levels are only partially elevated in the presence of oxLDL.

Human platelets 2×10^8/ml were incubated on 50 µg/ml nLDL or 50 µg/ml oxLDL and 100 µg/ml fibrinogen coated wells. Platelets were spread for 20 mins and subsequently treated with 10 nM PGI_2 for 2 mins. Adhered platelets were lysed using Triton X-100 (0.1%) and analysed using a cAMP kit. Absorbance was measured on a spectrophotometer. Data shown as mean ± SD (n=5) * $p<0.05$. ** $p<0.01$ relative to control.
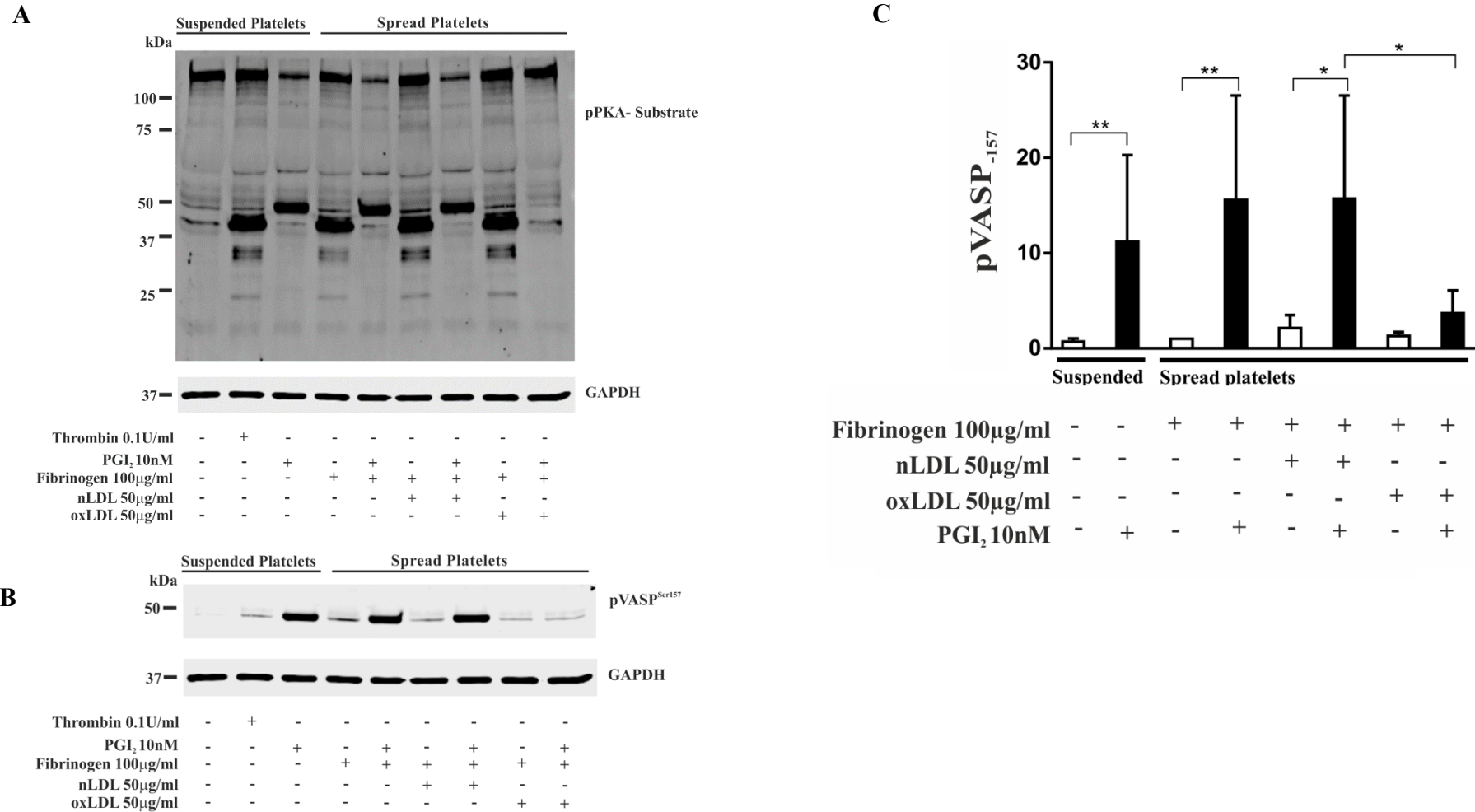
Figure 4.3. pVASP not elevated in platelets spread on oxLDL and fibrinogen.

Human platelets 2×10^8/ml were spread on 100 μg/ml fibrinogen or 50 μg/ml oxLDL or 50 μg/ml nLDL for 20 mins before treatment with 10 nM PGI$_2$ for 10 mins. The samples were then lysed, using the lysis before probing for pVASP, pPKA and GAPDH. **A+B)** Western blots for, pPKA pVASP relative to GAPDH. **C)** Western blot Densitometry analysis for pVASP relative to GAPDH. Data shown as mean ± SD (n=6). * $p<0.05$** $p<0.01$ relative to control.

4.3. Reduction in cAMP inhibits RhoGTPase activity in a differential manner

Figures 4.2-4.3 show that elevation of cAMP is altered in spread platelets on a combination of oxLDL and fibrinogen, but that there is still an elevation over the basal level. Chapter 3 identified that PGI$_2$ treatment could induce stress fibre reversal, but no effect in surface area. Therefore, we next sought to identify if the small change in cAMP correlated with a change in RhoA function and no change in Rac activity. Therefore, to identify if there were different activity levels of Rac and RhoA in these conditions we conducted experiments in two different ways.

1) We used the ROCK inhibitor, Y27632 or the Rac inhibitor, NSC23766 to identify if they induced a similar phenotype to that identified in the presence of PGI$_2$.

2) We completed Rac and RhoA pulldown assays to identify their activation status in platelets spread on fibrinogen, fibrinogen + oxLDL, fibrinogen + LDL in the presence and absence of PGI$_2$.

Therefore, to ensure that we had effective doses of Y27632 and NSC23766 washed human platelets 2×10^7/ml were incubated on 100 μg/ml fibrinogen coverslips and pre-treated with either 10 μM Y27632 or 50 μM NSC23766 for 30 mins. Adhered platelets were fixed using formaldehyde, permeabilised, stained using FITC phalloidin and visualised using an immunofluorescence microscope.

Furthermore, treatment with Y27632 or NSC23766 induced a significant reduction in surface area in comparison to the control to 13.05 ± 2.89 μm^2 and 8.13 ± 3.16 μm^2. There was also a marked reduction in platelets adhesion from 49.78 ± 6.00 in the control to 26.00 ± 0.88 in Y27632 treated platelets and 21.89 ± 3.79 in NSC23766 treated samples (figure 4.8 C).

As expected, treatment with Y27632 (3.84±0.87%) and NSC23766 (3.23±1.73%) resulted in inhibition of stress fibre formation with just 3.84±0.87% of Y27632 treated and 3.23±1.73% of NSC23766 treated platelets containing stress fibres respectively, in comparison to 81.81+/-3% in the control sample. In agreement with this the percentage of platelets with actin nodules significantly increased after treatment with Y27632 and NSC23766 (figure 4.8 D).

A

100μg/ml Fibrinogen   + Y27632   +NSC23766

B

Fibrinogen 100μg/ml	+	+	+
Y27632 10μM	-	+	-
NSC23766 50μM	-	-	+

C

Fibrinogen 100μg/ml	+	+	+
Y27632 10μM	-	+	-
NSC23766 50μM	-	-	+

D

Fibrinogen 100μg/ml	+	+	+
Y27632 10μM	-	+	-
NSC23766 50μM	-	-	+

E

Fibrinogen 100μg/ml	+	+	+
Y27632 10μM	-	+	-
NSC23766 50μM	-	-	+
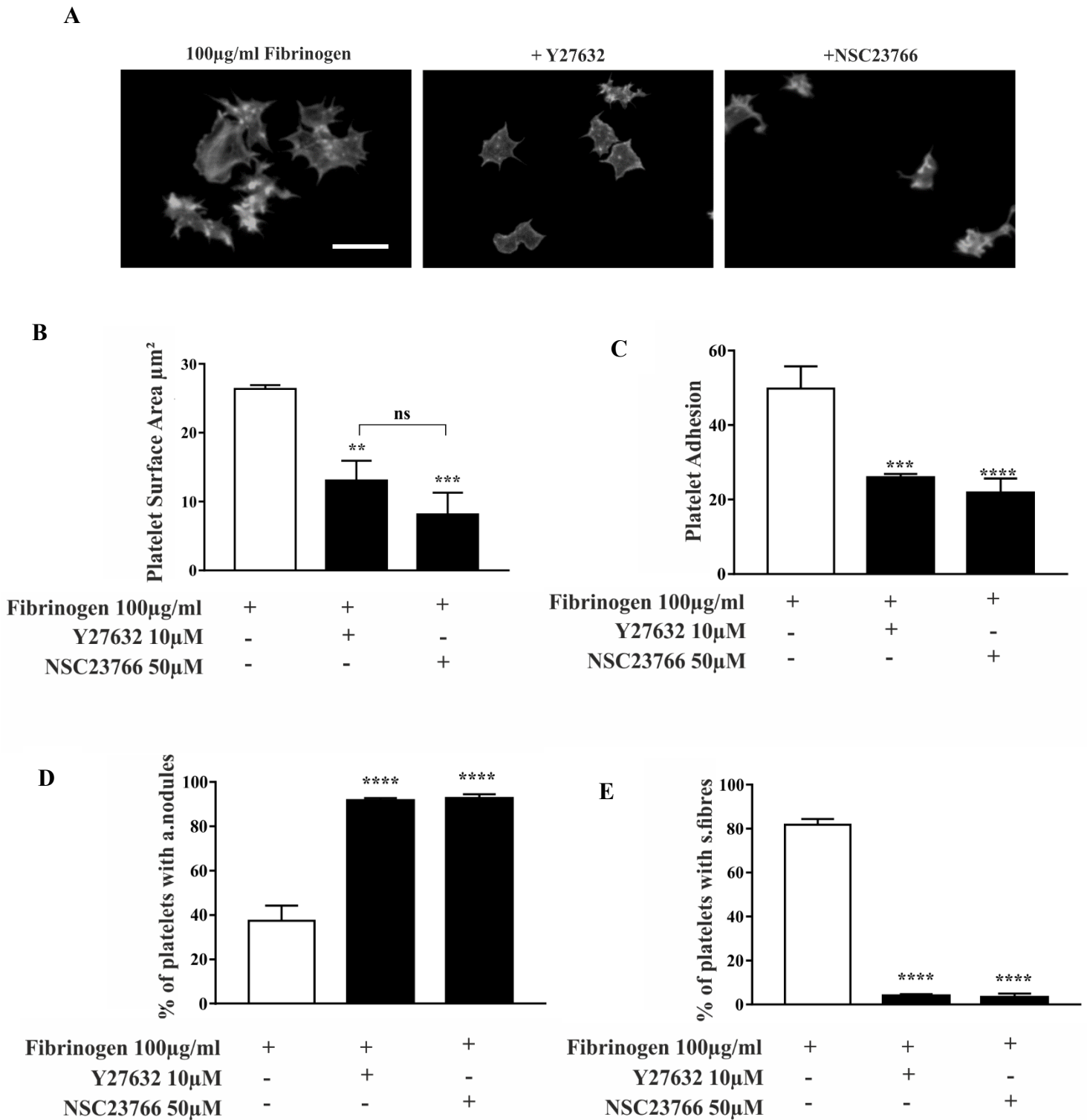
Figure 4.4. Pre-treatment of Y27632 and NSC3766 reduces platelet surface area in platelets spread on fibrinogen. Coverslips were coated on 100 μg/ml fibrinogen overnight at 4°C. Human platelets $2x10^7$/ml were pre-treated with either 10 μM Y27632 or 50 μM NSC23766 for 30 mins prior to spreading for 30 mins. Adhered platelets were fixed using formaldehyde, permeabilised using Triton X-100 (0.1%) and stained using FITC phalloidin. **A)** Images are representative of each condition. **B)** Average surface area. **C)** Platelet adhesion. **D)** % of platelets with actin nodules **E)** % of platelets with stress fibres. Data shown as mean ± SD (n=3). ** p<0.01 *** p<0.001**** p<0.0001 relative to control. Scale bar= 20μm.

4.4. Post-treatment of Y27632 and NSC3766 reduces platelet surface area in platelets spread on fibrinogen

Upon establishing the effect of pre-treating platelets with the ROCK inhibitor, Y27632 and Rac inhibitor, NSC3766, we then sought to identify if post treatment of Y27632 or NSC 23766 would show a similar phenotype to that shown by PGI_2 on oxLDL and fibrinogen. Therefore, human platelets $2x10^7$/ml were spread on either 100 µg/ml fibrinogen, 50 µg/ml oxLDL, 50 µg/ml nLDL, 100 µg/ml fibrinogen + 50 µg/ml oxLDL, or 100 µg/ml fibrinogen + 50 µg/ml nLDL coated coverslips for 20 minutes and post-treated with either 10 nM PGI_2 (for 10 mins) or 10 µM Y27632 or 50 µM NSC23766 for 30 mins. Adhered platelets were fixed using formaldehyde, permeabilised, stained using FITC phalloidin and visualised using an immunofluorescence microscope.

As expected, treatment of platelets spread on fibrinogen with 10 nM PGI_2 caused a reduction in surface area (16.06 ± 0.26 μm^2) in comparison to the control sample (25.73 ± 0.68 μm^2). There was also a significant reduction in surface area in platelets treated with Y27632 (11.21 ± 2.38 μm^2) or NSC23766 (7.84 ± 1.31 μm^2). There was no significant change between platelets treated with Y27632 or NSC23766. No change was displayed in number of platelets adhered for all conditions (figure 4.5 C). In addition, the percentage of platelets with actin nodules significantly increased after treatment with PGI_2 ($96.94\pm.29\%$), Y27632 ($96.74\pm1.21\%$) and NSC23766 ($75.50\pm4.61\%$) in contrast to the control ($46.51\pm8.19\%$) (figure 4.5 D). Interestingly, a marked reduction in actin nodules was induced in platelets treated with 50 µM NSC23766 than 10 µM Y27632. There was also a concurrent reduction in platelets with stress fibres with $18.45\pm6.07\%$ after PGI_2 treatment, $5.77\pm2.24\%$ after Y27632 treatment, and $3.67\pm1.26\%$ after NSC23766 treatment in comparison to the control sample ($88.80+2.79\%$)

(figure 4.5 E). Further, stress fibre formation in platelets was more pronounced in platelets treated with 10 µM Y27632 and 50 µM NSC23766 compared to 10 nM PGI$_2$.

Analysis of platelets spread on nLDL and fibrinogen showed a very similar effect to that seen on fibrinogen alone across all parameters except for platelet adhesion (figure 4.6).

Analysis of spread platelets on fibrinogen + oxLDL indicated that as expected the effect of 10nM PGI$_2$ was attenuated (figure 4.8 B). Post treatment with Y27632 and NSC23766 reduced surface area to 14.08.49±0.43µm^2 and 8.05±1.04 µm^2 respectively in contrast to the control (42.90±2.57 µm^2) (figure 4.8 B). In agreement with figure 4.7 B, treatment with NSC23766 had a stronger effect in reducing platelet surface area than Y27632. Platelet adhesion was significantly reduced after post-treatment with 10 µM Y27632 (40.22±2.12) and 50 µM NSC23766 (41.78±3.89) in comparison to treatment with 10 nM PGI$_2$ (74.00±3.18) (4.8 C). Again, the percentage of platelets spread with actin nodules increased from the control sample (46.51±8.19%) to 93.31±1.08%, 93.706±2.75% and 86.53±1.51% after treatment with 10 nM PGI$_2$, 10 µM Y27632 and 50 µM NSC23766 respectively (figure 4.8 D). Additionally, in figure 4.8 E, stress fibre reversal was induced upon treating platelets with 10 nM PGI$_2$ (26.32±13.42%), 10 µM Y27632 (2.58±0.75%) and 50 µM NSC23766 (1.98±1.02%) in comparison to the control (91.31±3.57%). Stress fibre reversal was more pronounced in platelets treated with 10 µM Y27632 and 10 µM Y27632 than 10 nM PGI$_2$ (figure 4.8 E).
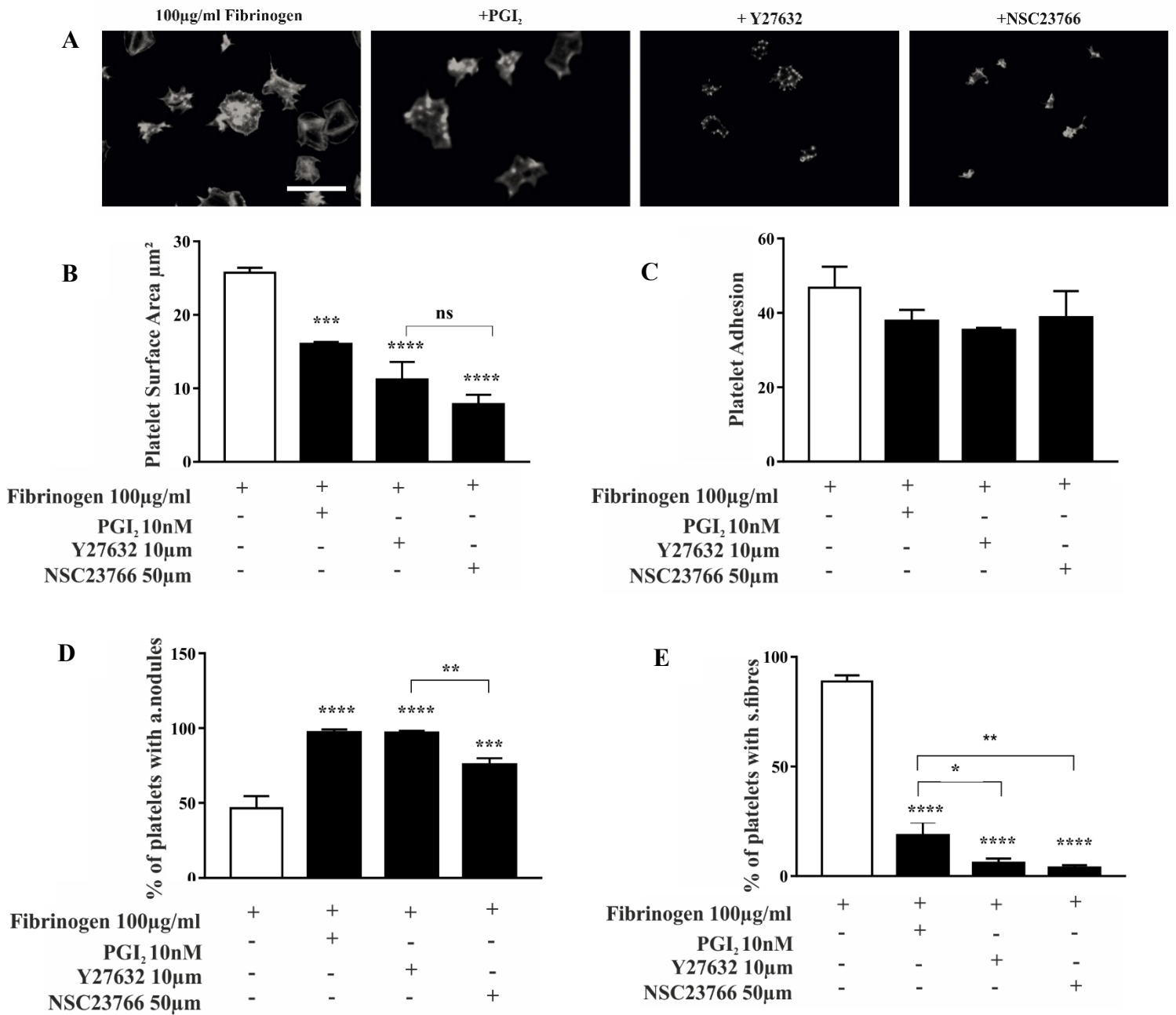
Figure 4.5. Post-treatment of Y27632 and NSC23766 reduces platelet surface area in platelets spread on fibrinogen. Coverslips were coated on 100 µg/ml fibrinogen overnight at 4°C. Human platelets 2×10^7/ml were spread for 20 mins and then post-treated with either 10 µM Y27632 or 50 µM NSC23766 for 30 mins or PGI$_2$ for 10 mins. Adhered platelets were fixed using formaldehyde, permeabilised using Triton X-100 (0.1%) stained using FITC phalloidin. **A)** Images are representative of each condition. **B)** Post-treatment of NSC23766 or Y27632 reduces platelet spreading. **C)** No effect in platelet adhesion. **D+E)** Increased actin nodule formation and induced stress fibre reversal in the presence of PGI$_2$, Y27632 and NSC3766). Data shown as mean ± SD (n=3). * $p<0.05$ ** $p<0.01$ *** $p<0.001$**** $p<0.0001$ relative to control. Scale bar= 20µm.
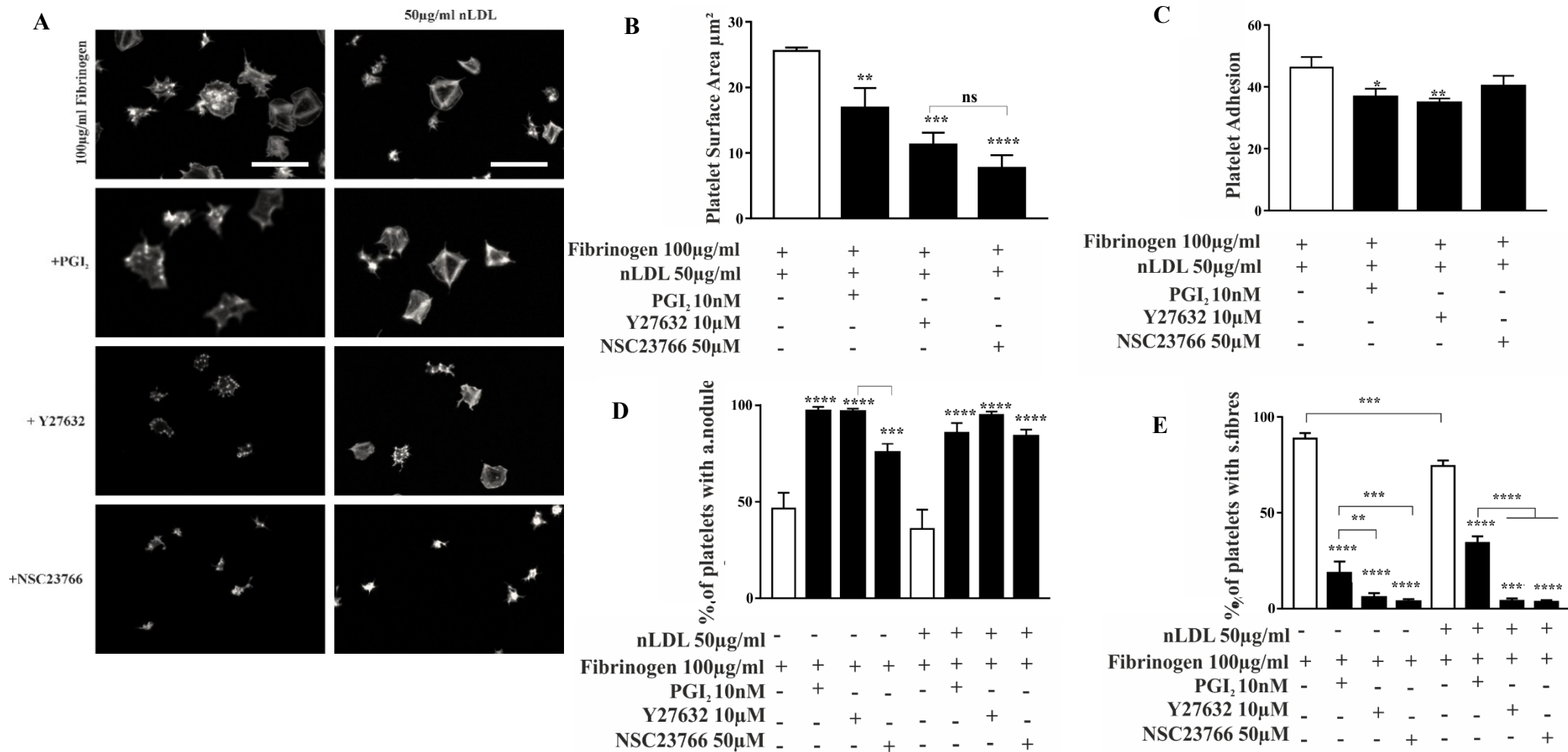
Figure 4.6 Post-treatment with Y27632 and NSC3766 reduces platelet surface area in platelets spread on fibrinogen and nLDL. Coverslips were coated on 100 µg/ml fibrinogen overnight at 4°C or 50 µg/ml nLDL for 1 hour at room temperature. Human platelets 2×10^7/ml were spread for 20 mins before post-treatment with either 10 µM Y27632 or 50 µM NSC23766 for 30 mins or with 10nM PGI$_2$ for 10 mins. Adhered platelets were fixed using formaldehyde, permeabilised using Triton X-100 (0.1%) and stained using FITC phalloidin. **A)** Images are representative of each condition. **B)** Post-treatment of NSC23766 + Y27632 reduces platelet spreading. **C)** Reduced platelet adhesion on PGI$_2$ and Y27632 treated platelets. **D+E)** Increased actin nodule formation and induced stress fibre reversal in the presence of PGI$_2$, Y27632 or NSC23766 VS figure 4.5 D, E). Data shown as mean ± SD (n=3). * $p<0.05$ ** $p<0.01$ *** $p<0.001$ **** $p<0.0001$ relative to control. Scale bar= 20µm.
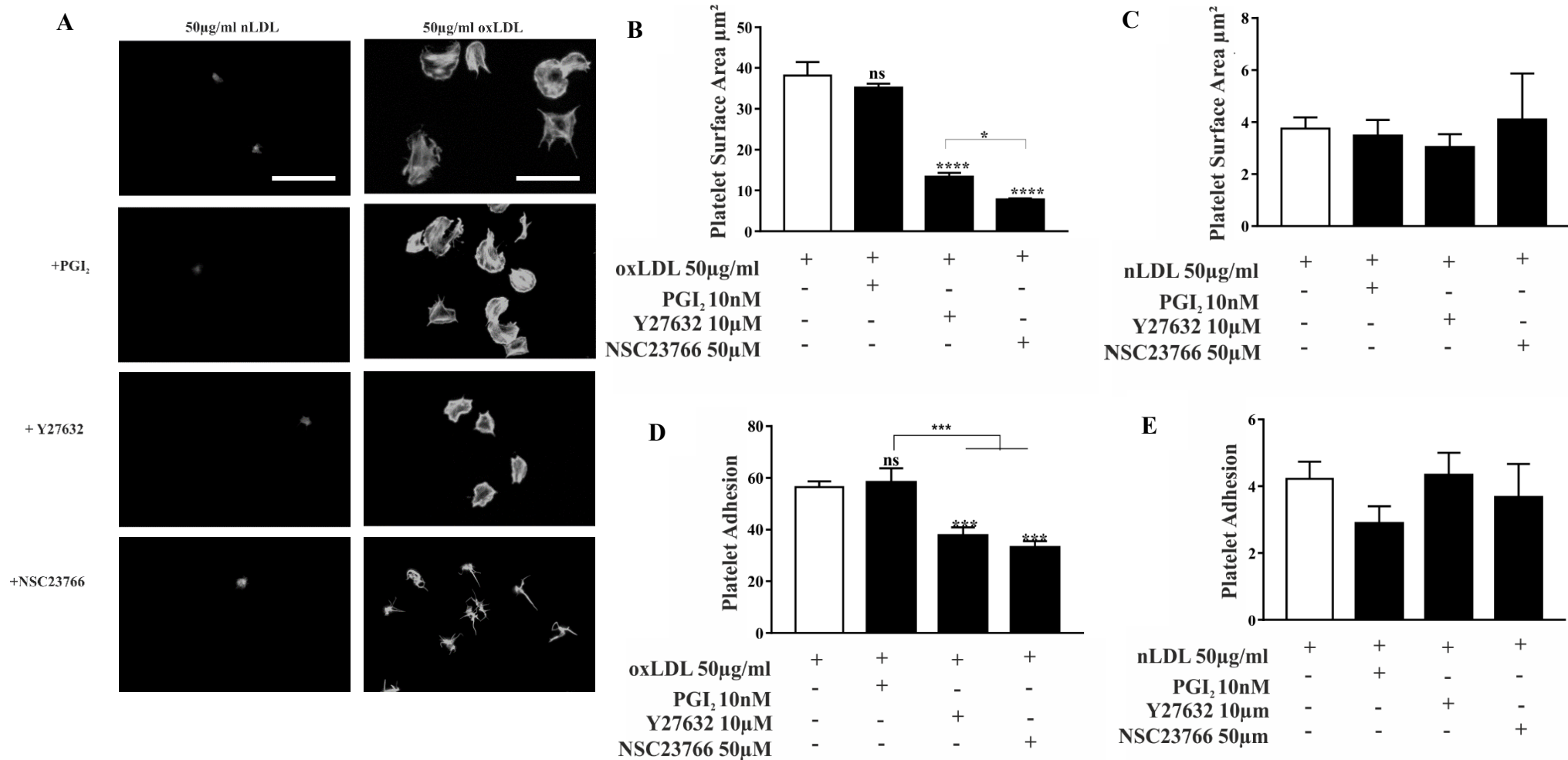
Figure 4.7. Post-treatment with NSC3766 inhibits platelet spreading more significantly than Y27632 in the presence of oxLDL. Coverslips were coated on 100 µg/ml fibrinogen overnight at 4°C or 50 µg/ml oxLDL for 1 hour at room temperature. Human platelets 2×10^7/ml were spread for 20 mins and then post-treated with either 10 µM Y27632 or 50 µM NSC23766 for 30 mins or with PGI$_2$ for 10 mins. Adhered platelets were fixed using formaldehyde, permeabilised using Triton X-100 (0.1%) and stained using FITC phalloidin. **A)** Images are representative of each condition. **B&C)** Average platelet surface area **D&E)** Platelet adhesion. Data shown as mean ± SD (n=3). * $p<0.05$ *** $p<0.001$ **** $p<0.0001$ relative to the control. Scale bar= 20µm.

A

100µg/ml Fibrinogen

50µg/ml oxLDL

+PGI₂

+Y27632

+NSC23766

B

Platelet Surface Area µm²

Fibrinogen 100µg/ml	+	+	+	+
oxLDL 50µg/ml	+	+	+	+
PGI₂ 10nM	-	+	-	-
Y27632 10µM	-	-	+	-
NSC23766 50µM	-	-	-	+

C

Platelet Adhesion

Fibrinogen 100µg/ml	+	+	+	+
oxLDL 50µg/ml	+	+	+	+
PGI₂ 10nM	-	+	-	-
Y27632 10µM	-	-	+	-
NSC23766 50µM	-	-	-	+

D

% of platelets with a.nodules

oxLDL 50µg/ml	-	-	-	-	+	+	+	+
Fibrinogen 100µg/ml	+	+	+	+	+	+	+	+
PGI₂ 10nM	-	+	-	-	+	-	-
Y27632 10µM	-	-	+	-	-	+	-
NSC23766 50µM	-	-	-	+	-	-	-	+

E

% of platelets with s.fibres

oxLDL 50µg/ml	-	-	-	-	+	+	+	+
Fibrinogen 100µg/ml	+	+	+	+	+	+	+	+
PGI₂ 10nM	-	+	-	-	+	-	-
Y27632 10µM	-	-	+	-	-	+	-
NSC23766 50µM	-	-	-	+	-	-	-	+

Figure 4.8. Post-treatment with Y27632 and NSC3766 reduces platelet surface area in platelets spread on fibrinogen and oxLDL. Coverslips were coated on 100 µg/ml fibrinogen overnight at 4°C or 50 µg/ml oxLDL for 1 hour at room temperature. Human platelets 2×10^7/ml were spread for 20 mins before post-treatment with either 10 µM Y27632 or 50 µM NSC23766 for 30 mins or PGI₂ for 10 mins. Adhered platelets were fixed using formaldehyde, permeabilised using Triton X-100 (0.1%) and stained using FITC phalloidin. **A)** Images are representative of each condition. **B)** NSC23766 induces a marked reduction in surface area than Y27632 in presence of oxLDL. **C)** Y27632 and NSC23766 reduce platelet adhesion **D+E)** Increased actin nodule formation and induced stress fibre reversal in the presence of forskolin and PGI₂. Data shown as mean ± SD (n=3). * $p<0.05$ ** $p<0.01$ *** $p<0.001$ **** $p<0.0001$ relative to control. Scale bar= 20µm.

The spreading data suggested that on oxLDL, inhibition of Rac and Rho A induced a different response in surface area as indicated by post treatment with PGI$_2$. Therefore, to extend this data we determined the activity levels of both of these key Rho GTPases. Therefore, washed human platelets 2x10^8/ml were spread on 100 μg/ml fibrinogen +/- oxLDL (50 μg/ml), 100 μg/ml fibrinogen +/- nLDL (50 μg/ml) for 20 minutes before stimulation with 10 nM PGI$_2$ for 10 minutes. Platelets were then lysed, and the lysates incubated with PAK-PBD beads. Suspended platelets treated with 10 nM PGI$_2$ for one minute were used as a positive control. Lysates were then blotted and probed for Rac and RhoA activity levels. It was previously established that 50 μg beads show optimal results (Verma and Ihler, 2002; Yusuf et al, 2017).

Quantification by densitometry showed that suspended platelets had 0.0629±0.0527 active Rac at the basal level whilst the addition of PGI$_2$ did not affect Rac activity (figure 4.9 B). However, upon spreading of platelets on fibrinogen, fibrinogen + oxLDL or fibrinogen + nLDL, there was a significant increase in activity to 0.270±0.0201, 0.276±0.0664 or 0.334±0.0617 respectively (figure 4.9 B). Importantly, the level of active Rac was significantly reduced in the presence of 10 nM PGI$_2$ in platelets spread on 100 μg/ml fibrinogen (0.0518±0.0184) and 100 μg/ml fibrinogen + 50 μg/ml nLDL (0.0457±0.0179) but there was no reduction in Rac activity in the presence of oxLDL. This correlated with the lack of reduction of surface area induced by PGI$_2$ in the presence of oxLDL (Figure 4.8).

A

	Suspended Platelets		Spread Platelets					
Fibrinogen 100μg/ml	-	-	+	+	+	+	+	+
nLDL 50μg/ml	-	-	-	-	+	+	-	-
oxLDL 50μg/ml	-	-	-	-	-	-	+	+
PGI$_2$ 10nM	-	+	-	+	-	+	-	+

B

	Suspended Platelets		Spread platelets					
Fibrinogen 100μg/ml	-	-	+	+	+	+	+	+
nLDL 50μg/ml	-	-	-	-	+	+	-	-
oxLDL 50μg/ml	-	-	-	-	-	-	+	+
PGI$_2$ 10nM	-	+	-	+	-	+	-	+
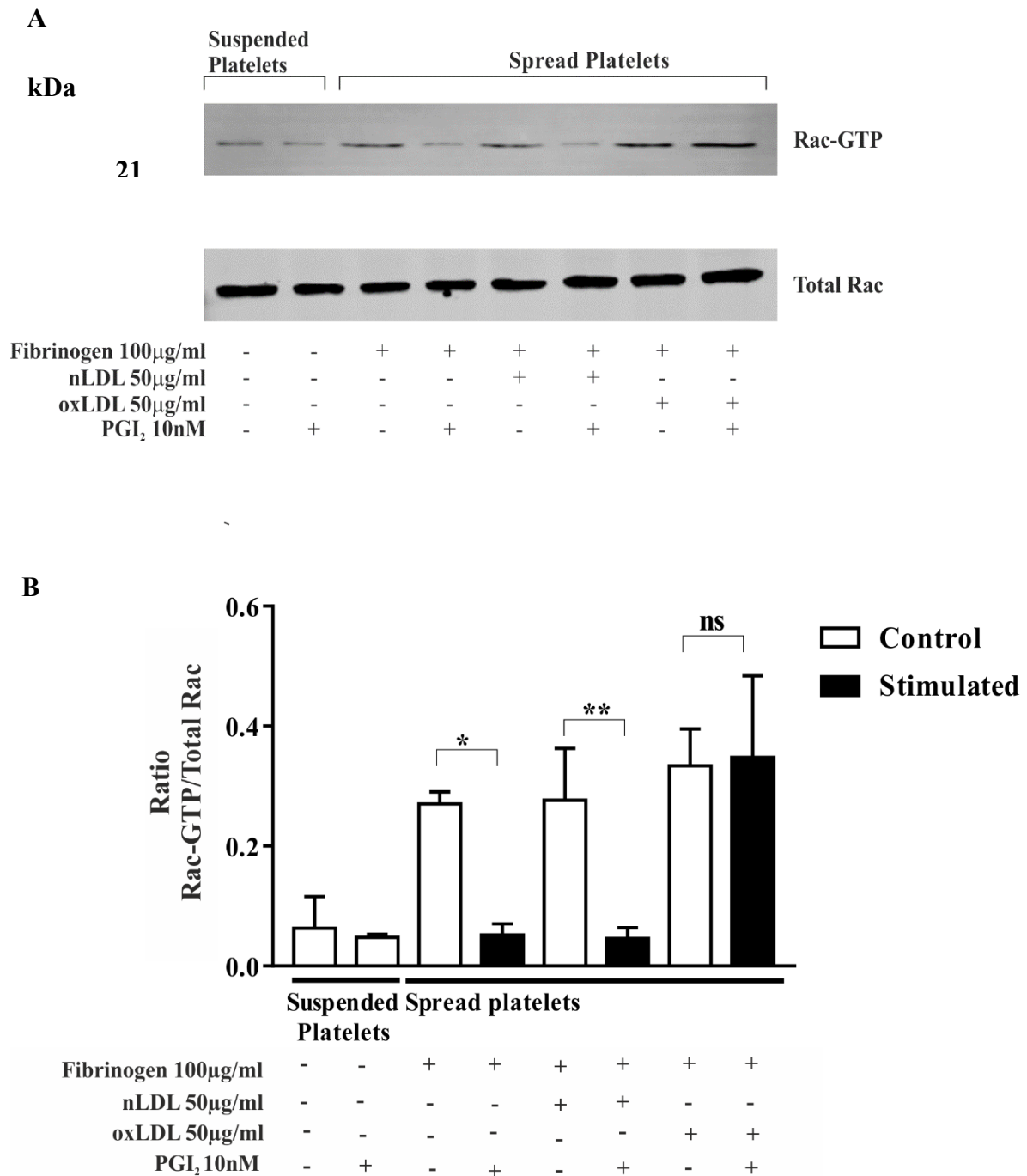
Figure 4.9. PGI$_2$ does not reverse Rac activity in the presence of oxLDL.

Human platelets 2×10^8/ml were spread on 100 μg/ml fibrinogen, 100 μg/ml fibrinogen and 50 μg/ml oxLDL or 100 μg/ml fibrinogen and 50 μg/ml nLDL for 20 mins before treatment with 10 nM PGI$_2$ for 10 mins. The samples were then lysed, using the lysis buffer supplemented with protease inhibitors in the commercial kit, before the addition of 50 μg PAK-PBD beads and completion of a Rac-GTP pulldown assay. Samples were immunoblotted for active Rac & total Rac. **A)** Representative blots for active and total Rac. **B)** Quantification by densitometry for Rac pull down. Data shown as mean ± SD (n=3). * $p < 0.05$. ** $p < 0.01$ relative to control.

After establishing the role of PGI$_2$ in modulating Rac activity, it was essential to understand whether PGI$_2$ regulates Rho activity. Therefore, the experiment was completed as for Rac but Rhotekin beads used to identify RhoA activity levels.

Figure 4.10 B showed that the quantification by densitometry in suspended platelets had 0.0912±0.0453 active Rho at the basal level, 0.113±0.071 in the presence of 10 nM PGI$_2$. There was a significant increase in platelets spread on 100 µg/ml fibrinogen (1.036±0.242), 100 µg/ml fibrinogen & 50 µg/ml nLDL (1.576±0.253) and 100 µg/ml fibrinogen & 50 µg/ml oxLDL (1.73±0.0.579) (figure 4.10 B) in comparison to the basal. Importantly RhoA activity was significantly reduced in the presence of 10 nM PGI$_2$ in platelets spread in all conditions. This is in agreement with the dissolution of stress fibres and the formation of actin nodules upon treatment with PGI$_2$ and demonstrates that there is differential regulation of Rac and RhoA upon addition of PGI$_2$.

Importantly pMLC which is a marker of myosin II activity was also monitored. In addition, in figure 4.11 suspended platelets, no significant difference was shown pMLC levels between basal conditions and platelets stimulated with 10 nM PGI$_2$. An increase in pMLC levels was observed in the presence of 0.1 U/ml thrombin (1.23±0.26). Nevertheless, a decrease in pMLC levels was shown in 10nM PGI$_2$ stimulated platelets that were spread on 100 µg/ml fibrinogen (0.13±0.14), the combination of 100 µg/ml fibrinogen and 50 µg/ml nLDL (0.085±0.032) as well as in the presence of 50 µg/ml oxLDL (1.31±0.21) (figure 4.11 B).

A

	Suspended Platelets		Spread Platelets					

RhoA-GTP

Total RhoA

Fibrinogen 100μg/ml	-	-	+	+	+	+	+	+
nLDL 50μg/ml	-	-	-	-	+	+	-	-
oxLDL 50μg/ml	-	-	-	-	-	-	+	+
PGI$_2$ 10nM	-	+	-	+	-	+	-	+

B

Fibrinogen 100μg/ml	-	-	+	+	+	+	+	+
nLDL 50μg/ml	-	-	-	-	+	+	-	-
oxLDL 50μg/ml	-	-	-	-	-	-	+	+
PGI$_2$ 10nM	-	+	-	+	-	+	-	+
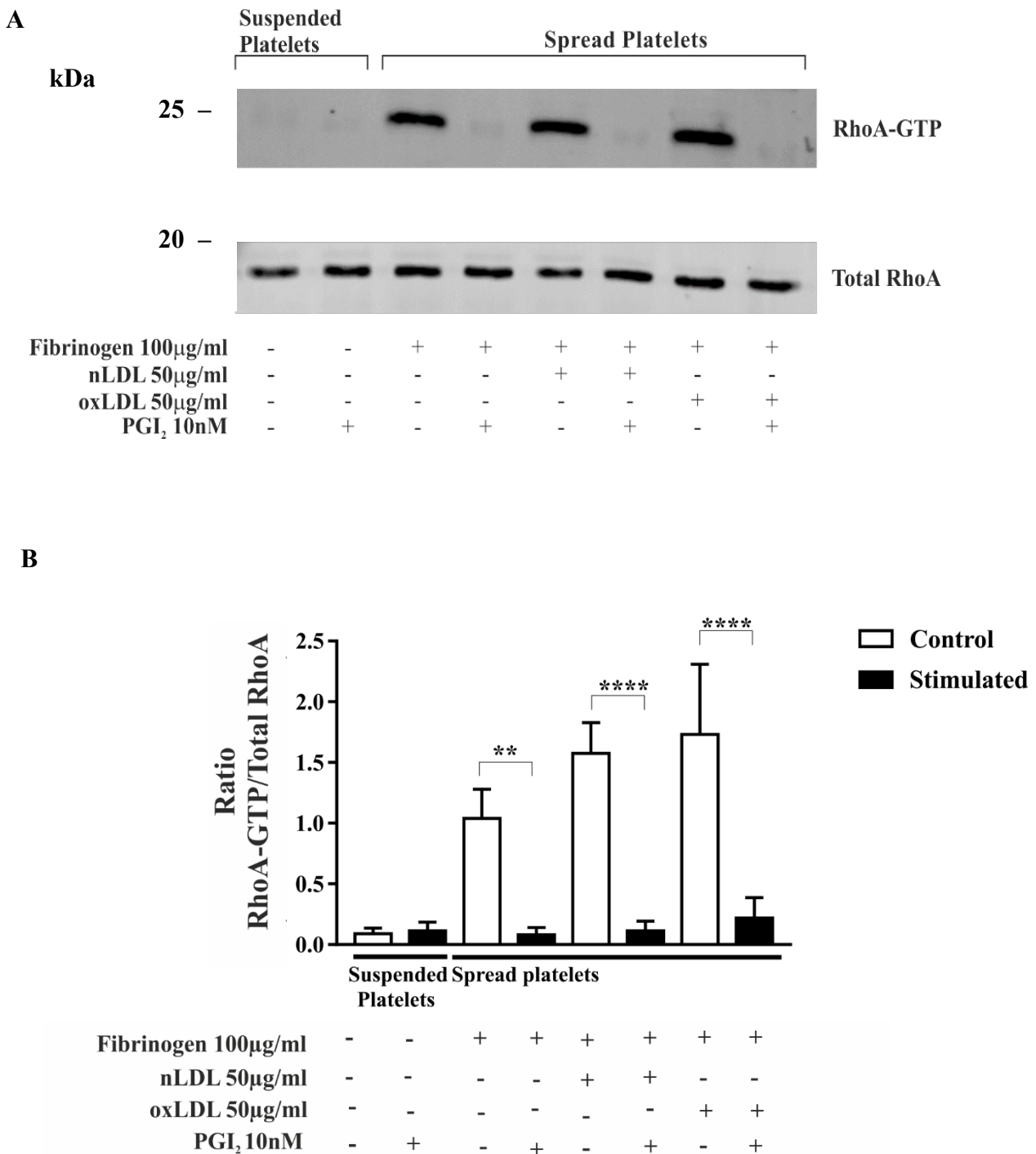
Figure 4.10. Reduced levels of active RhoA in the presence of PGI$_2$.

Human platelets 2×10^8/ml were spread on 100 μg/ml fibrinogen, 100 μg/ml fibrinogen & 50 μg/ml oxLDL or 100 μg/ml fibrinogen & 50 μg/ml nLDL for 20 mins before treatment with 10 nM PGI$_2$ for 10 mins. The samples were then lysed, using the lysis buffer supplemented with protease inhibitors in the commercial kit, before the addition of 50 μg Rhotekin beads and completion of a RhoA pulldown assay. Samples were immunoblotted for active RhoA and total RhoA. **A)** Images are representative of blots for active & total RhoA. **B)** Densitometry analysis for RhoA pull down. Data shown as mean ± SD (n=3). ** $p < 0.01$. **** $p < 0.0001$ relative to control.

A

	Suspended Platelets			Spread Platelets					
Thrombin 0.1U/ml	-	+	-	-	-	-	-	-	-
PGI$_2$ 10nM	-	-	+	-	+	-	+	-	+
Fibrinogen 100μg/ml	-	-	-	+	+	+	+	+	+
nLDL 50μg/ml	-	-	-	-	-	+	+	-	-
oxLDL 50μg/ml	-	-	-	-	-	-	-	+	+

B

	Suspended Platelets			Spread platelets					
Fibrinogen 100μg/ml	-	-	-	+	+	+	+	+	+
nLDL 50μg/ml	-	-	-	-	-	+	+	-	-
oxLDL 50μg/ml	-	-	-	-	-	-	-	+	+
Thrombin 0.1 U/ml	-	-	+	-	-	-	-	-	-
PGI$_2$ 10nM	-	+	-	-	+	-	+	-	+
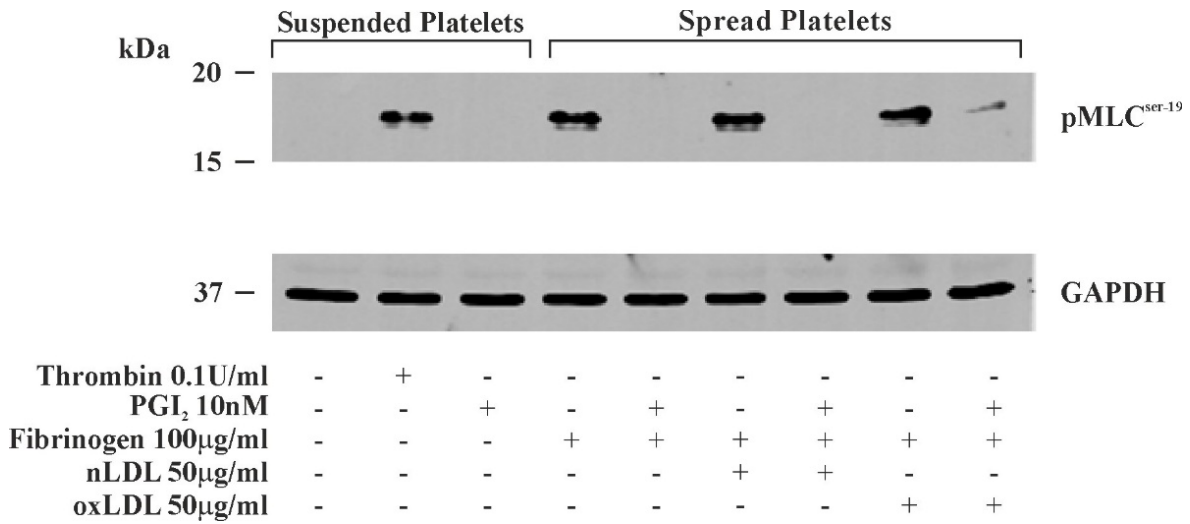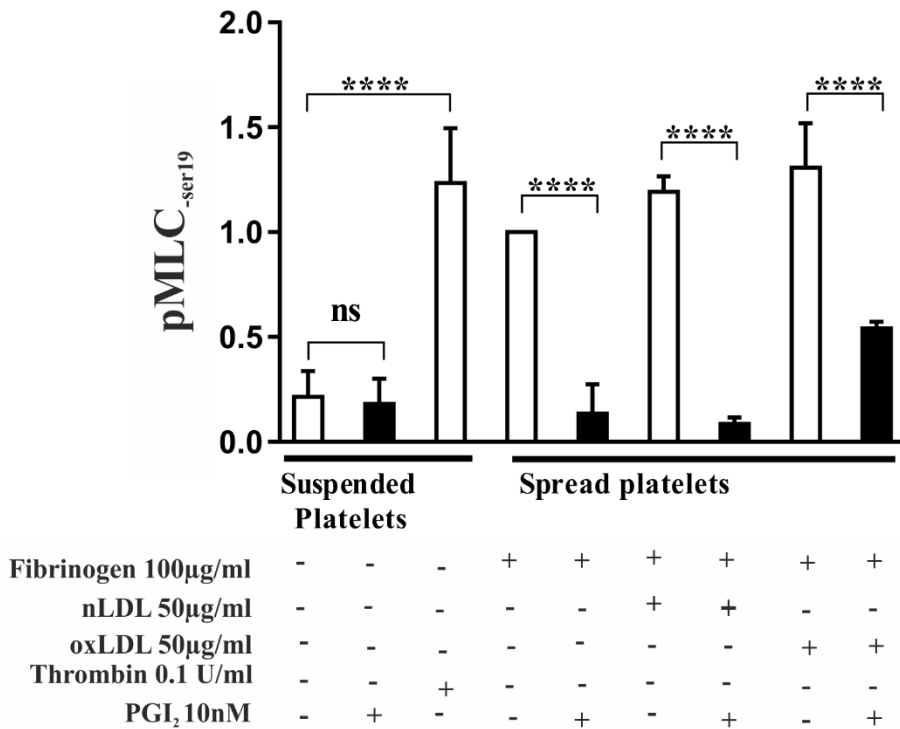
Figure 4.11. pMLC is downregulated in the presence of PGI$_2$.

Human platelets 2×10^8/ml were spread on 100 μg/ml fibrinogen or 50 μg/ml oxLDL or 50 μg/ml nLDL for 20 mins before treatment with 10 nM PGI$_2$ for 10 mins. The samples were then lysed, using the lysis before probing for pMLC and GAPDH. **A)** Western blots or pMLC and GAPDH. **B)** Densitometry analysis for pMLC. Data shown as mean ± SD (n=6). **** $p<0.0001$ relative to control.

4.5. The effect of forskolin is attenuated in platelets spread on oxLDL and fibrinogen

Having identified that there was a reduction in the level of cAMP, we next identified if this was due to an inhibition of AC or activation of PDE3 activity as previously identified by Berger et al. 2019. To identify if oxLDL could also inhibit the activity of AC, as well as activating PDE3, washed human platelets $2x10^7$/ml were allowed to spread on 100 µg/ml fibrinogen, 100 µg/ml fibrinogen with 50 µg/ml oxLDL, or 100 µg/ml fibrinogen and 50 µg/ml nLDL coated coverslips for 20 minutes and subsequently treated with 10 nM PGI_2, 10 nM PGI_2 in combination with 1µM Fsk and 1µM Fsk alone for 10 minutes. Adhered platelets were fixed using formaldehyde, permeabilised, stained using FITC phalloidin and visualised using an immunofluorescence microscope.

Figure 4.12B identified that the addition of 10 nM PGI_2 (19.25±0.73 µm^2), 10 nM PGI_2 in combination with 1 µM Fsk (19.97±0.42 µm^2) or 1 µM Fsk (20.00±0.50 µm^2) on 100 µg/ml fibrinogen spread platelets reduced the surface area of platelets significantly compared to the control conditions (26.09±0.62 µm^2). Analysis for percentage of platelets with actin nodules showed an increase in platelets stimulated with 10 nM PGI_2 (81.64±2.05%), 10 nM PGI_2 and 1 µM Fsk (94.25±0.90%) and 1 µM Fsk (82.36±2.37%) (figure 4.12 D). In contrast, figure 4.12 E showed that stress fibre reversal was reduced in the presence of 10 nM PGI_2 (18.72±2.24%), 10 nM PGI_2 and 1 µM Fsk (19.21±4.26%) as well as 1 µM Fsk (21.59±3.80%) alone in comparison to the control (75.92±3.49%).

Likewise, the same effect was seen in spread platelets in a combination of 100 µg/ml fibrinogen and 50 µg/ml nLDL. The percentage of platelets with actin nodules dramatically increased to 87.06±3.10% in 10 nM PGI_2 treated platelets, 95.01±1.26% in the presence of 10 nM PGI_2 and 1 µM Fsk and 93.05±1.47% after treatment with 1 µM Fsk alone (figure 4.13 D). As expected,

there was no change in number of platelets adhered on 100 µg/ml fibrinogen in any condition (figure 4.12 B). However, with the nLDL and fibrinogen combination unexpectedly platelet treated with 10 nM PGI_2 and 1 µM Fsk showed a significant increase in adhesion in comparison to the control condition (figure 4.13 B).

Figure 4.14 B shows the expected reversal of area in platelet spreading on fibrinogen and 50 µg/ml oxLDL for platelets treated with 10 nM PGI_2. This was phenocopied by FSK treatment. An increase in actin nodules is evident in the presence of 10 nM PGI_2 (76.27±2.36%), 10 nM PGI_2 and 1 µM Fsk (78.45±1.73%) and 1 µM Fsk (82.07±2.22%) in comparison to the control (5.95±1.06%) (figure 4.14 D). Analysis for percentage of platelets with stress fibres revealed a reduction in stress fibres upon treatment with 10 nM PGI_2 (23.48±2.16%), 10 nM PGI_2 in combination with 1 µM Fsk (21.05±1.59%) and 1 µM Fsk alone (19.75±1.10%) in contrast to the control condition (77.81±2.97%) (figure 4.14 E). Surprisingly, figure 4.14 C shows an increase was seen in adhered platelets stimulated with the combination of 10 nM PGI_2 and 1 µM Fsk at 50 µg/ml oxLDL (108.78±3.89) compared to the control condition at (44.67±4.33) as well as platelets inhibited with 10 nM PGI_2 (38.00±2.03) and 1 µM Fsk (39.22±2.54).

This data indicates that Fsk can still induce a reversal of stress fibres similar to that seen within PGI_2 treatment and therefore AC is less likely to be affected by oxLDL treatment.
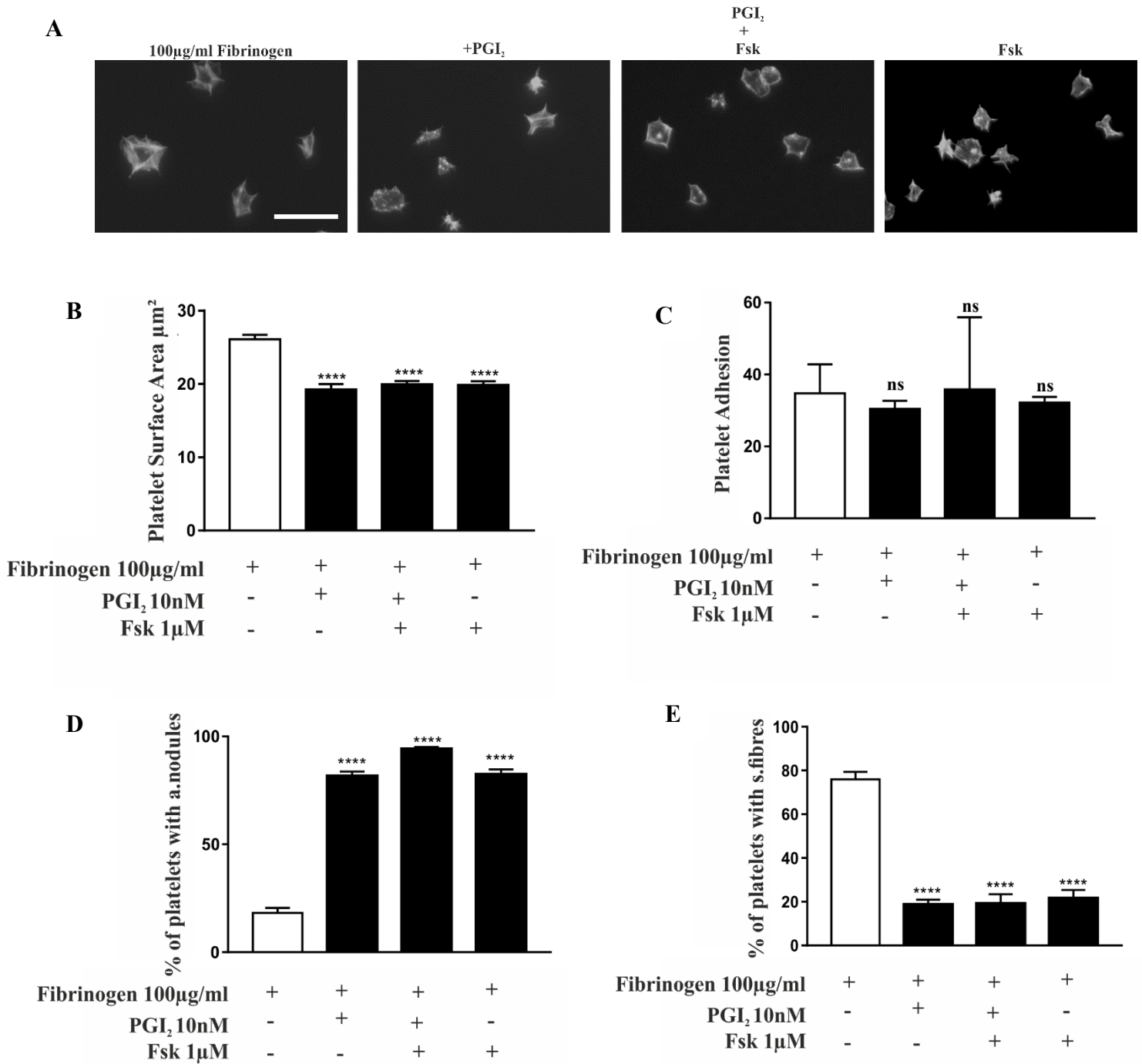
Figure 4.12. Forskolin induces reversal in platelet spreading on fibrinogen.

Coverslips were coated with 100 μg/ml overnight at 4°C. Human platelets 2×10^7/ml spread for 20 mins and subsequently treated with 10 nM PGI_2, combination of 10 nM PGI_2 and 1 μM forskolin and 1 μM forskolin alone for 10 mins. Adhered platelets were subsequently fixed using formaldehyde, permeabilised using Triton X-100 (0.1%) and stained using FITC phalloidin. **A)** Images are representative of each condition. **B)** Forskolin reduces surface area in fibrinogen spread platelets. **C)** No effect seen in adhered platelets. D+E) Forskolin and PGI_2 induce actin nodule formation and stress fibre reversal. Data shown as mean ± SD (n=3). **** $p < 0.0001$ relative to control. Scale bar= 20μm.
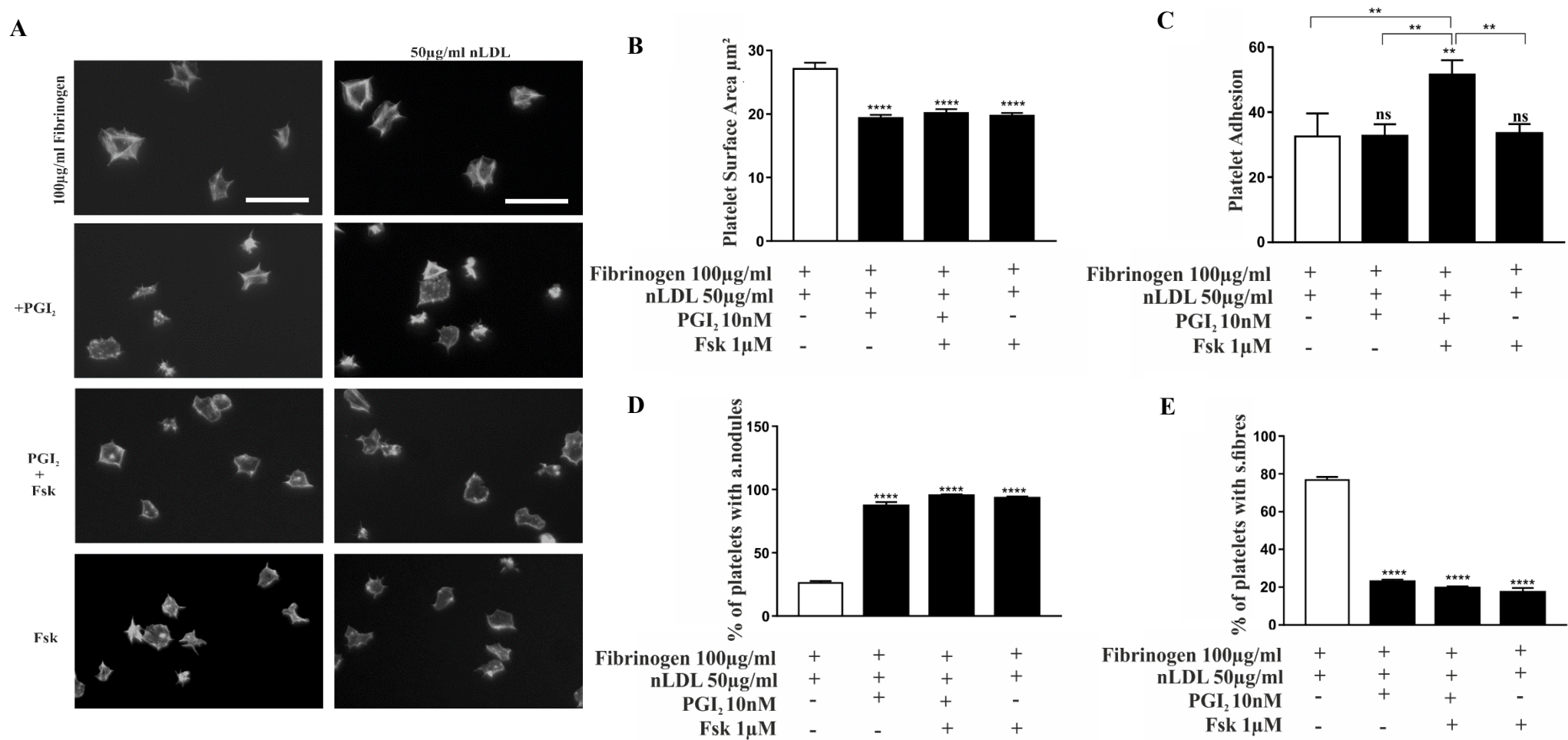
Figure 4.13. Forskolin induces reversal in platelet spreading on nLDL and fibrinogen.

Coverslips were coated with 100 µg/ml overnight at 4°C and 50 µg/ml nLDL for 1 hour at room temperature. Human platelets 2×10^7/ml spread for 20 mins and subsequently treated with 10 nM PGI$_2$, combination of 10 nM PGI$_2$ and 1 µM forskolin as well as 1 µM forskolin alone for 10 mins. Adhered platelets were subsequently fixed using formaldehyde, permeabilised using Triton X-100 (0.1%) and stained using FITC phalloidin. **A)** Images are representative of each condition. **B)** Forskolin reduces platelets spreading on nLDL and fibrinogen **C)** No effect seen in adhered platelets. **D+E)** Forskolin induces actin nodule formation and stress fibre reversal. Data shown as mean ± SD (n=3) ** $p<0.01$ **** $p<0.0001$ relative to control. Scale bar= 20µm.
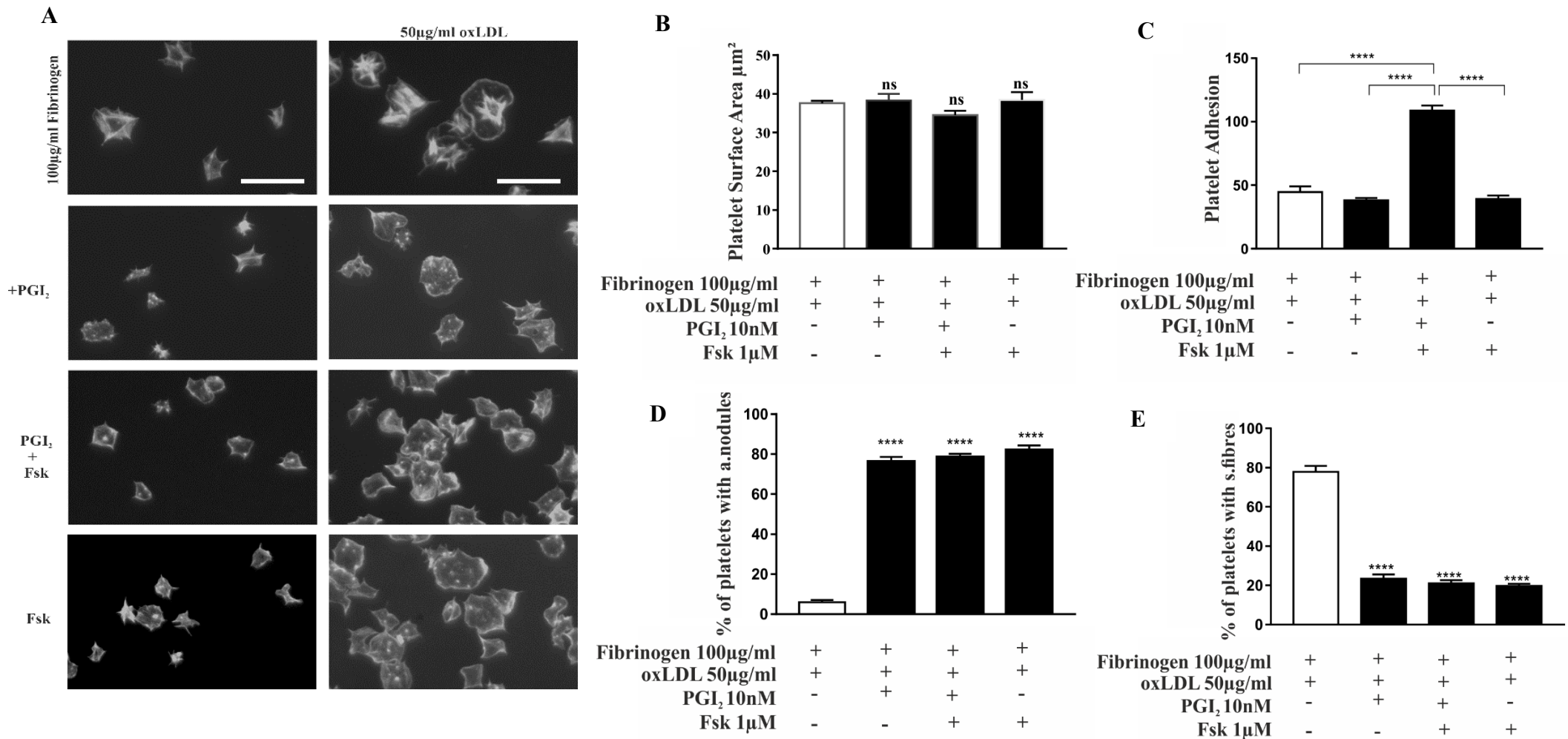
Figure 4.14. Forskolin mimics the effect of PGI$_2$ in platelet spreading on oxLDL and fibrinogen.
Coverslips were coated with 100 µg/ml overnight at 4°C and 50 µg/ml oxLDL for 1 hour at room temperature. Human platelets 2x10^7/ml spread for 20 mins and subsequently treated with 10nM PGI$_2$, combination of 10 nM PGI$_2$ and 1 µM forskolin and 1 µM forskolin alone for 10 mins. Adhered platelets were subsequently fixed using formaldehyde, permeabilised using Triton X-100 (0.1%) and stained using FITC phalloidin. **A)** Images are representative of each condition. **B)** Forskolin inhibits the effect of PGI$_2$ in platelets spread on oxLDL. **C)** No effect seen in adhered platelets. **D+E)** Increased actin nodule formation and induced stress fibre reversal in the presence of forskolin and PGI$_2$. Data shown as mean ± SD (n=3). **** $p<0.0001$ relative to control. Scale bar= 20µm.

4.6. The effect of PGI$_2$ is attenuated in a PDE3 dependent manner in platelets spread on oxLDL and fibrinogen.

After establishing that the use of Forskolin induced a similar phenotype to PGI$_2$, we next identified the effect of PDE3 inhibition on platelet spreading, with the use of Milrinone. As a result, washed human platelets 2×10^7/ml were allowed to spread on either 100 µg/ml fibrinogen, 50µg/ml oxLDL or 50µg/ml nLDL coated coverslips for 20 minutes and subsequently treated with Tyrodes, or Tyrodes containing either 10 nM PGI$_2$, 10 nM PGI$_2$ in combination with 10 µM milrinone or 10 µM milrinone alone for 10 minutes. Adhered platelets were fixed using formaldehyde, permeabilised, stained using FITC phalloidin and visualised using an immunofluorescence microscope.

Figure 4.15 B shows a significant decrease in platelets spread on 100 µg/ml fibrinogen in the presence of 10 nM PGI$_2$ (17.87 ± 2.56 µm^2), 10 nM PGI$_2$ and 10 µM milrinone 17.63 ± 2.35 µm^2) and 10 µM milrinone alone (15.64 ± 0.27 µm^2) in comparison to the control (27.31 ± 1.69 µm^2). Overall, no change in platelet adhesion was observed in all conditions (figure 4.15 C). In addition, the percentage of platelets with actin nodules increased from $28.03 \pm 7.99\%$ in the control to $82.27 \pm 2.97\%$ after 10 nM PGI$_2$ treatment, $96.52 \pm 1.08\%$ after 10 nM PGI$_2$ and 10 µM milrinone treatment and $96.00 \pm 4.80\%$ when treated with 10 µM milrinone alone (figure 4.15 D). Figure 4.15 E identifies the reciprocal reversal of stress fibres, with a decrease of stress fibres from $68.22 \pm 4.53\%$ in the control sample to $15.75 \pm 2.89\%$ upon treatment with 10 nM PGI$_2$, $0.50 \pm 1.67\%$ in platelets treated with the combination of 10 nM PGI$_2$ and 10 µM milrinone and $0.55 \pm 0.29\%$ in the presence of 10 µM milrinone.

Having identified that the individual matrix proteins had variable responses to PGI$_2$ but similar responses to milrinone treatment, we next identified the effect of both PGI$_2$ and milrinone on the combinations of fibrinogen with nLDL or oxLDL. Therefore, washed human platelets $2x10^7$/ml were allowed to spread on 100 µg/ml fibrinogen alone, 100 µg/ml fibrinogen and 50 µg/ml oxLDL, or 100 µg/ml fibrinogen and 50 µg/ml nLDL coated coverslips for 20 minutes and subsequently treated with Tyrode's as a control, tyrode's containing either 10 nM PGI$_2$, 10 nM PGI$_2$ in combination with 10 µM milrinone or 10 µM milrinone alone for 10 minutes. Adhered platelets were fixed using formaldehyde, permeabilised, stained using FITC phalloidin and visualised using an immunofluorescence microscope.

Analysis of platelets spread on fibrinogen +-/ nLDL showed a very similar profile to that shown on fibrinogen. Surface area analysis showed a significant reduction after treatment with 10 nM PGI$_2$ ($15.24\pm.1.82\mu m^2$), 10 nM PGI$_2$ and 10 µM milrinone (14.85 ± 1.21 μm^2) as well as 10 µM milrinone (14.65 ± 1.43 μm^2) in comparison to the control (25.46 ± 2.34 μm^2) (figure 4.16 B). There was no change observed in the number of platelets adhered for all conditions (figure 4.16C). In addition, figure 4.16 D showed that the percentage of platelets spread on 100 µg/ml fibrinogen and 50 µg/ml nLDL that had actin nodules significantly increased from $25.59\pm7.49\%$ in the control sample to $74.23\pm2.12\%$ after treatment with 10 nM PGI$_2$, $97.44\pm1.26\%$ in the presence of 10 nM PGI$_2$ and 10 µM milrinone and $95.11\pm2.80\%$ after the addition of 10 µM milrinone alone. Additionally, a significant increase in actin nodules was seen in the presence of 10µM milrinone than platelets treated with 10 nM PGI$_2$ alone. Interestingly, figure 4.16 D showed a reduced percentage of platelets that had actin nodules in the presence of 50 µg/ml nLDL ($25.59\pm7.49\%$) compared to platelets spread on 100 µg/ml fibrinogen alone ($38.50\pm8.34\%$). However, more platelets treated with 10 nM PGI$_2$ had actin

nodules in the presence of 50 µg/ml nLDL (74.23±2.12%) than the control platelets spread on 100 µg/ml fibrinogen alone.

Importantly there was the reciprocal relationship between actin nodule formation and stress fibre dissolution as expected. Figure 4.16 E established that the percentage of platelets with stress fibres reduced from 69.25±5.93% in the control to 10.55±1.00% after they were treated with 10 nM PGI_2, 0.46±0.18% in the presence of 10 nM PGI_2 and 10 µM milrinone and 0.43±0.15% upon treatment with 10 µM milrinone alone (figure 4.16 E). There was no difference in stress fibres in platelets spread in the presence or lack of nLDL for all conditions.

In agreement with the responsiveness of spread platelets on fibrinogen to Milrinone, platelets spread on oxLDL also readily responded to treatment with milrinone either on its own (15.83±1.21 μm^2) or in combination with PGI_2 10 nM (18.74±1.44 μm^2) in comparison to the control 40.24±0.98 μm^2 and PGI_2 samples 39.62±0.83 μm^2 um^2). As expected, samples treated with 50 µg/ml nLDL showed little adhesion and spreading, with all treatments (figure 4.17). PGI_2 and Milrinone had no effect on platelets spread on nLDL.

As shown previously, platelets spread on the combination of 100 µg/ml fibrinogen and 50 µg/ml oxLDL had a significant increase in surface area in comparison to those spread on 100 µg/ml fibrinogen alone (39.95±2.00 μm^2 V 27.31±1.69 μm^2) (figure 4.18 B). As expected, upon addition of 10 nM PGI_2 although platelets spread on fibrinogen reduced in surface area, those spread on the combination did not alter their surface area in comparison to the control. However, treatment with Milrinone, either alone or in combination with PGI_2, caused a significant reduction in platelet surface area (figure 4.18 B). No significant change was seen in number of platelets adhered for all treatments (figure 4.18 C). Again, as expected although

PGI$_2$ treatment did not affect the surface area of the platelet on the combination matrix, it did affect the actin structures. Analysis of stress fibres and actin nodules show that there was a dramatic increase in actin nodules from 21.00±10.99% in the control sample to 71.00±43.12% upon PGI$_2$ treatment, and a decrease in stress fibre formation (figure 4.18 D, E). There was no additional increased effect on actin nodule formation in the presence of milrinone.

This data indicates that milrinone treatment re-establishes the ability of PGI$_2$ to induce platelet inhibition. It also indicates that Rac activity is linked to higher levels of cAMP and potentially could be controlled via the activity of PDE3.
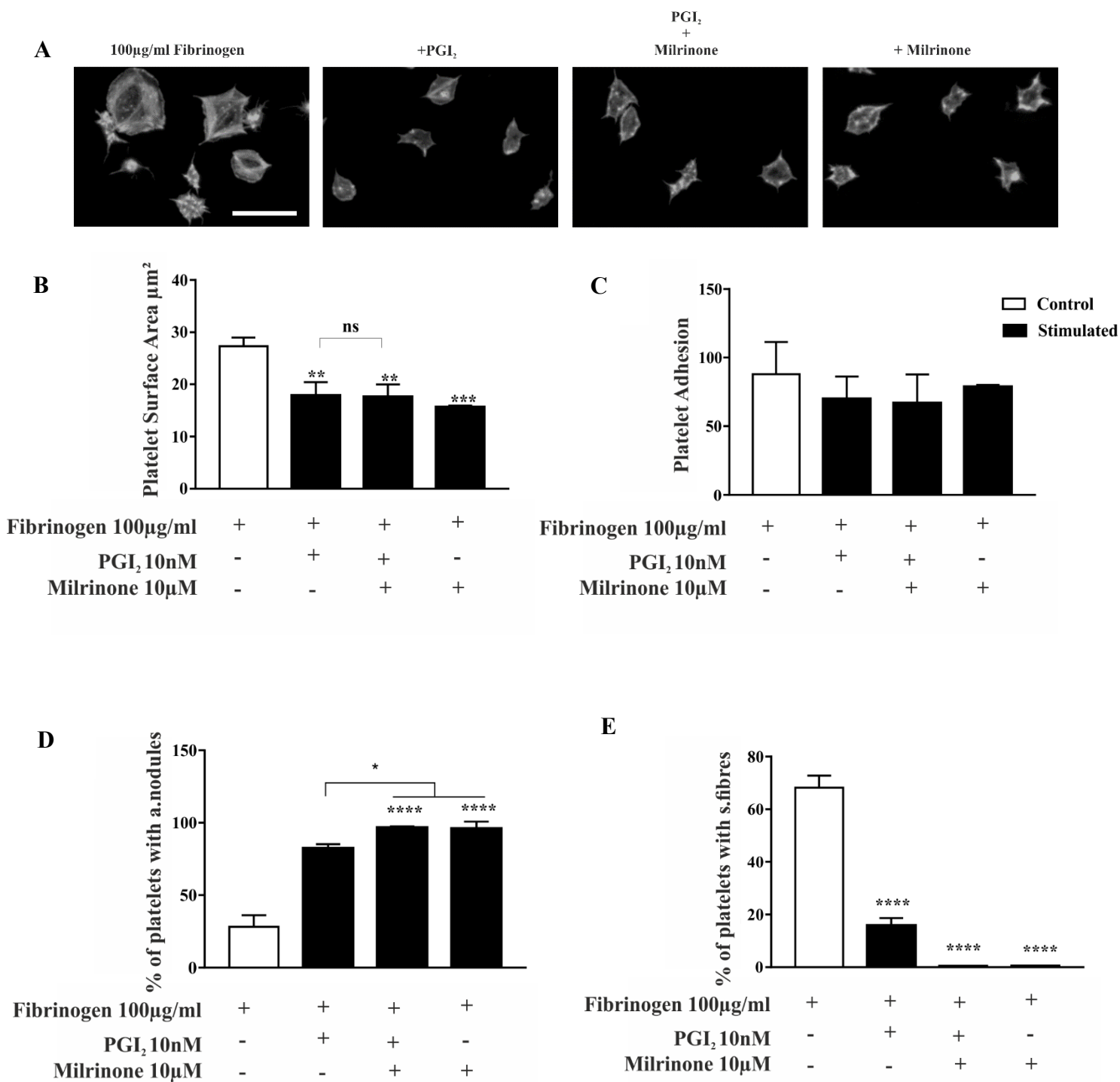
Figure 4.15. Platelet spreading on fibrinogen is reduced in a PDE3 mediated manner.

Coverslips were coated with 100 μg/ml overnight at 4°C. Human platelets 2×10^7/ml spread for 20 mins and subsequently treated with 10 nM PGI$_2$, and 10 μM milrinone alone for 10 minutes. Adhered platelets were subsequently fixed using formaldehyde, permeabilised using Triton X-100 (0.1%) and stained using FITC phalloidin. **A)** Images are representative of each condition. **B)** Platelet surface area is reduced in a PDE3 dependent manner. **C)** Platelet adhesion is unaffected in all conditions. **D+E)** Actin nodules is increased and stress fibre reversal is induced in PGI$_2$ treated platelets in a PDE3 dependent fashion. Data shown as mean ± SD (n=3). **** $p < 0.0001$ relative to control. Scale bar= 20μm.
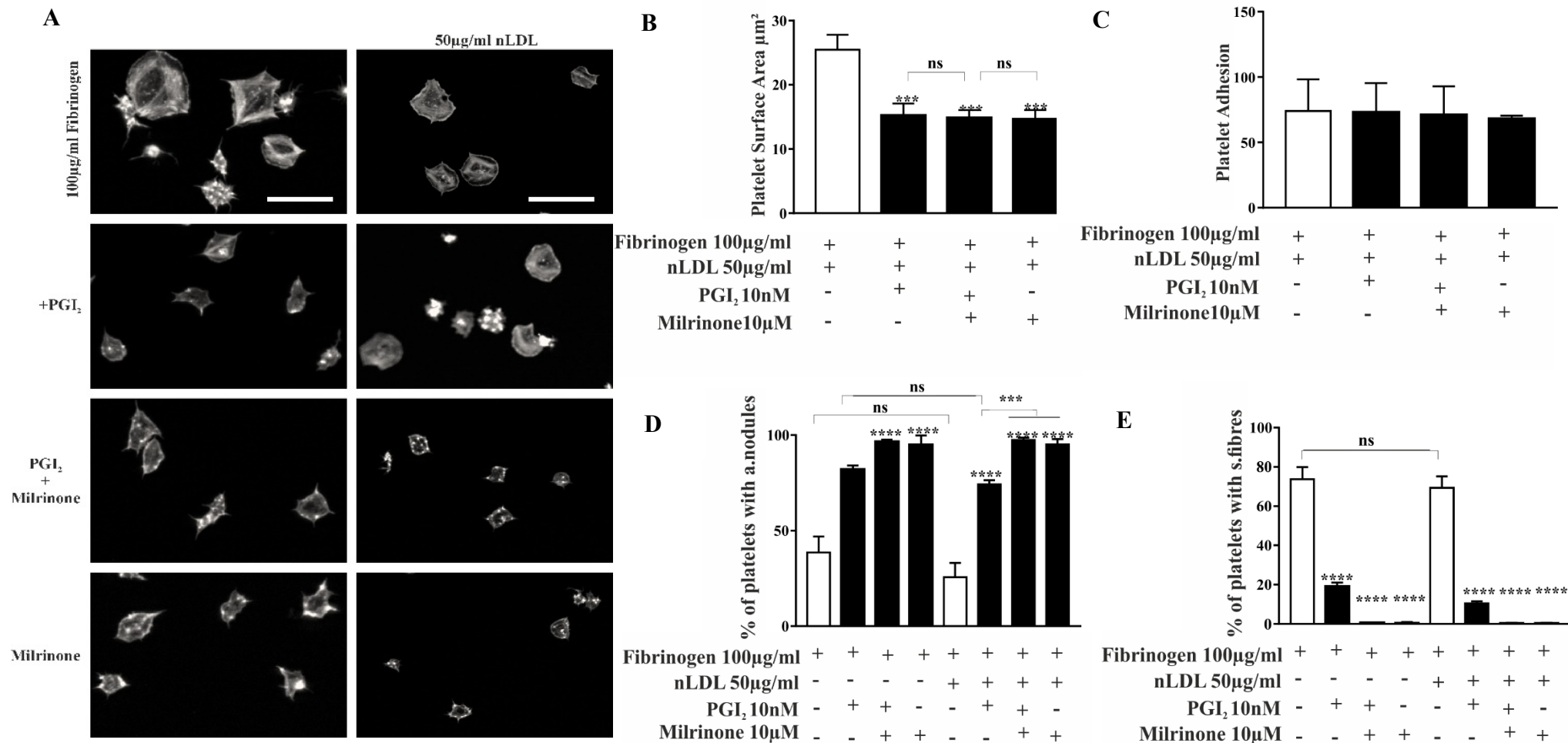
Figure 4.16. Platelet spreading on fibrinogen and nLDL is reduced in a PDE3 mediated manner. Coverslips were coated with 100 µg/ml fibrinogen overnight at 4°C or 50 µg/ml nLDL for 1 hour at room temperature. Human platelets 2×10^7/ml spread for 20 mins and subsequently treated with 10 nM PGI$_2$, and 10 µM milrinone alone for 10 mins. Adhered platelets were fixed using formaldehyde, permeabilised using Triton X-100 (0.1%) and stained using FITC phalloidin. **A)** Images are representative of each condition. **B)** Platelet surface area on fibrinogen and nLDL is reduced in a PDE3 mediated manner **C)** Platelet adhesion is unaffected in all conditions**. D+E)** actin nodule is increased and stress fibre reversal induced in a PDE3 VS figure 4.15 D, E. Data shown as mean ± SD (n=3). *** $p<0.001$ **** $p<0.0001$ relative to control. Scale bar= 20µm.
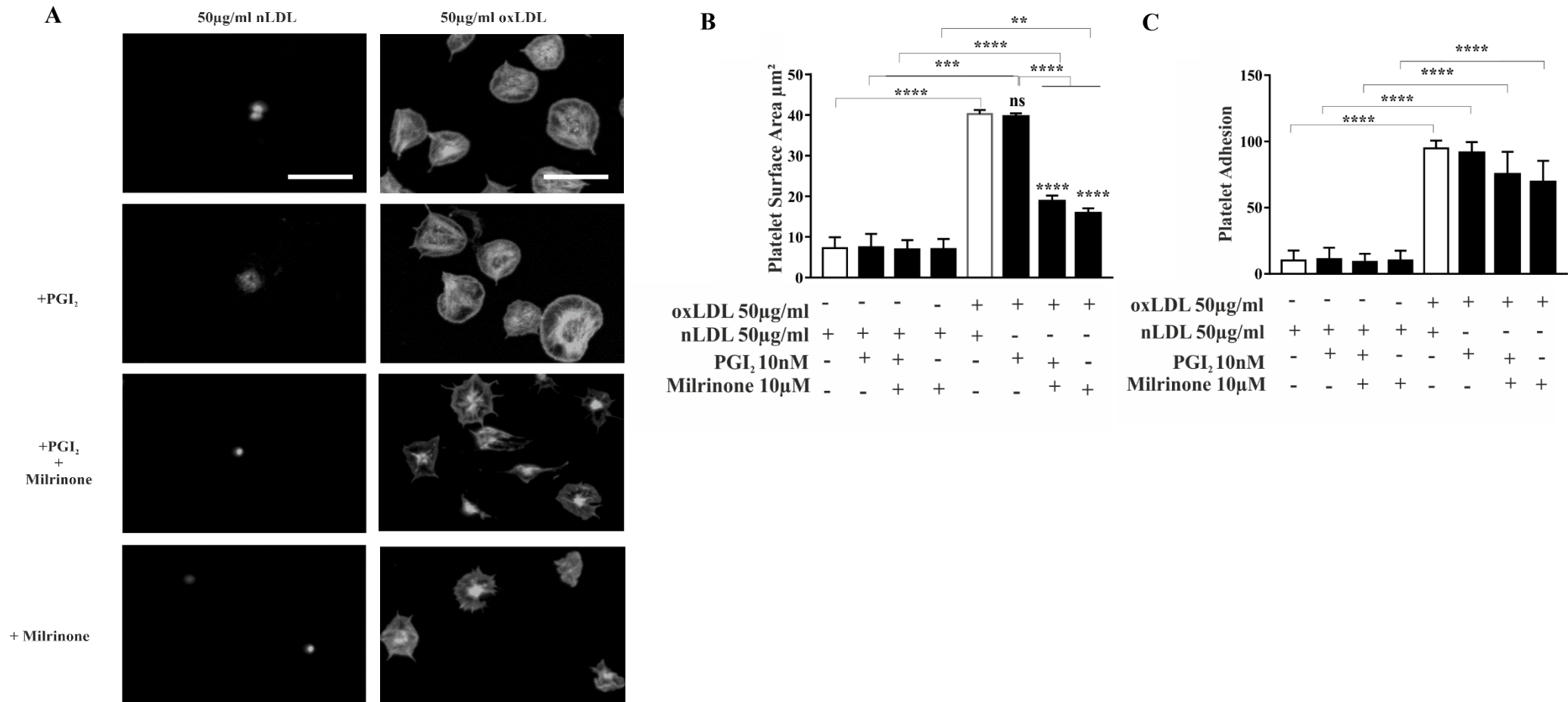
Figure 4.17. oxLDL attenuates the effect of PGI$_2$ in spread platelets in a PDE3 dependent manner.
Coverslips were coated with 50 µg/ml nLDL or 50 µg/ml oxLDL for 1 hour at room temperature. Human platelets 2×10^7/ml spread for 20 mins and subsequently treated with 10 nM PGI$_2$, and 10 µM milrinone alone for 10 mins. Adhered platelets were subsequently fixed using formaldehyde, permeabilised using Triton X-100 (0.1%) and stained using FITC phalloidin. **A)** Images are representative of each condition. **B)** Platelet surface area is not reduced in PGI$_2$ treated platelets in the presence of oxLDL in a PDE3 dependent fashion. **C)** Increased platelet adhesion in platelets spread on oxLDL. Data shown as mean ± SD (n=3). **** $p<0.0001$ relative to control. Scale bar= 20µm.
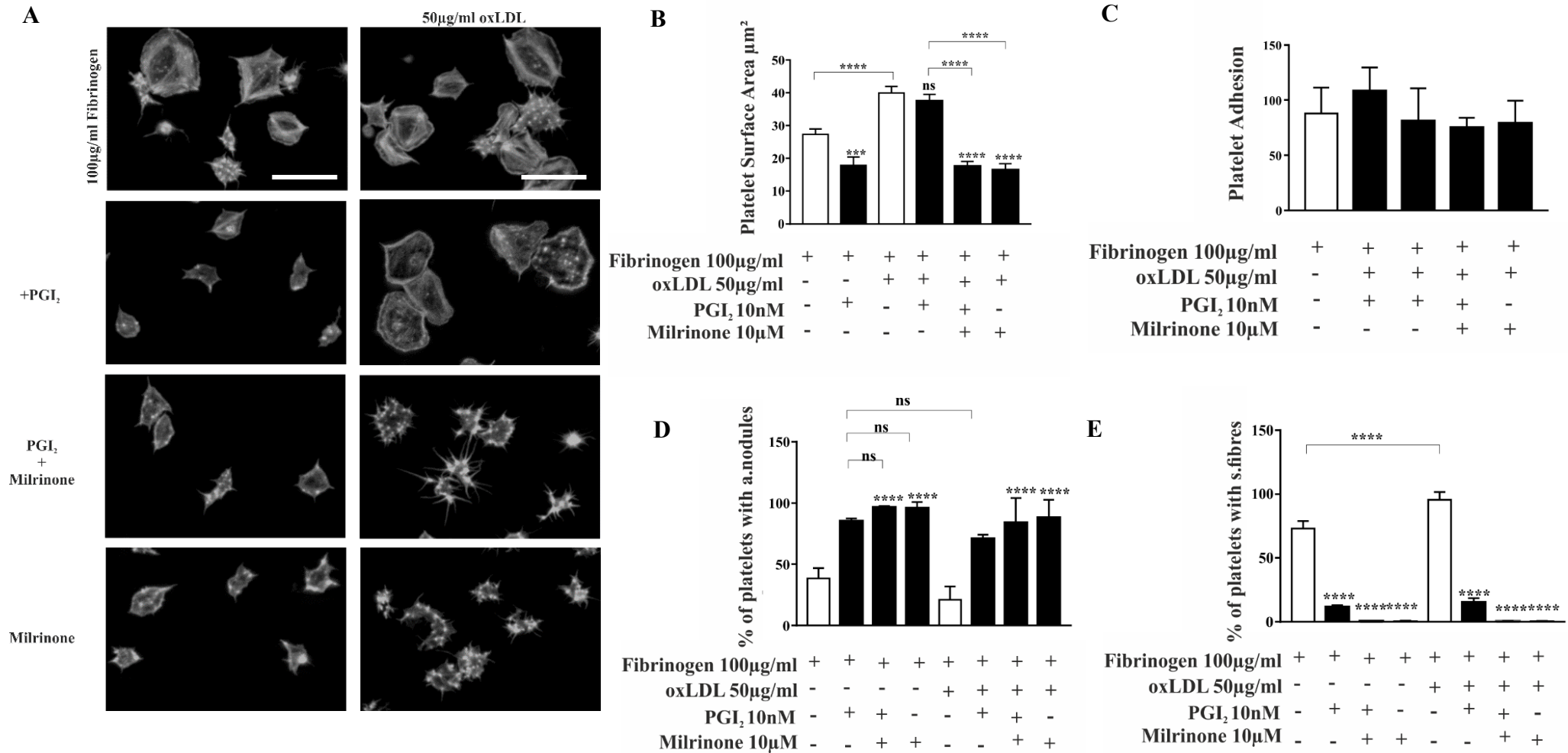
Figure 4.18. oxLDL and fibrinogen spread platelets attenuate PGI$_2$ in a PDE3 dependent manner.
Coverslips were coated with 100 µg/ml fibrinogen overnight at 4°C and then washed with PBS and treated with either 50 µg/ml oxLDL or PBS for 1 hour at room temperature. Human platelets 2x10^7/ml spread for 20 mins and subsequently treated with 10nm PGI$_2$, and 10µM milrinone alone for 10 mins. Adhered platelets were subsequently fixed using formaldehyde, permeabilised using Triton X-100 (0.1%) and stained using FITC phalloidin. **A)** Images are representative of each condition. **B)** oxLDL attenuates the effect of PGI$_2$ in spread platelets in a PDE3 dependent manner. **C)** No effect seen in adhered platelets. Data shown as mean ± SD (n=3). *** $p<0.001$ **** $p<0.0001$ relative to control. Scale bar= 20µm.

4.7. Discussion

Chapter 3 identified that oxLDL blocks the effect of PGI$_2$ on fibrinogen spread platelets, inducing stress fibre reversal while surface area and lamellipodia were unaffected. Thus, this chapter explores if RhoGTPases activity are dependent on the level of cAMP present in the platelet.

Platelets spread on fibrinogen showed a robust elevation in cAMP upon treatment with PGI$_2$. Likewise, platelets spread on fibrinogen and nLDL also showed elevated levels of cAMP. Elevated cAMP levels were also observed in the presence of oxLDL nevertheless, the elevation was significantly lower to the control condition.

Increase in cAMP levels leads to PKA mediated phosphorylation of downstream targets such as VASP. Thus, to identify this effect on PKA signalling downstream of cAMP, platelets were probed for the downstream pVASPSer[157]. This determined that stimulation with PGI$_2$ induces elevation of pVASPSer[157] marker and pPKA substrate phosphorylation. This effect however was not seen in the presence of oxLDL. However, pMLC was elevated in platelets spread on fibrinogen, fibrinogen and nLDL as well as oxLDL, in line with stress fibre formation and increase in Rho activity in the absence of PGI$_2$.

As it was hypothesised that oxLDL altered cAMP signalling played a role in regulating the different RhoGTPases, platelets were pre-treated with the RhoA inhibitor, Y27632 (selectively inhibits ROCK as a result of competitive binding with ATP) or the Rac inhibitor, NSC3766. As expected, it was found that both Y27632 and NSC3766 reduced platelet surface area and induced stress fibre reversal and actin nodule formation in platelets spread for 20 minutes on both fibrinogen and oxLDL. This experiment determined that platelet surface area is markedly

reduced with NSC3766 than Y27632 in the presence of oxLDL and the same effect was seen after post-treatment with Y27632 and NSC3766. These findings postulate that oxLDL differentially regulates the different RhoGTPases.

To determine this theory, Rho and Rac activity were identified. After spreading the platelets on oxLDL and fibrinogen for 20 minutes and treatment with PGI_2 for 10 minutes, there was a reduction in active GTP-bound form of RhoA in fibrinogen spread platelets. in agreement with this, platelets spread on nLDL or oxLDL also showed this reduction. This is consistent with the stress fibre reversal phenotype observed under these conditions. However, Rac activity was reduced in platelets spread on fibrinogen and nLDL but it was not reduced in the presence of oxLDL. Again, this is in line with the maintenance of lamellipodia formation in these conditions. It was thus deduced that in the presence of oxLDL, Rho but not Rac is downregulated in platelets treated with PGI_2, suggesting that different cAMP levels may regulate the different RhoGTPases. Scott and Leopardi, 2003 have described that elevated cAMP levels cause differential regulation of RhoGTPases in dendrite formation whereby RhoA activity was downregulated whereas the activity of Rac was upregulated due to RhoGDI preferentially binding to RhoA than Rac. Furthermore, phospholipids, arachidonic acid and phosphatidic acid can control the disassociation of the Rac-GDI complex, (Chuang, Bohl and Bokoch, 1993; Tolias, Couvillon, Cantley and Carpenter, 1998).

After establishing that oxLDL plays a role in modulating cAMP activity, we further explored if cAMP elevating agents such as forskolin induce the same effect to understand its role in rearranging the cytoskeleton and identified that forskolin mimics the effect of PGI_2 by inducing stress fibre reversal and actin nodule formation while surface area and lamellipodia remain

unaffected. This phenotype was previously established in vascular smooth muscle cells where oxLDL inhibited forskolin-mediated cAMP elevation (Jing et al., 1999).

Furthermore, to explore the inhibitory effect that was induced in oxLDL and fibrinogen spread platelets, it was postulated that oxLDL induced degradation of the cAMP which in turn diminished the effect of PGI_2. Therefore, to determine if oxLDL accelerated the breakdown of cAMP by PDE3, the PDE3 inhibitor milrinone was used. This experiment confirmed that oxLDL partially inhibits the reversal of platelet spreading on fibrinogen in a PDE3 dependent fashion. This agrees with findings that identified that oxLDL inhibits the effect of PGI_2 in a PDE3 dependent manner (Berger et al., 2019).

oxLDL-mediated Rac activation has been previously described in macrophages and linked to increased formation of atherosclerotic plaques (Park et al., 2012). It has been previously established that oxLDL activates PI3K, inducing PDE activity. It is well described that all PI3K isoforms can activate Rac however only PI3Kα activates RhoA and is inhibited by PI3Kδ. (Papakonstanti, Ridley and Vanhaesebroeck, 2007). It is attractive to speculate that oxLDL activates Rac by triggering the activation of some PI3K isoforms that are hyposensitive to cAMP. Upregulation of Rac may be driven by P-Rex1, a Rac-specific GEF which is activated by PIP3 upstream of PI3K (Welch et al., 2002). This GEF is also involved in the production of ROS through the activation of Rac, conveying an important role for Rac in oxidative stress (Welch et al., 2005). This further highlights the idea that oxidative stress such as ROS production potentiates the effect of oxLDL in platelet activation and may attenuate the effect of cAMP, proving potential implications of Rac in promoting atherogenicity.

In addition, the increased PDE3 activity induced by oxLDL reduces the response to cAMP elevating agents such as forskolin and oxLDL may play a role in regulating forskolin mediated activation of ACs by differential control of PDE3.

Conclusion

Within this chapter it was identified (i) cAMP production is attenuated significantly by the presence of oxLDL causing a marked reduction in PKA mediated signalling (ii) Rac activation is maintained in oxLDL treated spread platelets whilst RhoA activation is reversed on all matrix proteins (iii) PDE inhibition drives Rac inhibition, whereas FSK induces reversal of stress fibres while not reducing platelet surface area.

This chapter identifies that the effect of PGI_2 is inhibited in a PDE3 dependent manner on oxLDL and fibrinogen spread platelets. In oxLDL and fibrinogen spread platelets, the presence of PGI_2 causes an increase in actin nodules and stress fibre reversal and downregulation of pMLC. However, surface area and lamellipodia remain the same and this is due to different levels of cAMP switching RhoA off while Rac activity is upregulated.

CHAPTER 5: PGI$_2$ treatment induces differential effects in the presence of oxLDL and fibrinogen dependent on shear stress

5.1. Introduction

The stable adhesion and aggregation mediated by $\alpha_{IIb}\beta_3$ results in the initiation of the haemostatic plug. Upon endothelial injury, phosphatidylserine is produced, leading to calcium-mediated binding between factor Xa to the platelet surface with factor Va and resulting in the formation of prothrombinase complex. The conversion of prothrombin to thrombin takes place in this complex which promotes the coagulation cascade by cleaving soluble fibrinogen to fibrin (Palta, Saroa & Palta, 2014). Recent studies give further insight into the architecture of the platelet-rich thrombi. Studies *in vivo* show that platelet activation does not occur in an even fashion throughout the haemostatic plug but rather displays a defined structure and very distinct architecture (Ivanciu, Krishnaswamy & Camire, 2014). Exploring the architecture of clots can also give insight into the different regions of the thrombus and may play a role in potential therapeutic strategies in terms of which areas of the thrombus to target.

Early observations in vivo show that the distribution of activated platelets varies in the platelet rich thrombi. It is believed that platelet rich thrombi are composed of two zones: the growing thrombi also known as the core which consists of tightly packed activated platelets and a high concentration of thrombin (Stalker et al., 2013). The second zone has an outer shell of less active platelets that are arranged in a loose manner and is predominantly mediated by ADP. Inhibition of the P2Y$_{12}$ blocks the formation of the outer shell. It was reported that transport of soluble agonists such as thrombin was slow in the core than the outer shell of the growing thrombus (Welsh et al., 2014). These observations identify that platelet activation and granule release occurs in the core of the thrombi and not at the outer shell which highlights that platelets

in the thrombi release their contents into the core of the growing thrombus and not into the circulation (Stalker et al., 2013).

Following vascular injury, thrombogenic proteins of the ECM such as collagen and vWF become exposed which leads to the formation of a thrombus. It is believed that there are two independent pathways to platelet activation: one pathway is the principal concept whereby exposure of the subendothelial collagen propagates the activation of platelets whereas the other pathway suggests that thrombin produced by tissue factor (present in the vessel wall and in circulation) initiates platelet activation. Both pathways are crucial for platelet activation and thrombus formation however, the dominating pathway is dependent on the injury. As mentioned previously, the binding of collagen to platelet GPVI and GPIb-V-IX with collagen bound vWF leads to platelet adhesion. The shear rate at the vessel wall is a major determinant for the initial tethering of platelets.

At high shear rates 1000-10000 s-1 i.e. arterial blood flow, reversible aggregation is mediated by vWF which binds to immobilized collage via GPIb-IX-V. This results in the formation of thin membrane protrusions referred to as tethers. The formation of platelet tethers is in-dependent of soluble agonists such as ADP, serotonin, TXA_2 and thrombin. Additionally, tethers are formed by the binding of vWF to its receptor GPIbα at the A1 region before firm irreversible platelet adhesion and stable aggregation via $\alpha_{IIb}\beta_3$ (Savage, Saldívar and Ruggeri, 1996; Parise, 1999; Kasirer-Friede et al., 2004). vWF-GPα is essential for the formation of tethers as inhibiting the A1 domain of vWF results in reduced tether formation (Dopheide, Maxwell and Jackson, 2002). The formation of tethers is essential for causing the platelets in circulation to slow down for sustained interactions to occur between platelets, enabling firm and stable platelet aggregation.

Under low shear rates (<1000 s-1) in large veins and venules, GPVI binds to collagen and thus activates $\alpha_{IIb}\beta_3$ integrin mediated platelet activation. It is thought that $\alpha_{IIb}\beta_3$ is more predominant in mediating platelet aggregation at low shear rates as inhibition of vWF does not inhibit platelet aggregation, suggesting that platelet aggregation at low shear rates is independent of vWF-GPIbα (Savage, Almus-Jacobs and Ruggeri, 1998). Nevertheless, other in vivo studies have shown that vWF also plays a role in platelet aggregation under these conditions (Brill et al., 2011).

It is well established that various cells play a role in the atherosclerotic process such as monocytes, macrophages, endothelial cells, smooth muscle cells as well as platelets. In the blood of atherosclerotic patients, autoantibodies that react with oxidation specific epitopes of oxLDL are present, highlighting the presence of oxLDL in the circulation (Korporaal et al., 2007). It is thought that once the atherosclerotic plaque ruptures, platelets in the circulation associate with oxLDL, initiating the formation of a thrombus. oxLDL promotes platelet hyperactivity and thrombosis. However, the mechanism by which oxLDL promotes thrombus formation remain to be elucidated.

A small portion of LDL in circulation is thought to travel to the subendothelial space where LDL oxidation takes place in vivo as there is a plethora of antioxidants in circulation which prevent oxidation. Thus, the bidirectional transport of LDL may cause the presence of oxLDL in the circulation. oxLDL has been found in the plasma of CVD patients and it is involved in playing a principal role in activating inflammation in atherosclerotic plaques (Meisinger et al., 2005). Circulating oxLDL levels are significantly higher in patients with coronary heart disease and is a possible biochemical risk marker for patients with atherosclerotic disease. Furthermore, it has been previously shown that oxLDL activated platelets internalise oxLDL

compared to resting platelets (Daub et al., 2010). Similarly, clinical studies have consistently reported elevated levels of fibrinogen in patients with cardiovascular disease and thrombosis (Kannel, 1987). It is therefore important to postulate that circulating fibrinogen and oxLDL interact in the circulation. It has been previously established that elevated levels of fibrinogen promote the interaction of platelets as a result of increased binding affinity to the platelet $\alpha_{IIb}\beta_3$ receptor and increased clot viscosity, leading to enhanced thrombus formation. This, alongside circulating oxLDL has the potential to pose an increased cardiovascular risk to atherosclerotic patients. Clinical studies have further shown that elevated levels of oxLDL are strongly correlated to development of CVD and a poorer prognosis, with use as a clinically useful biomarker (Meisinger et al., 2005; Johnston et al., 2006).

Venous or arterial thrombosis is dependent on the anatomical site of the thrombotic event. Arterial thrombosis is primarily thought to be related to atherosclerotic plaque rupture and high shear stress, leading to the exposure and high concentrations of prothrombotic materials. On the other hand, venous thrombosis is believed to be associated to low shear stress and occurs without endothelial disruption. While the pathological modifications that take place in arterial and venous thrombosis are different, the common mechanisms are present for both. Oxidising products have been found on surfaces of microvesicles, suggesting a role for atherogenic lipids beyond arterial thrombosis (Obermayer, Afonyushkin and Binder, 2018). Furthermore, increasing clinical evidence shows a strong correlation between venous thrombosis and inflammation (Zöller, Li, Sundquist and Sundquist, 2012). Although oxLDL contributes heavily to atherogenesis and atherosclerosis associated inflammation, its role in venous thrombosis remains to be elucidated.

This chapter aims to explore the role of oxLDL and fibrinogen in vitro. The following experiments aim to:

- Determine the effect of oxLDL combining oxLDL and fibrinogen in thrombus formation in vitro.

- Identify the role of cAMP elevating agents such as PGI_2 and Fsk in thrombus formation.

- Explore the effect of shear stress on PGI_2 mediated reversal of thrombus formation on oxLDL and fibrinogen.

5.2. oxLDL in combination with fibrinogen induces enhanced thrombus formation

To understand how addition of oxLDL to fibrinogen affects thrombus formation initially thrombus formation was monitored on different concentrations of fibrinogen. Therefore, fibrinogen at 100, 300 and 1000 µg/ml was coated on Cellix biochips overnight at 4°C under humid conditions. Human whole blood was pre-treated with the anticoagulant 100 µM PPACK and stained with $DIOC_6$ for 20 minutes. The blood was subsequently flown at a shear rate of 1000 sec^{-1} (45.0 dynes/cm^2) through the biochip chambers for 2 minutes. The thrombi were as a result fixed with 4% formaldehyde for 15 minutes and re-stained with $DIOC_6$ for 1 hour at room temperature. Z-stack images were generated using the Apotome microscope and images were analysed for thrombi surface area coverage.

Figure 5.1 A shows an increase in surface area coverage by the platelets in whole blood with increasing fibrinogen concentrations. At 100 µg/ml and 300 µg/ml fibrinogen, the surface area coverage by platelets was 6.85±0.95% and 11.59±6.71% respectively which significantly increased to 24.03±1.19% at 1000 µg/ml fibrinogen (figure 5.1 B). No significant difference was observed between 100 µg/ml and 300 µg/ml fibrinogen however a significant increase in surface area coverage by platelets was observed between 300 µg/ml and 1000 µg/ml fibrinogen.

After establishing that surface area coverage increases with increasing fibrinogen concentrations, the effect of oxLDL on thrombus in vitro was investigated by coating biochip channels with 300 or 1000 µg/ml fibrinogen overnight at 4°C under humid conditions followed by the addition of 50 µg/ml nLDL or 50 µg/ml oxLDL for 1 hour at room temperature (figure 5.2). Figure 5.2 B showed no significant difference in surface area coverage by platelets between 300 µg/ml fibrinogen and the combination of 300 µg/ml fibrinogen and 50 µg/ml

nLDL. However, the percentage surface area coverage by platelets spread on 300 µg/ml fibrinogen and in combination with 50 µg/ml nLDL increased from 11.59±0.95% and 12.95±4.07% respectively to 25.72±0.32% in the presence of 50 µg/ml oxLDL (figure 5.2 B).

Interestingly analysis of surface area coverage on 1000 mg/ml fibrinogen +/- 50 mg/ml oxLDL showed no difference (figure 5.3). This indicated that although oxLDL could potentiate the adhesion of platelets on fibrinogen under shear at lower concentrations of fibrinogen once a maximum surface area coverage was achieved the addition of oxLDL caused no increase in surface area coverage.

A

B
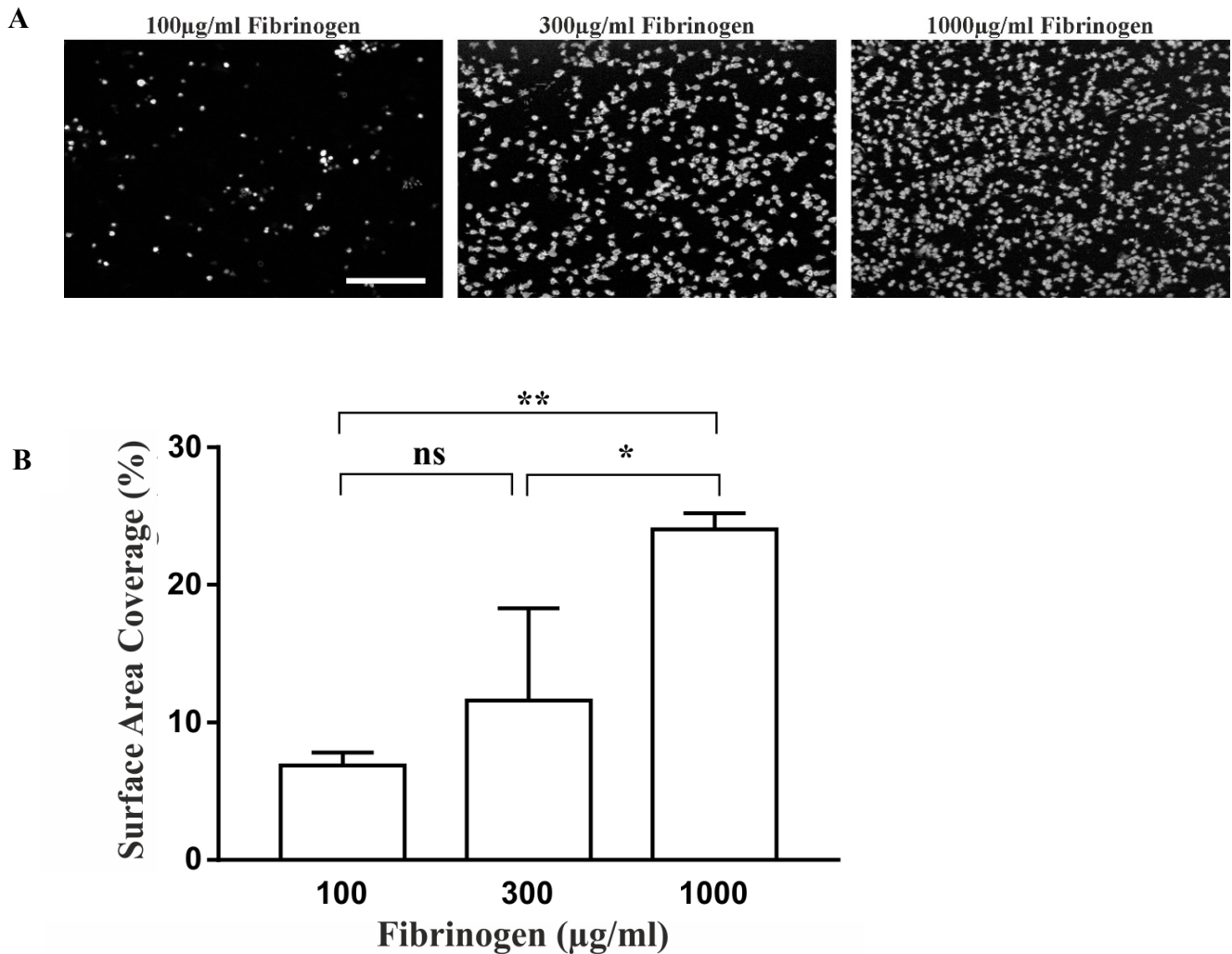
Figure 5.1. Increase in thrombus formation occurs in a dose dependent manner.

Biochips were coated with fibrinogen (100, 300 and 1000 µg/ml) overnight at 4°C. Human whole blood was preincubated with PPACK and stained with $DIOC_6$ before flowing at a shear rate of 1000 sec^{-1} (45.0 dynes/cm^2) over biochips for 2 minutes and subsequently fixed with 4% formaldehyde and re-stained with $DIOC_6$ for 1 hour at room temperature. Z-stack images were generated using the Apotome microscope and images were analysed for thrombi surface area coverage. **A)** Images are representative for each condition. **B)** Increased surface area coverage with increasing concentrations of fibrinogen. Data shown as mean ± SD (n=3). * $p<0.05$ ** $p<0.01$ relative to control. Scale bar= 20µm.

A

B

Fibrinogen 300µg/ml	+	+	+
nLDL 50µg/ml	-	+	-
oxLDL 50µg/ml	-	-	+
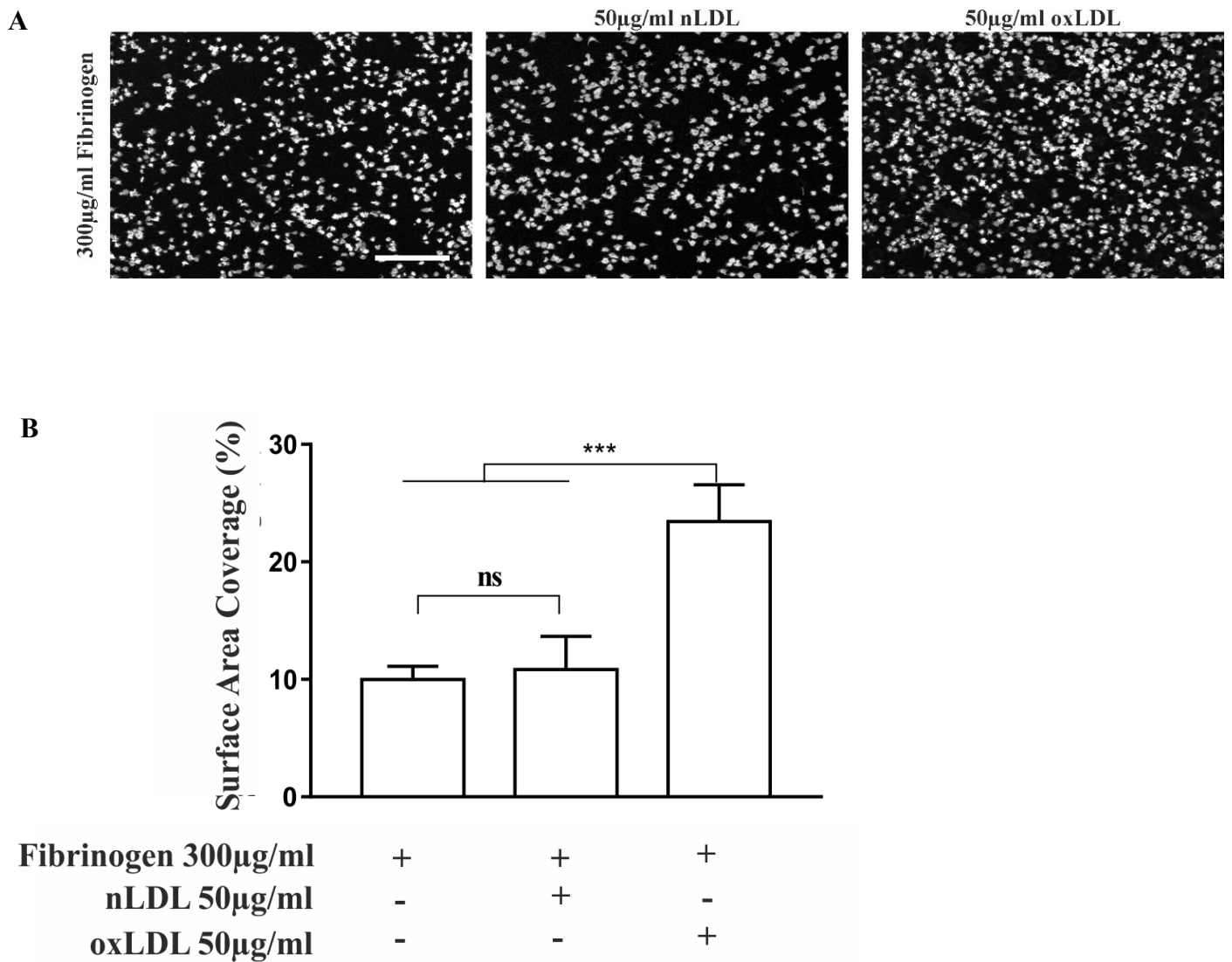
Figure 5.2. oxLDL in combination with fibrinogen induces enhanced thrombus formation.

Biochips were coated with fibrinogen 300 µg/ml overnight at 4°C and 50 µg/ml oxLDL or nLDL for 1 hour at room temperature. Human whole blood was preincubated with PPACK and stained with $DIOC_6$ before flowing at a shear rate of 1000 sec^{-1} (45.0 dynes/cm^2) over biochips for 2 minutes and subsequently fixed with 4% formaldehyde and re-stained with $DIOC_6$ for 1 hour at room temperature. Z-stack images were generated using the Apotome microscope and images were analysed for thrombi surface area coverage. **A)** Images are representative for each condition. **B)** Surface area coverage of platelets increased in the presence of oxLDL and fibrinogen. Data shown as mean ± SD (n=3). *** $p<0.001$ relative to control. Scale bar= 20µm.

A

50μg/ml nLDL 50μg/ml oxLDL

1000μg/ml Fibrinogen

B

Fibrinogen 1000μg/ml	+	+	+
nLDL 50μg/ml	-	+	-
oxLDL 50μg/ml	-	-	+
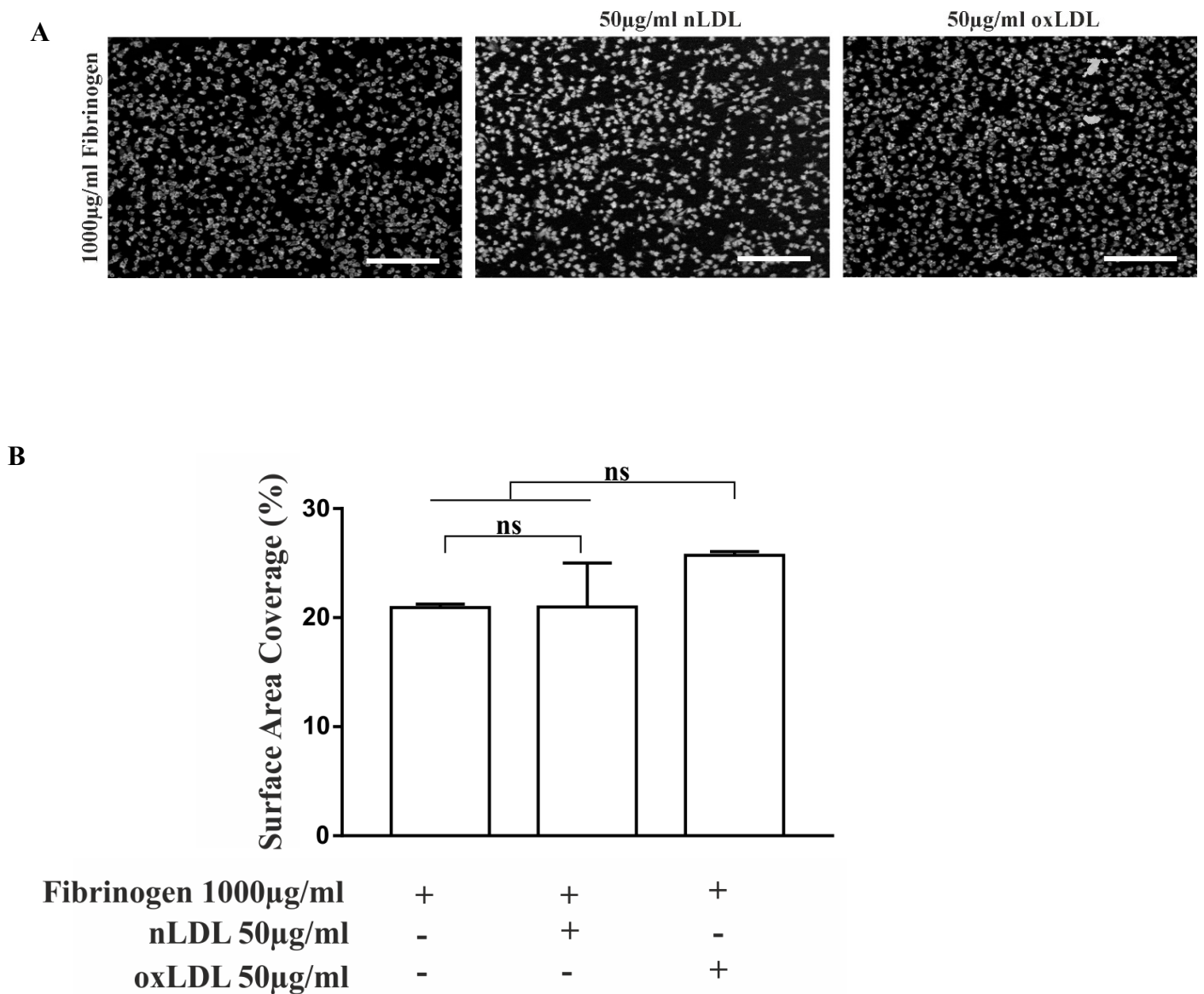
Figure 5.3. oxLDL has no effect in thrombus formation in combination with high dose fibrinogen.

Biochips were coated with fibrinogen 1000 μg/ml overnight at 4°C and 50 μg/ml oxLDL or nLDL for 1 hour at room temperature. Human whole blood was preincubated with PPACK and stained with $DIOC_6$ before flowing at a shear rate of 1000 sec^{-1} (45.0 dynes/cm^2) over biochips for 2 minutes and subsequently fixed with 4% formaldehyde and re-stained with $DIOC_6$ for 1 hour at room temperature. Z-stack images were generated using the Apotome microscope and images were analysed for thrombi surface area coverage. **A)** Images are representative for each condition. **B)** No affect seen in surface area coverage of platelets. Data shown as mean ± SD (n=3). Scale bar= 20μm.

5.3. Effect of treatment with PGI$_2$ prior to the formation of thrombus on fibrinogen and oxLDL

To understand the effect that PGI$_2$ might have on platelets in the presence of fibrinogen +/- oxLDL in high shear conditions, we first examined the effect on fibrinogen alone. Human whole blood was pre-treated with the anticoagulant 100 μM PPACK and stained with DIOC$_6$ for 20 minutes. The blood was subsequently pre-treated with PGI$_2$ for 2 minutes in suspension flown at a shear rate of 1000 sec^{-1} (45.0 dynes/cm^2) through the biochip chambers for 2 minutes. The thrombi were as a result fixed with 4% formaldehyde for 15 minutes and re-stained with DIOC$_6$ for 1 hour at room temperature. Z-stack images were generated using the Apotome microscope and images were analysed for thrombi surface area coverage.

Figure 5.4 showed that there was no significant difference between the control conditions and pre-treatment of platelets with 10 nM PGI$_2$ for all conditions. Upon identifying that pre-treatment with 10 nM PGI$_2$ had no effect on the surface area coverage by platelets, post-treatment with PGI$_2$ was investigated to determine the effect of PGI$_2$ on platelets that have adhered on the matrix.

A

300µg/ml Fibrinogen

50µg/ml nLDL

50µg/ml oxLDL

+PGI$_2$

B

Fibrinogen 300µg/ml	+	+	-	-	+	+
nLDL 50µg/ml	-	-	+	+	-	-
oxLDL 50µg/ml	-	-	-	-	+	+
PGI$_2$ 10nM	-	+	-	+	-	+
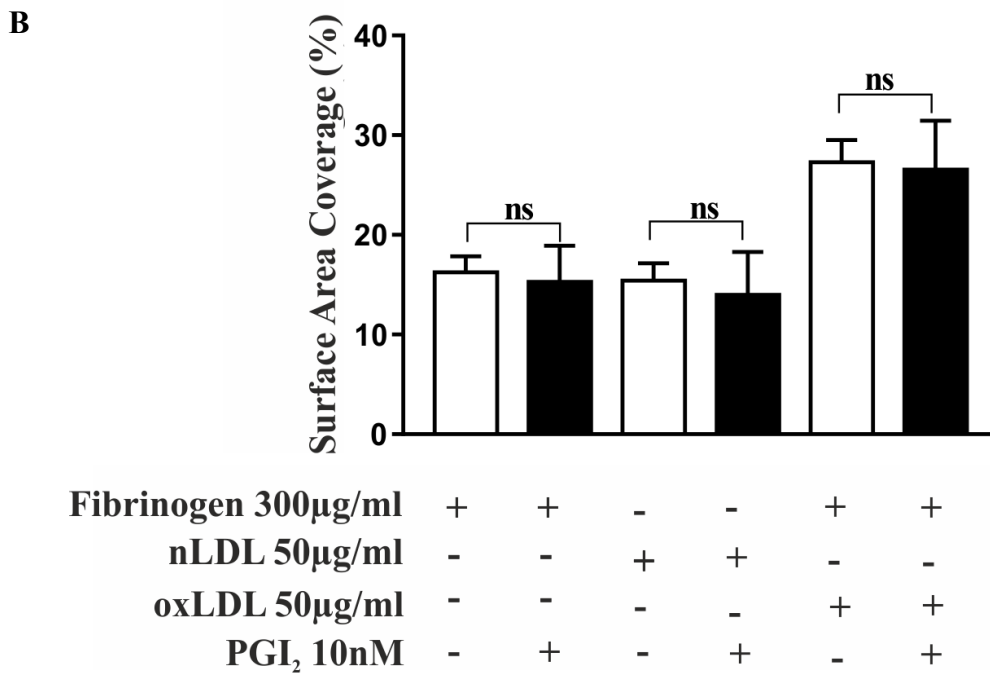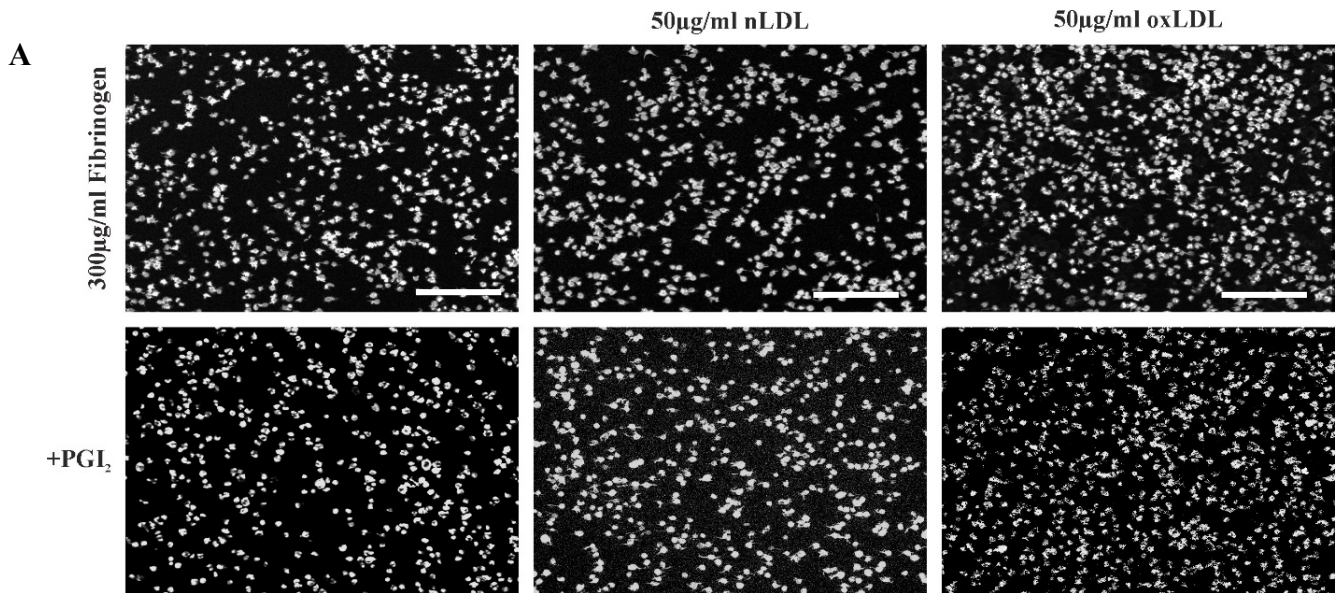
Figure 5.4. Pre-treatment with PGI$_2$ does not affect the surface area coverage of platelets.

Biochips were coated with fibrinogen 300 µg/ml overnight at 4°C, washed and then coated with 50 µg/ml oxLDL or nLDL for 1 hour at room temperature. Human whole blood was preincubated with PPACK, stained with DIOC$_6$ and pretreated with 10 nM PGI$_2$ before flowing at a shear rate of 1000 sec^{-1} (45.0 dynes/cm^2) over biochips for 2 minutes and subsequently fixed with 4% formaldehyde and re-stained with DIOC$_6$ for 1 hour at room temperature. Z-stack images were generated using the Apotome microscope and images were analysed for thrombi surface area coverage. **A)** Images are representative for each condition. **B)** Pre-treatment with PGI$_2$ does not affect surface area coverage of platelets. Data shown as mean ± SD (n=3). Scale bar= 20µm.

5.4. oxLDL attenuates the effect of PGI$_2$ on thrombus formation

We had previously identified that addition of PGI$_2$ caused a partial reversal of platelet activation with the reversal of stress fibres, but no effect on surface area coverage due to differential control of RhoA and Rac activation. Therefore, it was important to understand if this effect still occurred under high shear, or if shear induced a change in this response. Therefore, biochip chambers were coated initially with 300 µg/ml fibrinogen overnight at 4°C under humid conditions before washing, and addition of 50 µg/ml nLDL or 50 µg/ml oxLDL for 1 hour at room temperature. Human whole blood was pre-treated with the anticoagulant 100 µM PPACK and stained with DIOC$_6$ for 20 minutes before undergoing suspension flown at a shear rate of 1000 sec^{-1} (45.0 dynes/cm^2) through the biochip chambers for 2 minutes (figure 5.5). Flow was continued with Tyrodes buffer or Tyrode's buffer containing 10 nM PGI$_2$ for 20 minutes. The thrombi were as a result fixed with 4% formaldehyde for 15 minutes and re-stained with DIOC$_6$ and stained with Rhodamine B phalloidin for 1 hour at room temperature. Z-stack images were generated using the Apotome microscope and images were analysed for thrombi surface area coverage.

Platelet adhesion to fibrinogen and fibrinogen & 50 µg/ml nLDL was very similar with a coverage of 33.61±6.22% and 32.62±2.81% respectively. As expected, platelet adhesion to fibrinogen + 50 µg/ml oxLDL was significantly higher at 61.59±2.96% (figure 5.5 B). Addition of 10 nM PGI$_2$ reduced the surface area coverage of platelets spread on 300 µg/ml fibrinogen and in the presence of 50 µg/ml nLDL to 19.38±1.02 and 18.26±1.35% respectively (figure 5.5 B). Interestingly, the surface area coverage was unaffected by PGI$_2$ in the presence of 50 µg/ml oxLDL. In agreement with this Figure 5.5 C identified a significant increase in actin nodule formation in the presence of PGI$_2$ to 65.90±1.71% on 300 µg/ml fibrinogen, and 73.05±4.55%

on 300 µg/ml fibrinogen + 50 µg/ml nLDL spread platelets compared to the relevant control. Alongside this formation of actin nodules there was a reduction in stress fibre formation within these platelets, with stress fibres present in 32.42±3.65% platelets on 300 µg/ml fibrinogen and 26.22±3.08% platelets on fibrinogen + 50 µg/ml nLDL in comparison to their respective control conditions (78.91±3.75% and 85.79±2.02%). However, actin nodules did not form after treatment with PGI_2 in the presence of fibrinogen and 50 µg/ml oxLDL, with all platelets retaining clear and thick stress fibres (figure 5.5 D).

As we showed no effect with PGI_2 at 20 minutes of post flow, a shorter time point was used to identify if this might identify if PGI_2 could induce actin nodules in platelets as per section 3.6.
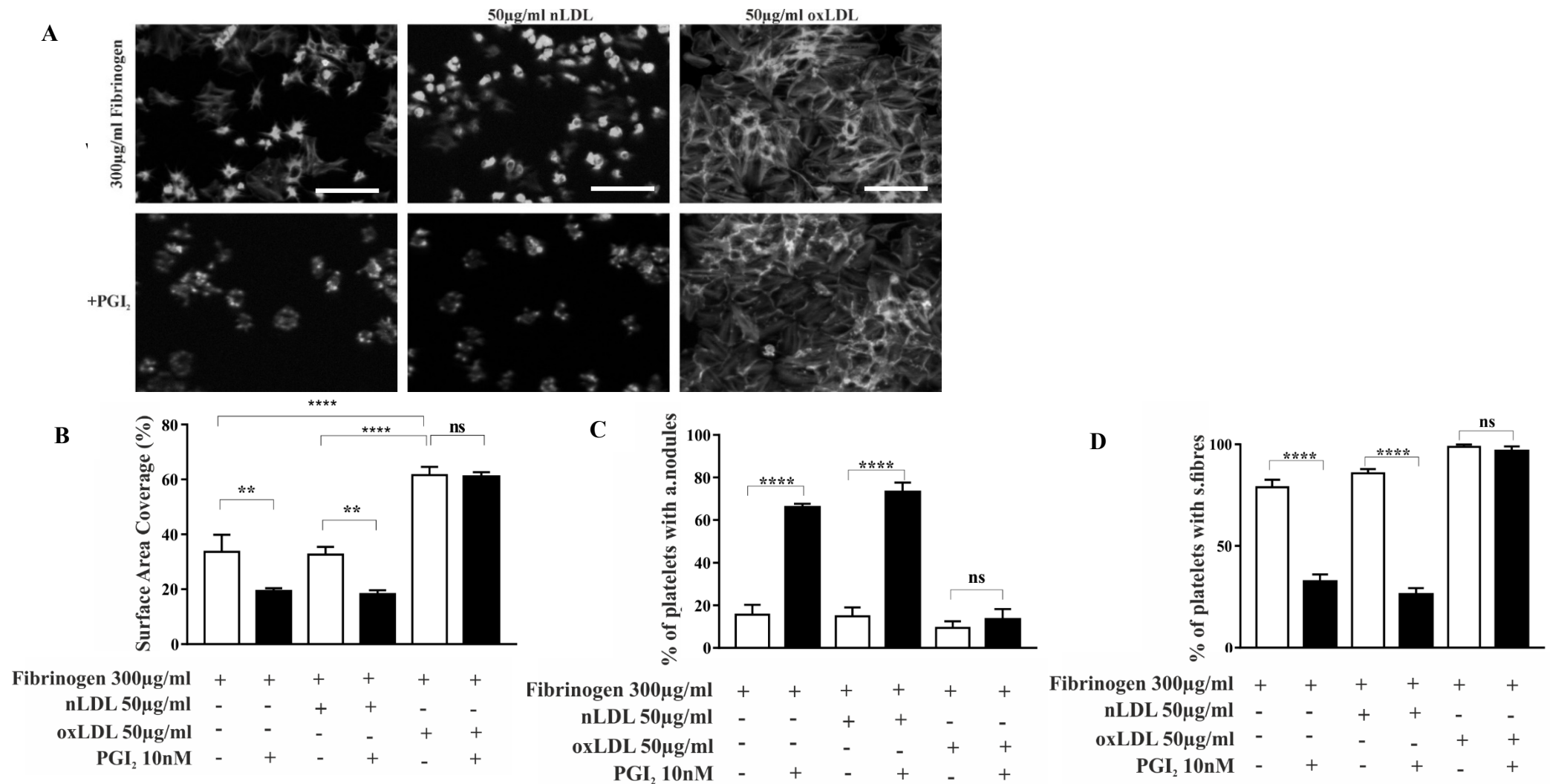
Figure 5.5. oxLDL attenuates the effect of PGI$_2$ on thrombus formation. Biochips were coated with fibrinogen 300 μg/ml overnight at 4°C and 50 μg/ml oxLDL or nLDL for 1 hour at room temperature. Human whole blood was preincubated with PPACK, stained with DIOC$_6$. Tyrodes buffer in the presence or absence of 10 nM PGI$_2$ were perfused over the formed thrombi for 18 mins at 1000 sec^{-1} (45.0 dynes/cm^2). Platelets were subsequently fixed with 4% formaldehyde and re-stained with DIOC$_6$ for 1 hour at room temperature. Z-stack images were generated using the Apotome microscope and images were analysed for thrombi surface area coverage. **A)** Images are representative for each condition. **B)** Surface area coverage not reduced by PGI$_2$ in the presence of oxLDL. **C+D)** Actin nodules and stress fibre reversal not induced in the presence of oxLDL. Data shown as mean ± SD (n=3). ** $p<0.01$ ****$p<0.0001$ relative to control. Scale bar= 20μm.

5.5. The effect of PGI$_2$ and forskolin is attenuated in the presence of oxLDL

After establishing the lack of response to 10 nM PGI$_2$ post flow in in platelets spread on fibrinogen + oxLDL after 20 minutes, we sought to

1) Identify if a shorter timepoint would identify a change in actin structures induced by PGI$_2$

2) identify if other cAMP elevating agents could drive reversal of platelet spreading under high shear, as previously identified in platelet spreading assays.

Therefore, the effect of Fsk, PGI$_2$ and milrinone were further explored using a shorter time course. Biochip chambers were coated with 300 µg/ml fibrinogen overnight at 4°C under humid conditions and 50 µg/ml nLDL or 50 µg/ml oxLDL for 1 hour at room temperature (figure 5.6). Human whole blood was pre-treated with the anticoagulant 100 µM PPACK and stained with DIOC$_6$ for 20 minutes before undergoing suspension flown at a shear rate of 1000 sec^{-1} (45.0 dynes/cm^2) through the biochip chambers for 2 minutes. Flow was continued with Tyrodes buffer or 10 nM PGI$_2$, 1 µM Fsk and 10 µM milrinone for 10 minutes. The thrombi were as a result fixed with 4% formaldehyde for 15 minutes and re-stained with 10 µM DIOC$_6$ and stained with Rhodamine B phalloidin for 1 hour at room temperature. Z-stack images were generated using the Apotome microscope and images were analysed for thrombi surface area coverage.

The surface area coverage analysis revealed that 31.53±2.42% was attained at 300 µg/ml fibrinogen and this markedly reduced as expected in the presence of 10 nM PGI$_2$ (22.39±1.59%), 1 µM Fsk (19.19±2.48%) and 10 µM milrinone (21.85±5.90%) (figure 5.6 B).

Likewise, a similar effect was observed in platelets spread in the presence of 50 μg/ml nLDL where 30.72±72% was attained and a significant reduction was observed after stimulation with 10 nM PGI_2 (22.32±3.50%), 1 μM Fsk (17.13±0.25%) and 10 μM milrinone (16.87±1.84%) (figure 5.6 C). Figure 5.6 D shows an increase in percentage of platelets with actin nodules in the presence of 300 μg/ml fibrinogen upon 10 nM PGI_2 (89.32±2.36%), 1 μM Fsk (92.75±2.87%) and 10 μM milrinone (94.84±3.67%) treatment in comparison to the control (16.32±1.24%). An induction in actin nodule formation was also demonstrated in platelets spread on 300 μg/ml fibrinogen and 50 μg/ml nLDL (figure 5.6 D). In the presence of 300 μg/ml fibrinogen, stress fibre reversal was induced in platelets treated with 10 nM PGI_2 (14.81±2.47%), 1 μM Fsk (11.80±4.31%) and 10 μM milrinone (10.79±3.20%) compared to the control (76.78±3.15%) (figure 5.6 E). Likewise, stress fibre reversal was also observed in the presence of 50 μg/ml nLDL for all treated conditions (figure 5.6 E).

This was further investigated in the presence of 50 μg/ml oxLDL whereby there was an elevated platelet adhesion at 45.38±2.39%. FSK did not reduce the surface area coverage, induce actin nodules, or reverse stress fibre formation in agreement with the PGI_2 results. However, milrinone induced a marked reduction in surface area coverage to 26.87±1.44% (figure 5.7 B) an increase in actin nodules (88.20±1.44%) compared to the control condition (9.29±3.23%) (figure 5.7 C) and significant stress fibre reversal (11.21±1.46%) compared to control (89.26±2.12%).
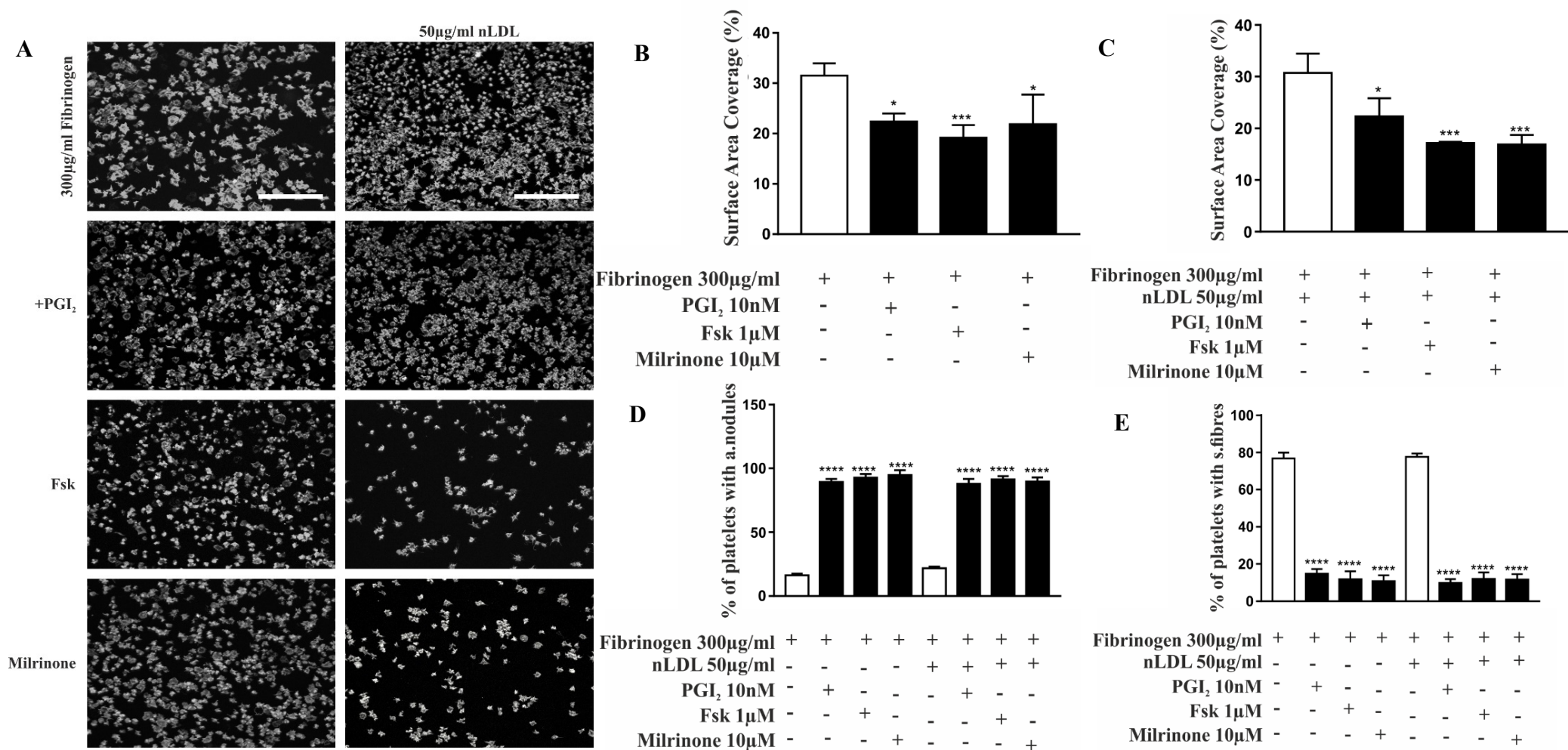
Figure 5.6. Thrombus formation on fibrinogen and nLDL is reduced in the presence of PGI₂, forskolin and milrinone. Biochips were coated with fibrinogen 300 µg/ml overnight at 4°C and 50 µg/ml nLDL for 1 hour at room temperature. Human whole blood was preincubated with PPACK, stained with $DIOC_6$. Tyrodes buffer in the presence or absence of 10 nM PGI₂, 1 µM Fsk or 10 µM milrinone were perfused over the formed thrombi for 8 mins at 1000 sec^{-1} (45.0 dynes/cm^2). Platelets were subsequently fixed with 4% formaldehyde and re-stained with $DIOC_6$ for 1 hour at room temperature. Z-stack images were generated using the Apotome microscope and images were analysed for thrombi surface area coverage. **A)** images are representative for each condition. **B+C)** Surface area coverage is reduced in the presence of PGI₂. **D+E)** Actin nodule formation is induced, and stress fibre is reversed in the presence of PGI₂, forskolin and milrinone. Data shown as mean ± SD (n=3). * $p<0.05$ ** $p<0.01$ *** $p<0.001$ **** $p<0.0001$ relative to control. Scale bar= 20µm.
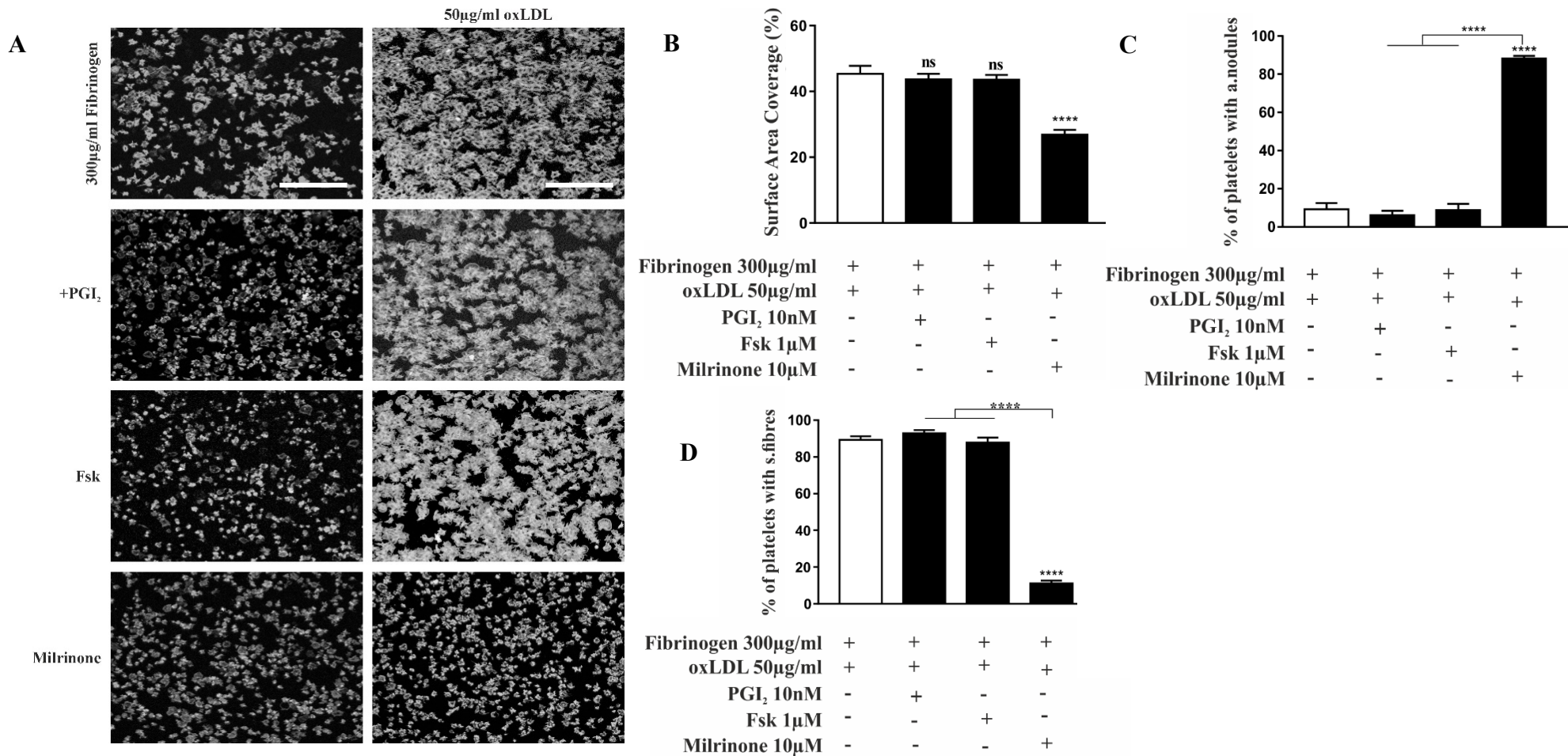
Figure 5.7. The effect of PGI₂ and forskolin is attenuated in the presence of oxLDL.
Biochips were coated with fibrinogen 300 µg/ml overnight at 4°C and 50 µg/ml oxLDL or nLDL for 1 hour at room temperature. Human whole blood was preincubated with PPACK, stained with DIOC₆. Tyrodes buffer in the presence or absence of 10 nM PGI₂, 1 µM Fsk or 10 µM milrinone were perfused over the formed thrombi for 8 mins at 1000 sec⁻¹ (45.0 dynes/cm²). Platelets were subsequently fixed with 4% formaldehyde and re-stained with DIOC₆ for 1 hour at room temperature. Z-stack images were generated using the Apotome microscope and images were analysed for thrombi surface area coverage. **A)** Images are representative for each condition. **B)** Surface area coverage is not reduced by PGI₂ and forskolin in the presence of oxLDL. **C+D)** PGI₂ and Forskolin does not induce actin nodules and stress fibre reversal in the presence of oxLDL. Data shown as mean ± SD (n=3). **** $p<0.0001$ relative to control. Scale bar= 20µm.

5.6. PGI$_2$ reduced thrombus formation and induced leukocyte adhesion in the presence of oxLDL under low shear rates

As PGI$_2$ and Fsk did not induce reversal of stress fibres within a high shear environment, we then investigated if reducing shear to that identified within the venule system (200 sec^{-1} (25.0 dynes/cm^2)) would affect platelet reversal. Thus, biochip chambers were coated with 300 µg/ml fibrinogen overnight at 4°C under humid conditions and 50 µg/ml nLDL or 50 µg/ml oxLDL for 1 hour at room temperature (figure 5.8). Human whole blood was pre-treated with the anticoagulant 100 µM PPACK and stained with 10 µM DIOC$_6$ for 20 minutes before undergoing suspension flown through the biochip chambers for 2 minutes. Flow was continued with Tyrodes buffer or 10 nM PGI$_2$ for 10 minutes. The thrombi were as a result fixed with 4% formaldehyde for 15 minutes and re-stained with 10 µM DIOC$_6$ and stained with Rhodamine B phalloidin for 1 hour at room temperature. Leukocytes were stained with DAPI. Z-stack images were generated using the Apotome microscope and images were analysed for thrombi surface area coverage.

Surface area coverage analysis showed that reduction in shear rates caused a reduction in platelet adhesion to fibrinogen. There was also no difference between each matrix protein in regard to surface area coverage. However, upon addition of PGI$_2$, there was no difference between post-treatment with 10 nM PGI$_2$ and the control conditions at 300 µg/ml fibrinogen (P value= 0.41), 50 µg/ml nLDL combination (P value= 0.40) and 50 µg/ml oxLDL (P value= 0.97) (figure 5.8 B). Our data shows number of adhered leukocytes increase in the presence of 10 nM PGI$_2$ in oxLDL and fibrinogen spread platelets (figure 5.8 C). Importantly analysis of the adhered platelets showed that PGI$_2$ could reverse stress fibre formation and induce actin nodules on all matrix combinations (figure 5.8 D + E).

This data indicates that shear stress plays a key role in the resistance of oxLDL to PGI_2 on fibrinogen, and therefore indicates why oxLDL plays a key role in arterial thrombosis rather than venous thrombosis.
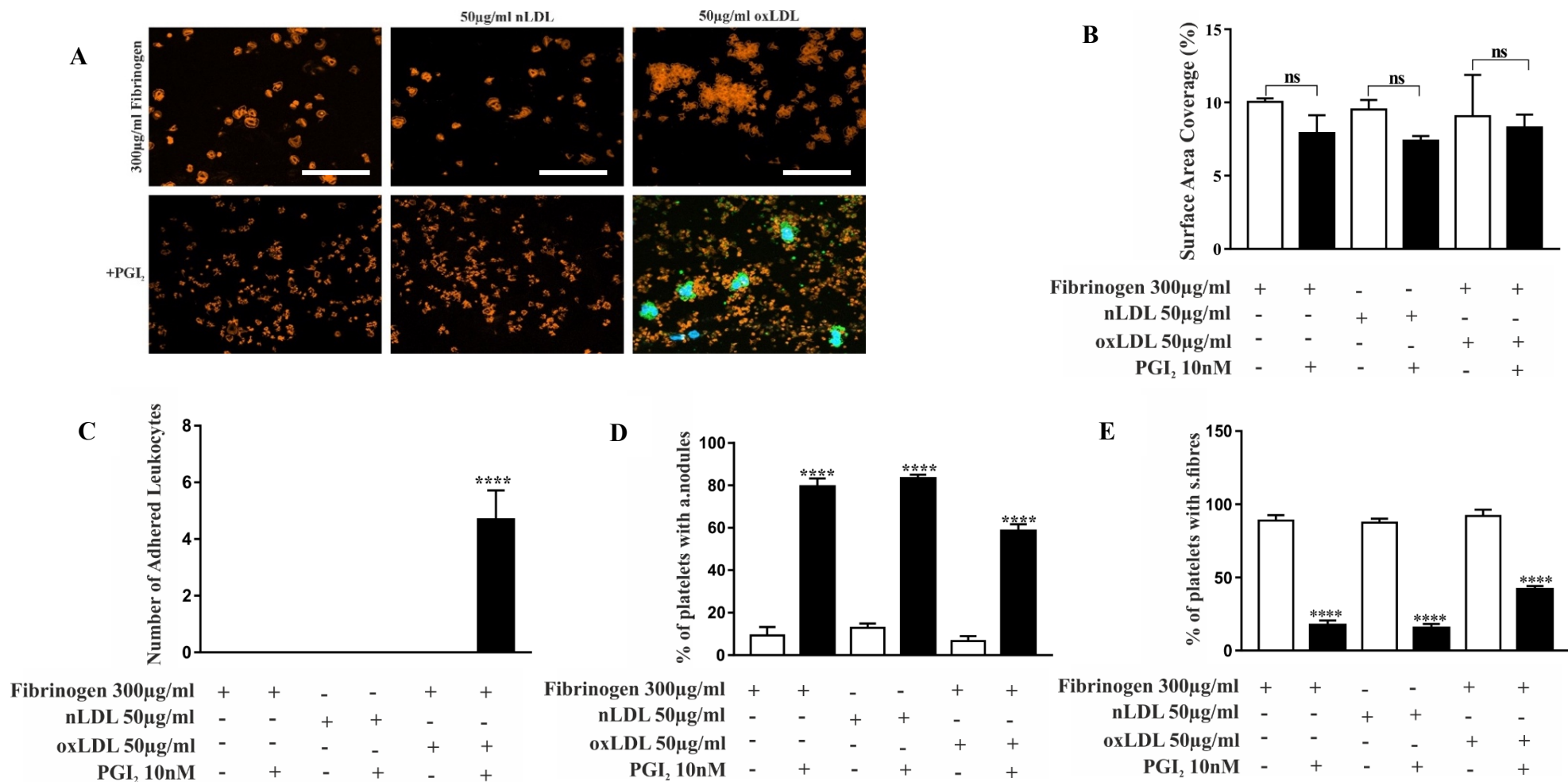
Figure 5.8. PGI$_2$ reduces thrombus formation under low shear conditions and induces the formation of leukocytes in the presence of oxLDL. Biochips were coated with fibrinogen 300 μg/ml overnight at 4°C and 50 μg/ml oxLDL or nLDL for 1 hour at room temperature. Human whole blood was preincubated with PPACK, stained with DIOC$_6$. Tyrodes buffer in the presence or absence of 10 nM PGI$_2$ was perfused over the formed thrombi for 8 mins at 200 sec^{-1} (25.0 dynes/cm^2). Platelets were subsequently fixed with 4% formaldehyde and re-stained for 1 hour with DIOC$_6$ and 15 minutes with Dapi at room temperature. Z-stack images were generated using the Apotome microscope and images were analysed for thrombi surface area coverage. **A)** Images are representative for each condition. **B)** Surface area coverage is reduced in the presence of PGI$_2$. **C)** Number of leukocytes. **D+E)**. Induced actin nodule formation and stress fibre reversal. Data shown as mean ± SD (n=3). ** $p<0.01$ **** $p<0.0001$. Scale bar= 20μm.

5.7. Discussion

Previous chapters established that oxLDL and fibrinogen enhanced platelet spreading and that the effect of cAMP inducing agents such as PGI_2 and Fsk were partially inhibited in the presence of oxLDL under static conditions. Under these conditions, platelet surface area was unaffected, however, stress fibre reversal and actin nodule formation were induced. Thus, this chapter aimed to explore the physiological relevance of this change to the role of PGI_2 in the presence of oxLDL, especially since Rac and RhoA have been implicated in thrombus stability and formation previously (McCarty et al., 2005).

Analysis of in vitro flow experiments identified that increasing concentrations of fibrinogen induced elevated surface area coverage. This agrees with the concept of elevated fibrinogen levels enhancing the interaction of platelets as a result of increased binding affinity to the platelet. It was also imperative to determine the effect of cAMP inducing agents such as PGI_2 in reorganising the actin cytoskeleton. Pre-treatment of whole blood with PGI_2 showed no effect in thrombus formation. This is an unexpected result that contradicts previous findings; however, additional n numbers may show an effect (Yusuf et al., 2017). Furthermore, we found that the surface area coverage was significantly reduced and actin nodules as well as stress fibre reversal induced upon post-treatment of PGI_2 on blood flown over 300 µg/ml fibrinogen as shown by Yusuf et al., 2017. As expected, this effect was also evident in the presence of 50 µg/ml nLDL. Post perfusion of another cAMP elevating agent, forskolin also induced a similar effect where the surface area coverage was markedly reduced and an increase in actin nodule formation and stress fibre reversal was observed, agreeing with our findings under the static system. On the other hand, in agreement with the phenotype observed in static conditions, the presence of 50 µg/ml oxLDL the effect of cAMP elevating agents such as PGI_2 and forskolin did not cause a reduction in surface area in vitro. Importantly, in contrast to static conditions,

under arterial shear rates, reversal of stress fibres and increased actin nodules were not seen after the perfusion of PGI_2 and forskolin on blood flown on 300 μg/ml fibrinogen and 50 μg/ml oxLDL. These results suggest that oxLDL modulates cAMP levels and thus induces a prothrombotic phenotype.

As atherogenicity and intimal lesions are increased in areas of low levels of shear stress we therefore postulated that this effect was dependent on shear rate. Thus, the following experiments were repeated under venous shear rates 200 sec^{-1} (25.0 dynes/cm^2). Analysis showed that although surface area coverage was not affected (although this maybe significant with additional n numbers), actin nodule formation and stress fibre reversal was present after the perfusion of PGI_2 in platelets spread on 300 μg/ml fibrinogen and/or 50 μg/ml nLDL.

In the presence of fibrinogen and 50 μg/ml oxLDL PGI_2 could now induce stress fibre reversal and actin nodule formation in contrast to the high shear results. This therefore indicates that shear stress could play a key role in PDE3 activity alongside oxLDL and therefore could partially underpin why oxLDL plays such an important role in thrombus formation in arterial conditions. Interestingly, the surface area coverage was increased in the presence of PGI_2 due to the appearance of significant number of leukocytes. It has been established that at low shear stress, endothelial ROS is generated which leads to endothelial dysfunction and subsequent activation of leukocytes (Kuiper, Sun, Magalhães and Glogauer, 2011). In addition, it has been previously shown that cAMP causes ROS production and therefore it can be postulated that elevated levels of cAMP coupled with oxLDL leads to pronounced production of ROS under low shear rates, inducing an atherogenic and immunothrombotic microenvironment for leukocytes to adhere which explains our observation of leukocyte adhesion on platelets treated with PGI_2 in the presence of oxLDL at low shear stress (Isoni et al., 2009).

PGI$_2$ is more effective at inhibiting platelets in low shear in contrast to high shear rates. This could be due to platelets adhering strongly on high shear conditions which are as a result more difficult to reverse. In addition, this phenotype could also be due to cAMP signalling requiring to be switched off effectively in order to maintain adhesion of platelets under high shear, suggesting high levels of PDE3 in high shear conditions. It is also postulated that there is an increase in contact time between adhesion molecules on leukocytes and endothelial cells, enabling stronger adhesion of leukocytes at lower shear rates (Panés and Granger, 1998). Studies have reported that oxLDL promotes leukocyte rolling and adhesion on the endothelium. Nevertheless, it has been previously established that the activation of RhoA promotes the detachment of leukocytes in postcapillary venules of mice and other cell types which may suggest that the inhibition of RhoA induces leukocyte adhesion in the presence of PGI$_2$ (Alblas, Ulfman, Hordijk and Koenderman, 2001). It is established that leukocytes protrude extensively when RhoA is inactive whereas leukocyte adhesion is inhibited when RhoA is activated (Worthylake, Lemoine, Watson and Burridge, 2001). Together, it can be suggested that although oxLDL promotes leukocyte adhesion strongly under low shear stress conditions, inhibition of RhoA induces leukocyte adhesion and spreading which is in line with our findings as we show leukocyte adhesion and spreading in the presence of PGI$_2$ where stress fibre reversal is observed.

Conclusion

This chapter identifies that oxLDL induces a prothrombotic phenotype under high shear, that is not present under low shear. This correlates with the changes in the actin cytoskeleton, where in low shear stress fibres are reversed, but in high shear surface area and stress fibres

are maintained. Intriguingly we also identified that PGI$_2$ in the presence of oxLDL and fibrinogen induced the adhesion of elevated numbers of leucocytes in comparison to all other conditions.

CHAPTER 6: General Discussion

6.1. Discussion

Atherosclerosis is a chronic inflammatory process, resulting in atheromatous plaques and atherosclerotic lesions. Underlying atherosclerosis is the process of dyslipidaemia. Dyslipidaemia is associated with hyperlipidaemia and elevated levels of LDL. These changes in lipid profile can cause increased platelet reactivity, elevating the chance of thrombosis. In addition, rupture of an atherosclerotic plaque increases the development of coronary thrombosis due to the release of the plaque contents (Lacoste et al., 1995).

Part of the mechanism by which LDL functions to elevate platelet reactivity is through the production of oxLDL. In 1989, Daniel Steinberg and his colleagues proposed the oxidative modification hypothesis. It was predicted that the oxidation of low-density lipoproteins (LDL) is an early event in the atherosclerotic process-giving rise to foam cells. Furthermore, modified LDL enhances the pathogenesis of atherosclerosis by altering the functions of cells. oxLDL adheres to endothelial cells and triggers their activation, leading to adhesion and rolling of leukocytes and thus, promoting an inflammatory response (Liao, Starzyk & Granger, 1997). It is well established that various cells play a role in the atherosclerotic process such as monocytes, macrophages, endothelial cells, smooth muscle cells as well as platelets (Su et al., 2016). In the blood of atherosclerotic patients, autoantibodies that react with oxidation specific epitopes of oxLDL are present, highlighting the presence of oxLDL in the circulation (Korporaal et al., 2007). It is thought that once the atherosclerotic plaque ruptures, platelets in the circulation associate with oxLDL, initiating the formation of a thrombus. oxLDL promotes platelet hyperactivity and thrombosis. However, the mechanisms by which oxLDL promotes

thrombus formation remain to be elucidated. One of the main aims of this thesis was to explore how oxLDL plays a role in regulating the actin cytoskeleton of spread platelets.

Previous studies have established that oxLDL but not nLDL induces platelet aggregation, adhesion and shape change (Wraith et al.,2013). However, the role of oxLDL in combination with fibrinogen in reorganising the actin cytoskeleton of spread platelets and inducing a prothrombotic phenotype remains to be investigated. It has been established that fibrinogen plays a crucial role in arterial thrombosis as a result of promoting the crosslinking of platelets during the growth of a thrombus (Buitrago, Coller & Zafar, 2019). In addition, conformational change in the platelet integrin receptor $\alpha_{IIb}\beta_3$ triggers inside-out signalling, changing the integrin from a low affinity to a high affinity state (Shen, Delaney & Du, 2012). Fibrinogen binding results in the elevation of intracellular calcium levels and induces the phosphorylation of MLC and thus, the formation of stress fibres (Aburima et al., 2013). As well as having a crucial role in platelet activation and aggregation, fibrinogen also plays an important role in atherogenesis. Increasing evidence from studies have reported that elevated fibrinogen levels are related to the formation of plaques in atherosclerosis as well as inducing a prothrombotic or hypercoagulable state (Levenson et al., 1995; Zhang et al., 2014). Therefore, we investigated whether a hypercoagulable state was induced upon the interaction between circulating oxLDL and fibrinogen. We found that the combination of oxLDL and fibrinogen under a static system resulted in a significant increase in surface area of platelets compared to those platelets spread on fibrinogen alone or in the presence of nLDL, suggesting that oxLDL is involved in promoting a prothrombotic phenotype.

Interestingly, oxLDL in combination with fibrinogen significantly increases thrombus formation in vitro. We specifically found that this effect was potentiated in higher

concentrations of fibrinogen suggesting that elevated levels of fibrinogen and oxLDL contribute to atherogenesis. It has been previously described that fibrinogen is susceptible to oxidation. Studies have shown that exposure of fibrinogen to oxidants induces the formation of fibrin and induces platelet aggregation while regulating the structure of fibrin in an oxidation dependent fashion (Olinescu and Kummerow, 2001). Although the mechanisms by which oxidative stress affects the properties of a fibrin clot remain to be investigated, oxidative stress is thought to encourage prothrombotic alterations in the formation and architecture of fibrin (Feng and Hart, 1995; Upchurch, Ramdev, Walsh and Loscalzo, 1998). Taken together, oxLDL and oxidative products of LDL peroxidation may play a role in the oxidation of fibrinogen and as a result induce fibrin formation, reducing fibrinolysis and clot permeability and promoting a prothrombotic phenotype.

The interaction of platelets with oxLDL is a key feature in atherothrombosis which inevitably leads to platelet hyperreactivity. Although the mechanism by which this happens is poorly understood, studies have suggested this phenotype is due to an increase in Ca^{2+} levels and increased secretion of P-selectin in a CD36 dependent manner (Chen, Febbraio and Silverstein, 2007). Another reason for the prothrombotic activity we observed can be due to changes in the platelet lipidome as a result of lipid uptake via CXCL12/CXCR4-7 axis through oxidation and peroxidation processes regulated by mitochondrion-dependent ROS generation (Chatterjee et al., 2015). As a result, this suggests that platelets have the ability to store large amounts of oxLDL in atherosclerotic lesions which further signifies the role of platelets in atherothrombosis.

6.1.2 Role of cytoskeleton in immunothrombosis

We found an increase in the formation of stress fibres in platelets spread on oxLDL and fibrinogen. RhoA activation regulates stress fibre assembly as a result of inactivating actin depolymerising factors like cofilins and causing platelet contractility via the phosphorylation of MLC. Furthermore, we found that pMLC was elevated in platelets spread on fibrinogen, fibrinogen and nLDL as well as oxLDL, in line with stress fibre formation and increase in Rho activity in the absence of PGI$_2$. In addition, after spreading the platelets on oxLDL and fibrinogen and treating with PGI$_2$, we found a reduction in active GTP-bound form of RhoA in fibrinogen spread platelets. In agreement with this, platelets spread on nLDL or fibrinogen also showed this reduction. This is consistent with the stress fibre reversal phenotype observed under these conditions.

The ability of RhoA to induce shape change is dependent on the G12/G13 signalling pathway although Rac1 is mediated by Gq, thus illustrating that Rho and Rac are differentially regulated (Gratacap et al., 2001). This further suggests that cAMP signalling may affect the downstream signalling of G12/G13 and Gq differentially. During the early stages of outside-in signalling, Rac1 drives actin polymerisation as well as lamellipodia formation while RhoA is inhibited to allow spreading highlighting their antagonistic relationship (Flevaris et al., 2007). Ultimately, calcium-dependent proteases like calpain promote platelet contraction and clot retraction, facilitating the interaction between RhoA and Rac to phosphorylate MLC. While Rho and Rac are both involved in the first pMLC peak activated by the inside-out signalling during clot retraction, Rac1 is also involved in the second pMLC peak that is mediated by actin polymerisation and Rac1 activation (Egot et al., 2013). Furthermore, role for Rac1 in inducing MLC phosphorylation and regulating Rac-1-MAPK dependent integrin outside-in signalling has been established (Flevaris et al., 2008).

Rac has a specific role in platelet lamellipodia formation, spreading and reorganising the cytoskeleton. Of the Rac isoforms, Rac 1 and Rac 2 have been reported to be expressed in platelets. Nevertheless, Rac1 has been shown to be the most principal isoform in platelets as shown in the murine platelets from Rac1 $^{-/-}$Rac2$^{-/-}$ mice, emphasising the pivotal role of Rac1 for lamellipodia formation (McCarty et al., 2005). Rac1 plays a role in the cytoskeletal reorganisation of engagement of receptors for collagen and laminin. We found that Rac activity was reduced in platelets spread on fibrinogen and nLDL but it was not reduced in the presence of oxLDL. Again, this is in line with the maintenance of lamellipodia formation in these conditions. It was thus deduced that in the presence oxLDL, Rho but not Rac is downregulated in platelets treated with PGI$_2$, suggesting that different cAMP levels may regulate the different RhoGTPases. Differential regulation of RhoGTPases was previously established in dendrite formation where elevated cAMP levels induced down regulation of Rho activity and upregulation of Rac activity as a result of Rho GDI preferentially bound to RhoA than Rac (Scott and Leopardi, 2003).

After establishing that cAMP elevating agents induced actin nodule formation and stress fibre reversal while lamellipodia and surface area remained the same in oxLDL and fibrinogen spread platelets, this led to the hypothesis that cAMP plays a role in differentially regulating the different RhoGTPases in the presence of oxLDL, specifically downregulating RhoA and upregulating Rac. To explore the effect observed under PGI$_2$ treated platelets further, platelets were pre-treated with the RhoA inhibitor, Y27632 or the Rac inhibitor, NSC3766. As expected, it was found that both Y27632 and NSC3766 reduced platelet surface area and induced stress fibre reversal and actin nodule formation in all conditions, including platelets spread on both fibrinogen and oxLDL. However, importantly this experiment determined that there is a

significant difference in the surface area reduction in response to Y27632 and NSC23766 in the presence of oxLDL. These findings emphasised the theory that different levels of cAMP regulate the different RhoGTPases in the presence of oxLDL.

It is believed that phospholipids, arachidonic acid and phosphatidic acid can control the disassociation of the Rac-GDI complex (Chuang, Bohl and Bokoch, 1993; Tolias, Couvillon, Cantley and Carpenter, 1998). Phosphatidic acid is activated by oxLDL and thus it can be hypothesised that the differential regulation of the RhoGTPases we identified is due to the disassociation of Rac-GDI mediated by Phospholipase D (PLD) activation via oxLDL (Natarajan, Scribner, Hart and Parthasarathy, 1995). The activation of PLD is thought to increase smooth muscle cell proliferation which in turn contributes to the hardening of the plaque in atherosclerotic lesions. PA is metabolised to LPA and DAG which on plaque rupture, LPA activates the circulating platelets, contributing to the formation of a thrombus.

It has been hypothesised in the literature that RhoGTPases are crucial in regulating a redox feedback loop that controls leukocyte chemotaxis (Kuiper, Sun, Magalhães and Glogauer, 2011). Rac1 is thought to trigger ROS production directly, promoting oxidant formation which in turn regulates GEF activation of Rac whereas RhoA downregulates oxidant generating enzymes, confirming that Rac and Rho have antagonistic roles. Another study showed that oxLDL results in oxidative stress and upregulates Rac1 in a LOX-1 dependent fashion (Yang et al., 2015). Together, this leads to the theory that Rac1 is involved in oxLDL induced ROS production in platelets thus emphasising that the activation of Rac can increase the atherogenicity of atherosclerotic lesions and platelet hyperreactivity. It is well described that all PI3K isoforms can activate Rac however only PI3Kα activates RhoA and is inhibited by

PI3Kδ (Papakonstanti, Ridley and Vanhaesebroeck, 2007). It is therefore attractive to speculate that in the presence of PGI$_2$ oxLDL may activate Rac upstream of selective isoforms of PI3K that are hyposensitive to cAMP. In addition, upregulation of Rac may be driven by P-Rex1, a Rac-specific GEF which is activated by PIP3 upstream of PI3K (Welch et al., 2002). This GEF is present in platelets and is also involved in the production of ROS through the activation of Rac, conveying an important role for Rac in oxidative stress (Welch et al., 2005; Morgan-Spencer & Greenberg, 2007). This further highlights the idea that oxLDL contributes to ROS production, therefore inducing platelet activation and may attenuate the effect of cAMP, proving potential implications of Rac in promoting atherogenicity.

6.2 Role of inhibitory signalling in thrombus formation

Under normal physiological conditions, the endothelium is intact and spontaneous activation of platelets is prevented to avoid thrombosis. Intracellular signalling pathways that promote platelet activation are controlled meticulously by mechanisms that negatively regulate platelet activation. Negative regulators of platelet activation such as NO and PGI$_2$ are platelet antagonists that inhibit adhesion, activation and aggregation. As PGI$_2$ is implicated in the regulation of a thrombus and plays a pivotal role in inhibiting platelets in the vasculature, understanding its role in spread platelets would help identify how it would affect thrombus formation. It is currently believed that PGI$_2$ has a dual role in regulating the formation of a thrombus. It is thought that PGI$_2$ is involved in continuously inhibiting platelets before activation and is present in the circulation at 10 pM whereby 0.1 nM is the threshold concentration essential in the body (FitzGerad et al., 1981). On the other hand, it is also thought that PGI$_2$ and NO are responsible for the reversal of platelets after their activation which is initiated by thrombin (Weksler, Ley and Jaffe, 1978). It has previously been established by Yusuf et al., 2017 that PGI$_2$ induces a strong elevation in cAMP within fully spread platelets

as well as stress fibre reversal in a PKA dependent manner. Together, this therefore emphasises the idea that PGI_2 is essential in controlling the formation of a thrombus initiated by vascular injury. Thus, we explored the effect of PGI_2 in oxLDL and fibrinogen spread platelets and identified that actin nodule formation and reversal of stress fibres were induced while surface area remained the same, suggesting that oxLDL attenuates the effect of PGI_2. It was therefore postulated that oxLDL was responsible for the degradation of the cyclic nucleotide, cAMP. Therefore, the experiment was consequently repeated with the addition of the PDE3 inhibitor milrinone where we found a marked reduction in platelet surface area, highlighting that oxLDL caused the attenuation of PGI_2 in a PDE3 dependent manner. This agrees with findings described by Berger et al., 2019. After establishing that oxLDL plays a role in degrading cAMP, we further explored the effect it may have on regulating the adenylyl cyclase enzyme. ACs are directly activated by forskolin, elevating cAMP levels in platelets and a variety of other cell types. As a result, we used forskolin as a cAMP elevating agent to understand its effect in mediating the cytoskeleton of spread platelets. We identified that in the presence of oxLDL, forskolin treatment mimics the effect of PGI_2 and results in stress fibre reversal and actin nodule formation while surface area and lamellipodia remained unaffected. This was previously established in vascular smooth muscle cells where forskolin did not elevate cAMP levels in the presence of oxLDL, (Jing et al., 1999). Therefore, it is evident that oxLDL can reduce cAMP levels in platelets as well as other cell types.

6.3 Role of oxLDL in thrombus formation

It was also critical to determine the effect of cAMP inducing agents such as PGI_2 in reorganising the actin cytoskeleton. We found that the surface area coverage was significantly reduced and actin nodules as well as stress fibre reversal induced upon post-treatment with PGI_2 on blood flown over fibrinogen as shown by Yusuf et al., 2017. As expected, this effect

was also evident in the presence of nLDL in combination with fibrinogen. Post perfusion of another cAMP elevating agent, forskolin also induced a similar effect where the surface area coverage was markedly reduced and an increase in actin nodule formation and stress fibre reversal was observed, agreeing with our findings under the static system. On the other hand, in agreement with the phenotype observed in static conditions, the presence of oxLDL did not cause a reduction in surface area in vitro upon post perfusion of forskolin. Interestingly, under arterial shear rates, reversal of stress fibres and increased actin nodules were not induced after the perfusion of PGI_2 and forskolin on blood flown on the combination of oxLDL and fibrinogen, contradicting our previous observations in the static system. This indicated that shear can alter the effectiveness of PGI_2 to reverse platelet activation.

Venous or arterial thrombosis is dependent on the anatomical site of the thrombotic event. Arterial thrombosis is primarily thought to be related to atherosclerotic plaque rupture and high shear stress, leading to the exposure and high concentrations of prothrombotic materials. On the other hand, venous thrombosis is believed to be associated to low shear stress and occurs without endothelial disruption. Although the pathological alterations that take place in arterial and venous thrombosis are different, common mechanisms are present for both. Lipid peroxidation products have been found on surfaces of microvesicles, suggesting a role for atherogenic lipids beyond arterial thrombosis (Obermayer, Afonyushkin and Binder, 2018). Furthermore, increasing clinical evidence shows a strong correlation between venous thrombosis and inflammation. For example, inflammatory bowel disease, rheumatoid arthritis, and Behçet's disease, are linked to an increased risk of venous thrombosis (Zöller, Li, Sundquist and Sundquist, 2012). Although oxLDL contributes heavily to atherogenesis and atherosclerosis associated inflammation, its role in venous thrombosis remains to be elucidated.

Thus, our experiments repeated under venous shear rates 200sec^{-1} (25.0 dynes/cm^2) showed that although surface area coverage was not affected, actin nodule formation and stress fibre reversal was present after the perfusion of PGI$_2$ in platelets spread on fibrinogen and/or nLDL. However, in the presence of oxLDL stress fibre reversal and actin nodule formation occurred in platelets post-treated with PGI$_2$. Interestingly, the surface area coverage increased although this was due to the recruitment of leukocytes.

PGI$_2$ is more effective at inhibiting platelets under low shear conditions in contrast to high shear rates. This could be due to platelets adhering strongly on high shear conditions which are as a result more difficult to reverse, however the structure of thrombi formed at different shear rates remains to be elucidated. Studies have reported that oxLDL promotes leukocyte rolling and adhesion on the endothelium. However, it has been established that the activation of RhoA promotes the detachment of leukocytes in postcapillary venules of mice and other cell types which may suggest that the inhibition of RhoA induces leukocyte adhesion and spreading in the presence of PGI$_2$ (Alblas, Ulfman, Hordijk and Koenderman, 2001). More recent studies have shown that leukocytes protrude extensively when RhoA is inactive whereas leukocyte adhesion is inhibited when RhoA is activated (Worthylake, Lemoine, Watson and Burridge, 2001). Taken together, we can postulate that although oxLDL promotes leukocyte adhesion strongly under low shear stress conditions, inhibition of RhoA induces leukocyte adhesion and spreading which is in line with our findings as we show leukocyte adhesion and spreading in the presence of PGI$_2$ where stress fibres are reversed.

6.4 Clinical relevance

Atherosclerosis is a pathophysiological disease which causes narrowing of the arteries, reducing their elasticity and impeding blood flow. A series of oxidation products are generated after the oxidation of LDL. These oxidative by products play a pivotal role in the pathogenesis of atherosclerosis as a result of pathogenic macrophage recruitment and foam cell formation.

 LDL is found in the circulation of which a small portion travel to the subendothelial space. Nonetheless, the subendothelial space is thought to be the site of LDL oxidation in vivo as there is a plethora of antioxidants in circulation which prevent oxidation. Thus, the bidirectional transport of LDL may consequently lead to oxLDL in the circulation which can be led to a poor prognosis in CVD patients (Nishi et al., 2002). oxLDL has been found in the plasma of CVD patients and it is involved in playing primary role in triggering inflammation in atherosclerotic plaques. Circulating oxLDL levels are significantly higher in patients with coronary heart disease and is a possible biochemical risk marker for patients with CVD (Trpkovic et al., 2015). Furthermore, it has been previously shown that oxLDL activated platelets internalise oxLDL compared to resting platelets (Daub et al., 2010).

Likewise, clinical studies have consistently shown elevated levels of fibrinogen in patients with CVD and thrombosis (Wilhelmsen et al., 1984). Thus, it is attractive to postulate that circulating fibrinogen and oxLDL interact. Furthermore, our results are clinically relevant as we show that high concentrations of fibrinogen and oxLDL induce a prothrombotic phenotype. It has been previously established that increasing levels of fibrinogen promote the interaction of platelets as a result of increased binding affinity to the platelet $\alpha_{IIb}\beta_3$ receptor and increased clot viscosity, leading to enhanced thrombus formation. This, alongside circulating oxLDL has

the potential to pose an increased cardiovascular risk to atherosclerotic patients. Clinical studies have further shown that elevated levels of oxLDL are strongly correlated to development of CVD and a poorer prognosis, with use as a clinically useful biomarker (Wang et al., 2019).

Although elevated levels of oxLDL and fibrinogen induce a prothrombotic phenotype, increased levels of oxLDL are associated to plaque rupture and vulnerability as circulating oxLDL may undergo further oxidation in the atherosclerotic plaque, which may lead to plaque instability as well as an increased risk of thrombosis and result in a poor prognosis (Nishi et al., 2002).

PGI_2 regulates platelet activation and thrombosis via cAMP signalling pathways however, its protective mechanism is inhibited in patients with CVD. Our novel finding shows that the effect of PGI_2 is attenuated and cAMP levels are diminished in the presence of elevated oxLDL and fibrinogen. Thus, these results convey that oxLDL plays an important role in promoting a prothrombotic phenotype by impairing PGI_2 sensitivity. Pharmacological inhibition of PDE3 resulted in the inhibition of platelet activity suggesting the attenuation of PGI_2 in the presence of oxLDL occurs in a PDE3 dependent fashion. This data highlights the clinical importance of PGI_2 hyposensitivity in high risk dyslipidaemic populations as these patients may still be at atherothrombotic and residual cardiovascular risk due to impaired inhibition of platelets. Likewise, in the presence of oxLDL and fibrinogen, forskolin mimics the effect of PGI_2 by partially inhibiting platelet function as stress fibre reversal and actin nodule formation is induced while surface area remains unaffected. In this context our findings suggest a novel pro-atherothrombotic role of oxLDL as impaired platelet inhibition constitute a greater atherogenic and prothrombotic risk for dyslipidaemic patients.

Furthermore, we found that the effect of PGI_2 affected actin cytoskeletal rearrangement in platelets treated with oxLDL and fibrinogen where partial inhibition was observed as stress fibre reversal is induced but surface area and lamellipodia formation were unaffected. This is confirmed by the downregulation of RhoA and upregulation of Rac, demonstrating that increased atherothrombotic risk remains despite treatment with PGI_2. It is appropriate to speculate this differential regulation alongside Rac mediated ROS production potentiates Rac activation, exacerbating the oxidising products from LDL oxidation which leads to further oxidation of LDL. This promotes atherogenicity of atherosclerotic lesions and platelet hyperreactivity, posing increased risk for CVD patients.

The interaction of platelets with oxLDL and fibrinogen leads to platelet hyperreactivity. This phenotype may be due to an increase in Ca^{2+} levels due to changes in the platelet lipidome as a result of lipid uptake via CXCL12/CXCR4-7 axis through oxidation and peroxidation processes regulated by mitochondrion-dependent ROS generation (Chatterjee et al., 2015). As a result, it is evident that platelets have the ability to store large amounts of oxLDL to atherosclerotic lesions which further signifies the role of platelets on atherothrombosis (Daub et al., 2010). Additionally, very low concentrations of oxLDL (5 µg/ml) is required to generate a small amount of ROS, highlighting the significance of oxidative agents in increasing the atherogenicity of atherosclerotic plaques (Dandapat, Hu, Sun and Mehta, 2007). Again, ROS production may play a significant role in inducing an increased risk for atherosclerotic patients and targeting ROS and oxidising components may be a potential therapeutic target.

We found that PGI_2 is more effective at inhibiting platelets under low shear conditions in contrast to high shear rates. We hypothesised that this could be due to platelets adhering

strongly on high shear conditions which are as a result more difficult to reverse, thus contributing to the theory that arterial thrombosis is primarily thought to be related to atherosclerotic plaque rupture and high shear stress, leading to the exposure and high concentrations of prothrombotic materials. Nevertheless, a variety of CVD as well as inflammatory related diseases such as inflammatory bowel disease, rheumatoid arthritis, and Behçet's disease, are linked to an increased risk of venous thrombosis (Zöller, Li, Sundquist and Sundquist, 2012).

Under low shear stress conditions, PGI_2 treatment results in leukocyte recruitment in the presence of oxLDL and fibrinogen. It is thought that leukocytes protrude extensively when RhoA is inactive whereas leukocyte adhesion is inhibited when RhoA is activated (Worthylake, Lemoine, Watson and Burridge, 2001). It can therefore be postulated that the combination of oxLDL and fibrinogen promotes leukocyte adhesion strongly under low shear stress conditions, suggesting that oxLDL has an important role in inflammation beyond arterial thrombosis. Atherogenesis is a complex and meticulously controlled physiological process where inflammation plays a key role in activating a variety of immune cells, causing the upregulation of inflammatory molecules and triggers a pro-inflammatory phenotype. More recently, it has become increasingly evident that the main cause of CVD, atherosclerosis, propagates the inflammatory process that occurs in the vascular wall (Wolf & Ley, 2019).

This data is clinically relevant as leukocyte recruitment under these conditions may lead to platelet-leukocyte interactions, suggesting an important clinical role for oxLDL in immunothrombosis, increasing the risk for CVD patients with venous thrombosis.

6.5 Future work

The role of oxLDL in inducing a prothrombotic and inflammatory phenotype has opened up a variety of avenues that need attention in future experiments. Future studies should explore the role of scavenger receptors in atherothrombosis. It has been established that CD36 binds to oxLDL with an affinity as great or even greater than some of the scavenger family receptors described in the literature (Greaves and Gordon, 2008). The CD36-oxLDL interaction also promotes platelet activation as well as promote the atherogenicity of the atherosclerotic plaque therefore, further studies should be carried out in CD36 knock out models in order to better understand the effect of targeting this receptor in improving the prognosis of patients suffering from atherogenesis (Magwenzi et al., 2015). Focusing on strategies that target inflammatory regulators that change the platelet lipidome such as CXCL12/CXCR4-7 via oxidation and peroxidation processes regulated by mitochondrion-dependent ROS generation may be of importance (Chatterjee et al., 2015).

Indeed, oxLDL adheres to endothelial cells, inducing a significant inflammatory response and thus triggers platelet accumulation and promotes atherosclerosis. A plethora of studies have shown that LOX-1 mediates many ox-LDL induced processes involved in inflammation and that the interaction between oxLDL and LOX-1 regulates the expression of various genes that play a role in the proliferation of SMCs, inducing foam cell formation in macrophages. Thus, targeting LOX-1 by blocking its expression may potentially be a therapeutic target in reducing processes such as inflammation and subsequently, atherosclerotic lesion formation. It is possible that LOX-1 plays an important role in oxLDL mediated platelet hyperreactivity and atherothrombosis and this is an attractive theory for research. Another study showed that oxLDL results in oxidative stress and upregulates Rac1 in a LOX-1 dependent fashion (Yang et al., 2015). Together, this leads to the theory that Rac1 is involved in oxLDL induced

oxidative stress, leading to rearrangement of the actin cytoskeleton of platelets and thus emphasising that targeting LOX-1 may be a therapeutic strategy by reducing atherogenicity of atherosclerotic lesions and platelet hyperreactivity.

As well as their importance in CVD, studies are now focusing on the importance of CD36 and LOX-1 in tumour progression. LOX-1 is upregulated in myeloid derived suppressor cells in cancer patients, suggesting the potential involvement in inflammation of oxLDL in immunotherapy (Condamine et al., 2016). It is well known that cancer is associated with thromboembolic disease however the mechanisms involved in thromboembolic events remain to be elucidated. Given that oxLDL plays a role in platelet hyperactivity and thrombosis as well as tumour progression, it can nonetheless be postulated that oxLDL may play a more complex role by also inducing tumour-associated thrombosis. Thus far, there is enough data to show oxLDL involvement in tumour progression as well as metastasis however, there is currently a lack of knowledge regarding oxLDL as an attractive therapeutic target for high-risk CVD patients that have cancer.

In addition, we have established that the effect of PGI_2 is inhibited in the combination of oxLDL and fibrinogen in a PDE3 dependent pathway. Pharmacological inhibition of PDE3 in human and murine platelets reduces thrombotic potential. Thus, factors that regulate platelet inhibition by influencing the synthesis or hydrolysis of cAMP may be critical modulators of atherothrombosis and may lead to a prothrombotic phenotype. Therefore, future studies should explore the isoforms of PDE3 and their clinical importance in atherothrombosis.

Although we established that inhibiting platelets in the presence of oxLDL causes the downregulation of RhoA and upregulation of Rac, demonstrating these results in Rac knock

out models to further explore the role of Rac in regulating the actin cytoskeleton and promoting atherothrombotic events is crucial. Furthermore, it will be interesting to explore the effect of Rho GDI in order to test the theory that lipid stress causes Rho-GDI to preferentially bind RhoA compared to Rac and that oxidising components activated by oxLDL control the disassociation of the Rac-GDI complex. Since Rac specific GEFs such as P-Rex1are involved in ROS production, it is important to investigate this in platelets as targeting Rac specific GEFS may reduce atherothrombotic phenotypes in CVD patients.

Conclusion

In summary, this thesis identifies that the combination of oxLDL and fibrinogen induces a prothrombotic phenotype. Firstly, our results show that platelets spread on oxLDL and fibrinogen result in the attenuation of cAMP elevating agents such as PGI_2 and forskolin, indicating that oxLDL triggers the activation of platelets by altering the inhibitory signalling pathway. Likewise, we found that PGI_2 downregulates RhoA activity while upregulating the activation of Rac in the presence of oxLDL, suggesting that oxLDL promotes platelet hyperactivity through the modulation of the RhoGTPases involved in the platelet actin cytoskeleton. We identify that the presence of PGI_2 at low shear rates 200 s^{-1} in vitro induce the formation of leukocytes in platelets spread on oxLDL and fibrinogen, suggesting that at low shear rates, leukocytes protrude extensively when RhoA is inactive whereas leukocyte adhesion is inhibited when RhoA is activated (Worthylake, Lemoine, Watson and Burridge, 2001). Therefore, suggesting that the combination of oxLDL and fibrinogen promotes leukocyte adhesion strongly under low shear stress conditions. Future work should investigate the role of oxLDL in inflammation beyond arterial thrombosis. Investigating the contribution of oxidised lipoproteins and fibrinogen and their involvement in promoting platelet

hyperreactivity, inflammation, atherogenicity and atherothrombosis, in the context of these results will provide novel insights and identify new pathways of immunothrombosis.

References

Abi-Gerges, A., Richter, W., Lefebvre, F., Mateo, P., Varin, A., Heymes, C., Samuel, J., Lugnier, C., Conti, M., Fischmeister, R. and Vandecasteele, G. (2009). Decreased Expression and Activity of cAMP Phosphodiesterases in Cardiac Hypertrophy and Its Impact on β-Adrenergic cAMP Signals. *Circulation Research*, 105(8), pp.784-792

Akbar, H., Shang, X., Perveen, R., Berryman, M., Funk, K., Johnson, J., Tandon, N. and Zheng, Y., 2011. Gene Targeting Implicates Cdc42 GTPase in GPVI and Non-GPVI Mediated Platelet Filopodia Formation, Secretion and Aggregation. *PLOS ONE*, 6(7), p.E22117.

Alblas, J., Ulfman, L., Hordijk, P. and Koenderman, L., 2001. Activation of RhoA and ROCK Are Essential for Detachment of Migrating Leukocytes. *Molecular Biology of the Cell*, 12(7), pp.2137-2145.

Alexopoulos, N. and Raggi, P., 2009. Calcification in atherosclerosis. *Nature Reviews Cardiology*, (6), pp.681–688.

André, P., Prasad, K., Denis, C., He, M., Papalia, J., Hynes, R., Phillips, D. and Wagner, D. (2002). CD40L stabilizes arterial thrombi by a β3 integrin–dependent mechanism. *Nature Medicine*, 8(3), pp.247-252.

Andrews, R., Kamiguti, A., Berlanga, O., Leduc, M., Theakston, R. and Watson, S., 2001. The Use of Snake Venom Toxins as Tools to Study Platelet Receptors for Collagen and von Willebrand Factor. *Pathophysiology of Haemostasis and Thrombosis*, 31(3-6), pp.155-172.

Ardlie, N., Selley, M. and Simons, L., 1989. Platelet activation by oxidatively modified low density lipoproteins. *Atherosclerosis*, 76(2-3), pp.117-124.

Aschoff, L. (1893) Ueber capilläre Embolie von riesenkernhaltigen Zellen. Archiv für *Pathologische Anatomie und Physiologie und für Klinische Medicin*, 134(1), 11-25.

Aslan, J. and McCarty, O., 2013. Rho GTPases in platelet function. *Journal of Thrombosis and Haemostasis*, 11(1), pp.35-46.

Atkinson, B., Stafford, M., Pears, C. and Watson, S., 2001. Signalling events underlying platelet aggregation induced by the glycoprotein VI agonist convulxin. *European Journal of Biochemistry*, 268(20), pp.5242-5248.

Auger, J. and Watson, S., 2008. Dynamic Tyrosine Kinase-Regulated Signaling and Actin Polymerisation Mediate Aggregate Stability Under Shear. *Arteriosclerosis, Thrombosis, and Vascular Biology*, 28(8), pp.1499-1504.

Avecilla, S., Hattori, K., Heissig, B., Tejada, R., Liao, F., Shido, K., Jin, D., Dias, S., Zhang, F., Hartman, T., Hackett, N., Crystal, R., Witte, L., Hicklin, D., Bohlen, P., Eaton, D., Lyden, D., de Sauvage, F. and Rafii, S. (2004) Chemokine-mediated interaction of hematopoietic progenitors with the bone marrow vascular niche is required for thrombopoiesis. *Nature Medicine*, 10(1), 64-71.

Backer, S., Lokmane, L., Landragin, C., Deck, M., Garel, S. and Bloch-Gallego, E., 2018. Trio GEF mediates RhoA activation downstream of Slit2 and coordinates telencephalic wiring. *Development*, 145(19), p.dev153692.

Badrnya, S., Schrottmaier, W., Kral, J., Yaiw, K., Volf, I., Schabbauer, G., Soderberg-Naucler, C. and Assinger, A. (2014) Platelets Mediate Oxidized Low-Density Lipoprotein-Induced Monocyte Extravasation and Foam Cell Formation. *Arteriosclerosis, Thrombosis, and Vascular Biology*, 34(3), 571-580.

Balduini, A., Di Buduo, C., Malara, A., Lecchi, A., Rebuzzini, P., Currao, M., Pallotta, I., Jakubowski, J. and Cattaneo, M. (2012) Constitutively released adenosine diphosphate regulates proplatelet formation by human megakaryocytes. *Haematologica*, 97(11), 1657-1665.

Barnes, M., Knight, C. and Farndale, R. (1999). 1.W01.1 Collagens and atherosclerosis: Collagen-cell interaction. *Atherosclerosis*, 134(1-2), p.8.

Bauriedel, G., Hutter, R. and Welsch, U. (1999). Role of smooth muscle cell death in advanced coronary primary lesions: implications for plaque instability. *Cardiovascular Research*, 41(2), pp.480-488.

Blair, A., Shaul, P., Yuhanna, I., Conrad, P. and Smart, E. (1999) Oxidized Low Density Lipoprotein Displaces Endothelial Nitric-oxide Synthase (eNOS) from Plasmalemmal Caveolae and Impairs eNOS Activation. *Journal of Biological Chemistry*, 274(45), 32512-32519.

Behnke, O., 1967. Electron microscopic observations on the membrane systems of the rat blood platelet. *The Anatomical Record*, 158(2), pp.121-137.

Behnke, O. (1968) An electron microscope study of the megacaryocyte of the rat bone marrow. *Journal of Ultrastructure Research*, 24(5-6), 412-433.

Bender, A. and Beavo, J. (2006). Cyclic Nucleotide Phosphodiesterases: Molecular. Regulation to Clinical Use. *Pharmacological Reviews*, 58(3), pp.488-520.

Berger, M., Raslan, Z., Aburima, A., Magwenzi, S., Wraith, K., Spurgeon, B., Hindle, M., Law, R., Febbraio, M. and Naseem, K., 2019. Atherogenic lipid stress induces platelet hyperactivity through CD36-mediated hyposensitivity to prostacyclin: the role of phosphodiesterase 3A. *Haematologica*, 105(3), pp.808-819.

Borgognone, A., Navarro-Núñez, L., Correia, J., Pollitt, A., Thomas, S., Eble, J., Pulcinelli, F., Madhani, M. and Watson, S., 2014. CLEC-2-dependent activation of mouse platelets is weakly inhibited by cAMP but not by cGMP. *Journal of thrombsis and haemostasis*, 12(4), pp.550-559.

Born, G., 1962. Aggregation of Blood Platelets by Adenosine Diphosphate and its Reversal. *Nature*, 194(4832), pp.927-929.

Brill, A., Fuchs, T., Chauhan, A., Yang, J., De Meyer, S., Köllnberger, M., Wakefield, T., Lämmle, B., Massberg, S. and Wagner, D. (2011). von Willebrand factor–mediated platelet adhesion is critical for deep vein thrombosis in mouse models. *Blood*, 117(4), pp.1400-1407.

Brown, B., Dean, R. and Davies, M., 2005. Glycation of low-density lipoproteins by methylglyoxal and glycolaldehyde gives rise to the in vitro formation of lipid-laden cells. *Diabetologia*, 48(2), pp.361-369.

Butcher, R. and Sutherland, E. (1962). Adenosine 3',5'-phosphate in biological materials. I. Purification and properties of cyclic 3',5'-nucleotide phosphodiesterase and use of this enzyme to characterize adenosine 3',5'-phosphate in human urine. *The Journal of Biological Chemistry*, 237, pp.1244-1250.-p90

Buitrago, C., Coller, B. & Zafar, H. (2019) Dominant Role of αIIbβ3 in Platelet Interactions with Polymerizing Cross-Linked Fibrin. Blood, 134(Supplement_1), 1061-1061.

Calderwood, D., Zent, R., Grant, R., Rees, D., Hynes, R. and Ginsberg, M. (1999). The Talin Head Domain Binds to Integrin β Subunit Cytoplasmic Tails and Regulates Integrin Activation. *Journal of Biological Chemistry*, 274(40), pp.28071-28074.

Carvalho, A., Colman, R. and Lees, R. (1974) Platelet Function in Hyperlipoproteinemia. New England Journal of Medicine, 290(8), 434-438.

Cathcart, M., Morel, D. and Chisolm, G., 1985. Monocytes and Neutrophils Oxidize Low Density Lipoprotein Making It Cytotoxic. *Journal of Leukocyte Biology*, 38(2), pp.341-350.

Chatterjee, M., von Ungern-Sternberg, S., Seizer, P., Schlegel, F., Büttcher, M., Sindhu, N., Müller, S., Mack, A. and Gawaz, M., 2015. Platelet-derived CXCL12 regulates monocyte function, survival, differentiation into macrophages and foam cells through differential involvement of CXCR4–CXCR7. *Cell Death & Disease*, 6(11), pp.e1989-e1989.

Chen, K., Febbraio, M. and Silverstein, R., 2007. Prothrombotic Platelet Signaling by the Scavenger Receptor, CD36. *Blood*, 110(11), pp.3642-3642.

Chen, K., Febbraio, M., Li, W. and Silverstein, R. (2008). A Specific CD36-Dependent Signaling Pathway Is Required for Platelet Activation by Oxidized Low-Density Lipoprotein. *Circulation Research*, 102(12), pp.1512-1519.

Chen, M., Kakutani, M., Minami, M., Kataoka, H., Kume, N., Narumiya, S., Kita, T., Masaki, T. and Sawamura, T. (2000) Increased Expression of Lectinlike Oxidized Low Density Lipoprotein Receptor-1 in Initial Atherosclerotic Lesions of Watanabe Heritable Hyperlipidemic Rabbits. *Arteriosclerosis, Thrombosis, and Vascular Biology*, 20(4), 1107-1115.

Cheng, Y., Austin, S. and Rocca, B. (2002). Role of Prostacyclin in the Cardiovascular Response to Thromboxane A2. *Science*, 296(5567), pp.539-541.

Chuang, T., Bohl, B. and Bokoch, G., 1993. Biologically Active Lipids Are Regulators of Rac. GDI Complexation. *Journal of Biology and Chemistry*, 268(35), pp.26206-26211.

Chung, B., Wilkinson, T., Geer, J. and Segrest, J., 1980. Preparative and quantitative isolation of plasma lipoproteins: rapid, single discontinuous density gradient ultracentrifugation in a vertical rotor. *Journal of lipid research*, 21(3), pp.284-291.

Condamine, T., Dominguez, G., Youn, J., Kossenkov, A., Mony, S., Alicea-Torres, K., Tcyganov, E., Hashimoto, A., Nefedova, Y., Lin, C., Partlova, S., Garfall, A., Vogl, D., Xu, X., Knight, S., Malietzis, G., Lee, G., Eruslanov, E., Albelda, S., Wang, X., Mehta, J., Bewtra, M., Rustgi, A., Hockstein, N., Witt, R., Masters, G., Nam, B., Smirnov, D., Sepulveda, M. and Gabrilovich, D., 2016. Lectin-type oxidized LDL receptor-1 distinguishes population of human polymorphonuclear myeloid-derived suppressor cells in cancer patients. *Science Immunology*, 1(2), pp.8943-aaf8943.

Courtemanche, N. and Pollard, T. (2013). Interaction of Profilin with the Barbed End of Actin Filaments. *Biochemistry*, 52(37), pp.6456-6466.

Crittenden, J., Bergmeier, W., Zhang, Y., Piffath, C., Liang, Y., Wagner, D., Housman, D. and Graybiel, A. (2004). CalDAG-GEFI integrates signaling for platelet aggregation and thrombus formation. *Nature Medicine*, 10(9), pp.982-986.

Curtiss, L., Black, A., Takagi, Y. and Plow, E. (1987) New mechanism for foam cell generation in atherosclerotic lesions. *Journal of Clinical Investigation,* 80(2), 367-373.

Dandapat, A., Hu, C., Sun, L. and Mehta, J., 2007. Small Concentrations of oxLDL Induce Capillary Tube Formation From Endothelial Cells via LOX-1–Dependent Redox-Sensitive Pathway. *Arteriosclerosis, Thrombosis, and Vascular Biology*, 27(11), pp.2435-2442.

Dash, D., Aepfelbacher, M. and Siess, W., 1995. The association of pp125FAK, pp60Src, CDC42Hs and Rap1B with the cytoskeleton of aggregated platelets is a reversible process regulated by calcium. *FEBS Letters*, 363(3), pp.231-234.

Daub, K., Seizer, P., Stellos, K., Krämer, B., Bigalke, B., Schaller, M., Fateh-Moghadam, S., Gawaz, M. and Lindemann, S., 2010. Oxidized LDL-Activated Platelets Induce Vascular Inflammation. *Seminars in Thrombosis and Hemostasis*, 36(02), pp.146-156.

Davi, G., Averna, M., Catalano, I., Barbagallo, C., Ganci, A., Notarbartolo, A., Ciabattoni, G. and Patrono, C. (1992) Increased thromboxane biosynthesis in type IIa hypercholesterolemia. *Circulation*, 85(5), 1792-1798.

Dejager, S., Mietus-Synder, M. and Pitas, R. (1993). Oxidized low density lipoproteins bind to the scavenger receptor expressed by rabbit smooth muscle cells and macrophages. *Arteriosclerosis and Thrombosis: A Journal of Vascular Biology*, 13(3), pp.371-378.

Disanza†, A., Steffen†, A., Hertzog†, M., Frittoli, E., Rottner, K. and Scita, G., 2005. Actin polymerization machinery: the finish line of signaling networks, the starting point of cellular movement. *CMLS Cellular and Molecular Life Sciences*,.

Dlaboga, D., Hajjhussein, H. and O'Donnell, J. (2006). Regulation of phosphodiesterase-4 (PDE4) expression in mouse brain by repeated antidepressant treatment: Comparison with rolipram. *Brain Research*, 1096(1), pp.104-112.

Dopheide, S., Maxwell, M. and Jackson, S. (2002). Shear-dependent tether formation during platelet translocation on von Willebrand factor. *Blood*, 99(1), pp.159-167.

Ehrenwald, E., Chisolm, G. and Fox, P., 1994. Intact human ceruloplasmin oxidatively modifies low density lipoprotein. *Journal of Clinical Investigation*, 93(4), pp.1493-1501.

Eitzman, D., Westrick, R., Xu, Z., Tyson, J. & Ginsburg, D. (2000) Hyperlipidemia Promotes Thrombosis After Injury to Atherosclerotic Vessels in Apolipoprotein E–Deficient Mice. Arteriosclerosis, Thrombosis, and Vascular Biology, 20(7), 1831-1834.

Endemann, G., Stanton, L., Madden, K., Bryant, C., White, R. and Protter, A. (1993). CD36 is a receptor for oxidized low density lipoprotein. *The Journal of Biological Chemistry*, 268, pp.11811–11816.

Escolar, G. and White, J. (1991). The platelet open canalicular system: a final common pathway. *Blood Cells*, 17, pp.467–485.

Feng, Y. and Hart, G., 1995. In vitro oxidative damage to tissue-type plasminogen activator: a selective modification of the biological functions. *Cardiovascular Research*, 30(2), pp.255-261.

Fox, J. (2001) Cytoskeletal Proteins and Platelet Signaling. Thrombosis Haemostasis, 86(1), 198-213.

Fibrinogen matrix deposited on the surface of biomaterials acts as a natural anti-adhesive coating. *Biomaterials*, 67, pp.151-159.

Flevaris, P., Stojanovic, A., Gong, H., Chishti, A., Welch, E. and Du, X., 2007. A molecular switch that controls cell spreading and retraction. *Journal of Cell Biology*, 179(3), pp.553-565.

Forstermann, U. and Sessa, W., 2011. Nitric oxide synthases: regulation and function. *European Heart Journal*, 33(7), pp.829-837.

Foster, C., Prosser, D., Agans, J., Zhai, Y., Smith, M., Lachowicz, J., Zhang, F., Gustafson, E., Monsma, F., Wiekowski, M., Abbondanzo, S., Cook, D., Bayne, M., Lira, S. and

Chintala, M. (2001). Molecular identification and characterization of the platelet ADP receptor targeted by thienopyridine antithrombotic drugs. *Journal of Clinical Investigation*, 107(12), pp.1591-1598.

Freedman, J., Loscalzo, J., Barnard, M., Alpert, C., Keaney, J. and Michelson, A. (1997). Nitric oxide released from activated platelets inhibits platelet recruitment. *Journal of Clinical Investigation*, 100(2), pp.350-356.

Freedman, J., Sauter, R., Battinelli, E., Ault, K., Knowles, C., Huang, P. and Loscalzo, J. (1999). Deficient Platelet-Derived Nitric Oxide and Enhanced Hemostasis in Mice Lacking the NOSIII Gene. *Circulation Research*, 84(12), pp.1416-1421.

Freeman, M., Ekkel, Y., Rohrer, L., Penman, M., Freedman, N., Chisolm, G. and Krieger, M. (1991). Expression of type I and type II bovine scavenger receptors in Chinese hamster ovary cells: lipid droplet accumulation and nonreciprocal cross competition by acetylated and oxidized low density lipoprotein. *Proceedings of the National Academy of Sciences*, 88(11), pp.4931-4935.

Frenette, P., Johnson, R., Hynes, R. and Wagner, D. (1995) Platelets roll on stimulated endothelium in vivo: an interaction mediated by endothelial P-selectin. Proceedings of the National Academy of Sciences, 92(16), 7450-7454.

Fukuhara, S., Chikumi, H. and Gutkind, J. (2001). RGS-containing RhoGEFs: the missing link between transforming G proteins and Rho?. *Oncogene*, 20(13), pp.1661-1668.

Galis, Z., Sukhova, G., Lark, M. and Libby, P., 1994. Increased expression of matrix metalloproteinases and matrix degrading activity in vulnerable regions of human atherosclerotic plaques. *Journal of Clinical Investigation*, 94(6), pp.2493-2503.

Gambaryan, S., Friebe, A. and Walter, U. (2012). Does the NO/sGC/cGMP/PKG pathway play a stimulatory role in platelets?. *Blood*, 119(22), pp.5335-5336.

Gerry, A., Satchell, L. and Leake, D. (2008). A novel method for production of lipid hydroperoxide- or oxysterol-rich low-density lipoprotein. *Atherosclerosis*, 197(2), pp.579-587.

Gardener, H., Morte, D., Elkind, M., Sacco, R. and Rundek, T., 2009. Lipids and carotid plaque in the Northern Manhattan Study (NOMAS). BMC Cardiovasc Disord, 9(55), pp.2261-2269.

Gerry, A., Satchell, L. and Leake, D., 2008. A novel method for production of lipid hydroperoxide- or oxysterol-rich low-density lipoprotein. *Atherosclerosis*, 197(2), pp.579-587.

Glomset, J., Nichols, A., Norum, K., King, W. and Forte, T., 1973. Plasma Lipoproteins in Familial Lecithin:Cholesterol Acyltransferase Deficiency Further Studies of Very Low and Low Density Lipoprotein Abnormalities. *Journal of Clinical Investigation*, 52(5), pp.1078-1092.4

Gong, H., Shen, B., Flevaris, P., Chow, C., Lam, S., Voyno-Yasenetskaya, T., Kozasa, T. and Du, X., 2010. G Protein Subunit G 13 Binds to Integrin IIb 3 and Mediates Integrin "Outside-In" Signaling. *Science*, 327(5963), pp.340-343.

Gordon, P., Woodruff, C., Anderson, H. and O'Dell, B., 1982. Effect of acute zinc deprivation on plasma zinc and platelet aggregation in adult males. *The American Journal of Clinical Nutrition*, 35(1), pp.113-119.

Gorodetsky, R., Mou, X., Blankenfeld, A. and Marx, G., 1993. Platelet multielemental composition, lability, and subcellular localization. *American Journal of Hematology*, 42(3), pp.278-283.

Gough, P., Greaves, D., Suzuki, H., Hakkinen, T., Hiltunen, M., Turunen, M., Herttuala, S., Kodama, T. and Gordon, S. (1999). Analysis of Macrophage Scavenger Receptor (SR-A) Expression in Human Aortic Atherosclerotic Lesions. *Arteriosclerosis, Thrombosis, and Vascular Biology*, 19(3), pp.461-471.

Gowen, B., Borg, T., Ghaffar, A. and Mayer, E. (2001). The collagenous domain of class A scavenger receptors is involved in macrophage adhesion to collagens. *Journal of Leukocyte Biology*, 69(4), pp.575-582.

Graham, G., 2015. Disparities in Cardiovascular Disease Risk in the United States. *Current Cardiology Reviews*, 11(3), pp.238-245.

Grant, P. and Colman, R. (1984). Purification and characterization of a human platelet cyclic nucleotide phosphodiesterase. *Biochemistry*, 23(8), pp.1801-1807.Hidaka, H. and Asano, T. (1976). Human blood platelet 3′:5′-cyclic nucleotide phosphodiesterase. *Biochimica et Biophysica Acta (BBA) - Enzymology*, 429(2), pp.485-497.

Greaves, D. and Gordon, S., 2008. The macrophage scavenger receptor at 30 years of age: current knowledge and future challenges: TABLE 1. *Journal of Lipid Research*, 50(Supplement), pp.S282-S286.

Gebuhrer, V., Murphy, J., Bordet, J., Reck, M. and McGregor, J. (1995) Oxidized low-density lipoprotein induces the expression of P-selectin (GMP140/PADGEM/CD62) on human endothelial cells. Biochem. J., 306(1), 293-298.

Guilbert, J., 2003. The World Health Report 2002‑Reducing Risks, Promoting Healthy Life. *Education for Health: Change in Learning & Practice*, 16(2), pp.230-230.

Guo, C., Xie, S., Chi, Z., Zhang, J., Liu, Y., Zhang, L., Zheng, M., Zhang, X., Xia, D., Ke, Y., Lu, L. and Wang, D., 2016. Bile Acids Control Inflammation and Metabolic Disorder through Inhibition of NLRP3 Inflammasome. *Immunity*, 45(4), p.944.

Hart, M., Jiang, X., Kozasa, T., Roscoe, W., Singer, W., Gilman, A., Sternweis, P. and Bollag, G. (1998). Direct Stimulation of the Guanine Nucleotide Exchange Activity of p115 RhoGEF by G13. *Science*, 280(5372), pp.2112-2114.

Heijnen, H. and Korporaal, S., 2017. *Platelet Morphology And Ultrastructure.Platelets In Thrombotic And Non-Thrombotic Disorders*. Cham: Springer, pp.21-37.

Heinecke, J., Baker, L., Rosen, H. and Chait, A., 1986. Superoxide-mediated modification of low density lipoprotein by arterial smooth muscle cells. *Journal of Clinical Investigation*, 77(3), pp.757-761.

Hoylaerts, M., Yamamoto, H., Nuyts, K., Vreys, I., Deckmyn, H. and Vermylen, J. (1997).

Howell, W. and Donahue, D. (1937) The production of blood platelets in the lungs. Journal of Experimental Medicine, 65(2), 177-203.

Ireton, K., 2013. Molecular mechanisms of cell–cell spread of intracellular bacterial pathogens. *Open Biology*, 3(7), p.130079.

Isoni, C., Borges, É., Veloso, C., Mattos, R., Chaves, M. and Nogueira-Machado, J., 2009. cAMP Activates The generation of Reactive Oxygen Species and Inhibits The Secretion of IL-6 in Peripheral Blood Mononuclear Cells from Type 2 Diabetic Patients. *Oxidative Medicine and Cellular Longevity*, 2(5), pp.317-321.

Italiano, J., Lecine, P., Shivdasani, R. and Hartwig, J. (1999) Blood Platelets Are Assembled Principally at the Ends of Proplatelet Processes Produced by Differentiated Megakaryocytes. J Cell Biol, 147(6), 1299-1312.

Ivanciu, L., Krishnaswamy, S. & Camire, R. (2014) New insights into the spatiotemporal localization of prothrombinase in vivo. Blood, 124(11), 1705-1714.

Jing, Q., Xin, S., Cheng, Z., Zhang, W., Zhang, R., Qin, Y. and Pei, G., 1999. Activation of p38 Mitogen-Activated Protein Kinase by Oxidized LDL in Vascular Smooth Muscle Cells. *Circulation Research*, 84(7), pp.831-839.

Jiroušková, M., Jaiswal, J. and Coller, B., 2007. Ligand density dramatically affects integrin αIIbβ3-mediated platelet signaling and spreading. *Blood*, 109(12), pp.5260-5269.

Johnston, N., Jernberg, T., Lagerqvist, B., Siegbahn, A. and Wallentin, L., 2006. Oxidized low-density lipoprotein as a predictor of outcome in patients with unstable coronary artery disease. *International Journal of Cardiology*, 113(2), pp.167-173.

Jones, K., Hughan, S., Dopheide, S., Farndale, R., Jackson, S. and Jackson, D. (2001). Platelet endothelial cell adhesion molecule-1 is a negative regulator of platelet-collagen interactions. *Blood*, 98(5), pp.1456-1463.

Jung, S., Moroi, M., Soejima, K., Nakagaki, T., Miura, Y., Berndt, M., Gardiner, E., Howes, J., Pugh, N., Bihan, D., Watson, S. and Farndale, R. (2012). Constitutive Dimerization of Glycoprotein VI (GPVI) in Resting Platelets Is Essential for Binding to Collagen and Activation in Flowing Blood. *Journal of Biological Chemistry*, 287(35), pp.30000-30013.

Junt, T., Schulze, H., Chen, Z., Massberg, S., Goerge, T., Krueger, A., Wagner, D., Graf, T., Italiano, J., Shivdasani, R. and von Andrian, U. (2007) Dynamic Visualization of Thrombopoiesis Within Bone Marrow. *Science*, 317(5845), 1767-1770.

Kannel, W. (1987) Fibrinogen and Risk of Cardiovascular Disease. JAMA, 258(9), 1183.

Kasirer-Friede, A., Cozzi, M., Mazzucato, M., De Marco, L., Ruggeri, Z. and Shattil, S. (2004). Signaling through GP Ib-IX-V activates αIIbβ3 independently of other receptors. *Blood*, 103(9), pp.3403-3411.

Kiyan, Y., Tkachuk, S., Hilfiker-Kleiner, D., Haller, H., Fuhrman, B. and Dumler, I. (2014) OxLDL induces inflammatory responses in vascular smooth muscle cells via urokinase receptor association with CD36 and TLR4. *Journal of Molecular and Cellular Cardiology*, 66, 72-82.

Klages, B., Brandt, U., Simon, M., Schultz, G. and Offermanns, S., 1999. Activation of G12/G13 Results in Shape Change and Rho/Rho-Kinase–mediated Myosin Light Chain Phosphorylation in Mouse Platelets. *Journal of Cell Biology*, 144(4), pp.745-754.

Kockx, M. & Herman, A. (2000) Apoptosis in atherosclerosis: beneficial or detrimental?. Cardiovascular Research, 45(3), 736-746.

Kodama, T., Reddy, P., Kishimoto, C. and Krieger, M. (1988). Purification and characterization of a bovine acetyl low density lipoprotein receptor. *Proceedings of the National Academy of Sciences*, 85(23), pp.9238-9242.

Korporaal, S., Van Eck, M., Adelmeijer, J., Ijsseldijk, M., Out, R., Lisman, T., Lenting, P., Van Berkel, T. and Akkerman, J. (2007) Platelet Activation by Oxidized Low Density Lipoprotein Is Mediated by Cd36 and Scavenger Receptor-A. *Arteriosclerosis, Thrombosis, and Vascular Biology*, 27(11), 2476-2483.

Krumwiede, M. and White, J., 2007. Some contributions of electron microscopy to knowledge of human platelets. *Thrombosis and Haemostasis*, 98(07), pp.69-72.

Kuiper, J., Sun, C., Magalhães, M. and Glogauer, M., 2011. Rac regulates PtdInsP3 signaling and the chemotactic compass through a redox-mediated feedback loop. *Blood*, 118(23), pp.6164-6171.

Kurian, A. and Cardarelli, K., 2007. Racial and ethnic differences in cardiovascular disease risk factors: a systematic review. *Ethnicity and Disease*, 17(1), pp.143-152.

Lacoste, L., Lam, J., Hung, J., Letchacovski, G., Solymoss, C. and Waters, D. (1995) Hyperlipidemia and Coronary Disease : Correction of the Increased Thrombogenic Potential With Cholesterol Reduction. *Circulation*, 92(11), 3172-3177.

Laemmli, U., 1970. Cleavage of Structural Proteins during the Assembly of the Head of Bacteriophage T4. *Nature*, 227(5259), pp.680-685.

Lafuente, E., van Puijenbroek, A., Krause, M., Carman, C., Freeman, G., Berezovskaya, A., Constantine, E., Springer, T., Gertler, F. and Boussiotis, V. (2004). RIAM, an Ena/VASP and Profilin Ligand, Interacts with Rap1-GTP and Mediates Rap1-Induced Adhesion. *Developmental Cell*, 7(4), pp.585-595.

Lankhof, H., van Hoeij, M., Schiphorst, M., Bracke, M., Wu, Y., Ijsseldijk, M., Vink, T., de Groot, P. and Sixma, J. (1996). A3 Domain Is Essential for Interaction of von Willebrand Factor with Collagen Type III. *Thrombosis and Haemostasis*, 76(06), pp.950-958.

Leake, D. and Rankin, S., 1990. The oxidative modification of low-density lipoproteins by macrophages. *Biochemical Journal*, 270(3), pp.741-748.

Lee, D., Carmichael, D., Krebs, E. and McKnight, G. (1983). Isolation of a cDNA clone for the type I regulatory subunit of bovine cAMP-dependent protein kinase. *Proceedings of the National Academy of Sciences*, 80(12), pp.3608-3612.

Lee, G., Subramanian, N., Kim, A., Aksentijevich, I., Goldbach-Mansky, R., Sacks, D., Germain, R., Kastner, D. and Chae, J., 2012. The calcium-sensing receptor regulates the NLRP3 inflammasome through Ca2+ and cAMP. *Nature*, 492(7427), pp.123-127.

Lefrançais, E., Ortiz-Muñoz, G., Caudrillier, A., Mallavia, B., Liu, F., Sayah, D., Thornton, E., Headley, M., David, T., Coughlin, S., Krummel, M., Leavitt, A., Passegué, E. and Looney, M., 2017. The lung is a site of platelet biogenesis and a reservoir for haematopoietic progenitors. *Nature*, 544(7648), pp.105-109.

Léon, C., Hechler, B., Freund, M., Eckly, A., Vial, C., Ohlmann, P., Dierich, A., LeMeur, M., Cazenave, J. and Gachet, C. (1999). Defective platelet aggregation and increased resistance to thrombosis in purinergic P2Y1 receptor–null mice. *Journal of Clinical Investigation*, 104(12), pp.1731-1737.

Li, H., Freeman, M. and Libby, P. (1995). Regulation of smooth muscle cell scavenger receptor expression in vivo by atherogenic diets and in vitro by cytokines. *Journal of Clinical Investigation*, 95(1), pp.122-133.

Li, R., Mitra, N., Gratkowski, H., Vilaire, G., Litvinov, R., Nagasami, C., Weisel, J., Lear, J., DeGrado, W. and Bennett, J. (2003). Activation of Integrin alphaIIbbeta3 by Modulation of Transmembrane Helix Associations. *Science*, 300(5620), pp.795-798.

Liao, L., Starzyk, R. and Granger, D., 1997. Molecular Determinants of Oxidized Low-Density Lipoprotein–Induced Leukocyte Adhesion and Microvascular Dysfunction. *Arteriosclerosis, Thrombosis, and Vascular Biology*, 17(3), pp.437-444.

Libby, P., Buring, J., Badimon, L., Hansson, G., Deanfield, J., Bittencourt, M., Tokgözoğlu, L. and Lewis, E., 2019. Atherosclerosis. *Nature Reviews Disease Primers*, 56(5).

Liu, Z., Italiano, J., Ferrer-Marin, F., Gutti, R., Bailey, M., Poterjoy, B., Rimsza, L. and Sola-Visner, M. (2011) Developmental differences in megakaryocytopoiesis are associated with up-regulated TPO signaling through mTOR and elevated GATA-1 levels in neonatal megakaryocytes. Blood, 117(15), 4106-4117.

Magwenzi, S., Woodward, C., Wraith, K., Aburima, A., Raslan, Z., Jones, H., McNeil, C., Wheatcroft, S., Yuldasheva, N., Febbriao, M., Kearney, M. and Naseem, K., 2015. Oxidized LDL activates blood platelets through CD36/NOX2–mediated inhibition of the cGMP/protein kinase G signaling cascade. *Blood*, 125(17), pp.2693-2703.

Mahfouz, M. and Kummerow, F. (1998) Oxysterols and TBARS are among the LDL oxidation products which enhance thromboxane A2 synthesis by platelets. *Prostaglandins & Other Lipid Mediators*, 56(4), 197-217.

Mahfouz, M. and Kummerow, F. (2001) Oxidized low density lipoprotein inhibits prostacyclin generation by rat aorta in vitro: A key role of lysolecithin. *Prostaglandins & Other Lipid Mediators*, 66(4), 283-304.

Mallat, Z. & Tedgui, A. (2001) Apoptosis as a Determinant of Atherothrombosis. Thrombosis and Haemostasis, 86(07), 420-426.

Mallat, Z., Hugel, B., Ohan, J., Lesèche, G., Freyssinet, J. & Tedgui, A. (1999) Shed Membrane Microparticles With Procoagulant Potential in Human Atherosclerotic Plaques. Circulation, 99(3), 348-353.

Martonosii, A., Molino, C. and Gergely, J. (1964). The binding of divalent cations to actin. *The Journal of Biology Chemistry*, 239, pp.1057-1064.

Marx, G., Korner, G., Mou, X. and Gorodetsky, R., 1993. Packaging zinc, fibrinogen, and factor XIII in platelet granules. *Journal of Cellular Physiology*, 156(3), pp.437-442.

Marx, G., Krugliak, J. and Shaklai, M., 1991. Nutritional zinc increases platelet reactivity. *American Journal of Hematology*, 38(3), pp.161-165.

Mauriello, A., Sangiorgi, G., Palmieri, G., Virmani, R., Holmes, D., Schwartz, R., Pistolese, R., Ippoliti, A. and Spagnoli, L., 2000. Hyperfibrinogenemia Is Associated With Specific Histocytological Composition and Complications of Atherosclerotic Carotid Plaques in Patients Affected by Transient Ischemic Attacks. *Circulation*, 101(7), pp.744-750.

Meisinger, C., Baumert, J., Khuseyinova, N., Loewel, H. and Koenig, W., 2005. Plasma Oxidized Low-Density Lipoprotein, a Strong Predictor for Acute Coronary Heart Disease Events in Apparently Healthy, Middle-Aged Men From the General Population. *Circulation*, 112(5), pp.651-657.

Meisinger, C., Baumert, J., Khuseyinova, N., Loewel, H. & Koenig, W. (2005) Plasma Oxidized Low-Density Lipoprotein, a Strong Predictor for Acute Coronary Heart Disease Events in Apparently Healthy, Middle-Aged Men From the General Population. ACC Current Journal Review, 14(12), 17.

Mensah, G., Wei, G., Sorlie, P., Fine, L., Rosenberg, Y., Kaufmann, P., Mussolino, M., Hsu, L., Addou, E., Engelgau, M. and Gordon, D., 2017. Decline in Cardiovascular Mortality. *Circulation Research*, 120(2), pp.366-380.

Miller, Y. and Shyy, J., 2017. Context-Dependent Role of Oxidized Lipids and Lipoproteins in Inflammation. *Trends in Endocrinology & Metabolism*, 28(2), pp.143-152.

Mitchell, J., Ali, F., Bailey, L., Moreno, L. and Harrington, L., 2007. Role of nitric oxide and prostacyclin as vasoactive hormones released by the endothelium. *Experimental Physiology*, 93(1), pp.141-147.

Moore, G., Smith, R. and Hutchins, G. (1982) Pulmonary artery atherosclerosis: correlation with systemic atherosclerosis and hypertensive pulmonary vascular disease. Arch Pathol Lab Med, 106(8), 378-380.

Morel, D., DiCorleto, P. and Chisolm, G., 1984. Endothelial and smooth muscle cells alter low density lipoprotein in vitro by free radical oxidation. *Arteriosclerosis: An Official Journal of the American Heart Association, Inc.*, 4(4), pp.357-364.

Morgan-Spencer, A. & Greenberg, D. (2007) P-REX1: A Novel RAC Activing Guanine-Nucleotide Exchange Factor in Human Platelets. Blood, 110(11), 3639-3639.

Moser, M., Nieswandt, B., Ussar, S., Pozgajova, M. and Fässler, R. (2008). Kindlin-3 is essential for integrin activation and platelet aggregation. *Nature Medicine*, 14(3), pp.325-330.

Mullins, R., Heuser, J. and Pollard, T., 1998. The interaction of Arp2/3 complex with actin: Nucleation, high affinity pointed end capping, and formation of branching networks of filaments. *Proceedings of the National Academy of Sciences*, 95(11), pp.6181-6186.

Murata, T., Ushikubi, F., Matsuoka, T., Hirata, M., Yamasaki, A., Sugimoto, Y., Ichikawa, A., Aze, Y., Tanaka, T., Yoshida, N., Ueno, A., Oh-ishi, S. and Narumiya, S. (1997). Altered pain perception and inflammatory response in mice lacking prostacyclin receptor. *Nature*, 388(6643), pp.678-682.

Murray, A., 2008. Pharmacological PKA Inhibition: All May Not Be What It Seems. *Pharmacolgy*, 1(22), p.pp. re4.

Nagy, Z. and Smolenski, A., 2018. Cyclic nucleotide-dependent inhibitory signaling interweaves with activating pathways to determine platelet responses. *Research and Practice in Thrombosis and Haemostasis*, 2(3), pp.558-571.

Narumiya, S., Sugimoto, Y. and Ushikubi, F. (1999). Prostanoid receptors; structures, properties and distribution. *Pathophysiology*, 1, p.36.

Naseem, K. (2005). The role of nitric oxide in cardiovascular diseases. *Molecular Aspects of Medicine*, 26(1-2), pp.33-65.

Naseem, K., Goodall, A. and Bruckdorfer, K. (1997). Differential effects of native and oxidatively modified low-density lipoproteins on platelet function. *Platelets*, 8(2), pp.163-174.

Nergiz-Unal, R., Lamers, M., Van Kruchten, R., Luiken, J., Cosemans, J., Glatz, J., Kuijpers, M. and Heemskerk, J., 2011. Signaling Role of CD36 in Platelet Activation and Thrombus Formation on Immobilized Thrombospondin or Oxidized Low-Density Lipoprotein. *Journal of Thrombosis and Haemostasis*, 9(9), pp.1835-1846.

Nobes, C. and Hall, A., 1995. Rho, Rac, and Cdc42 GTPases regulate the assembly of multimolecular focal complexes associated with actin stress fibers, lamellipodia, and filopodia. *Cell*, 81(1), pp.53-62.

Nurden, A., Fiore, M., Nurden, P. and Pillois, X. (2011). Glanzmann thrombasthenia: a review of ITGA2B and ITGB3 defects with emphasis on variants, phenotypic variability, and mouse models. *Blood*, 118(23), pp.5996-6005.

Obermayer, G., Afonyushkin, T. and Binder, C., 2018. Oxidized low-density lipoprotein in inflammation-driven thrombosis. *Journal of Thrombosis and Haemostasis*, 16(3), pp.418-428.

O'Dell, B. and Emery, M., 1991. Compromised Zinc Status in Rats Adversely Affects Calcium Metabolism in Platelets. *The Journal of Nutrition*, 121(11), pp.1763-1768.

Olinescu, R. and Kummerow, F., 2001. Fibrinogen is an efficient antioxidant. *The Journal of Nutritional Biochemistry*, 12(3), pp.162-169.

Olivecrona, G., 2016. Role of lipoprotein lipase in lipid metabolism. *Current Opinion in Lipidology*, 27(3), pp.233-241.

Pagidipati, N. and Gaziano, T., 2013. Estimating Deaths From Cardiovascular Disease: A Review of Global Methodologies of Mortality Measurement. *Circulation*, 127(6), pp.749-756.

Palta, S., Saroa, R. & Palta, A. (2014) Overview of the coagulation system. Indian Journal of Anaesthesia, 58(5), 515.

Panés, J. and Granger, D., 1998. Leukocyte-endothelial cell interactions: Molecular mechanisms and implications in gastrointestinal disease. *Gastroenterology*, 114(5), pp.1066-1090.

Pantaloni, D. and Carlier, M. (1993). How profilin promotes actin filament assembly in the presence of thymosin β4. *Cell*, 75(5), pp.1007-1014.

Papakonstanti, E., Ridley, A. and Vanhaesebroeck, B., 2007. The p110δ isoform of PI 3-kinase negatively controls RhoA and PTEN. *The EMBO Journal*, 26(13), pp.3050-3061.

Parise, L. (1999). Integrin αIIbβ3 signaling in platelet adhesion and aggregation. *Current Opinion in Cell Biology*, 11(5), pp.597-601.

Parise, L. (1999). Integrin αIIbβ3 signaling in platelet adhesion and aggregation. *Current Opinion in Cell Biology*, 11(5), pp.597-601.

Park, Y., Drazba, J., Vasanji, A., Egelhoff, T., Febbraio, M. and Silverstein, R., 2012. Oxidized LDL/CD36 interaction induces loss of cell polarity and inhibits macrophage locomotion. *Molecular Biology of the Cell*, 23(16), pp.3057-3068.

Patel, S., Hartwig, J. and Italiano, Jr, J., 2005. The biogenesis of platelets from megakaryocyte proplatelets. *Journal of Clinical Investigation*, 115(12), pp.3348-3354.

Patel, B., Dunn, R., Jeong, S., Zhu, Q., Julien, J. & David, S. (2002) Ceruloplasmin Regulates Iron Levels in the CNS and Prevents Free Radical Injury. The Journal of Neuroscience, 22(15), 6578-6586.

Patil, S., Newman, D. and Newman, P. (2001). Platelet endothelial cell adhesion molecule-1 serves as an inhibitory receptor that modulates platelet responses to collagen. *Blood*, 97(6), pp.1727-1732.

Pleines, I., Eckly, A., Elvers, M., Hagedorn, I., Eliautou, S., Bender, M., Wu, X., Lanza, F., Gachet, C., Brakebusch, C. and Nieswandt, B., 2010. Multiple alterations of platelet functions dominated by increased secretion in mice lacking Cdc42 in platelets. *Blood*, 115(16), pp.3364–3373.

Podrez, E., Byzova, T., Febbraio, M., Salomon, R., Ma, Y., Valiyaveettil, M., Poliakov, E., Sun, M., Finton, P., Curtis, B., Chen, J., Zhang, R., Silverstein, R. and Hazen, S. (2007) Platelet CD36 links hyperlipidemia, oxidant stress and a prothrombotic phenotype. *Nature Medicine*, 13(9), 1086-1095.

Pula, G. and Poole, A., 2008. Critical roles for the actin cytoskeleton and cdc42 in regulating platelet integrinα2β1. *Platelets*, 19(3), pp.199-210.

Qiu, Y., Brown, A., Myers, D., Sakurai, Y., Mannino, R., Tran, R., Ahn, B., Hardy, E., Kee, M., Kumar, S., Bao, G., Barker, T. and Lam, W., 2014. Platelet mechanosensing of substrate stiffness during clot formation mediates adhesion, spreading, and activation. *Proceedings of the National Academy of Sciences*, 111(40), pp.14430-14435.

Qiu, Y., Brown, A., Myers, D., Sakurai, Y., Mannino, R., Tran, R., Ahn, B., Hardy, E., Kee, M., Kumar, S., Bao, G., Barker, T. and Lam, W., 2014. Platelet mechanosensing of substrate stiffness during clot formation mediates adhesion, spreading, and activation. *Proceedings of the National Academy of Sciences*, 111(40), pp.14430-14435.

Quinn, M., Parthasarathy, S., Fong, L. and Steinberg, D. (1987) Oxidatively modified low density lipoproteins: a potential role in recruitment and retention of monocyte/macrophages during atherogenesis. *Proceedings of the National Academy of Sciences*, 84(9), 2995-2998.

Richardson, J. (2005) Mechanisms of organelle transport and capture along proplatelets during platelet production. *Blood*, 106(13), 4066-4075.

Rahaman, S., Lennon, D., Febbraio, M., Podrez, E., Hazen, S. and Silverstein, R., 2006. A CD36-dependent signaling cascade is necessary for macrophage foam cell formation. *Cell Metabolism*, 4(3), pp.211-221.

Reid, H., Mulvaney, E., Turner, E. and Kinsella, B. (2010). Interaction of the human prostacyclin receptor with Rab11. Characterization of a novel Rab11 binding domain within α-helix 8 that is regulated by palmitoylation. *Journal of Biological Chemistry*, 293(31), pp.12287-12287.

Ren, Q., Ye, S. and Whiteheart, S. (2008). The platelet release reaction: just when you thought platelet secretion was simple. *Current Opinion in Hematology*, 15(5), pp.537-541.

Repetto, M., Ferrarotti, N. and Boveris, A., 2010. The involvement of transition metal ions on iron-dependent lipid peroxidation. *Archives of Toxicology*, 84(4), pp.255-262.

Riazy, M., Chen, J., Yamamato, Y., Yamamato, H., Duronio, V. and Steinbrecher, U., 2011. OxLDL-mediated survival of macrophages does not require LDL internalization or signalling by major pattern recognition receptors. *Biochemistry and Cell Biology*, 89(4), pp.387-395.

Rohrer, L., Freeman, M., Kodama, T., Penman, M. and Krieger, M. (1990). Coiled-coil fibrous domains mediate ligand binding by macrophage scavenger receptor type II. *Nature*, 343(6258), pp.570-572.

Ruggeri, Z. and Mendolicchio, G., 2007. Adhesion Mechanisms in Platelet Function. *Circulation Research*, 100(12), pp.1673-1685.

Ruiz, J., Hutcheson, J. and Aikawa, E., 2015. Cardiovascular calcification: current controversies and novel concepts. *Cardiovascular Pathology*, 24(4), pp.207-212.

Ruiz, J., Weinbaum, S., Aikawa, E. and Hutcheson, J., 2016. Zooming in on the genesis of atherosclerotic plaque microcalcifications. *The Journal of Physiology*, 594(11), pp.2915-2927.

Rybalkin, S., Bornfeldt, K., Sonnenburg, W., Rybalkina, I., Kwak, K., Hanson, K., Krebs, E. and Beavo, J. (1997). Calmodulin-stimulated cyclic nucleotide phosphodiesterase (PDE1C) is induced in human arterial smooth muscle cells of the synthetic, proliferative phenotype. *Journal of Clinical Investigation*, 100(10), pp.2611-2621.

Safiullin, R., Christenson, W., Owaynat, H., Yermolenko, I., Kadirov, M., Ros, R. and Ugarova, T., 2015.

Sasaki, Y., Takahashi, T., Tanaka, I., Nakamura, K., Okuno, Y., Nakagawa, O., Narumiya, S. and Nakao, K. (1997) Expression of Prostacyclin Receptor in Human Megakaryocytes. *Blood*, 90(3), 1039-1046.

Savage, B., Almus-Jacobs, F. and Ruggeri, Z. (1998). Specific Synergy of Multiple Substrate–Receptor Interactions in Platelet Thrombus Formation under Flow. *Cell*, 94(5), pp.657-666.

Savage, B., Saldívar, E. and Ruggeri, Z. (1996). Initiation of Platelet Adhesion by Arrest onto Fibrinogen or Translocation on von Willebrand Factor. *Cell*, 84(2), pp.289-297.

Schlossmann, J., Ammendola, A., Ashman, K., Zong, X., Huber, A., Neubauer, G., Wang, G., Allescher, H., Korth, M., Wilm, M., Hofmann, F. and Ruth, P. (2000). Regulation of intracellular calcium by a signalling complex of IRAG, IP3 receptor and cGMP kinase Iβ. *Nature*, 404(6774), pp.197-201.

Scott, G. and Leopardi, S., 2003. The cAMP Signaling Pathway has Opposing Effects on Rac and Rho in B16F10 Cells: Implications for Dendrite Formation in Melanocytic Cells. *Pigment Cell Research*, 16(2), pp.139-148.

Scott, J., Glaccum, M., Zoller, M., Uhler, M., Helfman, D., McKnight, G. and Krebs, E. (1987). The molecular cloning of a type II regulatory subunit of the cAMP-dependent protein kinase from rat skeletal muscle and mouse brain. *Proceedings of the National Academy of Sciences*, 84(15), pp.5192-5196.

Shah, P., Falk, E., Badimon, J., Fernandez-Ortiz, A., Mailhac, A., Villareal-Levy, G., Fallon, J., Regnstrom, J. and Fuster, V. (1995). Human monocyte-derived macrophages induce collagen breakdown in fibrous caps of atherosclerotic plaques. Potential role of

matrix-degrading metalloproteinases and implications for plaque rupture. *Circulation*, 92(6), pp.1565-1569.

Shen, B., Delaney, M. & Du, X. (2012) Inside-out, outside-in, and inside–outside-in: G protein signaling in integrin-mediated cell adhesion, spreading, and retraction. Current Opinion in Cell Biology, 24(5), 600-606.

Shepherd, J., 2001. The role of the exogenous pathway in hypercholesterolaemia. *European Heart Journal Supplements*, 3, pp.E2-E5.

Shvartsman, M., Kikkeri, R., Shanzer, A. and Cabantchik, Z. (2007). Non-transferrin-bound iron reaches mitochondria by a chelator-inaccessible mechanism: biological and clinical implications. *American Journal of Physiology-Cell Physiology*, 293(4), pp.C1383-C1394.

Siegel-Axel, D., Daub, K., Seizer, P., Lindemann, S. and Gawaz, M. (2008) Platelet lipoprotein interplay: trigger of foam cell formation and driver of atherosclerosis. *Cardiovascular Research*, 78(1), 8-17.

Sjoberg, T., Kornev, A. and Taylor, S. (2010). Dissecting the cAMP-inducible allosteric switch in protein kinase A RIα. *Protein Science*, 19(6), pp.1213-1221.

Smith, F., Reichow, S., Esseltine, J., Shi, D., Langeberg, L., Scott, J. and Gonen, T. (2013). Intrinsic disorder within an AKAP-protein kinase A complex guides local substrate phosphorylation. *eLife*, 2.

Smyth, E. and FitzGerald, G. (2002). Human prostacyclin receptor. *Vitamin and Hormones*, 65, pp.149-165.

Smyth, E., Li, W. and FitzGerald, G. (1998). Phosphorylation of the Prostacyclin Receptor during Homologous Desensitization. *Journal of Biological Chemistry*, 273(36), pp.23258-23266.

Stalker, T., Traxler, E., Wu, J., Wannemacher, K., Cermignano, S., Voronov, R., Diamond, S. and Brass, L. (2013). Hierarchical organization in the hemostatic response and its relationship to the platelet-signaling network. *Blood*, 121(10), pp.1875-1885.

Steinberg, D. (1997) Low Density Lipoprotein Oxidation and Its Pathobiological Significance. Journal of Biological Chemistry, 272(34), 20963-20966.

Steinberg, D., Parthasarathy, S., Crew, T., Khoo, J. and Witztum, J. (1989) Beyond cholesterol: modification of low-density lipoprotein that increase its atherogenecity. *N Engl J Med*, 320(14), 915-924.

Steinberg, D. and Witztum, J., 2002. Is the Oxidative Modification Hypothesis Relevant to Human Atherosclerosis? *Circulation*, 105(17), pp.2107-2111.

Stenberg, P., Shuman, M., Levine, S. and Bainton, D. (1984). Redistribution of alpha-granules and their contents in thrombin- stimulated platelets. *The Journal of Cell Biology*, 98(2), pp.748-760.

Stitham, J., Stojanovic, A., Merenick, B., O'Hara, K. and Hwa, J. (2003). The Unique Ligand-binding Pocket for the Human Prostacyclin Receptor. *Journal of Biological Chemistry*, 278(6), pp.4250-4257.

Stuart, M., Gerrard, J. and White, J. (1980) Effect of Cholesterol on Production of Thromboxane B2by Platelets in Vitro. *New England Journal of Medicine*, 302(1), 6-10

Su, J., Zhou, H., Liu, X., Nilsson, J., Fredrikson, G. & Zhao, M. (2016) oxLDL antibody inhibits MCP-1 release in monocytes/macrophages by regulating Ca2+/K+channel flow. Journal of Cellular and Molecular Medicine, 21(5), 929-940.

Sun, B., Li, H., Shakur, Y., Hensley, J., Hockman, S., Kambayashi, J., Manganiello, V. and Liu, Y. (2007). Role of phosphodiesterase type 3A and 3B in regulating platelet and cardiac function using subtype-selective knockout mice. *Cellular Signalling*, 19(8), pp.1765-1771.

Sutton, R., Fasshauer, D., Jahn, R. and Brunger, A. (1998). Crystal structure of a SNARE complex involved in synaptic exocytosis at 2.4 Å resolution. *Nature*, 395(6700), pp.347-353.

Tadokoro, S., Shattil, S., Eto, K., Tai, V., Liddington, R., de Pereda, J., Ginsberg, M. and Calderwood, D. (2003). Talin Binding to Integrin Tails: A Final Common Step in Integrin Activation. *Science*, 302(5642), pp.103-106.

Takahashi, K., Naito, M., Kodama, T., Suzuki, H., Mori, T. and Matsumoto, A. (1992). Expression of macrophage scavenger receptors in various human tissues and atherosclerotic lesions. *Clinical Biochemistry*, 25(5), pp.365-368.

Taylor, S., Buechler, J. and Yonemoto, W. (1990). cAMP-Dependent Protein Kinase: Framework for a Diverse Family of Regulatory Enzymes. *Annual Review of Biochemistry*, 59(1), pp.971-1005.

Taylor, S., Kim, C., Cheng, C., Brown, S., Wu, J. and Kannan, N. (2008). Signaling through cAMP and cAMP-dependent protein kinase: Diverse strategies for drug design. *Biochimica et Biophysica Acta (BBA) - Proteins and Proteomics*, 1784(1), pp.16-26.

The British Journal of Cardiology. (2019). *Lipids module 1: lipid metabolism and its role in atherosclerosis - The British Journal of Cardiology*. [online] Available at: https://bjcardio.co.uk/2015/07/lipids-module-1-lipid-metabolism-and-its-role-in-atherosclerosis-3/# [Accessed 6 Nov. 2019].

Thomas, D., Mannon, R., Mannon, P., Latour, A., Oliver, J., Hoffman, M., Smithies, O., Koller, B. and Coffman, T. (1998). Coagulation defects and altered hemodynamic responses in mice lacking receptors for thromboxane A2. *Journal of Clinical Investigation*, 102(11), pp.1994-2001.

Thompson, R., Allam, A., Lombardi, G., Wann, L., Sutherland, M., Sutherland, J., Soliman, M., Frohlich, B., Mininberg, D., Monge, J., Vallodolid, C., Cox, S., Abd el-Maksoud, G., Badr, I., Miyamoto, M., el-Halim Nur el-din, A., Narula, J., Finch, C. and Thomas, G. (2013) Atherosclerosis across 4000 years of human history: the Horus study of four ancient populations. *The Lancet*, 381(9873), 1211-1222.

Thorin, E., Hamilton, C., Dominiczak, M. and Reid, J. (1994) Chronic exposure of cultured bovine endothelial cells to oxidized LDL abolishes prostacyclin release. Arteriosclerosis, Thrombosis, and Vascular Biology, 14(3), 453-459.

Tolias, K., Couvillon, A., Cantley, L. and Carpenter, C., 1998. Characterization of a Rac1- and RhoGDI-Associated Lipid Kinase Signaling Complex. *Molecular and Cellular Biology*, 18(2), pp.762-770.

Trepakova, E., Cohen, R. and Bolotina, V. (1999). Nitric Oxide Inhibits Capacitative Cation Influx in Human Platelets by Promoting Sarcoplasmic/Endoplasmic Reticulum Ca2+-ATPase–Dependent Refilling of Ca2+Stores. *Circulation Research*, 84(2), pp.201-209.

Trpkovic, A., Resanovic, I., Stanimirovic, J., Radak, D., Mousa, S., Cenic-Milosevic, D., Jevremovic, D. and Isenovic, E., 2015. Oxidized low-density lipoprotein as a biomarker of cardiovascular diseases. *Critical Reviews in Clinical Laboratory Sciences*, 52(2), pp.70-85.

Upchurch, G., Ramdev, N., Walsh, M. and Loscalzo, J., 1998. Prothrombotic consequences of the oxidation of fibrinogen and their inhibition by aspirin. *J Thromb Thrombolysis*, 5, pp.9–14.

van Tits, L., Stienstra, R., van Lent, P., Netea, M., Joosten, L. and Stalenhoef, A. (2011) Oxidized LDL enhances pro-inflammatory responses of alternatively activated M2 macrophages: A crucial role for Krüppel-like factor 2. *Atherosclerosis*, 214(2), 345-349.

van Willigen, G., Gorter, G. and Akkerman, J., 1994. LDLs increase the exposure of fibrinogen binding sites on platelets and secretion of dense granules. *Arteriosclerosis and Thrombosis: A Journal of Vascular Biology*, 14(1), pp.41-46.

Varga-Szabo, D., Braun, A. and Niewsandt, B., 2009. Calcium signaling in platelets. *Journal of Thrombosis and Haemostasis*, 7(7), pp.1057-1066.

Verma, A. and Ihler, G., 2002. Activation of Rac, Cdc42 and other downstream signalling molecules by Bartonella bacilliformis during entry into human endothelial cells. *Cellular Microbiology*, 4(9), pp.557-569.

Vinogradova, O., Velyvis, A., Velyviene, A., Hu, B., Haas, T., Plow, E. and Qin, J. (2002). A Structural Mechanism of Integrin αIIbβ3 "Inside-Out" Activation as Regulated by Its Cytoplasmic Face. *Cell*, 110(5), pp.587-597.

Virmani, R., Kolodgie, F., Burke, A., Farb, A. and Schwartz, S. (2000). Lessons From Sudden Coronary Death. *Arteriosclerosis, Thrombosis, and Vascular Biology*, 20(5), pp.1262-1275.

von Willebrand factor binds to native collagen VI primarily via its A1 domain. *Biochemical Journal*, 324(1), pp.185-191.

Vora, D., Fang, Z., Liva, S., Tyner, T., Parhami, F., Watson, A., Drake, T., Territo, M. and Berliner, J. (1997) Induction of P-Selectin by Oxidized Lipoproteins: Separate Effects on Synthesis and Surface Expression. *Circulation Research*, 80(6), 810-818.

Walkup, G., Burdette, S., Lippard, S. and Tsien, R., 2000. A New Cell-Permeable Fluorescent Probe for Zn2+. *Journal of the American Chemical Society*, 122(23), pp.5644-5645.

Wang, A., Zhang, X., Li, S., Zhao, X., Liu, L., Johnston, S., Meng, X., Lin, J., Zuo, Y., Li, H., Wang, Y. & Wang, Y. (2019) Oxidative lipoprotein markers predict poor functional outcome in patients with minor stroke or transient ischaemic attack. European Journal of Neurology, 26(8), 1082-1090.

Wang, F., Kohan, A., Lo, C., Liu, M., Howles, P. and Tso, P., 2015. Apolipoprotein A-IV: a protein intimately involved in metabolism. *Journal of Lipid Research*, 56(8), pp.1403-1418.

Wang, J., Jia, L., Li, X., Jin, S., Li, X., Liu, F., Shan, C., Zhang, Y. and Yang, Y., 2019. New Insights into the Association between Fibrinogen and Coronary Atherosclerotic Plaque Vulnerability: An Intravascular Optical Coherence Tomography Study. *Cardiovascular Therapeutics*, 2019, pp.1-12.

Watson, B., White, N., Taylor, K., Howes, J., Malcor, J., Bihan, D., Sage, S., Farndale, R. and Pugh, N., 2016. Zinc is a transmembrane agonist that induces platelet activation in a tyrosine phosphorylation-dependent manner. *Metallomics*, 8(1), pp.91-100.

Watt, J., Kennedy, S., Ahmed, N., Hayhurst, J., McClure, J., Berry, C., Wadsworth, R. and Oldroyd, K. (2016) The relationship between oxidised LDL, endothelial progenitor cells and coronary endothelial function in patients with CHD. *Open Heart*, 3(1), e000342.

Weiss, H. and Turitto, V., 1979. Prostacyclin (prostaglandin I2, PGI2) inhibits platelet adhesion and thrombus formation on subendothelium. *Blood*, 53(2), pp.244-250.

Weksler, B., Ley, C. and Jaffe, E., 1978. Stimulation of Endothelial Cell Prostacyclin Production by Thrombin, Trypsin, and the Ionophore A 23187. *Journal of Clinical Investigation*, 62(5), pp.923-930.

Welch, H., Coadwell, W., Ellson, C., Ferguson, G., Andrews, S., Erdjument-Bromage, H., Tempst, P., Hawkins, P. and Stephens, L., 2002. P-Rex1, a PtdIns(3,4,5)P3- and Gβγ-Regulated Guanine-Nucleotide Exchange Factor for Rac. *Cell*, 108(6), pp.809-821.

Welch, H., Condliffe, A., Milne, L., Ferguson, G., Hill, K., Webb, L., Okkenhaug, K., Coadwell, W., Andrews, S., Thelen, M., Jones, G., Hawkins, P. and Stephens, L., 2005. P-Rex1 Regulates Neutrophil Function. *Current Biology*, 15(20), pp.1867-1873.

Welsh, J., Stalker, T., Voronov, R., Muthard, R., Tomaiuolo, M., Diamond, S. and Brass, L. (2014). A systems approach to hemostasis: 1. The interdependence of thrombus architecture and agonist movements in the gaps between platelets. *Blood*, 124(11), pp.1808-1815.

White, J. (2007). *Platelet Structure*. 2nd ed. San Diego, CA: Michelson.

White, J. and Gerrard, J., 1976. Ultrastructural features of abnormal blood platelets. A review. *American Journal of Pathology*, 83, pp.589–632.

Wilhelmsen, L., Svärdsudd, K., Korsan-Bengtsen, K., Larsson, B., Welin, L. and Tibblin, G., 1984. Fibrinogen as a Risk Factor for Stroke and Myocardial Infarction. *New England Journal of Medicine*, 311(8), pp.501-505.

Willoughby, D. and Cooper, D. (2007). Organization and Ca2+ Regulation of Adenylyl Cyclases in cAMP Microdomains. *Physiological Reviews*, 87(3), pp.965-1010.

Wolf, D. & Ley, K. (2019) Immunity and Inflammation in Atherosclerosis. Circulation Research, 124(2), 315-327.

Worthylake, R., Lemoine, S., Watson, J. and Burridge, K., 2001. RhoA is required for monocyte tail retraction during transendothelial migration. *Journal of Cell Biology*, 154(1), pp.147-160.

Wraith, K., Magwenzi, S., Aburima, A., Wen, Y., Leake, D. and Naseem, K. (2013). Oxidized low-density lipoproteins induce rapid platelet activation and shape change through tyrosine kinase and Rho kinase–signaling pathways. *Blood*, 122(4), pp.580-589.

Wright, J. (1906) The Origin and Nature of the Blood Plates. *The Boston Medical and Surgical Journal*, 154(23), 643-645.

Wu, M., Atkinson, T. and Lindner, J., 2017. Platelets and von Willebrand factor in atherogenesis. *Blood*, 129(11), pp.1415-1419.

Xiao, C., Hara, A., Yuhki, K., Fujino, T., Ma, H., Okada, Y., Takahata, O., Yamada, T., Murata, T., Narumiya, S. and Ushikubi, F. (2001). Roles of Prostaglandin I 2 and Thromboxane A 2 in Cardiac Ischemia-Reperfusion Injury. *Circulation*, 104(18), pp.2210-2215.

Yadav, S. and Storrie, B., 2016. The cellular basis of platelet secretion: Emerging structure/function relationships. *Platelets*, 28(2), pp.108-118.

Yin, T. and Linheng, L., 2006. The stem cell niches in bone. *Journal of Clinical Investigation*, 116(5), pp.1195-1201.

Yun, S., Sim, E., Goh, R., Park, J. and Han, J., 2016. Platelet Activation: The Mechanisms and Potential Biomarkers. *BioMed Research International*, 2016, pp.1-5.

Zhang, G., Xiang, B., Skoda, R., Smyth, S., Du, X. and Li, Z. (2010). Biphasic Roles for the Soluble Guanylyl Cyclase (sGC) In Platelet Activation In Mice. *Blood*, 116(21), pp.486-486.

Zhang, Y., Zhu, C., Guo, Y., Xu, R., Li, S., Dong, Q. and Li, J. (2014). Higher Fibrinogen Level is Independently Linked with the Presence and Severity of New-Onset Coronary Atherosclerosis among Han Chinese Population. *PLoS ONE*, 9(11), p.e113460.

Zhang, Z., Austin, S. and Smyth, E. (2001). Glycosylation of the human prostacyclin receptor: role in ligand binding and signal transduction. *Molecular Pharmacology*, 60(3), pp.480-487.

Zöller, B., Li, X., Sundquist, J. and Sundquist, K., 2012. Autoimmune diseases and venous thromboembolism: a review of the literature. *Am J Cardiovasc Dis*, 2(3), pp.171–183.

Zwaal, R., Comfurius, P. and Bevers, E., 1998. Lipid–protein interactions in blood coagulation. *Biochimica et Biophysica Acta (BBA) - Reviews on Biomembranes*, 1376(3), pp.433-453.